## Swansea University
## Prifysgol Abertawe

# Methods to Identify Biomarkers

# to Predict Bacterial Sepsis

Heather Mair Chick

Submitted to Swansea University in fulfilment of the requirements for the Degree of
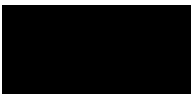Doctor of Philosophy

*Swansea University*

2019

## Summary

Bacterial sepsis represents a significant challenge for clinicians worldwide and causes 11 million deaths annually worldwide. In Wales, *Escherichia coli* and *Staphylococcus* species are the predominant causes. Predicting sepsis accurately is complicated by the multifactorial nature of the disorder resulting in very few useful biomarkers. This thesis aimed to characterise the immunological and cellular response to model and pathogenic bacteria and analyse the genomic composition of clinically relevant extraintestinal blood culture-positive *E. coli*. Eight strains comprising *E. coli, S. aureus* and *S. epidermidis* were applied to a whole blood infection model, incubated for up to eight hours and the supernatant used in ELISA, flow cytometry and mass spectrometry analysis. Clinically relevant *E. coli* were obtained from the Hywel Dda University Health Board in West Wales and submitted for DNA sequencing and whole genome analysis using the pan-genome pipeline Roary. *E. coli* induced significantly more IL-6, MIP-1α and MIP-3α and significantly less phagocytosis than that induced by both *Staphylococcus* species. Flow cytometry analysis of leukocyte subsets revealed a robust infection model that confirmed interactions seen in the blood were due to infection, and a loss of CD14 was characterised on the monocytes treated with bacteria. The oxysterol 25-HC was confirmed to be significantly elevated in blood treated with *E. coli* which challenges the previous dogma of virus restricted induction. Finally, blood culture-positive *E. coli* were found to be from a diverse range of sequence types and possessed virulence factors and antibiotic resistance genes in abundance. The genes *tufA* and *tufB* were found to be significantly associated with sepsis and certain origins of infection. The work undertaken in this thesis identifies biomarkers to predict bacterial sepsis that can be taken forward for clinical validation.

**Declaration**

This work has not previously been accepted in substance for any degree and is not being concurrently submitted in candidature for any degree.

Signed... █████ .............................................. Date..7.7.2020......

This thesis is the result of my own investigations, except where otherwise stated. Where correction services have been used, the extent and nature of the correction is clearly marked. Other sources are acknowledged by footnotes giving explicit references. A bibliography is appended.

Signed....... ████ .................................................Date....7.7.2020............

I hereby give consent for my thesis, if accepted, to be available for photocopying and for inter-library loan, and for the title and summary to be made available to outside organisations.

Signed........... ████ .................................................. Date...7.7.2020........

## Acknowledgments

First, I would like to thank Dr Tom Wilkinson for his excellent supervision during my time as a PhD student. This thesis would not have been possible if not for his continuing support throughout my time as a PhD student. His enthusiasm and good nature has largely boosted my confidence throughout the PhD and enabled me to explore my own ideas. I would also like to give a very special thanks to Dr Llinos Harris and Dr Lisa Williams for their much-appreciated efforts to help me with my laboratory work, professional development and of course with this thesis. Additionally, I would like to thank Prof. Tom Humphrey for his kind words of encouragement and his help with all my written work and conference material.

I would like to thank everyone at the Griffiths-Wang laboratory, including my supervisors Dr. William Griffiths and Dr. Yuqin Wang, for the opportunity to perform some of my studies in their lab and for their help with Chapter 5. I would also like to thank Dr. Eylan Yutec for his patience answering all my questions and for walking me through the method and to Alison Dickson, for not only helping me with all things mass spec. but also for being a good friend. Thanks also to Dr. Cathy Thornton, Dr. Nick Jones and Graham Botley for all their help with flow cytometry, and thanks to Dr Matt Hitchings for sequencing my *E. coli* isolates and for all his help with Chapter 6. Thank you also to Professor Keir Lewis and Dr Mike Simmons for kindly providing us with the isolates and for their help with Chapter 6. I would also like to extend a special thanks to the Joint Clinical Research Facility and all the staff for their help over the years; without the facility this thesis would not have been possible. I would also like to thank all the anonymous donors who provided me with blood over the years.

A massive thank you to everyone in the Microbiology and Infectious Diseases group who have been there throughout my time doing my PhD, especially Dr. Rhys Jones, Celeste Felion, Phacharapon Boonkhot and Nattinee Kittiwan. Thanks to all for keeping me sane throughout my PhD and all your help over the years. I would like to give a special thanks to both Dr. Susan Murray and Dr. Dan John for all your help with Roary and all the holidays over the years, and of course, thanks to all my friends everywhere, especially Elinor Parry, Rebecca Davis, Dennese Tan and Anwen Hamer.

Finally, I would like to thank my family, especially Rhys, Mum, Dad, Sean, Nanny and Taid. Thank you all for believing in me over the years and encouraging me to go far.

# Contents

## List of Tables

## List of Figures

**Abbreviations**

| | |
|---|---|
| 7α-HC | 7α-hydroxycholesterol |
| 7α,25-HC | 7α,25-dihydroxycholesterol |
| 7α,27-HC | 7α,27-dihydroxycholesterol |
| 24-HC | 24-hydroxycholesterol |
| 25-HC | 25-hydroxycholesterol |
| 27-HC | 27-hydroxycholesterol |
| AD | Alzheimer's disease |
| *agr* | accessory gene regulator |
| AIM | absent in melanoma |
| APACHE | Acute Physiology and Chronic Health Evaluation |
| APC | allophycocyanin |
| APCs | antigen-presenting cells |
| APP | acute phase protein |
| APR | acute phase response |
| ATP | adenosine triphosphate |
| BCR | B cell receptor |
| BSA | bovine serum albumin |
| CACO-2 | human caucasian colon adenocarcinoma |
| CD | cluster of differentiation |
| CDT | cytolethal distending toxin |
| cfDNA | cell-free DNA |
| cfu/ml | cell forming units per millilitre |
| CH25H | cholesterol 25-hydroxylase |
| CNF-1 | cytotoxic necrotising factor 1 |
| CoNS | coagulase-negative *Staphylococci* |
| CoV | coefficience of variation |
| CRP | c-reactive protein |
| DAMP | damage-associated molecular pattern |
| $dH_2O$ | distilled water |
| DIC | disseminated intravascular coagulation |
| DMEM | Dulbecco's modified eagle medium |

DNA          deoxyribonucleic acid

EF-tu         elongation factor thermo-unstable

ELISA        enzyme-linked immunosorbent assay

ELLecSA    enzyme-linked lectin-sorbent assay

EPS          extracellular polymeric substance

ESBL         extended-spectrum β-lactamase

*E. coli*        *Escherichia coli*

ESR          erythrocyte sedimentation rate

ExPEC       extraintestinal *Escherichia coli*

FACS         fluorescent activated cell sorting

FcMBL       Fc (IgG1) bound mannose binding lectin

FITC         fluorescein isothiocyanate

FTMS         fourier-transform mass spectrometry

GI           gastrointestinal

g/L          gram per litre

GLASS        global antimicrobial resistance surveillance system

GPCR         g-protein coupled receptor

GWAS         genome-wide association study

HDL          high-density lipoprotein

HDP          human defence peptide

HDUHB        Hywel Dda University Health Board

HLA-DR       human leukocyte antigen – DR isotype

HMGB1        high mobility group protein b2

HPLC         high performance liquid chromatography

ICU          intensive care unit

IFN          interferon

Ig           immunoglobulin

IL           interleukin

IreA          siderophore receptor A

LB           lennox broth

LBP           LPS-binding protein

| | |
|---|---|
| LC-MS | liquid chromatography – mass spectrometry |
| LDL | low-density lipoprotein |
| LPS | lipopolysaccharide |
| LRR | leucine-rich repeat |
| LTA | lipoteichoic acid |
| LXR | liver X receptor |
| M | mole |
| MAC | membrane attack complex |
| MAL | MYD88 adaptor-like |
| MAP | mitogen-activated protein |
| MBL | mannose-binding lectin |
| mCD14 | membrane bound CD14 |
| MD-2 | myeloid differentiation protein 2 |
| MFI | mean fluorescence intensity |
| mg/l | milligram per litre |
| mg/ml | milligram per millilitre |
| MHC | major histocompatibility complex |
| MIF | macrophage inhibitory factor |
| MIP | macrophage inflammatory protein |
| ml | millilitre |
| MLST | multi-locus sequence typing |
| mM | millimole |
| MOI | multiplicity of infection |
| MSCRAMM | microbial surface components recognising adhesive matrix molecule |
| MyD88 | myeloid differentiation – $1^o$ response gene 88 |
| NAIP | NLR family apoptosis inhibitory protein |
| NALP | NACHT leucine-rich-repeat protein |
| NET | neutrophil extracellular trap |
| NK | natural killer |
| NF-κB | nuclear factor – κB |
| nm | nanometre |

| | |
|---|---|
| NO | nitric oxide |
| NOD | nucleotide-binding oligomerization domain-containing protein |
| $O_2^-$ | superoxide anion |
| OD | optical density |
| ·OH | hydroxyl radical |
| PAb | polyclonal antibody |
| PAF | platelet-activating factor |
| PAI | pathogenicity island |
| PAI1 | plasminogen-activator inhibitor type 1 |
| PAMP | pathogen-associated molecular pattern |
| PBMC | peripheral blood mononuclear cell |
| PBP2A | penicillin-binding protein |
| PBS | phosphate buffered saline |
| PCT | procalcitonin |
| PE | phycoerythrin |
| pg/ml | picogram per millilitre |
| PGN | peptidoglycan |
| PI | propidium iodide |
| Poly I:C | polyinosine:polycytidylic acid |
| PPP | platelet poor plasma |
| PRR | pattern recognition receptor |
| PSM | phenol-soluble modulin |
| QC | quality control |
| RNS | reactive nitrogen species |
| ROS | reactive oxygen species |
| r.p.m | rotations per minute |
| RT | room temperature |
| SAT | secreted autotransporter toxin |
| SAG | *Staphylococcal* superantigen |
| SCC | *Staphylococcal* cassette chromosome |
| sCD14 | soluble CD14 |

| | |
|---|---|
| SCV | small colony variant |
| SEM | standard error of the mean |
| SREBP | sterol response element-binding protein |
| SOFA | sepsis-related organ failure assessment |
| ST | sequence type |
| *S. aureus* | *Staphylococcus aureus* |
| *S. epidermidis* | *Staphylococcus epidermidis* |
| TF | tissue factor |
| Th | t helper |
| TIC/ITMS | extracted ion chromatogram/ion trap mass spectrometry |
| TIR | toll/IL-2 cytoplasmic receptor |
| TLR | toll-like receptor |
| TNF-α | tumour necrosis factor - α |
| TRAM | toll receptor-associated molecule |
| Trif | toll receptor-associated activator of interferon |
| TSB | tryptic soy broth |
| TTSS | type III secretion system |
| μg/ml | microgram per millilitre |
| μl | microlitre |
| UM-UC-3 | human bladder transitional cell carcinoma |
| UPEC | uropathogenic *Escherichia coli* |
| UTI | urinary tract infection |
| VF | virulence factor |
| WHO | World Health Organisation |
| W/V | weight per volume |

# Chapter 1. Introduction

## 1.1. Sepsis

### 1.1.1. Definition

Sepsis is defined as an uncontrollable and overwhelming innate inflammatory response to an infection, often caused by the presence of bacteria in the bloodstream (bacteraemia) (Cohen, 2002; Becker *et al*., 2009; Charles *et al*., 2009; Burdette *et al*., 2010; Chan and Gu, 2011; Hughes *et al*., 2013; Singer *et al.,* 2016). Symptoms are typified by **S**lurred speech or confusion, **E**xtreme shivering or muscle pain, **P**assing no urine within 24 hours, **S**evere breathlessness, the patient (**I**t) feeling like they are going to die, and **S**kin mottled or discoloured in adult patients (abbreviated as **SEPSIS** by the UK Sepsis Trust as part of an awareness campaign). Sepsis in young children is further characterised by fast breathing, convulsions, a non-fading rash, lethargy and abnormally cold skin (UK Sepsis Trust, 2019). Further diagnosis is confirmed by the presence of two or more patient abnormalities including temperature, heart and respiratory rate and/or leukocyte counts, and sufficient diagnosis of an accompanying infection (Calandra and Cohen, 2005; Deutschman and Tracey, 2014). The final diagnosis is often dependent on the severity of the disease; severe sepsis is diagnosed when there is evidence of organ dysfunction, and septic shock is diagnosed when there is organ dysfunction accompanied with evidence of hypotension refractory to fluid resuscitation, or circulatory collapse (McPherson *et al*., 2013; Singer *et al.,* 2016).

### 1.1.2. Global Importance

Sepsis represents one of the biggest challenges to healthcare professionals in the United Kingdom, with global cases reaching as high as 19 million per year (Monneret and Venet, 2016). It is currently the third largest cause of death in the U.K. behind coronary heart disease and stroke, and is the leading cause of death among critically ill patients in Intensive Care Units (ICU; Charles *et al*., 2009; Chan and Gu, 2011). Current mortality rates reach as high as 60% and subsequently sepsis claims more lives than both bowel and breast cancer combined, with as much as 5% of all deaths in England being due to sepsis (Charles *et al*., 2009; Chan and Gu, 2011; McPherson *et al*., 2013; Monneret and Venet, 2016). The recent rise in cases is believed to be caused by a number of modern factors, including an increase in the life expectancy of the population, a better recognition of the disorder and improved medical and surgical care for patients with comorbidities such as diabetes that until recently would have been fatal (Deutschman and Tracey, 2014;

Monneret and Venet, 2016; Singer *et al*., 2016). Often, the resolution of a septic episode is complicated by a large variety of factors, including issues with diagnosis, treatment, and the rise in antibiotic resistance  (Charles *et al*., 2009; Singer *et al*., 2016). Many of these factors negatively impact on the time from onset of the disease to diagnosis, where the 'golden hours' for effective treatment of sepsis are often missed (Charles *et al*., 2009). Amongst those who are most vulnerable are the immunocompromised, including the elderly, new-born babies, and patients with previous or current trauma and conditions, such as diabetes and cancer (Lever and Mackenzie, 2007).

### 1.1.3. Complications and ICU Management

Overall, approximately 27% of patients admitted to ICUs in England and Wales have been diagnosed with severe sepsis, and almost half of these patients will later die (McPherson *et al*., 2013). Factors and symptoms associated with sepsis syndrome include fever, leukocytosis or leukopenia, hypotension, hypothermia, tachycardia and tachypnoea (Feezor *et al*., 2003; Becker *et al.,* 2008). Severe complications arise in the form of organ dysfunction, altered mental state, cardiac failure, coma, renal failure and intravascular coagulation (Nguyen *et al*., 2006; Becker *et al*., 2009). People who survive sepsis are often left with long-term complications that can affect them physically and physiologically with significant impacts on the quality of their lives (Singer *et al*., 2016) and often, the outcome is death (Becker *et al*., 2008). Early recognition and appropriate application of antibiotic therapy is crucial to prevent overt patient harm and death. Clinically, physicians are encouraged to apply the "Sepsis 6", a care bundle that, if applied within one hour of admission, has been shown to reduce mortality in sepsis patients (McGregor, 2014). The Sepsis 6 is characterised by the delivery of high flow oxygen, the preparation of blood cultures, administration of empiric intravenous antibiotics, measurement of serum lactate and full blood counts, application of intravenous fluid resuscitation and accurate measurement of urine output (Daniels, 2011). Application of severity scoring systems, such as the Acute Physiology and Chronic Health Evaluation (APACHE II) and the Sequential Sepsis-related Organ Failure Assessment (SOFA), are also applied within one hour of admission to assist in determination of severity and advise on treatment options (Bouch and Thompson, 2008). Outlined in Table 1.1 are ICU admission statistics assessed by six separate studies from 2006-2018.

Table 1.1. Intensive Care Unit admission statistics for critically ill patients and patients with sepsis from six papers.

| Study | Countries Included | Patient Number | % ICU Patients +ve Sepsis | Gender | Age (mean) | Length of ICU Stay (mean) | % patients with organ failure | Comorbidities |
|---|---|---|---|---|---|---|---|---|
| Capuzzo *et al.* 2014 | 17 European Countries | 5834 | ██████ | ██████ | ██████ | 3.5 days | ██████ | ██████ |
| Williams *et al.* 2010 | Australia | 22298 | 4.6% (<10 days) 23.9% (>10 days) | Male 68% (<10 days) 66% (>10 days) | 57 (<10 days) 49 (>10 days) | 17 days (>10 days) | ██████ | ██████ |
| Sakr *et al.* 2018 | Worldwide | 10069 | 17.9% | 60.1% Male | 59.4 | 6 days | ██████ | Sepsis-related: COPD (452) Cancer (339) Diabetes (308) Heart Failure (333) Immunosuppression (169) % Comorbidities: None (46%) 1 (30.9%) 2 (15.7%) 3 (5.6%) |

| | | | | | | | | |
|---|---|---|---|---|---|---|---|---|
| Shankar-Hari *et al.* 2017 | England | 654918 | 30.2% | 65%-66.4% Male | 63.3-65.3 | | Cardiovascular (46.2%) Respiratory (10.6-14.1%) Renal (17.2-17.6%) Haematological (15.1%-17.5%) Neurological (10.9%-14.3%) Hepatic (97.5-98.9%) | Cardiovascular (1.7-1.8%) Respiratory (2.8-4.2%) Liver (2.4-3.3%) Renal (2.1-2.2%) Metastatic disease (2.5-2.8%) Haematological (3.7-4.2%) Immunosuppressed (8.5-9%) |
| Vincent *et al.* 2006 | Europe | 3147 | 66% | 63% Male | 65 | 6.9 days | 71% 42% in sepsis patients | |
| Vincent *et al.* 2009 | Worldwide | 14414 | | 63% Male | 60.9 | | | 52% ≥ 1 Comorbidity COPD (20.2%) Cancer (15.7%) Heart Failure (10.4%) Diabetes mellitus (10.3%) Immunosuppression (5.8%) |

### 1.1.4. Antibiotic Resistance and Stewardship

Antibiotic resistance is considered to be one of the largest threats to health and development worldwide (Morgan, 2019). The over-use and inappropriate application of antibiotics in the clinic has resulted in the rise of multi-drug resistant bacteria, and recent estimates suggest that 70% of antibiotics are inappropriately prescribed (Schuetz *et al*., 2011; Adhikari *et al*., 2012; Public Health England, 2015; Morgan, 2019). However, the use of broad-spectrum antibiotics early in a septic episode is critical, and often it's the only option available to a doctor when it comes to treatment (Reinhart *et al*., 2012). These patients and those with chronic conditions and immunocompromised systems are most at risk for developing lethal infections that cannot be treated with currently used antibiotics. In Europe, approximately 25,000 people die each year due to hospital infections caused by resistant *Escherichia coli, Klebsiella pneumoniae, Enterococcus faecium, Pseudomonas aeruginosa* and methicillin-resistant *Staphylococcus aureus* (MRSA; Public Health England, 2015). Globally, approximately 700,000 people die annually due to drug-resistant infections (O'Neill, 2016). It is currently estimated that without measures to safeguard our current antibiotic pool, approximately 10 million deaths will occur annually by 2050, and result in a loss of £66 trillion of the global economy (Public Health England, 2015; O'Neill, 2016). This is directly comparable to the 8.2 million deaths that will be attributed to cancer by the same year (O'Neill, 2016). The World Health Organisation (WHO), launched the Global Antimicrobial Resistance Surveillance System (GLASS) in 2015, which focused on collating data on the eight bacterial pathogens they considered a priority in antibiotic resistance context; *E. coli*, *K. pneumoniae*, *Acinetobacter baumannii, S. aureus, Streptococcus pneumoniae, Salmonella* spp., *Shigella* spp., and *Neisseria gonorrhoeae,* of which *E. coli* and *S. aureus* are regarded as the major sepsis pathogens. Recent efforts have been made in establishing antibiotic stewardship initiatives that focus on primarily antibiotic prescribing and their use in the clinic. Antibiotic stewardship is defined as interventions designed to monitor and improve the appropriate use of antibiotics by promoting optimal dosing, duration and route of administration  (Morgan, 2019).

### 1.1.5. Sepsis Pathogens

The presence of an infection is critical to the diagnosis of sepsis, as sepsis in the absence of an infection is defined as systemic inflammatory response syndrome (SIRS; Becker *et al.,* 2009). Sepsis can be characterised by the presence or absence of a bacteraemia (bacteria in the blood; Becker *et al.,* 2009). These distinctions are very important when we take into consideration the treatments for these very different conditions. Presence of a bacteraemia will dictate the appropriate application of antibiotics, and extra care is required to avoid inappropriate applications and the development of antibiotic resistance. In addition to this, an infection as the cause of the septic attack is often very difficult to diagnose, and thus clinicians are often faced with very difficult choices on how to approach the case. The terms culture-positive and culture-negative are often used to describe a sepsis case, and sepsis is rarely confirmed, as often clinicians rely on a presumed diagnosis (Becker *et al*., 2009). Approximately one third of sepsis patients are infected with a pathogen that cannot be identified (Reinhart *et al.*, 2012).

The major cause of sepsis in Europe and the U.K. is a bacterial infection, and likewise sepsis is the predominant cause of death due to an infection (Schuetz *et al*., 2011; Opota *et al.,* 2015; Singer *et al*., 2016). The predominant bacterial cause is often dependent on many factors, including the geographical area in which the patient lives and whether the primary cause of infection is community or nosocomial-based. It has been reported in the past that Gram-negative bacteria are more commonly the cause of sepsis than Gram-positive bacteria. However, this trend is rapidly changing with the rise in hospital-acquired Gram-positive infections (Feezor *et al*., 2003; Becker *et al*., 2009; Abe *et al.*, 2010; Ramachandran, 2014; Surbatovic *et al*., 2015). The most common Gram-positive bacteria isolated in such sepsis cases are *S. aureus* and *S. pneumonia*e, and the most common Gram-negative bacteria are *E. coli, Klebsiella* spp. and *P. aeruginosa* (Ramachandran, 2014; Opota *et al.,* 2015). In England and Wales, *E. coli* is the most common cause of bacteraemia (Public Health England, 2015). More recently, coagulase-negative staphylococci (CoNS), such as *S. epidermidis,* have emerged as a large cause of neonatal and device-associated infections in hospitals (Dong and Speer, 2014). The bacteria most commonly isolated during sepsis from four worldwide studies are shown in Table 1.2.

Table 1.2. Sources of infection and most commonly isolated bacteria in sepsis patients.

| Study | Sources of Infection | % Positive Isolates | % Gram-positive isolates | % Gram-negative isolates | Most frequently isolated species | No. of patients receiving antibiotics | Mortality rate | Infection mortality rate |
|---|---|---|---|---|---|---|---|---|
| Sakr *et al.* 2018 | 67.4% Respiratory Tract 21.8% Abdomen 10.8% Respiratory & Catheter-associated | 69.6% 51.6% Patients >1 pathogen isolated | 50% | 66.6% | Coagulase-negative *Staphylococcus* (24.2%) Methicillin-sensitive *S. aureus* (12.4%) *Escherichia coli* (22.7%) *Pseudomonas* spp. (16.3%) | 5975 (59.3%) | 25.8% for Sepsis Patients | 26.2% Gram-positive 26.6% Gram-negative |
| Vincent *et al.* 2006 | Lung (68%) Abdomen (22%) Blood (20%) Urinary Tract (14%) | 60% | 40% | 38% | MRSA (14%) *Pseudomonas* spp. (14%) *E. coli* (13%) | 64% | 18.50% | 27% |
| Vincent *et al.* 2009 | Lung (64%) Abdomen (20%) Blood (15%) Genitourinary (14%) | 70% | 47% | 62% | *S. aureus* (20%) *Pseudomonas* spp. (20%) *E. coli* (16%) *S. epidermidis* (10.8%) | 71% | 18.20% | 25.30% |
| Opota *et al.* 2015 | | <30% Contamination | 35.4% | 62% | *E. coli* (28.6%) *S. aureus* (13.6%) Coagulase-negative *staphylococci* (10.09%) *Pseudomonas aeruginosa* (8.52%) *Klebsiella* spp. (7.11%) | | | |

### 1.1.5.1. *Staphylococcus aureus*

*Staphylococcus aureus* is a Gram-positive bacteria that colonises approximately 20-30% of the population and can be found on the anterior nares of asymptomatic carriers (Gordon and Lowy, 2008). Carriers that are persistently colonised are most at risk of infection but are more likely to survive an infection than non-carriers (Adhikari *et al.*, 2012). In addition, those infected are very often done so by the colonising strain (Gordon and Lowy, 2008). This colonisation serves as a reservoir from which the bacteria can establish an infection when host defences are compromised (Gordon and Lowy, 2008). Primary infection sites often occur at a breach in the skin, such as a cut or a burn, which can lead to minor wound or skin infections. However, *S. aureus* can disseminate within the host and infect any tissue, and subsequently infection can rapidly lead to sepsis. Key to the pathogenicity of *S. aureus* is the arsenal of toxins (alpha-haemolysin, toxic shock syndrome protein; Otto, 2014), enzymes (serine proteases, staphylokinase; Otto, 2014) and adhesins (surface protein adhesins [MSCRAMMs]; Foster *et al.,* 2014) that it uses to establish an infection. The coordination of these numerous virulence factors (VFs) allows *S. aureus* to be one of the most successful pathogens in the community (Fournier and Philpott, 2005).

### 1.1.5.2. *Staphylococcus epidermidis*

Coagulase negative Staphylococci (CoNS), particularly *S. epidermidis*, have emerged as the predominant cause of neonatal sepsis (Dong and Speer, 2014). It is persistently present in both nosocomial and community environments and is found worldwide; it is the most commonly isolated bacteria from human skin (Kloos & Musselwhite, 1975; Otto, 2009). *S. epidermidis* is a natural coloniser of human skin and is beneficial to the host by aiding in defence and immune maturation as well as preventing colonisation of pathogenic bacteria (Otto, 2009; Dong and Speer, 2014). However, the increase in the number of implanted medical devices (catheters, pacemakers *etc.*) has led to disruption of the usually intact skin and mucosal barriers, and coupled with the use of antibiotics and immunosuppressive drugs has contributed to the switch from commensal to pathogen (Dong and Speer, 2014). Although infections are rare, they are difficult to treat, and their frequency associated with devices represents a significant public health risk. In fact, approximately 22% of bloodborne infections in the US ICU are attributed to *S. epidermidis* infection (Otto, 2009).

*Staphylococcus epidermidis* shows a high degree of genetic diversity and as of 2009 74 sequence types had been identified (Otto, 2009). Most isolates belong to clonal complex 2 and the most frequently isolated sequence type ST2. All ST2 isolates contain the biofilm *icaADBC* operon and the IS256 insertion sequences (Otto, 2009), both of which confer invasiveness to the organism and the ability to form biofilms. *Staphylococcus epidermidis* also serves as a significant reservoir of antibiotic resistance genes that can be transferred to other, more virulent bacterial species, such as *S. aureus* (Otto, 2009).

### 1.1.5.3. *Escherichia coli*

*Escherichia coli* is a ubiquitous Gram-negative bacterium that asymptomatically colonises the mammalian colon (Kaper *et al*., 2004). Infants are colonised within a few hours after birth, and the bacterium often exerts a beneficial effect upon its host, contributing to good gut health and preventing colonisation by pathogenic Enterobacteriaceae (Kaper *et al*., 2004). These colonising strains rarely cause disease except in immunocompromised individuals or when the gut barrier is breached. However, many strains are highly adapted to colonise new niches and cause a wide range of diseases through the acquisition of VFs that are encoded on mobile genetic elements known as pathogenicity islands (PAIs) that can be horizontally transferred to other strains resulting in novel combinations of virulence genes (Kaper *et al.*, 2004). These pathotypes tend to be clonal and are characterised by their O (LPS) and H (flagellar) antigens (Kaper *et al*., 2004). *Escherichia coli* is capable of colonising and causing disease in almost any intestinal and extraintestinal site. Generally, two clinical syndromes result from *E. coli* infection; enteric disease, further subdivided into enterohemorrhagic, enterotoxigenic, enteropathogenic and enteroaggregative; and extraintestinal disease (ExPEC), where certain strains colonise normally sterile body sites and cause severe disease (Vila *et al*., 2016). The most common manifestation of ExPEC is urinary tract infections (UTIs), caused by uropathogenic *E. coli* (Kaper *et al*., 2004). *Escherichia coli* is the most common cause of sepsis and UTIs among the Gram-negative bacteria. The ExPEC tend to belong within phylogenetic groups B2 and D and are distinguished genetically by certain traits associated with attachment to host tissue, nutrient acquisition, avoidance of host defence and damage to host tissue (Emody *et al*., 2003). These traits broadly promote survival within hostile host tissue (Vila *et al*., 2016). Virulence in ExPEC are encoded by a variety of PAIs, which characterise the high plasticity of ExPEC genomes, and allow for the emergence of highly virulent ExPEC (Emody *et al*., 2003).

## 1.1.6. Origins of Infection

Common origins of infection in sepsis include cases of pneumonia, intra-abdominal infections, UTIs, skin infections and soft tissue infections and infections of indwelling medical devices (Nguyen *et al*., 2006; Adhikari *et al*., 2012; Deitch, 2012; Menendez *et al.,* 2012; Vila *et al.,* 2016). Systemic Inflammatory Response Syndrome, which is a systemic response in the absence of an infection, is often caused by trauma, surgery, heat stroke, pancreatitis and burns. However, bacteria and bacterial components are believed to play a role to some extent in the development of SIRS. For example, symptoms of patients with SIRS can be exacerbated by the translocation of bacteria or bacterial components such as lipopolysaccharide (LPS) across the gut wall, thus further blurring the line between sepsis and SIRS (Becker *et al*., 2009). Indeed, LPS levels in the blood are elevated (>300pg/ml) in the plasma of approximately 70-80% of patients with advanced cases of sepsis (Alexander and Rietschel, 2001).

## 1.2. The Immune System

The human body is well equipped to resist bacterial invasion and to resolve bacterial infection, through physical, cellular, and molecular defences (Lever and Mackenzie, 2007). Classically, the human immune system is characterised by an early non-specific innate immune response followed by a later specific adaptive immune response which are intricately linked (Gallo and Nizet, 2008; Turvey and Broide, 2010). Inflammation is the collective natural response of the immune system to a foreign or dangerous stimulus that can be chemical, traumatic or infectious *(*Burdette *et al*., 2010). The normal inflammatory response involves recognition and 'marking' of the stimulus, the recruitment of leukocytes to the site of inflammation, and the initiation of phagocytosis and killing of the pathogen (Heumann and Roger, 2002). Later adaptive responses require antigen presentation and processing, followed by clonal lymphocyte amplification and production of specific T-cell derived cytokines and B cell derived antibodies that subtly modify the immune response to target distinct pathogens (Gallo and Nizet, 2008). In healthy individuals, resolution of the infection allows the individual to recover normally and maintain a state of homeostasis (Burdette *et al*., 2010).

## 1.2.1. Barriers to Infection

Physical barriers to microbial invasion involve the skin and the mucous membranes that line the gastrointestinal (GI), genitourinary and respiratory systems (Goto and Kiyono, 2012). Primarily, intact skin prevents colonisation and infection of subcutaneous tissue, and disruption of skin often results in either localised or systemic severe infections, indicating the importance of intact physiological barriers. Aside from intact skin, internal epithelial cell layers lining the airways, gut and urethra offer an additional barrier to external pathogens. These cells experience a high turnover and are equipped with membrane-bound recognition molecules that recognise pathogens, recruiting the immune system to quickly eliminate pathogens before substantial damage to vulnerable cells can be done. Tight junctions exist between the tightly packed epithelial cells that forms an impermeable barrier that not only prevents diffusion of soluble molecules but also prevents bacterial invasion between cells (Shen, 2012). In the GI tract, a thick mucus layer lining the GI tract further separates microorganisms from the epithelial cell layers and contains antimicrobial secretions that prevent colonisation by pathogenic species (Goto and Kiyono, 2012). Bacteriolytic lysozyme is also produced and secreted in tears and saliva to prevent colonisation of sensitive areas, such as the eyes and mouth (Turvey and Broide, 2010). Commensal microflora that colonise both the skin and the digestive tract also offer some measure of protection from pathogenic microorganisms (Goto and Kiyono, 2012). Colonising skin microbes, such as *S. epidermidis*, promote the production of host defence peptides (HDPs) that provide an antimicrobial protective role against pathogenic skin bacteria such as *S. aureus, S. pyogenes, H. influenzae, Pseudomonas* sp. and *Bacteroides* sp. (Chiller *et al*., 2001; Coates *et al*., 2018). Human HDPs, such as cathelicidin and β-defensin, are expressed at the surface of exposed tissues and surfaces such as the skin, GI tract, lungs and UT, and have a range of broad-spectrum antimicrobial functions including inhibiting bacterial growth and promoting wound healing (Wang, 2014).

## 1.2.2. Innate Immune System

The innate immune system is a highly evolved system of identifying and eliminating pathogens that have breached the protective barriers of the skin and mucous membranes. This system is incredibly fast in responding, as within a few minutes of pathogen recognition a protective response is generated (Turvey and Broide, 2010). It is composed of a system of molecular and cellular mechanisms through which it identifies a pathogen and coordinates a response to eliminate it (Gabay and Kushner, 1999; Heumann and Roger, 2002; Gallo and Nizet, 2008). The innate immune system is also integral in activating and coordinating the adaptive immune response (Iwasaki and Medzhitov, 2015). Pathogen recognition is achieved through the production of a limited number of evolutionary conserved receptors that are expressed on both innate immune cells and epithelial cells and recognise a limited number of pathogen-associated molecules that are shared by numerous microorganisms (Turvey and Broide, 2010; Iwasaki and Medzhitov, 2015).

## 1.2.3. Pathogen Recognition

The recognition of pathogens by the innate immune system occurs through germline-encoded pattern recognition receptors (PRRs) that are expressed on all cells involved in the inflammatory response such as monocytes/macrophages, neutrophils and dendritic cells as well as on certain epithelial cells, endothelial cells and fibroblasts (Fournier and Philpott, 2005). These PRRs are limited but highly specific for conserved molecules present in each pathogenic group, and require a stimulus originating from the pathogen, and the stimuli include both internal and external pathogenic structures and compounds (Table 1.3). Conserved pathogen associated molecular patterns (PAMPs) are responsible for the magnitude and the type of the immune response that is initiated (Figure 1.2; Degn and Thiel, 2013). Pattern recognition receptors are capable of recognising pathogens of different species and at different infective stages, for example coloniser, invading, infection and exhibit localisation to different cellular compartments (Saïd-Sadier and Ojcius, 2012). In addition to recognising PAMPs, certain PRRs recognise molecules released from stressed and dying cells that are known as damage-associated molecular patterns (DAMPs; Becker *et al*., 2009; Saïd-Sadier and Ojcius, 2012). Such DAMPs play a significant role both in sterile and infectious inflammation and include high mobility group protein b2 (HMGB1), extracellular ATP, DNA fragments, uric acid and heat shock proteins (Lotze *et al*., 2007; Kaczmarek *et al.*, 2013) .

Table 1.3. Bacterial PAMPs and their associated pathogen and PRR (Heumann and Roger, 2002; Dziarski and Gupta, 2005; Fournier and Philpott, 2005; Kawai & Akira, 2011).

| PAMP | Pathogen | PRR |
|---|---|---|
| LPS | Gram-negative bacteria | TLR4 |
| Peptidoglycan (PGN) Lipoteichoic Acid (LTA) Lipoproteins | Gram-positive bacteria Gram-negative bacteria | TLR1/2 TLR2/6 Nucleotide-binding oligomerization domain-containing protein 1 (NOD1) NOD2 NACHT leucine-rich-repeat protein 1 (NALP1) NALP3 |
| Flagellin | Flagellated bacteria | TLR5 IPAF NLR family apoptosis inhibitory protein 5 (NAIP5) |
| CpG DNA | Bacteria | TLR9 Absent in melanoma 2 (AIM2) |
| Pili | Bacteria | TLR2 |
| RNA | Bacteria | TLR7 NALP3 |

## 1.2.4. PRR Activation and Signal Transduction

The most well characterised PRRs are the Toll-like receptors (TLRs; Hoebe *et al*., 2004). These TLRs are composed of a leucine-rich repeat (LRR) extracellular domain that is involved with microbial sensing and binding and a Toll/IL-1 cytoplasmic receptor (TIR) that interacts with myeloid differentiation primary response gene 88 (MyD88; Saïd-Sadier and Ojcius, 2012). Toll-like receptor 4 is one of the most abundant TLRs expressed on the cell surface of leukocytes and epithelial cells (van Kessel *et al*., 2014). Bacterial LPS, derived from the outer membrane of Gram-negative bacteria, is closely associated with this TLR through which the lipid A portion of LPS is known to interact with and activate (Matera et al., 2012, Landsem et al., 2015). Toll-like receptor 2 recognises lipoproteins that are expressed on the cell surface of Gram-positive bacteria (Table 1.3; van Kessel *et al*., 2014). In addition to the TLRs, another group of PRRs exist

called the Nod proteins (Nod1 and Nod2): cytoplasmic PRRs that are also upstream activators of cytokine transcription and recognise Gram-positive bacteria (Dziarski and Gupta, 2005).

The signalling cascade triggered by TLR interactions with bacterial PAMPs is mediated by different signalling pathways and molecules. Lipopolysaccharide activation of TLR4 is well described and the molecule is comprised of extra- and intracellular toll-like receptor domains and the externally bound CD14 and myeloid differentiation protein 2 (MD-2). CD14 recognises and binds to LPS and exists in both a soluble (sCD14) and membrane-bound (mCD14) form (Wiersinga *et al*., 2008; Landsem *et al*., 2015). The amount of sCD14 increases rapidly immediately after activation of monocytic cells, as the mCD14 is shed in its scavenging form (Wiersinga *et al*., 2008). Professional phagocytes (monocytes, tissue macrophages and neutrophils) all show high expression of mCD14 (Alexander and Rietschel, 2001). MD-2 is the link between extracellular CD14-LPS binding and internal TLR signalling (Landsem *et al*., 2015). Similarly, the scavenger receptor CD36 is closely associated with TLR2, and thus recognises lipoteichoic acids (LTA) and peptidoglycan (PGN) from Gram-positive bacteria (Hoebe et al., 2004, Surbatovic et al., 2015). In general, four intracellular adaptor proteins convey the signal from the TLR to the nucleus. These are MyD88, MyD88 adaptor-like (MAL), toll receptor-associated activator of interferon (Trif), and toll receptor-associated molecule (TRAM). The majority of TLRs activate the MyD88-dependent pathway, which culminates in the activation of mitogen-activated protein (MAP) kinases and the transcription factor nuclear factor (NF) -kB (Hoebe *et al*., 2004). Nuclear factor-κB promotes expression of the initial cytokines tumour necrosis factor-alpha (TNF-α), interleukin-1β (IL-1β) and IL-18, the latter two of which are synthesised in their inactive pro-forms (Arango Duque & Descoteaux, 2014; Evavold and Kagan, 2019). Activation of these cytokines is initiated by the inflammasome, a macromolecular platform that recruits and activates inflammatory caspases, such as caspase-1 (Evavold and Kagan, 2019). Once activated caspase-1 is responsible for the cleavage of the inactive portion of IL-1β and IL-18 and the production of their active forms (Gasteiger *et al*., 2017).

### 1.2.5. Soluble Response

### 1.2.5.1. Cytokine Response

Much of the inflammatory response of the host is directed by the secretion profiles of cytokines, small intercellular signalling proteins that are produced upon activation by immune and epithelial cells (Gabay and Kushner, 1999; Arango Duque and Descoteaux, 2014). Cytokines exhibit functional redundancy; different cytokines often have similar functions, and they are pleiotropic in that they influence a diverse range of cell types. Each cytokine binds to a specific cell surface receptor on a target cell that generates a signalling cascade to influence cell function. Cytokines are primarily produced by macrophages and lymphocytes *in vivo*, but are also produced by neutrophils, epithelial cells and adipocytes (Arango Duque and Descoteaux, 2014). The earliest cytokines to be induced by NF-kB binding are TNF-α, IL-1β, IL-6 and IL-18 (Figure 1.1; Gruys *et al*., 2005; Arango Duque and Descoteaux, 2014). These cytokines are released in large quantities within 1 hour of pathogen detection by cells such as monocytes macrophages and endothelial cells, and are largely responsible for stimulating the acute phase response (APR) in the liver, which is composed of a number of proteins known as the acute phase proteins (APPs; section 1.2.5.2; Burdette *et al*., 2010). Additional functions of these early cytokines include inducing vasodilation and increasing vascular permeability (TNF-α, IL-1β), promoting expression of neutrophil-attracting chemokines (TNF-α, IL-1β), inducing fever (TNF-α, IL-1β, IL-6), promoting the differentiation of adaptive immune cells (IL-1β, IL-6, IL-18), mediating apoptosis (IL-6) and stimulating IFN-γ production (IL-18; Figure 1.1; Arango Duque and Descoteaux, 2014).

In addition to the secretion of pro-inflammatory cytokines, the innate immune system is also characterised by the late production of anti-inflammatory cytokines including IL-4, IL-10, IL-13, transforming growth factor β (TGF-β) and IL-1ra by activated macrophages, B cells and T cells (Arango Duque and Descoteaux, 2014; Hamers *et al*., 2015). Anti-inflammatory cytokines suppress the activities of pro-inflammatory cytokines such as TNF-α, IL-6, IL-1β and IL-8, suppress macrophage activation and antigen presentation, inhibit IFN-γ production, induce IgG secretion by B cells and promote the function of T regulatory cells (Tregs; Fournier and Philpott, 2005; Arango Duque and Descoteaux, 2014).

### 1.2.5.2. Acute Phase Response

The APR is essential for many immunological processes, including phagocytosis, clearance of pathogens, promotion of proinflammatory cytokines and host survival (Strnad *et al.,* 2016). It is characterised by a distinguished pattern of protein synthesis in the liver that results in either a large increase (positive) or decrease (negative) in certain APPs in the plasma. One well-researched APP is C-reactive protein (CRP) that is important in the activation of the classical complement pathway and therefore the induction of phagocytosis, as well as binding to phosphocholine present on the surface of many bacteria (Black *et al.*, 2004). In addition to pro-inflammatory cytokines, also induced are lipid-derived mediators, such as platelet-activating factor (PAF) and leukotrienes, and reactive oxygen species (ROS), such as the superoxide anion ($O_2^-$), hydroxyl radicals ($^\cdot OH$) and reactive nitrogen species (RNS) such as nitric oxide (NO; Alexander and Rietschel, 2001). All of these pro-inflammatory molecules function either directly on tissue or pathogens or via secondary mediators to activate further pathways including the coagulation and complement cascade (Burdette *et al.*, 2010). Other important APPs include haptoglobin, which accelerates the clearance of free haemoglobin, limiting its availability to bacteria, and serum amyloid A (SAA), which functions both as a transporting mediator for cholesterol and as a bacterial opsonin, behaving in a similar manner to CRP (Shah *et al.,* 2006; Wobeto *et al.,* 2008).

### 1.2.5.3. Chemokine Response

Chemokines are also secreted in conjunction with cytokines and are a specific group of proteins that serve to coordinate cellular migration in a process known as chemotaxis, in which the direction of a cell's movement is determined by an extracellular chemical gradient. Chemokines bind to G-protein coupled receptors (GPCRs) which in turn activate intracellular signalling pathways to promote chemotaxis and migration to inflammatory tissues (Jin *et al.*, 2008). In addition to this, chemokines promote interactions between immune effector cells, linking innate and adaptive immunity (Sokol and Luster, 2015). Important chemokines include CXCL1/CXCL2, also known as the macrophage inflammatory proteins (MIPs), and CXCL8-11 (Arango Duque and Descoteaux, 2014). A list of cytokines and chemokines secreted by monocytes in response to TLR engagement are outlined in Figure 1.1.

### 1.2.5.4. Complement System

The complement system is an essential player in driving chemotaxis, plasma protein oxidation and opsonisation of pathogens and damaged cells, resulting in their engulfment and destruction by professional phagocytes (Gabay and Kushner, 1999). Three pathways are currently defined: classical, alternative and lectin (Black *et al*., 2004), that are activated by immunoglobulin (Ig) complexes, foreign carbohydrates/lipids/proteins, and mannose-binding lectin, respectively (Sarma and Ward, 2011). The central proteins involved in the classical pathway are C1-9, which exist as inactive zymogens that are subsequently cleaved and activated during inflammation, with all pathways converging at C3 (Black et al., 2004; Sarma and Ward, 2011). Initial stages involve cleavage of the C3 and C4 proteins (opsonins), that bind to and coat the pathogen/dead tissue, and the later stages involve the proteins C5-C9 which are highly inflammatory and lead to further chemotaxis and formation of the membrane attack complex (MAC; Black *et al*., 2004). The MAC functions by forming pores in bacterial cell walls and directly inducing lysis of Gram-negative bacteria. Both the lectin and alternative pathways involve the deposition of C3b/C3bi on the bacteria which is then recognised by receptors on neutrophils, leading to the uptake of the pathogen (van Kessel *et al*., 2014).

## 1.2.6. Phagocytes and Monocytes

Derived from the haematopoietic system, these phagocytic cells are principally involved in eliminating pathogens, and include neutrophils, monocytes, macrophages, basophils and eosinophils (Gasteiger *et al*., 2017). Neutrophils are the predominant immune cell type in human blood, making up to 50-60% of all circulating leukocytes (white blood cells; Tecchio *et al*., 2014; van Kessel *et al*., 2014). They quickly respond to early cytokines and chemokines secreted by macrophages and epithelial cells, rapidly migrating to the site of inflammation. Migration of neutrophils is facilitated by the expression of selectins and integrins on the cell surface of vascular endothelium, which tethers the neutrophils to the surface and facilitate a 'rolling' effect, whereby neutrophils roll along the endothelium until binding of chemokines allows for transcytosis of the neutrophils across the endothelial barrier and into the inflamed tissue (Sokol and Luster, 2015).

Neutrophil phagocytosis killing involves the production of proteins directly related to pathogen elimination such as proteases, cytokines, chemokines and reactive species (Li and Tablin, 2018). Phagocytosis is a rapid process, with a single neutrophil internalising up to 50 bacteria in as little as three minutes. After uptake, bacteria reside within an intracellular compartment known as a phagosome. Within this compartment, the pathogen is destroyed via the generation of ROS and RNS, coupled with the release of toxic proteins such as proteases and antimicrobial peptides (van Kessel *et al*., 2014). Once the pathogen has been destroyed, the neutrophil is consumed via the formation of neutrophil extracellular traps (NETs), fibres composed of extracellular chromatin coupled with histones and granular proteins (van Kessel *et al*., 2014; Li and Tablin, 2018). These NETs possess potent antimicrobial activities via the presence of granular proteins, such as calprotectin (Urban *et al.,* 2009). Cell death is inevitable in neutrophils undergoing a unique form of apoptosis known as NETosis (Li and Tablin, 2018).

Neutrophils are also fast responders to activation and have a relatively short half-life in peripheral blood, perishing less than 7 hours after they first enter the circulation (van Kessel *et al*., 2014). They are also responsible for some level of cytokine and chemokine production during inflammation. Cytokine production is triggered by engagement of G protein-coupled, FCγ and complement receptors, and of TLRs. Neutrophils express all TLRs with the exception of TLR3 and TLR7, and produce chemokines that are primarily chemotactic for other neutrophils, as well as for monocytes, dendritic cells (DCs), natural

killer (NK) cells and T helper (Th) cells, enhancing their own migration to inflamed tissue as well as recruiting other inflammatory cells (Tecchio *et al.*, 2014).

Monocytes are the precursors for tissue macrophages. The average half-life of a circulating monocyte in healthy adults is approximately 70 hours (~3 days), and monocytes constitute 1-6% of the total circulating leukocyte pool (Arango Duque and Descoteaux, 2014). Three subsets circulate the body and are divided based on their expression of CD14 and CD16 (FcγRIII immunoglobulin receptor); classical ($CD14^{++}CD16^{-}$), intermediate ($CD14^{+}CD16^{+}$) and non-classical ($CD14^{+}CD16^{++}$; Kratofil *et al.*, 2017). Once monocytes are activated by PAMPs or chemokines, they rapidly leave the blood and migrate into inflamed tissue, thus differentiating into tissue macrophages (Gasteiger *et al.*, 2017; Kratofil *et al.*, 2017). Once differentiated, the principal purpose of tissue macrophages is to continuously monitor the tissue they colonise, and, when necessary, ingest pathogens and produce the inflammatory cytokines necessary to mount an efficient immune response to maintain homeostasis (Figure 1.1; Gasteiger *et al.*, 2017). Tissue macrophages are approximately 5-10 times bigger than their monocyte progenitors, and they possess significantly more organelles, as well as being more complex (Arango Duque and Descoteaux, 2014). They are ubiquitous in the body, and the average human has 0.2 trillion macrophages that inhabit almost every tissue compartment. Macrophages are broadly divided into two subgroups: M1 (classically activated) macrophages that are activated by Th1 cytokines and PAMPs, whereas M2 (alternatively activated) macrophages are activated by Th2 cytokines. M1 macrophages are the primary macrophage type involved with bacterial defence (Gasteiger *et al.*, 2017).

| Cytokine/Chemokine | Effects |
|---|---|
| TNF-α | Upregulation of APPs, suppression of appetite, fever, vasodilation, increased vascular permeability, neutrophil migration |
| IL-1 (α/β) | Upregulation of APPs, fever, prostaglandin production, histamine release, increased vascular permeability, chemoattraction, CD4+ T cell expansion and differentiation, upregulation of cell adhesion molecules |
| IL-6 | Differentiation of B cells, activation of CD8+ T cells, fever, upregulation of APPs, recruitment of monocytes, maintenance of Th17 cells, inhibition of T cell apoptosis and T-reg development |
| IL-12 | Stimulates Th1 cells, promotes IFN-γ production, promotes cytotoxicity, activates T and NK cells, attenuates fever |
| IL-18 | Induces IFN-γ and IL-17 production, activates T cells, augments IL-10 release |
| IL-23 | Induces IFN-γ and IL-17 synthesis, augments IL-10 release, activates T cells |
| IL-27 | Differentiation of naïve T cells to Th1 cells, induces IFN-γ production, inhibits differentiation of Th17 cells |
| IL-10 | Suppresses macrophage activation, suppresses production of pro-inflammatory cytokines and IFN-γ, suppresses MHC-II expression, induces IgG synthesis |
| TGF-β | Suppresses production of pro-inflammatory cytokines, promotes maintenance and function of T-regs |
| MIP-1/3α | Neutrophil chemotaxis |
| CCL5 | Chemoattraction, activation of NK cells |
| CXCL8/9/10/11 | Chemoattraction, induces degranulation in neutrophils |

Figure 1.1. List of cytokines and chemokines secreted by monocytes upon engagement of TLRs by PAMPs. Cytokines/chemokines highlighted in blue are proteins that are also secreted by neutrophils (Arango Duque and Descoteaux, 2014; Tecchio *et al*., 2014).

## 1.3. Adaptive Immune System

The adaptive immune system is so called due to its ability to adapt antigen exposure into antigen recognition, and it possesses an extremely diverse collection of receptors known as antibodies that recognise specific pathogenic antigens (Iwasaki and Medzhitov, 2015). This diversity and specificity allows the adaptive immune system to recognise any antigen, covering a large and robust coverage of all infectious diseases (Iwasaki and Medzhitov, 2015). Certain PRRs expressed on the surface of B and T lymphocytes determine the origin of the antigen (e.g. intracellular bacteria, fungal pathogen) and instruct the cell to induce the appropriate effector response (Iwasaki and Medzhitov, 2015).

Dendritic cells are professional antigen presenting cells (APCs) that link innate and adaptive immunity. They reside in tissues and continuously sample antigens prior to migrating to lymph nodes for presentation to T cells (Kaiko *et al*., 2008). They continuously express antigens on an MHC class II receptor, which facilitates activation of naïve T cells. Immature DCs take up antigens and rapidly degrade them into antigenic peptides that are able to bind MHC II, a process which facilitates their maturation (Lipscomb and Masten, 2002). Once matured, DCs migrate to lymphoid organs and activate naïve T cells with specific antigens and polarising factors that determine the T cell phenotype (Kaiko *et al*., 2008).

Naïve T cells naturally circulate in the blood of healthy individuals until they are activated by processed peptide bound on a class II MHC molecule on the surface of an APC via the T cell receptor (TCR). Upon activation, T cells begin to rapidly divide and differentiate into a variety of effector cells, which takes place several days after recognition of a pathogen. These differentiated cells are broadly divided into two subgroups: CD4+ T helper cells (Th cells) and CD8+ cytotoxic T cells (Tc cells). T helper cells are further divided into at least four subgroups: Th1, Th2, Th17 and Treg cells, all with very different phenotypes (Kaiko *et al*., 2008). The phenotype of these cells can be seen in Table 1.4. The differentiation of Th cells is characterised by four defined stages; activation of specific cytokine groups, commitment to a certain phenotype, suppression of cytokines not associated with the committed phenotype, and augmentation and stabilisation of the chosen phenotype (Kaiko *et al*., 2008).

Table 1.4. Phenotypical characteristics and cytokine secretion of Th cell subtypes (Kaiko *et al.*, 2008).

| T helper Cell | Cytokines secreted | Phenotype |
|---|---|---|
| Th1 | IFN-γ<br>TNF-β | Protection against intracellular infections<br>Mediate cellular responses |
| Th2 | IL-4<br>IL-5<br>IL-10<br>IL-13 | Enhance antibody production<br>Target parasitic organisms<br>Mediate humoral responses |
| Th17 | IL-17<br>IL-17F<br>IL-6<br>IL-22<br>TNF-α | Protection against extracellular bacteria |
| Treg | IL-10<br>TGF-β | Suppression of Th1 activity |

Cytotoxic CD8+ T cells are characterised by their potent ability to eliminate infected cells and produce high amounts of certain inflammatory mediators, such as granzyme B, which initiates apoptosis, proinflammatory cytokines such as IFN-γ and TNF-α, and anti-inflammatory cytokines, such as IL-10, to prevent excessive tissue injury (Zhang and Bevan, 2011; Halle *et al.*, 2017). Upon activation by IL-12, naïve CD8+ T cells undergo clonal expansion similar to all lymphocytes and can undergo up to 19 divisions within a week of pathogen recognition (500,000-fold expansion). Activation is characterised by a switch in metabolic patterns, as energy production is changed from oxidative phosphorylation to aerobic glycolysis. Cytotoxic CD8+ cells then migrate to infected tissue and facilitate the elimination of infected cells (Zhang and Bevan, 2011).

B-lymphocytes are a population of leukocytes that express clonally diverse Ig receptors that recognise specific unprocessed antigens. Terminally differentiated B cells are capable of recognising a distinct antigenic stimulus, and as a result deliver a robust pool of antibodies to target the originator of the particular stimulus. Specificity in B cell antigens is achieved via functional rearrangements of the Ig loci and various gene segments via selective expression. This process takes place when the B cells are resting in the adult bone marrow, and ultimately give rise to the B cell receptor (BCR). Clonal

expansion of these matured cells give rise to the population that targets the cause of the inflammation. B cells also promote T cell activity via processing of the antigen and presentation of the antigen by the BCR to unstimulated T cells (Kaiko *et al.*, 2008). Immunoglobulin G is the main antibody that is secreted by memory B cells and dominates adaptive immune responses. It binds to antigens via the Fab domain, while the Fc domain binds to Fcγ receptors on the surface of immune cells, and signals via these receptors to modulate adaptive responses, enhance T cell activity and select for high affinity B cells (Bournazos *et al.*, 2017).

## 1.4. The Host Response in Bacterial Sepsis

Resolution of a bacterial infection is crucial to prevent chronic infection and the development of sepsis. Under normal circumstances, the immune response can resolve an infection without it becoming detrimental to the host. However, in cases of blood borne bacterial disease, a systemic and dysregulated inflammatory response develops to the detriment of the host, which can have long-lasting, devastating effects (Figure 1.2; Cohen, 2002; Bosmann and Ward, 2013; Conway Morris *et al.,* 2018). This hyperactivity is uncontrollable while the infectious stimulus is still present, resulting in sepsis pathology directed by the immune system (Qureshi and Rajah, 2008). The symptoms and the pathology of sepsis is extremely variable and is governed by a combination of both host and bacterial factors (Lever and Mackenzie, 2007). The vast majority of these pathological interactions occurs at the vascular endothelium, resulting in the characteristic damage of sepsis such as tissue ischemia, hypoxia and organ failure (Nguyen *et al.*, 2006). The decline in organ function during sepsis dominates much of the pathology, and the pathways leading to this damage are not fully understood (Cohen, 2002). Both a hyperinflammatory and the dysfunctional counter-inflammatory response are considered to be important in the immunopathology of sepsis (Cohen, 2002). The vast majority of septic patients tend to succumb at later time points that are associated with an immunosuppressive state known as immunoparalysis (Rittirsch *et al.*, 2008). Subsequently, over-production of pro-inflammatory cytokines contributes significantly to the development of pathology, creating a unique condition where the patient experiences both pro-inflammatory and dysfunctional anti-inflammatory states, often at the same time (Fournier and Philpott, 2005; Degn and Thiel, 2013). This excessive response results in severe immunopathology, which exacerbates pathogen-induced pathology as they remain within the bloodstream (Iwasaki and Medzhitov, 2015). The

various immunopathological pathways involved in the development of severe sepsis are shown in Figure 1.2.
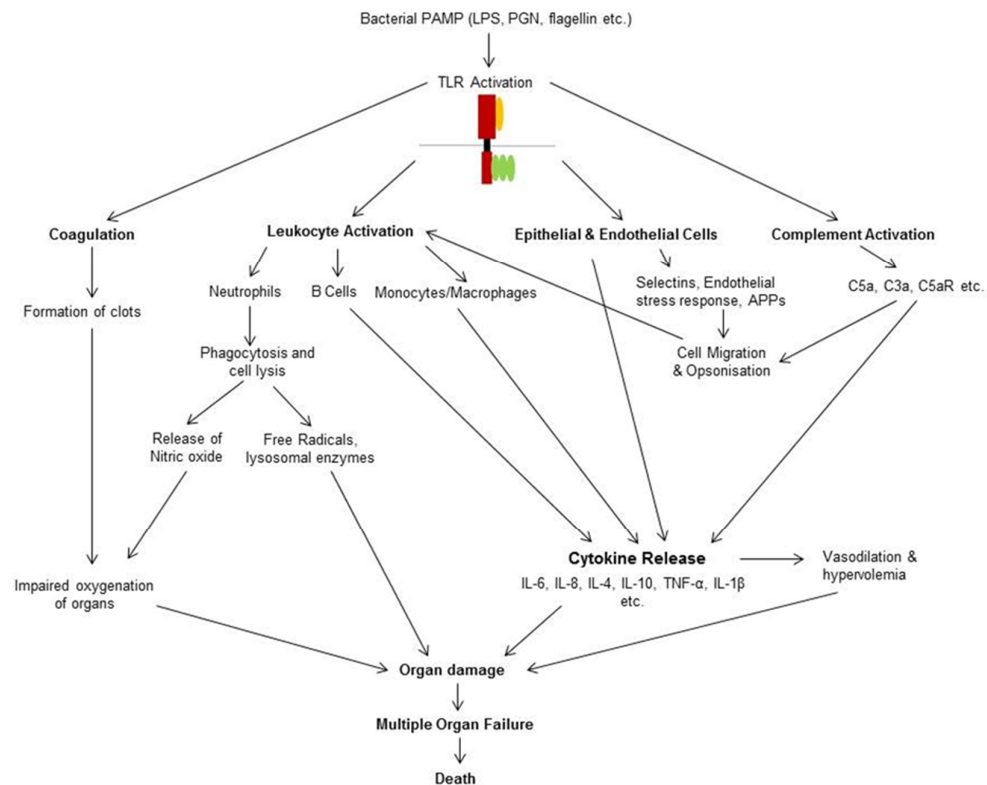


Figure 1.2. The basic pathway of immune activation and pathogenic processes during sepsis (adapted from Cohen, 2002; Rittirsch *et al*., 2008; Reinhart *et al*., 2012).

### 1.4.1. Cytokine Responses in Sepsis

Cytokines induced during a normal acute inflammatory response are key mediators of sepsis immunopathology. A characteristic profile of cytokine changes is evident in modern sepsis and septic shock (Figure 1.2). Initially, the presence of high concentrations of cytokines in the blood (cytokine storm) is later accompanied by a compensatory response of anti-inflammatory cytokines. This pattern of cytokine expression at the later stages of sepsis is associated with poor patient outcomes, and the immune response subsequently becomes severely downregulated, a phenomenon known as immunoparalysis (Brown *et al.*, 2006). Interestingly, there is evidence that immunoparalytic mechanisms are evident from the very start of sepsis (Hamers *et al.*, 2015).

Both mCD14 and sCD14, key recognition molecules in cases of Gram-negative bacteraemia, are found in elevated concentrations in the blood of septic patients. A high

circulating concentration of sCD14 has been found to be associated with a negative outcome during sepsis, and sCD14 that has been neutralised by blocking antibodies protected primates from sepsis mortality (Cohen, 2002; Chalupa *et al.*, 2011). Many early cytokines, such as TNF, have been found to remain at significantly high concentrations in septic patients even weeks after the initial acute response was initiated and these significantly high levels have been found to be associated with a negative outcome for patients (Cohen, 2002). Macrophage inhibitory factor (MIF), unlike most cytokines, is constitutively expressed by leukocytes and stored intracellularly. It normally promotes both innate and adaptive processes, but during sepsis it is detrimental in that it prevents anti-inflammatory apoptosis of monocytes, which promotes excessive inflammation (Rittirsch *et al.*, 2008).

## 1.4.2. Complement Dysfunction

Another molecular system involved in promoting excessive inflammation during sepsis is the complement system. Complement component 5a is activated very early on during sepsis, and at high concentrations it is particularly harmful. As well as causing direct harm, C5a is able to negatively influence other inflammatory processes such as coagulation, TLR4 responses, phagocytosis, oxidative burst and cytokine production (Rittirsch *et al.*, 2008; Ward, 2010; Bosmann and Ward, 2013). Thus, C5a broadly contributes to immunoparalysis at later stages of sepsis, multiple organ failure and dysfunction in coagulation (Rittirsch *et al.*, 2008). A sustained high concentration of C5a during sepsis is linked with poor outcome and survival (Rittirsch *et al.*, 2008).

## 1.4.3. Coagulation, Platelets and Endothelial Cells

Cytokines such as IL-1 and IL-6 promote a procoagulant effect, and coagulation disorders are very common in sepsis patients. Approximately 30-50% of sepsis patients have been found to have the most severe form, disseminated intravascular coagulation (DIC; Cohen, 2002). Central to coagulation processes are the platelets, anucleated cells that are found abundantly in blood. Early in sepsis, platelets experience an increase in activation coupled with a decrease in the circulating numbers of cells, a process which is facilitated by bacterial interactions promoting aggregation with other immune cells (Assinger *et al.,* 2019). The cytokine tissue factor (TF) is responsible for activating the proteolytic cascades that result in conversion of prothrombin to thrombin, and then the conversion of fibrinogen to fibrin (Cohen, 2002). Normally, regulatory mechanisms, such as fibrin breakdown by plasmin (precursor plasminogen), prevents excessive coagulation, but this

regulation becomes impaired during sepsis due to high levels of plasminogen-activator inhibitor type 1 (PAI1). The result of this and the decrease in circulating platelets is enhanced production and subsequent decreased removal of fibrin, which results in deposition of fibrin clots in blood vessels and subsequently microvascular occlusion, or DIC, which in turn leads to insufficient tissue perfusion and ultimately organ damage (Cohen, 2002; Assinger *et al.,* 2019).

### 1.4.4. Neutrophil Dysfunction in Sepsis

Early during sepsis pathogenesis it is clear that neutrophil maturation is significantly affected which later impairs their phagocytic functions (Monneret and Venet, 2016). Neutrophils are the predominant infiltrates present in tissues that later experience damage and failure, and these cells damage tissue directly by releasing lysosomal enzymes and reactive species (Cohen, 2002). These factors directly contribute to the formation of abscesses and subsequent organ dysfunction during sepsis (Brown *et al*., 2006). Production of NO is upregulated by the increased synthesis of inducible NO synthase, a key neutrophil enzyme whose synthesis is promoted by TNF-α activity. Levels of this cytokine are severely elevated during sepsis, and increased production of NO directly leads to vascular damage and myocardial depression. Imbalances in redox within phagocytes leads to an intracellular oxidant state, which is associated with reduced antioxidant levels and increased ROS and RNS generation. Reactive radicals, such as OH and NO, react with a wide range of targets to ultimately alter intracellular biochemistry, which can lead to DNA fragmentation that causes damage to cells and organs. Further, build-up of reactive species results in a nuclear decrease of the peroxisome proliferator activated receptors (PPARs) that suppress the expression of proinflammatory cytokines (Bosmann and Ward, 2013). Excessive NET formation by neutrophils during sepsis due to uncontrolled inflammation leads to the development of organ damage and dysfunction (Li and Tablin, 2018). Neutrophils also undergo immunoparalysis during severe sepsis, which broadly involves a decline in intracellular signalling and dysfunction of the adaptive immune system (Rittirsch *et al*., 2008).

## 1.4.5. Resolution of Inflammation

Poor co-ordination to resolve inflammation plays a number of significant roles in the immunopathology of sepsis. Lymphocyte apoptosis is a common occurrence in sepsis, with the majority of sepsis patients being lymphopenic (abnormally low plasma lymphocytes; Cohen, 2002). Another facet of this downregulation is the selective depletion of B and CD4+ lymphocytes, as well as T cell hyporesponsiveness (Cohen, 2002). This decrease in circulating lymphocytes is also coupled with impaired antigen presentation (Brown *et al*., 2006; Bosmann and Ward, 2013). The initial Th1 cell response that characterises acute inflammation ultimately switches to a Th2 cell response, which diverts the immune system from resolving an infection to promoting harmful processes (Rittirsch *et al*., 2008). This ultimately results in a severe state of immunosuppression that is characteristic of sepsis (Cohen, 2002).

Apoptosis and clearance of professional phagocytes during a normal inflammatory response ultimately leads to the downregulation of the immune response and the resolution of an infection (Cao *et al.,* 2019). However, in patients with sepsis, loss of professional phagocytes leads to a reduced defence against the pathogen in the bloodstream (Umlauf *et al*., 2013). Apoptosis in adaptive immune cells such as lymphocytes and DCs further contributes to the development of immunoparalysis. In septic patients, the majority of circulating monocytes and tissue macrophages experience cell death due to phagocytosis-induced apoptosis/pyroptosis and loss of function (Umlauf *et al*., 2013). This coupled with depletion and dysfunction of DCs, results in impaired antigen presentation and subsequent down-regulation of the adaptive immune response (Bosmann and Ward, 2013).

## 1.5. Biomarkers in sepsis

A physician treating a patient with unconfirmed sepsis must first decide if a patient has sepsis or SIRS (i.e. if an infection is present) and whether or not antibiotics are required to resolve the bacteraemia (Póvoa, 2002). Traditionally, bacteraemia has been identified through positive blood culture, which usually takes 24-48 hours (Jin and Khan, 2010), a lengthy process susceptible to contamination, and there is a direct correlation between time taken to treat and patient mortality (Jin *et al.*, 2008; Seymour *et al.,* 2017). In addition, this process often produces many false positive and negative results, with up to half of all patients with a suspected bacteraemia having no definitive proof of infection (Becker *et al.*, 2008; Jin and Khan, 2010). The terms culture-negative and culture-positive sepsis are often used to describe patients with suspected or confirmed bacteraemia respectively (Becker *et al.*, 2009). Increasingly, there is a high demand for accurate patient biomarkers that allow for differentiation between infected and non-infected (SIRS) patients (Póvoa, 2002). Current biomarkers have advantages and limitations.

## 1.5.1. C-reactive Protein (CRP)

C reactive protein is a well-established biomarker and is often used to test for inflammatory disorders (Póvoa, 2002). Upon immune stimulation, CRP is produced by hepatocytes in response to IL-6 (Pepys and Hirschfield, 2003). During bacterial infections, CRP binds to prokaryotic phosphocholine on the cell surface of invading bacteria, which in turn leads to the activation of the complement pathway, facilitating phagocytosis (Póvoa, 2002). Other CRP functions include preventing neutrophil adhesion to endothelial cells, inhibiting generation of superoxides and initiating synthesis of the IL-1 receptor agonist (Gabay and Kushner, 1999).

Monitoring levels of CRP in patients with inflammatory disorders are especially useful in disease management (Pepys and Hirschfield, 2003). In healthy people, the baseline level of CRP is 0.8mg/ml and following immune stimulation can increase to more than 500mg/ml (Pepys and Hirschfield, 2003). Increases can be seen as early as 6 hours after stimulation, and peaks at around 48 hours, representing a useful tool for monitoring acute inflammation in many different diseases (Pepys and Hirschfield, 2003). In general, CRP concentration is higher in bacterial infections than in viral or fungal infections, but this rule is not absolute (Póvoa, 2002; Chan and Gu, 2011). Non-infectious causes of SIRS, such as trauma and heat stroke, can also lead to elevated concentrations of CRP, making it a relatively non-specific marker of inflammation (Póvoa, 2002). Furthermore, there is

no correlation between CRP levels and infection, as CRP is a very sensitive marker of inflammation, but not a very specific marker (Vincent, 2016).

### 1.5.2. Procalcitonin

Procalcitonin (PCT) is considered to be the gold standard in sepsis diagnosis (Matwiyoff *et al.*, 2012). It is a 116 amino acid peptide with a molecular weight of 14.5 kDa, produced in liver and kidney tissue, but all tissues show increased PCT expression in response to an infection stimulus, including peripheral blood mononuclear cells (PBMCs; Jin and Khan, 2010; Matwiyoff *et al.*, 2012). Procalcitonin is a precursor of the protein calcitonin, and in healthy people it is not normally found in circulating blood (Maruna *et al.*, 2000; Hentschel *et al.*, 2014). It has a relatively short half-life in the blood, approximately 25-30 hours and a low concentration in non-sepsis patients (<10ng/ml), making it a useful means of monitoring patient status in the ICU (Jin and Khan, 2010; Hentschel *et al.*, 2014). In addition, PCT levels often increase 2-4 hours after stimulation, peaking at 6-8 hours, making it a useful early diagnostic marker (Chan and Gu, 2011), with levels of PCT rising up to 1000µg/ml in severe bacterial infections (Maruna *et al.*, 2000). These levels generally persist until the inflammatory event ends (Becker *et al.*, 2008). Procalcitonin is an immunomodulatory molecule, regulating calcium concentration in the blood, and plays a significant role in phagocytosis and inflammation (Jin and Khan, 2010; Matwiyoff *et al.*, 2012). Other functions of PCT during infection involve modulating cytokine and NO synthesis, analgesia, and neutralising bacterial LPS (Maruna *et al.*, 2000; Matera *et al.*, 2012). High levels of PCT in patients with inflammatory conditions is detrimental, and further correlate with high levels of pro-inflammatory cytokines (Matwiyoff *et al.*, 2012).

In its current clinical use, PCT has been used to rule out bacteraemia with more than 95% accuracy and is considered a marker exclusive to bacteraemia (Jin and Khan, 2010; Schuetz *et al.*, 2011; Matwiyoff *et al.*, 2012). In addition, PCT is virtually absent in healthy people, as it remains intracellular before being converted to the mature calcitonin protein in blood. In the ICU, PCT levels are measured using the BRAHMS assay, a chemiluminescence assay that uses monoclonal antibodies to detect PCT in serum (Jin and Khan, 2010). Gram-negative bacteria, and to a lesser degree Gram-positive bacteria, induce the highest levels of PCT detected in the blood (Matwiyoff *et al.*, 2012). In addition to PCT's use as a 'rule-in, rule-out' biomarker, blood PCT levels are known to strongly correlate with the severity of a septic episode and bacterial load, allowing for

PCT to be used as a marker of disease outcome and to monitor antibiotic therapy (Charles *et al.*, 2009; Schuetz *et al.*, 2011; Matwiyoff *et al.*, 2012). A decrease in PCT blood concentrations in septic patients is generally considered as a favourable sign (Becker *et al.*, 2009), suggesting recovery.

Despite the numerous benefits of using PCT as a diagnostic tool, there are still some drawbacks to its use with some researchers suggesting that PCT is incapable of distinguishing between Gram-positive and Gram-negative sepsis, and therefore does not inform empirical antibiotic therapy (Chan and Gu, 2011). In addition, antibiotic therapy has been shown to interfere with PCT kinetics; while this can be useful to inform the efficacy of the treatment, it can also be detrimental, if antibiotic therapy has been started before PCT levels were determined, as it is then difficult to monitor the effects of the antibiotic (Charles *et al.*, 2009). Conversely, some studies have failed to find a link between PCT levels and antibiotic therapy (Charles *et al.*, 2009). Despite PCT being regarded as specific to bacterial sepsis, many studies have found that it is elevated in the blood of patients suffering from lung injury (Nylén *et al.*, 1996), severe burns (von Heimburg *et al.*, 1998), pancreatitis (Ammori *et al.*, 2003), heat stroke (Nylen *et al.*, 1997), trauma (Maier *et al.*, 2009) and surgery (Meisner *et al.*, 1998), challenging its use in infection. Assays used to determine levels of PCT in septic patients may differ in their sensitivity and specificity, depending on the assay used and the clinic it is performed at, and different clinics may use different definitions of disease and disease parameters (Schuetz *et al.*, 2011), making its use as a biomarker difficult at present due to these variations and suggests that there needs to be a standardisation of methodology for PCT.

### 1.5.3. Cellular Biomarkers

Leukocytes undergo significant changes during sepsis and represent a rich source of biomarker information that can be used to monitor patient condition and assess the efficacy of antibiotic treatment. To date many cells are already used as markers for patient condition, including neutrophils, which are considered very sensitive markers of both bacterial infection and whole blood counts (Chalupa *et al.*, 2011). A neutrophil count that is higher, lower, or contains more than 10% immature cells are all considered markers of sepsis and other inflammatory conditions (Brown *et al.*, 2006). The erythrocyte sedimentation rate (ESR) is used in many hospitals as a non-specific marker of disease activity, particularly of the APR (Gruys *et al.*, 2005). The ESR is influenced by increases in plasma viscosity initiated by changes in total blood fibrinogen concentration and

reflects the activity of the APR as fibrinogen is a slow reacting APP, and increased activity reflects increased sedimentation (Gruys *et al*., 2005). Immature granulocyte counts and neutrophil phagocytic indexes including measuring NETosis via cell free DNA (cfDNA) have all recently found to be significant predictors of sepsis in burn patients (Hampson *et al*., 2017).

### 1.5.4. Pathogen-associated Biomarkers

Recent efforts in sepsis diagnosis have focused on the ability to detect carbohydrate amphiphilic PAMPs in the whole blood of patients with infection-related diseases. Detection of PAMPs such as LPS and PGN has been hampered in the past by natural molecular reactions between the hydrophobic lipid moieties of PAMPs and the core lipid structure of lipoproteins such as high-density lipoprotein (HDL) and low-density lipoprotein (LDL), which sequester the biomarkers and prevent their detection using traditional methods (Kupicek-Sutherland *et al.,* 2019). These interactions however can be exploited using two novel assays; membrane insertion and lipoprotein capture. Membrane insertion uses the interactions between PAMPs and lipoproteins by utilising a lipid bilayer to directly capture the biomarker and measure using a dye-conjugated biomarker; this method has been previously validated with *E. coli* LPS and lipoarabinomannan from *Mycobacterium tuberculosis.* Lipoprotein capture uses a specific antibody to anchor host lipid-PAMP complexes to a biosensor surface, which is then detected using a dye-conjugated antibody for the target (Kupicek-Sutherland *et al.,* 2019). Both these methods demonstrate a sensitive and specific means of detecting PAMPs in whole blood with minimal contamination and show considerable promise for clinical diagnosis and pathogen identification.

Another approach that specifically targets PAMPs uses a modified enzyme-linked immunosorbent assay (ELISA) known as the enzyme-linked lectin-sorbent assay (ELLecSA) that exploits the natural affinity that mannose-binding lectin (MBL) has for PAMPs such as LPS and LTA (Cartwright *et al.,* 2016; Seiler *et al.,* 2019). The MBL in this particular assay has been engineered to not only contain the carbohydrate-recognising domain of MBL but also the Fc portion of human IgG1 (FcMBL). This FcMBL recognises and binds to many different PAMPs and thus has broad range specificity for numerous PAMPs from a range of pathogens that can be identified within 1 hour of testing (Cartwright *et al.,* 2016; Seiler *et al.,* 2019). Early studies using this methodology identified the ability of ELLecSA to detect the presence of over 85% (47 out of 55) of living pathogen species in serum, a sensitivity that markedly increased upon mechanical

breakdown of the pathogens (Cartwright *et al.,* 2016). In human studies, this method was found to detect pathogen presence in more than 80% of blood samples, compared with less than 20% identified using traditional identification methods (Cartwright *et al.,* 2016). A follow-on study performed last year determined that this assay was able to detect 58% of live pathogens in blood and 89% of disrupted pathogens in blood (Seiler *et al.,* 2019). In this method, the mechanical disruption substantially increases the detection range of this assay, owing to the disruption of protective capsules surrounding pathogens that would have otherwise shielded membrane PAMPs from detection (Seiler *et al.,* 2019). This method shows increasing promise in clinical applications.

### 1.5.5. Other Biomarkers for Inflammatory Diseases

Interleukin-6 is a well-characterised pro-inflammatory cytokine that plays a significant role in the APR. An increase in IL-6 concentrations between sepsis and septic shock accurately reflects the change in severity, and one study found that IL-6 levels were significantly higher during Gram-negative infections than Gram-positive infections (Abe *et al.*, 2010). In one study (Hou *et al.*, 2015), using IL-6 as a diagnostic tool for sepsis had a pooled sensitivity of 80% and a specificity of 85%. However, despite these findings, IL-6 is frequently elevated in patients with SIRS and other non-infectious inflammatory illness, and is more generally used to identify inflammation (Hou *et al.*, 2015). Other soluble markers include TNF-α, IL-8 and sCD14 (Chalupa *et al.*, 2011). Several cell surface markers have also been investigated for their potential to identify sepsis, such as Fc gamma receptor 1 (CD64) and human leukocyte antigen DR isotype (HLA-DR; Umlauf *et al.*, 2013). CD64 binds IgG to facilitate phagocytosis and intracellular pathogen killing (Umlauf *et al.*, 2013). Upregulation of this marker on neutrophils occurs early in the septic response, and expression is enhanced during neonatal sepsis (Umlauf *et al.*, 2013; van Kessel *et al.*, 2014). Expression of HLA-DR is increased on monocytes following stimulation by cytokine expression. A decrease in this marker has been recorded during neonatal sepsis (Umlauf *et al.*, 2013). Interleukin-10, a key anti-inflammatory cytokine, has also been considered for use as a biomarker to monitor patient progress. Concentrations of IL-10 early in sepsis have shown promise in discriminating the severity and predicting the mortality of patients that later progress to septic shock (Hamers *et al.*, 2015). Function of the APR can also be measured by analysing changes such as decreases in serum cholesterol, increases in glucocorticoids, activation of complement and coagulation, decreased serum levels of calcium, zinc and iron, and changes in the concentrations of both positive and negative APPs (Gruys *et al.*, 2005).

Serum lactate levels are traditionally used as a biomarker of tissue hypoxia in septic patients and can be used to predict severity and progression to septic shock, although it is not a determinant of bacterial infection (Nolt *et al.,* 2018).

## 1.6. A New Class of Biomarkers: Sterols and Immunity

### 1.6.1. Cholesterol

Cholesterol is one of the most abundant lipids in mammalian cells and is essential for normal body function. Its structure is composed of four rings and an eight-carbon side chain; the 3β-hydroxyl group on ring A confers polarity to the molecule (Figure 1.3). Approximately 25% of cell plasma membrane lipid is made up of cholesterol, and its rigid, hydrophobic structure allows for efficient membrane packing and fluidity. Cholesterol-rich domains in cell membranes serve as 'rafts' for transmembrane receptor cell signalling (Cyster *et al.*, 2014). Humans obtain the majority of cholesterol through their diet, whilst the remainder is synthesised endogenously (Brown and Sharpe, 2016). The biosynthetic pathway that gives rise to cholesterol and sterols (isoprenoids, bile acids, steroid hormones and oxysterols) is active in all nucleated mammalian cells (Cyster *et al.*, 2014). Each day, approximately 500mg of cholesterol is converted into bile acids in a healthy adult, and all these by-products of cholesterol biosynthesis play further roles in maintaining healthy body functions (Russell, 2003). Sterol response element-binding proteins (SREBPs) regulate sterol biosynthesis and control expression of rate-limiting enzymes in the sterol biosynthetic pathway (Figure 1.3; Cyster *et al.*, 2014).
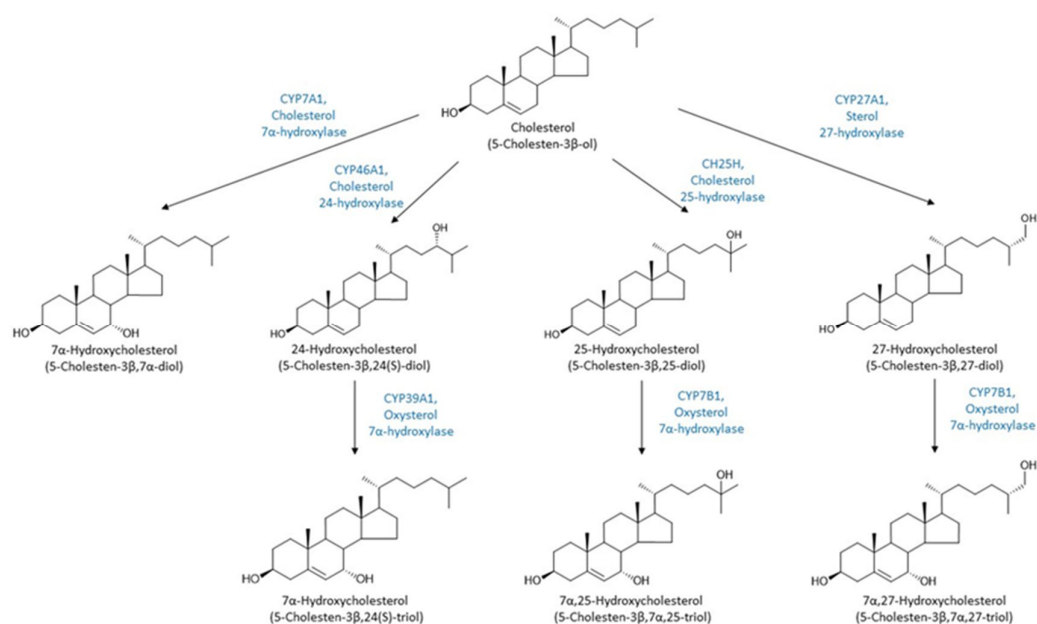
Figure 1.3. Bile acid synthetic pathway of cholesterol including enzymes required for synthesis of each sterol (Russell, 2003).

Cholesterol and other sterols play a significant role in immune defence, regulation and disease (Robertson and Ghazal, 2016). High-density lipoprotein opposes this process by promoting cellular efflux of cholesterol, reducing inflammation (Tall and Yvan-Charvet, 2015). Cholesterol has also been found to play a role in infectious diseases (Robertson and Ghazal, 2016). In particular, viral infections have often been associated with a downregulation in host plasma cholesterol levels, and viruses such as Human Immunodeficiency Virus (HIV) and Herpes Simplex Virus (HSV) have been found to depend on host sterol metabolism to drive their own survival and replication (Robertson and Ghazal, 2016). Inhibiting cholesterol biosynthetic pathways has been shown to limit virus entry and replication in mammalian cells (Cyster *et al*., 2014). Furthermore, lipid metabolic pathways and inflammatory pathways have recently been shown to converge, and oxysterols have emerged as key players in this interaction (Gold *et al*., 2014). Lipoproteins and lipids, including HDL, have been found to have direct immunomodulatory properties towards bacterial infection, binding to and neutralising toxic bacterial structures, such as LPS (Zou *et al*., 2016).

### 1.6.2. 25-Hydroxycholesterol (25-HC)

Oxysterols are minor constituents and precursors of bile acids. They are secreted into the small intestine from the liver where they act as emulsifiers of dietary lipids (Russell, 2003). Their synthesis is tightly regulated (Figure 1.3) to maintain homeostasis, and they initiate negative feedback loops when they are in high enough concentrations (Russell, 2003). Most of the enzymes that produce bile acids are expressed in the liver but some enzymes have been found in tissues, including tissue macrophages and neurons (Russell, 2003; Cyster *et al.*, 2014). 25-hydroxycholesterol (25-HC) is an oxysterol where the $25^{th}$ carbon has been modified by the addition of a hydroxyl group (-OH). The addition of this second hydroxyl group confers a more hydrophilic nature to this oxysterol. Previously, 25-HC was believed to play a role in mediating negative feedback during cholesterol biosynthesis (Cyster *et al.*, 2014). In recent experiments, mice deficient in 25-HC were found to have unaffected cholesterol metabolism, suggesting that 25-HC's role lies elsewhere (Cyster *et al.*, 2014). Recent data strongly suggests that 25-HC and its synthetic enzyme cholesterol 25-hydroxylase (CH25H), also known as CYP27A1, is involved in the immune response (Cyster *et al.*, 2014; Ning *et al.*, 2017). CH25H is upregulated in macrophages in response to activation by inflammatory mediators and is able to neutralise enveloped viral replication via the production of 25-HC (Cyster *et al.*, 2014; Ning *et al.*, 2017), as mice deficient in this enzyme were found to be more susceptible to viral septic shock and enveloped virus activity was reduced in cell culture treated with 25-HC (Blanc *et al.,* 2013; Liu *et al.,* 2013; Robertson and Ghazal, 2016). The mechanisms behind this action are still unclear but are thought to be linked to direct modifications of host cellular membranes by directly removing cholesterol from these membranes, limiting viral entry and the production of the virus envelope (Liu *et al.,* 2013; Cyster *et al.,* 2014). The majority of 25-HC secreted in response to stimulation occurs within 8 hours of incubation and levels continue to rise throughout a 24-hour time frame (Blanc *et al.*, 2013). Additional evidence arises from the discovery that synthesis of CH25H occurs in tissue not involved in lipid and cholesterol synthesis (McDonald and Russell, 2010). Expression of the CH25H gene is inactive in resting cells but is rapidly induced in response to activation of TLR ligands, in particular TLR3 (Poly I:C) and TLR4 (LPS; McDonald and Russell, 2010).

### 1.6.3. 25-HC Expression and Interferon Signalling

25-hydroxycholesterol synthesis is induced in macrophages and other phagocytes in response to type I and II IFN signalling (Figure 1.4; McDonald and Russell, 2010; Cyster *et al.*, 2014). Interferons induce signalling via the JAK-STAT pathway and promote interferon-stimulated gene (ISG) production (Wilkins and Gale, 2013). Type I IFN-α and IFN-β play a significant role in host defence during viral infections by promoting cytotoxic activities, increasing expression of MHC I and promoting apoptosis of infected cells (Pestka, 2007). The only type II IFN, IFN-γ, , is produced by adaptive immune cells to skew the immune response towards Th1, promote macrophage survival, enhance microbicidal processes and upregulate antigen processing and presentation (Schroder *et al.*, 2004).. It has also been found that Type I IFN signalling leads to a downregulation of sterol biosynthesis that ultimately leads to cell protection from the invading virus. Hence 25-HC, may have a significant role to play in this protective mechanism as a negative feedback molecule (Cyster *et al.*, 2014).
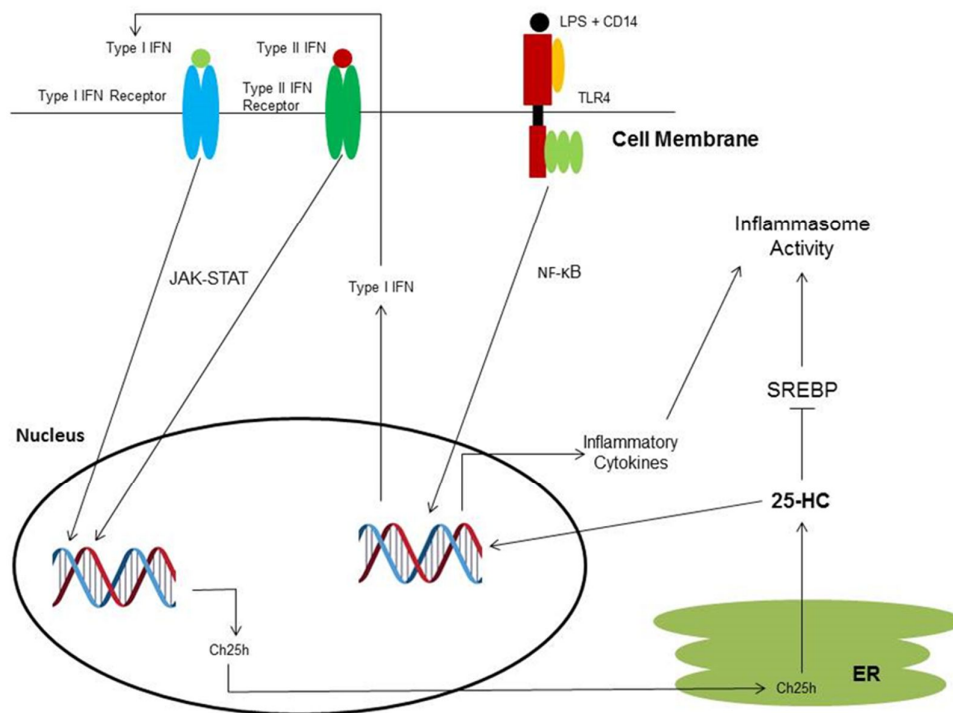


Figure 1.4. Induction pathways of CH25H expression and 25-HC synthesis in macrophages. ER refers to the endoplasmic reticulum (Wilkins and Gale, 2013; Cyster *et al.,* 2014).

### 1.6.4. Immune Functions of 25-HC

The immune functions of 25-HC that have been discovered to date are numerous. It has been found to regulate immunoglobulin (Ig) production, in particular IgA (Cyster *et al.,* 2014); promote macrophage foam cell formation and development of atherosclerosis (Koarai *et al.*, 2012); amplify the production of inflammatory cytokines (Cyster *et al.*, 2014); encourage neutrophil chemotaxis (Cyster *et al.*, 2014); interact with integrins to facilitate integrin-focal adhesion kinase (FAK) signalling after PRR activation (Pokharel *et al.,* 2019); and suppress inflammasome activity and mediate negative feedback of IL-1 family cytokine production (Koarai *et al.*, 2012; Cyster *et al.*, 2014). Suppression of inflammasome activity is mediated in part by 25-HC decreasing active sterol-regulatory binding protein 2 (SREBP2) levels intracellularly and thus decreasing the accumulation of sterols (Tall and Yvan-Charvet, 2015). It has also been suggested that 25-HC may aid in the recovery of septic shock and liver function after injury by LPS (Ning *et al.*, 2017). Another function of 25-HC is the inhibition of SREBPs, which play a central role in the regulation of cholesterol and fatty acid biosynthesis (Zou *et al.*, 2011).

### 1.6.5. 25-HC in Infection and Disease

25-HC has been implicated in a number of immune-related diseases and disorders, including atherosclerosis and Alzheimer's disease (Koarai *et al.*, 2012). In the airways, overproduction of 25-HC has been correlated with high numbers of neutrophils in circulating blood (Koarai *et al.*, 2012). These disease processes have been found to be mediated in part through liver X receptors (LXRs), which are essential in maintaining lipid homeostasis in healthy mammalian cells; 25-HC is a natural ligand for LXRs (Zou *et al.*, 2011). The majority of 25-HC and oxysterol immune research has been conducted using viral infection conditions (Amako *et al.*, 2009; Liu *et al.*, 2013; Anggakusuma *et al.*, 2015; Li *et al.,* 2017; Wang *et al.*, 2017; Shawli *et al.*, 2019). There is less research and evidence as to the role of 25-HC during a bacterial infection (Zou *et al.*, 2011). One piece of evidence that could link bacterial infection with 25-HC upregulation in mammalian cells is that the levels of 25-HC increase in response to TLR4 activation (Bauman *et al.*, 2009). Furthermore, the enzyme CH25H is induced by incubation with LPS, PGN, Poly I:C and LTA, which supports the hypothesis that 25-HC may have a role in innate immune activation of bacterial as well as viral pathogens (Bauman *et al.*, 2009). Recently, LXR metabolic signalling have been found to play an important role in defence

against bacterial infection (Zou *et al*., 2011). LXR knockout (KO) mice have increased susceptibility to *Listeria monocytogenes* infection (Zou *et al*., 2011).

Upon infection with *L. monocytogenes,* macrophages were found to detect bacterial cyclic di-AMP and induce Type I IFNs that are central to the upregulation of CH25H in macrophages (Zou *et al*., 2011). The mechanism underlying this protection against *L. monocytogenes* infection is through enhancing the survival of macrophages (Zou *et al*., 2011). Another investigation found that *ch25h*-deficient mice had more IL1-β and IL-18 in their sera than control mice when challenged with LPS, which coincided with the KO mice succumbing to LPS-induced death approximately 12 hours sooner (Reboldi *et al*., 2014). This strongly suggests that the CH25H enzyme is very important in pathogen clearance (Reboldi *et al*., 2014). Blood lipid parameters have been found to change during a septic episode, and one study found that high density lipoprotein (HDL)-cholesterol was markedly suppressed in sepsis patients and was inhibited to a greater extent during Gram-negative bacterial sepsis (Zou *et al*., 2016).

## 1.6.6. Other Oxysterols

Several other oxysterols have been implicated in the defence against pathogens, including 24-hydroxycholesterol (24-HC), 27-hydroxycholesterol (27-HC) and 7α-hydroxycholesterol (7α-HC; Testa *et al*., 2018). 27-HC selectively promotes survival of breast tumours by indirectly suppressing the cytotoxic activity of CD8+ T cells (Baek *et al.*, 2017), and also has roles in immunity, specifically blocking non-enveloped virus entry and replication via promoting the accumulation of cholesterol in endosomes and thus sequestering viral particles within them (Civra *et al*., 2018). 7α-HC has been identified as a major oxysterol found in atherosclerotic lesions, and facilitates immunopathology at the lesion by promoting monocyte differentiation into macrophages and inducing elevated concentrations of the chemokine IL-8 (Cho *et al*., 2017).

## 1.7. Current Issues and Gaps in the Literature

A major roadblock facing sepsis care and management is the lack of a robust panel of biomarkers that can accurately and rapidly predict the underlying infectious agent. While evidence points towards host biomarkers such as IL-6 and PCT as strong indicators of pathogenic cause, conflicting data from different laboratories puts the reliability of these two molecules into question. New host expressed biomarkers are urgently needed for potential future application to the clinic. Furthermore, a simple testing platform for measuring potential biomarker responses to sepsis relevant pathogens is needed.

Current work into 25-HC and other oxysterols have largely focused on viral infection. Indeed, certain researchers believe that 25-HC is a virus-specific oxysterol and is only upregulated in response to viral infection. In comparison, little work has investigated whether 'bacteria' or 'bacterial stimuli' can activate these pathways. There is evidence that LPS interactions with TLR4 lead to upregulation of 25-HC *in vitro* suggesting that 25-HC upregulation is a more general response to infection and not to a specific pathogen. Furthermore, bacterial stimulation of 25-HC expression in whole blood opens the real possibility for a diagnostic test that has not been conducted to date, and no information exists as to the expression profile of 25-HC in other body compartments where macrophages are absent.

It is also very clear that 'pathogen' (bacterial) expressed biomarkers (such as virulence genes) remain untested despite numerous collections of virulence factors defining important disease pathotypes. Identifying new bacterial genes associated with sepsis and survival in human blood could also be a useful approach to refine biomarker panels. Indeed, 16S rRNA genes have been used to detect infection in critical care units but whether virulence factors (that are generally expressed at lower levels) will be equally successful, is a good opportunity for research.

## 1.8. Aims and Objectives

The gaps in the literature identified above form the basis of the main aims of this thesis. This thesis aims to identify new host and pathogen-associated biomarkers to predict pathogen specific sepsis, that have the potential to take forward to the clinic. Host biomarker responses will be investigated in chapters 3, 4 and 5 and bacterial genes in chapter 6.

- Characterisation of the innate immune response towards model strains of *Staphylococcus* and *E. coli* in whole blood from healthy volunteers in order to identify new soluble biomarkers of infection. This will be characterised using ELISAs in chapter 3.

- Characterisation of the cellular response towards model strains of *Staphylococcus* and *E. coli* in healthy whole blood in order to design a robust model for understanding cellular interactions in healthy whole blood. This will be characterised using flow cytometry in chapter 4.

- Characterisation of the sterol response towards model strains of *Staphylococcus* and *E. coli* in healthy whole blood in order to determine any associations between bacterial infection and sterol regulation. This will be characterised using LC-MS in chapter 5.

- Genomic and phenotypic analysis of blood culture positive *E. coli* strains from Welsh hospitals in the Hywel Dda University Health Board (HDUHB) will investigate potential associations between origin of infection and virulence factors. This will be characterised using next generation sequencing pipeline and gentamicin protection assays of urinary and intestinal epithelial cells in chapter 6.

**Chapter 2. Materials and Methods**

**2.1. Media and Stock Solutions**

**2.1.1. Media**

Media were prepared using 200-1000 ml distilled water ($H_2O$) and sterilised by autoclaving.

**2.1.1.1. Luria Bertani (Lennox) Broth (LB)**

Luria Bertani (Lennox) Broth medium purchased in tablet form from Sigma-Aldrich (Gillingham, UK) and dissolved 1 tablet in 50 ml of $H_2O$.

10 g/L Tryptone

5 g/L Yeast Extract

5 g/L NaCl

2.2 g/L inert binding agents

**2.1.1.2. Bacto Tryptic Soy Broth (TSB)**

Tryptic Soy Broth medium was purchased in powder form from Thermo Fisher Scientific (Loughborough, UK) and dissolved 3.3 g per 10 ml in $H_2O$.

17 g/L Pancreatic digest of Casein

3 g/L Papaic digest of Soybean

2.5 g/L Dextrose

5 g/L Sodium chloride

2.5 g/L Dipotassium phosphate

**2.1.1.3. LB and TSB Agar**

Agar Technical (no. 3) was purchased from Oxoid (Basingstoke, UK) and dissolved 1.2% W/V (12 g) in 1000 ml LB or TSB prior to autoclaving.

### 2.1.1.4. Columbia Agar with Horse Blood

Agar plates come pre-sterilised and were purchased from Oxoid (Basingstoke, UK).

 25 g/L Special peptone

1 g/L Starch

5 g/L Sodium chloride

10.25 g/L Agar

50 ml Defibrinated horse blood

### 2.1.2. Stock Solutions

Stock solutions were prepared using either distilled $H_2O$ or phosphate buffered saline (PBS). Stock solutions used for microbiological work were sterilised by autoclaving.

### 2.1.3. Glycerol

>99% Glycerol was purchased from Sigma Aldrich (Gillingham, UK) and diluted in $dH_2O$ to an 80% stock solution.

### 2.1.4. Phosphate Buffered Saline (PBS)

Phosphate buffered saline in tablet form was purchased from VWR Life Sciences (Leicestershire, United Kingdom) and dissolved 1 tablet per 100 ml $dH_2O$. 1000 ml of stock solution was prepared for microbiological and blood work.

Per tablet, when dissolved:

137 mM Sodium chloride

2.7 mM Potassium chloride

10 mM phosphate buffer

### 2.1.5. ELISA Wash Buffer

0.05% Tween 20 (Sigma Aldrich; Gillingham, UK) in 1000 ml PBS.

### 2.1.6. ELISA Reagent Diluent

Bovine Serum Albumin (BSA) Protease free powder was purchased from Thermo Fisher Scientific (Loughborough, UK) and diluted 1% w/v in 1000 ml dH$_2$O.

### 2.1.7. ELISA Stop Solution

37% Hydrochloric acid (HCl) was purchased from Sigma Aldrich (Gillingham, UK) and diluted to a 1 M solution in dH$_2$O by adding 41.3 ml HCl to 458.7 ml dH$_2$O.

### 2.1.8. BD FACS Lysing Solution

Becton Dickinson FACS lyse was purchased from BD Biosciences (Berkshire, United Kingdom) and diluted to a 10% solution in dH$_2$O.

### 2.1.9. FACS Buffer

FACS Buffer was prepared with 0.2% BSA and 0.05% Sodium azide reagent plus >99.5% (Sigma Aldrich; Gillingham, UK), in 50 ml of PBS.

### 2.1.10. Triton X Solution

A 0.1% solution of Triton-X 100 (Sigma Aldrich; Gillingham, UK) was made using 100 ml PBS.

### 2.1.11. Deuterated Internal Standard

A 4 ml stock solution of the deuterated internal standard was made according to the table in Appendix A. All oxysterol standards were purchased from Avanti Polar Lipids (Alabaster, Alabama, United States).

### 2.1.12. Ethanol Solution

A 70% ethanol stock solution was made using >99% ethanol (Thermo Fisher Scientific; Loughborough, UK) and high-performance LC-MS grade water (Thermo Fischer Scientific; Loughborough, UK).

### 2.1.13. Methanol Solutions

Stock solutions of 10%, 17%, 35%, 70% and 95% methanol were made using >99% methanol (Thermo Fisher Scientific; Loughborough, UK) and high-performance LC-MS grade water (Thermo-Fisher Scientific; Loughborough, UK).

### 2.1.14. Sodium hydroxide (NaOH)

Sodium hydroxide >97% pellets were purchased from Sigma Aldrich (Gillingham, UK) and dissolved 1g per 25 ml high performance LC-MS grade water. pH was checked (pH 13) and adjusted as appropriate.

### 2.1.15. Potassium phosphate ($KH_2PO_4$)

340 mg $KH_2PO_4$ monobasic

1.5 ml Sodium hydroxide

48.5 ml high performance LC-MS grade water

This yields a 50 mM solution. pH was checked using indicator strips and adjusted as appropriate. Potassium phosphate monobasic was purchased from Sigma Aldrich (Gillingham, UK).

### 2.1.16. Cholesterol oxidase

Lyophilised Cholesterol oxidase from *Streptomyces* sp. was purchased from Sigma Aldrich (Gillingham, UK) and reconstituted in 1 ml of LC-MS grade water as per manufacturer instructions. Aliquots were stored at -20°C.

### 2.1.17. Deuterated Girard Reagent P ($D_5$)

$D_5$ Girard reagent was synthesised in house as per Crick *et al.* 2015 using Girard Reagent P 1-(carboxymethyl) pyridinium chloride ($D_0$) from TCI Europe (Zwijndrecht, Belgium).

### 2.1.18. Isopropanol/Methanol Solution

> 99% isopropanol (Thermo Fisher Scientific; Loughborough, UK) and methanol were mixed 50:50 to a final volume of 50 ml.

### 2.1.19. LC-MS Mobile Phases

Mobile Phase A (total volume 1000 ml):

33.3% Methanol

16.7% Acetonitrile

50% LC-MS grade water

0.1% Formic acid

Mobile Phase B (total volume 700 ml):

63.3% Methanol

31.7% Acetonitrile

5% LC-MS grade water

0.1% Formic acid

>99.8% acetonitrile and LC-MS grade Formic acid was purchased from Thermo Fisher Scientific (Loughborough, UK).

## 2.2. Reagents

### 2.2.1. ELISA Colour Solution

KPL SureBlue TMB Microwell Peroxidase Substrate was purchased from Sera Care (Milford, Massachusetts, United States) and used as the ELISA colour solution.

### 2.2.2. Microscopy Reagents

#### 2.2.2.1. Microscopy Stains

Red Microscopy Hemacolor and Purple Microscopy Hemacolor were purchased from Merck (Watford, UK).

#### 2.2.2.2. Microscopy Mountant and Immersion

Stained slides were mounted using DPX Mountant for histology and immersed using Immersion Oil for microscopy (both Sigma Aldrich; Gillingham, UK).

### 2.2.3. Glacial Acetic acid

Acetic acid glacial >99.85% was purchased from VWR life sciences (Leicestershire, UK).

### 2.2.4. Rnase A

100 mg/ml Rnase A enzyme was purchased from Qiagen (Manchester, UK) and stored at 4ºC.

### 2.2.5. Vacutainer Tubes

Vacutainer tubes were purchased from Becton Dickinson (Swindon, UK) and were for a final draw volume of 10 ml. Anticoagulants used were Lithium Heparin (BD Vacutainer Lithium Heparin Tubes) and EDTA (BD Vacutainer spray coated K2EDTA Tubes).

### 2.3. Cell Culture Media and Reagents

All cell culture reagents were purchased from Gibco (Thermo Fisher Scientific; Loughborough, UK) unless otherwise stated.

### 2.3.1. Phosphate Buffered Saline

Pre-made Phosphate Buffered Saline (PBS; 1X) pH 7.4 without $CaCl_2$, $MgCl_2$ was used for all cell culture work.

### 2.3.2. CACO-2 Growth Media

500 ml 1x Dulbecco's Modified Eagle Medium (DMEM) 4.5 g/L D-glucose, L-glutamine Pyruvate Positive

50 ml (10%) Foetal Bovine Serum, Qualified (FBS)

5 ml (1%) L-glutamine 200mM (100x)

5 ml (1%) MEM Non-essential Amino Acid Solution (100X) without L-glutamine (Sigma Aldrich)

5 ml (1%) Pen/Strep 10000 units/ml Penicillin, 10000µg/ml Streptomycin

Antibiotic-free media was made without Pen/Strep for all bacterial work.

### 2.3.3. UM-UC-3 Growth Media

500 ml 1x Dulbecco's Modified Eagle Medium (DMEM) 4.5 g/L D-glucose, L-glutamine Pyruvate Positive

50 ml (10%) Foetal Bovine Serum, Qualified (FBS)

5 ml (1%) MEM Non-essential Amino Acid Solution (100X) without L-glutamine (Sigma Aldrich)

5 ml (1%) Pen/Strep 10000 units/ml Penicillin, 10000 µg/ml Streptomycin

Antibiotic-free media was made without Pen/Strep for all bacterial work.

### 2.3.4. U937 Growth Media

500 ml RPMI-1640 Medium, phenol red, 2 mM L-glutamine, 10 mM HEPES, 1 mM Sodium pyruvate, 4500 mg/L glucose, 1500 mg/L Sodium bicarbonate

50 ml (10%) Foetal Bovine Serum, Qualified (FBS)

### 2.3.5. TrpyLE Express Enzyme

Adherent cells were disassociated using TrypLE Express Enzyme (1X) with no phenol red.

### 2.3.6. Gentamicin Solution

A working concentration of 300 µg/ml Gentamicin (Thermo Fisher Scientific; Loughborough, UK) was prepared using 50 mg/ml Gentamicin Solution diluted in sterile $dH_2O$.

### 2.3.7. Trypan Blue Stain

Adherent cells were stained with Trypan Blue Stain, 0.4%.

### 2.4. Antibodies and TLR Agonists

### 2.4.1. Antibodies

All antibodies were purchased from Miltenyi Biotec (Woking, UK) and were stored at 4ºC between tests. Antibodies were supplied in buffer containing stabiliser and 0.05% Sodium azide (Table 2.1).

Table 2.1. List of the antibodies used.

| Target Antigen | Conjugated Dye | Clone | Lot no. | Excitation/ Emission | Expression | Amount per Test |
|---|---|---|---|---|---|---|
| CD45 | Fluorescein isothiocyanate (FITC) | REA747 | 51711 10333 | 488 nm/520 nm (Green) | Leukocytes | 2 µl |
| CD14 | Phycoerythrin (PE) | REA599 | 51803 13090 | 488 nm/578 nm (Red-Orange) | Monocytes Activated Neutrophils | 5 µl |
| CD3 | Allophycocyanin (APC) | BW264/ 56 | 51803 16241 | 561 nm/660 nm (Red) | T Cells | 5 µl |
| CD19 | VioBlue | LT19 | 51803 13117 | 405 nm/452 nm (Violet) | B Cells | 5 µl |
| CD282 (TLR2) | Phycoerythrin (PE) | REA109 | 51809 25198 | 488 nm/578 nm (Red-Orange) | Leukocytes | 10 µl |
| CD284 (TLR4) | Allophycocyanin (APC) | HTA125 | 51809 25202 | 561 nm/660 nm (Red) | Leukocytes | 10 µl |

## 2.4.2. TLR Agonists and Blocking Antibodies

All Toll-like receptor (TLR) agonists and blocking antibodies were purchased from Invivogen (Toulouse, France) and were guaranteed free from LPS and lipoprotein contamination. All blocking antibodies were polyclonal rat IgG and are supplied in $H_2O$ 250 µg/ml Pen/Strep (Table 2.2).

Table 2.2. List of the PRR agonists and blocks used in the thesis.

| Agonist/Block | Reconstituted In | Amount Required Per Test | Lot no. |
|---|---|---|---|
| Lipopolysaccharide (LPS) B5 Ultrapure from *E. coli* serotype 055:K59 (B5H) 5 mg/ml stock | Contaminating LPS-free water Sterile PBS | 1 µl 1 µg/ml to 1 ml of whole blood | - |
| Peptidoglycan (PGN) BS from *Bacillus subtilis* 1 mg/ml stock | Contaminating LPS-free water Sterile PBS | 1 µl 1 µg/ml to 1 ml of whole blood | - |
| Polyinosine:polycytidylic acid (Poly I:C) High Molecular Weight 100 µg/ml stock | Contaminating LPS-free water Sterile PBS | 1 µl 1 µg/ml to 1 ml of whole blood | - |
| PAb Control 0.2 mg/ml stock | Sterile PBS | 100 µl 5 µg/ml to 1 ml whole blood | PCS-39-01 |
| PAb-hTLR2 0.2 mg/ml stock | Sterile PBS | 100 µl 5 µg/ml to 1 ml whole blood | T2S-39-01 |
| PAb-hTLR4 0.2 mg/ml stock | Sterile PBS | 100 µl 5 µg/ml to 1 ml whole blood | T4S-38-01 |

## 2.5. Microbiology

## 2.5.1. Bacterial Strains

Eight bacterial strains of *E. coli, S. aureus* and *S. epidermidis* used in Sections 2.5.2, 2.5.4 and 2.5.6 are listed in Table 2.3.

Table 2.3. List of the bacteria used in *ex vivo* study.

| Species | Strain | Comments | Source |
|---|---|---|---|
| *Escherichia coli* | ECOR26 | Human infant isolate Commensal strain | Part of the ECOR collection of isolates Ochman and Selander 1984 |
| *Escherichia coli* | GMB10 | Non-clinical plant isolate (Spinach) | Meric *et al.* 2013 |
| *Escherichia coli* | K12 | Model laboratory strain Descendent of a strain first isolated in 1922 from a stool sample | Bachmann 1972 |
| *Escherichia coli* | B | Laboratory strain from pathology laboratory, Singleton Descendent of a strain originally isolated in 1918 and named in 1942 | d'Herelle 1918 Delbruck and Luria 1942 |
| *Staphylococcus aureus* | VAP39 | An MRSA Cause of ventilator-associated pneumonia UK isolate | Conway Morris *et al.* 2009 Conway Morris *et al.* 2011 Wilkinson *et al.* 2012 |
| *Staphylococcus aureus* | SH1000 | Representative laboratory strain of *S. aureus* UK isolate Highly virulent derivative of NCTC 8325 | Horsburgh *et al.,* 2002 |
| *Staphylococcus epidermidis* | 1457 | Cause of central-venous catheter associated disease Biofilm producer | Mack *et al* 1992 |
| *Staphylococcus epidermidis* | RP62A | Isolated from a patient with intravascular catheter-associated sepsis | Christensen *et al.,* 1982 |

Ninety-eight clinically relevant strains of *E. coli* recovered from septic patients and water sources were obtained from the HDUHB in Wales. Isolates were sorted based on their isolation source (Reference, Urine, Intra-abdominal, Biliary, Other/Unknown and Water) and details can be found in Appendix B.

## 2.5.2. Culture of Microorganisms

Eight bacterial strains of *E. coli, S. aureus* and *S. epidermidis* were obtained from the Microbiology and Infectious Diseases collection at Swansea University (see section 2.5.1). Upon receipt of the strains, bacteria were cultured independently by streaking from freezer stocks onto agar plates. Plates were incubated for 24 hours in a 37°C Genlab Incubator. A single colony from each plate was inoculated in 5 ml of relevant media (LB for *E. coli* and TSB for *Staphylococcus*) and incubated for 24 hours at 37°C in a Kuhner Shaker X at 200 r.p.m. Freezer stocks were prepared using 80% glycerol stock solution diluted to 40% in a 50:50 2 ml cryotube. Strains were stored at -80$^0$C in a Thermo Fischer Scientific TSX Series Freezer.

Ninety-eight clinically relevant strains of *E. coli* were obtained from the HDUHB on agar slopes. Upon receipt of the strains, slopes were streaked and bacteria inoculated onto blood agar and incubated as described above. Freezer stocks were created using Cryobeads (Qiagen) and 2-3 colonies before storage at -80°C. A single colony from each plate was inoculated in 5 ml of corresponding media and incubated as described above.

## 2.5.3. Preparation of *E. coli* for Gentamicin Protection Assay

After 24 hours incubation, optical density of *E. coli* cultures was determined by spectrophotometry at 600 nm. Cultures were adjusted to an OD of 0.05 and diluted as appropriate in LB. Specifications for the Gentamicin Protection Assay are highlighted in Section 2.6.5.

## 2.5.4. Bacterial Enumeration and Standardisation

Total viable counts in 1 ml of media was determined for each strain used in the study by serial dilutions according to the method of Miles and Misra (1939). This suspension was mixed by inversion and serially diluted to $10^{-8}$. Three or 10 μl of the suspensions was placed on either LB agar, TSB agar or blood agar in triplicate and incubated 20-24 hours at 37$^0$C. Three microlitre suspensions were required for *E. coli* strains with large colony morphology characteristics to prevent merging of colonies and distortion of enumeration

results. Dilutions that had 1-20 distinct colonies on the plate were counted and the amount of cfu/ml was calculated for each species.

Bacterial suspensions were standardised by spectrophotometry. Optical densities were determined using a Jenway 7200 spectrophotometer set at 600 nm. Bacterial suspensions were standardised to an optical density of 0.1 and an approximate cell count of $10^7$ by diluting in RPMI to a final volume of 1 ml in a microcentrifuge tube. Tubes were centrifuged at 12000 r.p.m for 5 minutes in an Eppendorf Centrifuge 5415 R set at room temperature. Supernatants were discarded and the pellet resuspended in 1 ml of RPMI.

### 2.5.5. *E. coli* DNA Extraction and sequencing

All DNA extractions were carried out using the QIAamp DNA mini kit (Qiagen, Manchester, UK) according to manufacturer's instructions. An overnight culture of the strains in Appendix B was grown in 5 ml LB broth as described in Section 2.5.1, and then 1 ml of culture was pipetted into a 1.5 ml microcentrifuge tube and centrifuged for 5 minutes at 7500 r.p.m in a Eppendorf Centrifuge 5415 R. The supernatant was discarded and a further 1 ml of culture added and centrifuged as described previously. The DNA extraction protocol was then followed as per the manufacturer's instructions and quantified (ng/ml) using a Nanodrop spectrophotometer MD1000 (Labtech, East Sussex, UK). Samples were frozen at -20°C before being sequenced at the Swansea Genome Centre.

### 2.6. Whole Blood Model

### 2.6.1. Isolation of whole blood from healthy volunteers

Whole blood from healthy volunteers was obtained through the Joint Clinical Research Facility (JCRF) at Swansea University. Ethical approval was obtained for collection of blood by a trained nurse, and consent given by all participants. The work is one of the projects (13/WA/0190) assessed by the local ethics committee (Wales Rec 6) at Swansea University Medical School (SUMS). For each donor several 9 ml tubes (green top heparin or purple top EDTA as described in Section 2.2.5) were taken and used on the day of donation, with the exception of apoptotic samples (see section 2.7.2.2). Information sheets on the donations, as well as details on disposal and transfer of whole blood, were kept in a folder in the Microbiology & Infectious Diseases (MID) office.

### 2.6.2. Addition of Bacteria to Whole Blood

One millilitre of anticoagulated whole blood (Lithium Heparin or EDTA) was added to a microcentrifuge tube. To each tube, 100 µl of the bacteria:RPMI suspension was added and mixed gently by inversion. A blood sample was inoculated with RPMI alone as a control. The blood/bacteria inoculation (Multiplicity of Infection 0.2) was incubated on a Stuart SB3 rotator at 10 r.p.m at 37°C for 2-8 hours. After incubation, samples were centrifuged at 7000 r.p.m for 5 minutes at room temperature. The supernatant was removed and frozen at -20°C until further analysis. Multiplicity of infection was calculated using the following equation:

$$multiplicity\ of\ infection\ (MOI) = \frac{number\ of\ bacterial\ cells\ added}{number\ of\ leukocytes\ per\ 1ml\ of\ blood}$$

### 2.6.3. Purified Agonist and TLR Block Whole Blood Incubation

Blood was obtained as above (2.5.6.1.). Descriptions of both purified agonists and TLR blocking antibodies can be found in Table 2.2. For TLR stimulation, 1 µl of LPS, PGN or Poly I:C (all at 1 µg/ml) was added to 1 ml of whole blood prior to incubation for 2-8 hours as described above. For TLR blocking, 100 µl (5 µg/ml final concentration) of the relevant antibody was added to 1 ml of whole blood and incubated for half an hour prior to infection for 2-8 hours as described above.

### 2.7. Cell Culture

### 2.7.1. Culture of Gut and Bladder Epithelial Cells

Human gut and bladder epithelial cell lines were used to investigate invasive interactions between *E. coli* clinical isolates and epithelial cells. CACO-2 colon epithelial cells (ECACC 86010202) and UM-UC-3 bladder epithelial cells (ECACC 96020936) were obtained from Public Health England Culture Collections (Porton Down, Salisbury) and placed in liquid nitrogen until ready to culture (Table 2.4). All cell lines were cultured in DMEM high glucose media and supplemented as described in Section 2.3.2 and 2.3.3 and incubated in a 5% $CO_2$ incubator (Nuaire, Caerphilly, Wales) at 37°C.

Table 2.4. Human gut and bladder cell lines.

|  | UM-UC-3 | CACO-2 |
|---|---|---|
| Supplier | European Collection of Authenticated Cell Cultures (ECACC) | European Collection of Authenticated Cell Cultures (ECACC) |
| Catalogue Number | 96020936 | 86010202 |
| Cell Line Source | Human Bladder Transitional Cell Carcinoma | Human Caucasian colon adenocarcinoma |
| Species & Gender | Human Male | Human Male |
| Tissue of Origin | Bladder | Colon |
| Cell Type | Epithelial | Epithelial |
| Growth Mode | Adherent | Adherent |

## 2.7.2. Culture of U937 Cells

Monocytic non-adherent U937 cells were used as a positive control for monocyte populations described in Chapter 4.3.4.1. U937 monocytes (ECACC 85011440) were obtained from Public Health England Culture Collections and placed in liquid nitrogen until ready to culture. The cell line was sourced from a human Caucasian histiocytic lymphoma. Monocytic cells were cultured in RPMI media supplemented as described in Section 2.3.4. and incubated in a 5% $CO_2$ incubator (Nuaire) at 37$^{o}$C.

## 2.7.3. Recovery and sub-culture of Cells

Cells were recovered from liquid nitrogen storage by adding thawed cells to 25 ml of corresponding media in a T75 cell culture flask and incubated in a 37$^{o}$C $CO_2$ incubator until they reached confluency and were ready to be sub-cultured. Briefly, confluent CACO-2 and UM-UC-3 cells were washed three times in PBS before being treated with 5 ml TrypLE Express for up to 10 minutes to detach the cells from the base of the flask. TrypLE was then deactivated with either CACO-2 or UM-UC-3 supplemented media and centrifuged in a ThermoScientific Heraeus Megafuge 16R at 400 r.p.m for 5 minutes. U937 cells were centrifuged without washing at the same specifications. The supernatant was discarded and the pellet resuspended in relevant cell culture media. Cells were split into new T175 flasks by performing a 1 in 25 dilution. Cells were supplemented with media and incubated as previously described.

### 2.7.4. Seeding Cells onto 24-well Plates

CACO-2 and UM-UC-3 cells were washed and centrifuged as described in Section 2.6.3 and resuspended in 10 ml of relevant media after centrifugation. Cell viability was determined by mixing 10 μl of cell suspension with 10 μl of TrypanBlue and applying 10 μl to each side of a 0.0025 mm$^2$ haemocytometer (Hirschmann EM Technology, Neckartenzlingen, Germany). Cells were counted from each side of the slide and the calculation below used to calculate cell density:

$$(Average\ no.\ of\ cells\ X\ 10000)\ X\ 2 = n$$

$$\frac{n\ X\ 10\ (total\ volume)}{Area\ of\ Flask} = cells/cm2$$

The number of cells/cm$^2$ was used to calculate the number of cells required to cover a 2 cm$^2$ area of a 24-well plate (number of cells/cm$^2$ multiplied by 2). Cells were diluted appropriately and seeded into a 24-well plate. Plates were incubated in a 5% $CO_2$ incubator at 37°C allowed to grow to confluence.

### 2.7.5. Gentamicin Protection Assay

The gentamicin protection assay enables quantification of the cellular invasive potential of bacteria and depends on the inability of gentamicin to penetrate eukaryotic cell membranes. A subset of *E. coli* isolates outlined in Appendix B were inoculated in LB media overnight and standardised to 0.05 OD. Confluent UM-UC-3 and CACO-2 monolayers pre-seeded into a 24-well plate (Section 2.6.4.) were washed three times with warm PBS and 2 ml of antibiotic-free DMEM was added to each well. To test wells, 30 μl of 0.05 $OD_{600}$ bacterial suspension was added and the plates incubated in a 5% $CO_2$ incubator at 37°C for four hours. Each *E. coli* strain was added to duplicate wells and the original inoculum serially diluted on agar plates to determine cell density (cfu/ml) as described in section 2.5.4. After four hours, the samples were washed three times with warm PBS and 2 ml of PBS was added to each well. To each well, 4 μl of gentamicin (300 μg/ml) was added and the plates incubated in a 5% $CO_2$ incubator at 37°C for 90 minutes. After 90 minutes, the samples were checked for contamination by plating 10 μl of the mixture onto blood agar using a 10 μl inoculating loop and incubating the plate at 37°C overnight. Sample wells were then washed once in warm PBS before the inoculating loop step was repeated. This step was to ensure complete elimination of non-internalised bacteria. The plate was washed a further two times in warm PBS before 2 ml of 0.1% Triton-X100 in PBS was added to each well to lyse the cells and release the internalised

bacteria. Plates were then incubated for 10 minutes before each duplicate well was serially diluted. Dilutions were plated onto blood agar (20 µl) and incubated at 37°C overnight. Counts (cfu/ml) were determined and the number of bacteria that invaded compared to the original bacterial inocula added (as a percentage) calculated:

$$\frac{number\ of\ bacteria\ at\ end\ of\ experiment}{number\ of\ bacteria\ added\ to\ cell\ culture}\ x\ 100 = \%\ invasion$$

This percentage invasion value was then divided by the total number of epithelial cells to represent a ratio of bacterial cells to one epithelial cell. Values were then presented as the ratio of invasion per 1000 epithelial cells.

## 2.8. Cellular Analysis

### 2.8.1. Phagocytosis Analysis

Neutrophil phagocytosis of bacterial strains was investigated using microscopy. Whole blood was incubated for 2, 4 and 6 hours with each model bacterium (section 2.5.1.) and RPMI vehicle as a control. At the end of each incubation period, 100 µl of whole blood was added to 5 ml Falcon round bottom tubes. To each tube 1.5 ml of 1X FACS Lysing Solution (BD Biosciences, Wokingham) was added and incubated for up to 10 minutes in the dark at room temperature until the blood was fully lysed. Tubes were then centrifuged in an Eppendorf Centrifuge 5810 R at 300 r.p.m for 5 minutes and the supernatant discarded. The pellet was resuspended in 100 µl of PBS and vortexed. Then, 80 µl of each sample was pipetted into cytospin funnel cartridges and filters (Thermo Fisher Scientific) attached to microscope slides. Filters were then centrifuged in a Cytospin 3 (ThermoShandon, Thermo Fisher Scientific) at 300 r.p.m for 3 minutes or until all the blood in the filters had been transferred to the slides. After centrifugation, the microscope slides were removed and allowed to dry overnight. Once sample slides were dry, they were stained with 100% methanol fix, Red Microscopy Hemacolor, Purple Microscopy Hemacolor and 2x washes with distilled water for 30 seconds each respectively. The slides were then left to dry overnight before mounting with cover slips using DPX mountant and left to dry overnight.

Once dry, slides were viewed using a Nikon eclipse 50i microscope at a magnification of x1000 with oil immersion. Neutrophils were identified by their multi-lobed nuclei and counted (Figure 2.1). Neutrophils that had actively phagocytosed bacteria were identified by black dots (bacteria) within the cytoplasm of the cells. Neutrophils were counted until

100 of either phagocytosed or non-phagocytosed neutrophils had been scored, with random fields of view being selected. The calculation below was used to determine the degree of phagocytosis (%).

$$\frac{Number\ of\ Phagocytosed\ Neutrophils}{Total\ Number\ of\ Neutrophils}\ x\ 100$$



Figure 2.1. Cytospin showing morphology of neutrophil (A) and mononuclear leukocyte (B).

## 2.8.2. Flow Cytometry

### 2.8.2.1. Sample preparation and staining

Analysis of leukocyte sub-populations in whole blood treated with bacteria (section 2.5.6.) were measured using Flow Cytometry. One millilitre of whole blood with 100 µl *E. coli* K12, *S. epidermidis* RP62A or RPMI alone (control) was incubated for 2, 4, 6 and 8 hours. At the end of each incubation period, 100 µl of whole blood was placed into a 5 ml Falcon round bottom tube. To each tube, 2-10 µl of antibody was added and gently flicked to ensure mixing. Samples were incubated on ice in the dark for 30 minutes. An unstained control and a stained (time 0 control) were included. Additionally, stain isotype controls were included for each of the conjugated dyes used.

After the incubation period, 2 ml of 1X FACS Lysing Solution (BD Biosciences) was added to each tube, vortexed, and incubated in the dark at room temperature for up to 10 minutes until the sample was fully lysed. Samples were then centrifuged at 1600 r.p.m for 7 minutes using an Eppendorf Centrifuge 5810 R at 4°C and the supernatant discarded. Pellets were washed with 3 ml of FACS buffer and centrifuged again as previously described. The supernatant was discarded and the pellet resuspended in 100 µl of FACS buffer and vortexed. Samples were then analysed using the Novocyte NovoSampler Pro

(Acea Biosciences Inc., San Diego, California). Threshold conditions were set, including medium flow rate (Flow Rate 35 μl/min, Core Diameter 12.2 μm) and Stop Conditions of 12,000 ungated events or 70 μl volume. Laser parameters are shown in Table 2.5.

Table 2.5. Laser parameters included in FACS analysis.

| Parameter | Alias | Volt |
|---|---|---|
| FSC | Forward Scatter | - |
| SSC | Side Scatter | - |
| BL1 | FITC | 446 |
| BL2 | PE | 451 |
| BL3 | PE-Texas Red | 566 |
| BL4 | PerCP | 512 |
| BL5 | PE-Cy7 | 482 |
| RL1 | APC | 512 |
| RL2 | APC-Cy7 | 482 |
| VL1 | Pacific Blue | 493 |
| VL2 | AmCyan | 446 |
| VL3 | Pacific Orange | 451 |
| VL4 | Qdot 605 | 566 |
| VL5 | Qdot 655 | 512 |
| VL6 | Qdot 800 | 482 |

## 2.8.2.2. Cell Viability Measurements

A FITC Annexin V/Dead cell apoptosis kit (Invitrogen, Thermo Fisher Scientific) was used to measure the degree of apoptosis/cell death in the whole blood model. Briefly, whole blood samples incubated for 3-6 hours with *E. coli* K12, *S. epidermidis* RP62A or RPMI alone (control), were stained with the Annexin stain (binds to phosphatidylserine, a molecule exposed only on the cell surface of apoptotic mammalian cells) and propidium iodide (PI, stains DNA of permeabilised cells). Controls included an unstained sample, a stained time 0 sample, a cell death control (samples treated with 0.1% Triton-X100), and an apoptosis control (samples left for 24 hours after blood drawn).

Due to BD FACS lyse interfering with the integrity of leukocyte cell membranes, a separate purified source of monocytes was investigated. Histopaque-1077 (Sigma Aldrich) was used to separate mononuclear cells from red blood cells. Three 1 ml aliquots of blood was prepared for each sample and incubated as described above. To a 15 ml

conical centrifuge tube, 3 ml of Histopaque-1077 was added and brought to room temperature (RT). Then, 3 ml of whole blood was layered on top of the Histopaque and centrifuged at 1900 r.p.m for 30 minutes at 21°C. After centrifugation, the upper layer was aspirated with a Pasteur pipette to within 0.5 cm of the middle layer containing mononuclear cells (Figure 2.2) and discarded. The opaque layer of mononuclear cells was transferred using a Pasteur pipette to a clean 15 ml conical centrifuge tube. Mononuclear cells were then washed 3X with 10 ml PBS and centrifuged at 1200 r.p.m for 10 minutes per wash. The supernatant was discarded and the final pellet resuspended in 100 µl of 1X Annexin-binding buffer and transferred into a 5 ml round bottom Falcon tube. To this, 5 µl of FITC-Annexin V and 1 µl 100 µg/ml PI was added and incubated at room temperature (20-24°C) for 15 minutes. Then, 400 µl of 1X Annexin-binding buffer was added and mixed gently before being analysed on the Novocyte NovoSampler Pro under the same conditions outlined in section 2.7.2.1.
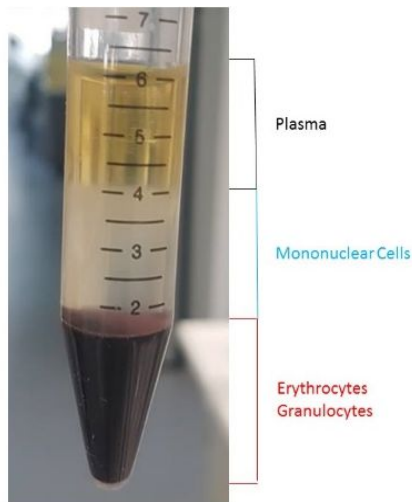


Figure 2.2. Separation of blood components after 30 minutes centrifugation with Histopaque-1077.

### 2.8.2.3. FACS Analysis

Novocyte flow cytometer results were processed with FlowJo v10 software (BD Biosciences). Compensation was performed using single-stain samples and applied to all multi-stain samples. A gating strategy was developed through which cell populations positive for the target antibody were isolated from negative populations based on both the histogram, mean fluorescence intensity (MFI) and the separation of the stained populations. For each target cell marker, plots were generated based on their relative cell counts and the MFI, and changes in cell population and marker expression were determined using the following techniques:

- Gating on positive populations of leukocytes, monocytes, neutrophils and lymphocytes to determine cell counts. Positive populations are defined as those with high expression of a given cell marker as determined by histograms and MFI (Figure 2.3 and Table 2.6).

- Mean fluorescence intensity is defined as the measure of expression of a marker-bound antibody on a certain population of cells. Positive cells are defined by an MFI that exceeds that of the unstained control.

- Cell proportions (i.e. the percentage of the total population that a given leukocyte population represents) were determined by using the following calculation:

$$\frac{Number\ of\ CD-positive\ cells}{Total\ Number\ of\ Sample\ Events}\ X\ 100$$
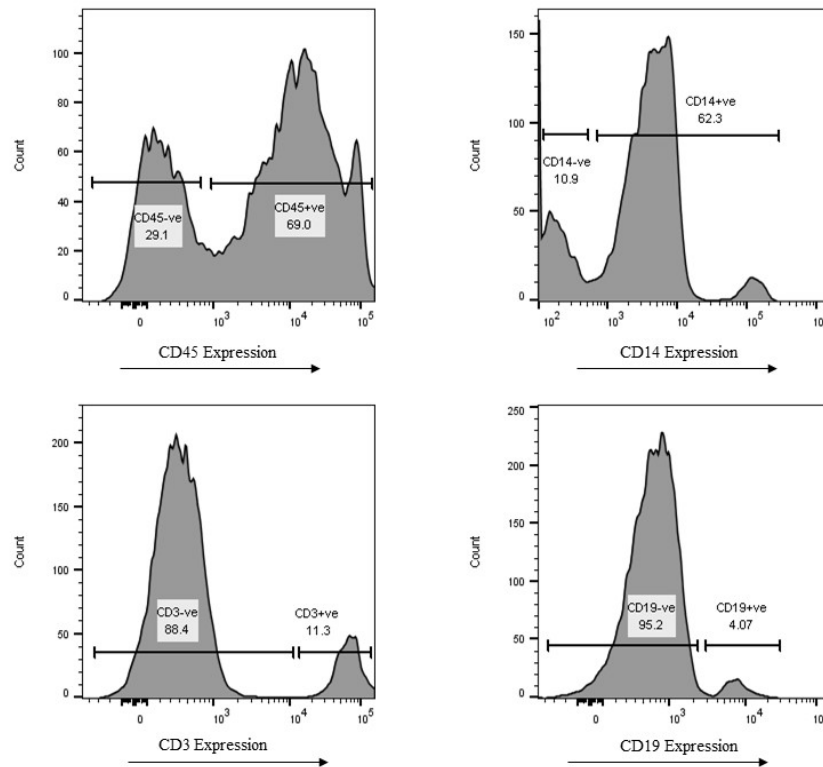


Figure 2.3. Histograms of each cellular marker (CD45, CD14, CD3 and CD19) included in whole blood characterisation. Both positive and negative populations are gated, and numbers represent the percentage of the total population that are positive or negative for that marker.

Table 2.6. Median fluorescence intensity of each cellular marker included in whole blood characterisation. Values are taken from one donor sample.

| Cell Marker | Unstained Control | Stained Positive Population | Stained Negative Population |
|---|---|---|---|
| CD45 | 254 | 21629 | 533 |
| CD14 | 255 | 49621 | 1180 |
| CD3 | 176 | 59642 | 516 |
| CD19 | 824 | 8100 | 713 |

## 2.9. Protein Analysis

## 2.9.1. Membrane Cytokine Array

The Human XL Cytokine Array Kit (R & D Systems, Biotechne Ltd, Abingdon) was used to analyse cytokine production from the whole blood of a single donor exposed to *E. coli* K12, *S. epidermidis* RP62A and *S. aureus* SH1000, with 6-hour untreated platelet-poor plasma (PPP) used as control (section 2.5.6.). Reagents were reconstituted and prepared according to the manufacturer's instructions. Membranes were also treated as per manufacturer's instructions. Membranes were imaged on the BioRad ChemiDoc XRS+ (Watford, Hertfordshire) for 15 minutes. Images were processed using ImageJ software (1.50i; Rasband, 2018) and density was averaged for each analyte spot. Background pixel density was determined from the negative control spots.

## 2.9.2. ELISA Analysis

Duoset ELISA kits (R & D Systems) were used to analyse the production of IL-6, C5a, TF3, IL-10, S100A8, S100A8/A9 (calprotectin), resistin, MIP-1α/β and MIP-3α in PPP from samples treated with the bacteria outlined in Table 2.3. Half-area plates (Greiner Bio-One, Stonehouse, UK) were used and all volumes used in the test were half that suggested in the manufacturer's protocol with the exception of the Stop Solution. For each sample, neat serum, a 1 in 10, 1 in 100 and 1 in 1000 dilution in Reagent Diluent were tested in duplicate. Solutions were reconstituted and the standards prepared corresponding to the concentrations specified in the manufacturer's instructions. The reagent diluent used in every test was 1% BSA in PBS, the Colour Reagent was SureBlue TMB 1-component microwell peroxidase substrate (SeraCare, Massachusetts) and the Stop Solution used was 1M HCl prepared as described in section 2.1.7.

For each duoset, 50 µl of the diluted Capture Antibody (provided in kit) was added to each well and incubated overnight at room temperature. The Capture Antibody was then removed by blotting the plates on absorbent paper and each well was washed with Wash Buffer (section 2.1.5.) three times. Plates were then blocked using 150 µl Reagent Diluent (section 2.1.6.) for at least one hour at room temperature. Plates were washed again three times with Wash Buffer, then 50 µl of standard (Table 2.7) or sample was added and the plates incubated at room temperature for 90 minutes. After incubation, plates were washed three times, 50 µl of Detection Antibody added to each well and incubated for 90 minutes at room temperature. Plates were then washed three times before being incubated for 20 minutes with 50 µl of the working dilution of Streptavidin-HRP in the dark at room temperature. Plates were again washed three times then 50 µl SureBlue Substrate Solution was added to each well. Plates were incubated for 10-20 minutes in the dark at room temperature until the standards changed to a blue gradient, then 50 µl Stop Solution was added to each well. The plates were then placed in a BMG Omega plate reader (BMG Labtech, Aylesbury) and the optical densities of the standards and samples measured at 450 nm. Optical densities of standards and samples were blank corrected and a 4-parameter fit was applied to generate a standard curve using the BMG Mars data analysis software (v3 02R2). An $r^2$ value of >0.8 was taken as cut-off. Sample concentrations were calculated from this standard curve.

Table 2.7. List of the standard concentrations of the kits used for ELISA analysis.

| Kit | Standard Concentrations |
|---|---|
| Human IL-6 | 9.38-600 pg/ml |
| Human C5a | 31.3-2000 pg/ml |
| Human TF3 | 7.81-500 pg/ml |
| Human IL-10 | 31.3-2000 pg/ml |
| Human S100A8 | 31.3-2000 pg/ml |
| Human S100A8/A9 | 93.8-6000 pg/ml |
| Human Resistin | 31.3-2000 pg/ml |
| Human MIP-1α | 7.81-500 pg/ml |
| Human MIP-3α | 15.6-1000 pg/ml |

## 2.10. Cholesterol and Oxysterol Determination using Mass Spectrometry

### 2.10.1. Oxidation, derivatisation and extraction of plasma for analysis of oxysterols

Changes in plasma oxysterol concentrations in blood treated with *Escherichia coli* K12 or *S. epidermidis* RP62A were measured using high performance Liquid Chromatography-Mass Spectrometry (LC-MS; Griffiths *et al.,* 2013; Crick *et al.*, 2015). All extractions and LC-MS were conducted at the Griffiths-Wang laboratory at Swansea University Medical School. Prior to extraction, standards were prepared as to the specifications outlined in Appendix A. The standard required for one extraction was multiplied by the total number of samples being extracted to give the final volume required for a batch extraction.

### 2.10.1.1. Preparation of Plasma

For each extraction batch, a water blank sample and a quality control (QC) sample was included. These QCs originate from plasma from a single donor at the Joint Clinical Research Facility (JCRF) at Swansea University. To a 1.5 ml microcentrifuge tube, 1.05 ml of prepared standards in ethanol was added. Samples were vortexed and pulsed in a centrifuge for 10 seconds before 100 µl of sample/QC/water was added drop wise to the corresponding microcentrifuge tube. Samples were then sonicated for 5 minutes before 350 µl of water was added to each tube. Samples were sonicated for a further 5 minutes before being centrifuged at 17,000 g for 30-60 minutes.

### 2.10.1.2. Solid-phase Extraction

A Vacuum Manifold Processing System (Agilent Technologies, Greater Manchester) was sterilised with 70% ethanol then fitted with Sep-Pak Vac 3cc (200 mg) Certified tc18 Cartridges (Sigma Aldrich), one for each sample that was to be extracted. Screw lock 12 ml tubes (Greiner Bio-One) were placed in the manifold to collect effluent. The cartridges were pre-conditioned using 100% then 70% ethanol, and the effluent discarded. New screw lock tubes were placed in the manifold before 1.5 ml of plasma sample/QC/water was added to the column and allowed to drip via gravity. Once the column was empty, it was washed with 6 ml 70% ethanol to elute the fraction containing oxysterols. The tubes were vortexed before the eluate was split into two tubes (3.5 ml per tube, labelled Fr1 A and B). Conditioning tubes were then placed back in the manifold and the columns washed with 70% ethanol. New tubes were placed in the manifold and fractions containing cholesterol were eluted using 2 ml 100% ethanol. The tubes were vortexed

and the eluate split into two 1 ml aliquots (labelled Fr3 A and B). All fractions were dried overnight in a Scanvac scanspeed vacuum concentrator (Thistle Scientific, Glasgow).

### 2.10.1.3. Cholesterol & Oxysterol Oxidation

After drying, the fractions were reconstituted using 100 µl 100% isopropanol. Fractions were then vortexed thoroughly before 1 ml $KH_2PO_4$ was added and samples vortexed for 1 minute. To tube A only, 3 µl of reconstituted Cholesterol Oxidase (section 2.1.16.) was added, the fractions vortexed to mix and incubated in a 37°C water bath for 1 hour. After this, the reaction in the oxysterol fraction was stopped with 100% methanol and 150 µl of glacial acetic acid. To tube A, 190 mg of $D_5$ Girard P (section 2.1.17.) was added and to tube B 150 mg of $D_0$ Girard P was added (section 2.1.17.). Fractions were vortexed until all Girard reagent had dissolved, and then incubated overnight in the dark at room temperature.

### 2.10.1.4. Reversed Solid-phase Extraction of Sterols

A Vacuum Manifold Processing System was sterilised with 70% ethanol and fitted with Oasis HLB 3cc (60 mg) Extraction Cartridges (Elstree, Herts, UK), one for each sample. The cartridges were preconditioned with 100%, 10% and 70% methanol, respectively. New tubes were placed in the manifold and both the oxysterol and cholesterol fractions were applied to the column and allowed to drip via gravity. One millilitre of 70% methanol was added to empty sample tubes, vortexed and added to the column to ensure complete addition of sterols to the column. Once the column was empty, it was washed with 35% methanol. The tubes containing the effluent were removed from the manifold and $H_2O$ added to each tube and vortexed. New tubes were placed in the manifold and the combined effluent/$H_2O$ reapplied to the column. The column was washed once empty with 17% methanol. The effluent was then combined with $H_2O$ to a final volume of 19 ml 17.5% methanol, vortexed, and reapplied to the column. Once the columns were empty, the effluent was discarded and the column washed once more with 10% methanol. Microcentrifuge tubes were placed into the manifold and the compounds of interest eluted with 3x applications of 1 ml 100% methanol and one application of 1 ml 100% ethanol. Samples were stored in a -20°C or -80°C freezer until analysis.

## 2.10.2. Preparation of Samples for MS Analysis

For each oxysterol sample, the first and second elutions of the A and B samples were centrifuged at 17000 g for 30-60 minutes. During this, mobile phases A and B (section 2.1.19.) for LC-MS were prepared and placed into the LTQ-Orbitrap Velos (Thermo Fischer Scientific). Liquid chromatography was performed with a Hypersil Gold reversed-phase column (1.9 μm particle size, 50x2.1 mm, Thermo Fischer Scientific). HPLC vials were collected and the following were prepared:

- 1-2 tubes of 19-Hydroxycholesterol (Avanti Polar Lipids).
- 2-4 tubes of 50% methanol/50% isopropanol.
- 1-2 tubes of 95% methanol.

After centrifugation of elutions A1, A2, B1 and B2 were complete, 22.5 μl of each fraction was added to 60 μl of water and vortexed. Each sample was then placed in a HPLC vial. All HPLC vials were flicked to ensure no air bubbles were present. Samples were then given to the Griffiths-Wang laboratory for analysis on the LTQ-Orbitrap Velos.

## 2.10.3. Analysis of Chromatograms

Chromatogram outputs from the LC-MS analysis were processed using Thermo Xcalibur Roadmap (Thermo Fischer Scientific). Layouts for each analyte were established using their mass ranges and the scan filters FTMS (non-targeted scan, for quantification) and TIC/ITMS (total ion chromatogram, for identification) were used to identify the analyte. Once the analyte had been identified, a peak was drawn on the FTMS chromatogram, and the peak was confirmed by checking the ion fingerprint in Xcalibur. The mass range of the peak was then exported into Excel. As the concentration of the internal standard was defined in Appendix A, the calculation below was used to determine the concentration of the target analyte:

$$\frac{Peak\ Area\ Target}{Peak\ Area\ Internal\ Standard}\ x\ Quantity\ Internal\ Standard$$

## 2.11. *E. coli* Bioinformatics and Genomics

### 2.11.1. Pan-genome Generation

*Escherichia coli* genome sequences were annotated using Prokka (Seemann 2014) and the output used to create the pan-genome in the Roary pan-genome pipeline (Page *et al*. 2015). Included in the pan-genome were the ECOR collection of genomes for reference (Ochman and Selander 1983), listed in Appendix C. The pan-genome was used to create maximum likelihood trees using iTOL v4 (Letunic and Bork, 2007).

The following command line was used to run Prokka:

```
Prokka -kingdom Bacteria -outdir E.coli_Genomes_Roary -genus Escherichia
```

The following command was used to run Roary:

```
Roary -f ./PanGenome -e -n -v ./gff/*.gff
```

### 2.11.2. Sequence Type and Phylotype Determination

The sequence type (ST) of *E. coli* isolates was determined using the following command:

```
-   mlst
```

Sequences were automatically recognised as *E. coli* and the Warwick MLST scheme was applied (Clermont 2000; Wirth 2006; Clermont 2015). Outputs included ST and allele number of each MLST gene. Phylotype was determined using the following command:

```
ezclermont .fasta
```

Isolates were assigned a phylogroup based on Clermont 2015.

### 2.11.3. GWAS using Scoary

Scoary microbial pan-GWAS (Brynildsrud *et al.* 2016) was used to assess gene associations using the file output "gene_presence_absence.csv" from Roary with a traits file that described the analysis.

The following command was used to run Scoary:

```
scoary –g gene_presence_absence.csv –t traits.csv
```

## 2.12. Statistical Analysis

Statistical analysis of all data was performed using GraphPad Prism version 7 (La Jolla, California, USA). Firstly, all data sets were tested for normality using the Shapiro-Wilks normality test, and where this was not possible ($n < 7$) data was assumed to be not normally distributed. For normally distributed data ($n > 7$), parametric T-tests, one-way ANOVAs or two-way ANOVAs with Dunn's multiple comparison tests were applied. For non-normal data, non-parametric Mann-Whitney tests or Kruskal-Wallis tests with Dunn's multiple comparison tests were applied. A p value of $<0.05$ was considered to be significant.

Other statistical representations used include coefficience of variance (CoV), which was calculated using Excel (Microsoft Office 365), and was applied where multiple controls had been used to analyse the reproducibility of the assay, and chi squared tests, which were applied to virulence data in Chapter 6.

The specified statistical tests used in each experiment are given in the individual results chapter.

## Chapter 3. Characterisation of Biomarkers in a Whole Blood Model of Bacterial Sepsis

### 3.1. Introduction

### 3.1.1. Classical Biomarkers of Sepsis

Biomarkers of the innate immune response have long been used by clinicians as useful tools for monitoring and diagnosing inflammatory diseases, such as atherosclerosis, Crohn's disease and rheumatoid arthritis (Becker *et al*., 2008; Jin and Khan, 2010). More recently, there is increasing demand for biomarkers that can specifically diagnose or exclude certain inflammatory disorders, such as sepsis, and to use them to guide antibiotic therapy and to monitor disease progression (Póvoa, 2002; Vincent, 2016). Current biomarkers in use for sepsis include CRP, IL-6, PCT and white blood cell counts (WBCCs). C reactive protein is a protein of the APR and is expressed very soon after recognition of an inflammatory insult. The expression is promoted by IL-6 in liver hepatocytes, and it has broad functions in pathogen recognition and elimination (Pepys and Hirschfield, 2003). Interleukin-6 is an acute cytokine responsible for the feverish immunopathology that manifests in numerous inflammatory disorders, and promotes differentiation of adaptive immune cells (Gruys *et al.*, 2005; Burdette *et al.*, 2010). Both CRP and IL-6 are regarded as having high sensitivity towards disease severity, but are relatively poor when it comes to specificity, often being present at elevated concentrations in numerous inflammatory and/or infectious diseases (Póvoa, 2002; Vincent, 2016). There is currently a concerted effort to identify new inflammatory biomarkers of sepsis that can be used to identify the cause of the bacteraemia with high sensitivity and specificity which in turn has applications in monitoring patient condition and the improving antibiotic therapy (Vincent, 2016).

### 3.1.2. Procalcitonin (PCT)

Procalcitonin is a biomarker that shows considerable promise. It is the pro-hormone for the calcium hormone calcitonin and is not found in the plasma of healthy people (Jin and Khan, 2010). Plasma PCT concentrations increase substantially during bacterial sepsis, and several studies have found that levels are elevated only in this condition (Gendrel and Bohuon, 2000; Schuetz *et al.,* 2007; Rowther *et al*., 2009)**.** Concentrations rise within 24 h of infection onset and remain elevated until the inflammatory insult has been removed, illustrating its use a marker of patient progress (Schuetz *et al.,* 2011). Assays have been developed that allow the clinic to quickly determine blood PCT concentrations, allowing

comprehensive results to be obtained in a short period. These factors have allowed PCT to be considered the current "gold standard" for bacterial sepsis (Jin and Khan, 2010; Schuetz *et al*., 2011). Despite this, there are still limitations to the efficacy and accuracy of using PCT as a biomarker (Jin and Khan, 2010). While most studies show consistency with the ability of PCT to distinguish bacterial sepsis from non-infectious SIRs, others have not been able to replicate this level of confidence in scrutinising different types of inflammation and informing antibiotic therapy (Chan and Gu, 2011; Schuetz *et al*., 2011; Giannakopoulos *et al*., 2017).This suggests that designing a panel of biomarkers that can accurately predict cause and course of the inflammatory response induced by infection is still a long way off.

### 3.1.3. Distinguishing Bacterial Infections

To be a clinically useful sepsis biomarker, the marker must provide additional information to the clinician that cannot be obtained from established assessments, which include the ability to accurately differentiate bacterial infection from other forms of inflammation. They must also rise above normal levels very early in the course of the infection (Kibe *et al*., 2011). Recent efforts have sought to differentiate further between classes of bacteria in blood, more specifically whether they are Gram-positive or Gram-negative (Opal and Cohen, 1999; Yu *et al*., 2004; Abe *et al*., 2010; Alexandraki and Palacio, 2010; Lang *et al*., 2017). While most studies suggest that Gram-negative organisms such as *E. coli* and *P. aeruginosa* induce much greater inflammatory responses than Gram-positive organisms such as *S. aureus* and *S. epidermidis*, there is conflicting evidence to suggest that this is not always the case (Opal and Cohen, 1999; Yu *et al*., 2004; Abe *et al.*, 2010; Alexandraki and Palacio, 2010; Lang *et al*., 2017).

### 3.1.4. Aims and Objectives

Sepsis biomarkers are often derived from the various inflammatory pathways that dictate the immunopathology of the syndrome. These pathways include, but are not limited to, proinflammatory, anti-inflammatory, coagulation, complement and phagocytic (Cohen, 2002). These pathways utilise numerous molecular mechanisms to promote their activities and represent a wealthy pool from which sepsis biomarkers can be mined. In this study, these pathways are used to investigate several candidate biomarkers of infection to determine their specificity and sensitivity towards the major sepsis causing organisms, *E. coli, S. aureus* and *S. epidermidis* (Opota *et al.,* 2015).

The aim of this chapter is to identify (cytokine microarray) and investigate (ELISA) the temporal changes in 8 candidate soluble biomarkers that represent different pathways of sepsis immunopathology in a bacterial whole blood model of sepsis. Two genera, three species, and eight strains of bacteria will be investigated over a six-hour time course to determine the diagnostic usefulness of these inflammatory molecules.

### 3.2. Methodology

### 3.2.1. Microbiology and Whole Blood

Eight bacterial strains (Table 2.3) were incubated for up to 24 hours in 5 ml of either LB or TSB media (2.5.2.) at 37°C and 200 r.p.m. Optical densities were determined at $OD_{600}$ and suspensions standardised to an OD of 0.1 in RPMI. Suspensions were centrifuged and the pellet washed with RPMI. To a 1.5 ml microcentrifuge tube, 100 µl of bacterial suspension was added to 1 ml whole blood and incubated at 37°C on a rotator set at 10 r.p.m for up to 6 hours. Samples were removed at 2, 4 and 6 hours, centrifuged and the PPP removed and frozen at -20°C (Chapter 2.5.6).

### 3.2.2. Membrane Cytokine Array

The Human XL Cytokine Array Kit was used to analyse cytokine production from the whole blood of a single donor exposed to *E. coli* K12, *S. epidermidis* RP62A and *S. aureus* SH1000 for 6 hours. Membranes were treated as per the manufacturer's instructions as described in Chapter 2.8.1 and imaged on a BioRad ChemiDoc XRS+ for 15 minutes. Images were processed using ImageJ software and density was averaged for each analyte spot. Background pixel density was determined from the negative control spots.

### 3.2.3. ELISA Analysis

The 8 molecules chosen for ELISA analysis are as follows:

- IL-6, identified by cytokine membrane array as showing promise in distinguishing between different infection types (Jones, 2005; Tanaka *et al.*, 2014). This cytokine is also currently considered a biomarker of inflammation (Harbarth *et al.*, 2001; Hou *et al.*, 2015).
- MIP-1α and MIP-3α, both identified by membrane cytokine array as showing promise as a marker of distinguishing bacterial infection. These are chemokines (Menten *et al.*, 2002).

- Resistin, identified by membrane cytokine array as showing potential as a marker of distinguishing bacterial infection. This cytokine is also linked to obesity and diabetes (Steppan and Lazar, 2002).

- S100A8 and S100A8/A9 (Calprotectin), both markers of neutrophil activation and potentially of phagocytic function (Decembrino *et al.*, 2015).

- Tissue factor 3 (TF3), a marker of coagulation pathways and of dysfunctional coagulation processes during sepsis (Landsem *et al.*, 2015).

- Complement component 5a (C5a), a marker of complement activation and indicative of bacterial clearance (Mollnes *et al.*, 2002; Klos *et al.*, 2009).

- IL-10, a marker of anti-inflammatory processes and compensatory anti-inflammatory response syndrome (CARS; Oberholzen *et al.*, 2002).

Duoset ELISA kits for IL-6, C5a, TF3, IL-10, S100A8, S100A8/A9, resistin, MIP-1α/β and MIP-3α in PPP were used to measure the production of the 8 candidate molecules in whole blood following experimental infection. Half-area plates were used and all volumes used in the test were half that suggested in the manufacturer's protocol with the exception of the Stop Solution. Solutions were prepared corresponding to the manufacturer's protocols per kit (Chapter 2.8.2). Plates were read using the BMG Omega plate reader set at 450 nm. Optical densities of standards and samples were blank corrected and a 4-parameter fit was applied to generate a standard curve using the BMG Mars data analysis software. Sample concentrations were calculated from the standard curve.

### 3.2.4. Statistical Analysis

Statistical analysis of ELISA data was performed using GraphPad Prism version 7. N numbers refer to the number of donors analysed in the test. All data was tested for normality using the Shapiro-Wilks normality test and where this was not possible ( $n < 7$ ) data was assumed to not be normally distributed. For normally distributed data, one-way ANOVAs with Dunn's multiple comparison tests were applied. For non-normal data, non-parametric Kruskal-Wallis tests with Dunn's multiple comparison tests were applied. A p value of $< 0.05$ was considered significant. On graphs, error is represented by the standard error of the mean (SEM).

### 3.3. Results

### 3.3.1. Membrane Cytokine Array

Human XL cytokine assay membranes were used to screen for biomarkers. In all four membranes, the positive reference spots were well defined, with a CoV of 18.6%. All negative reference spots showed no changes in pixel density and were not detected on the BioRad ChemiDoc XRS+ (Figure 3.1).
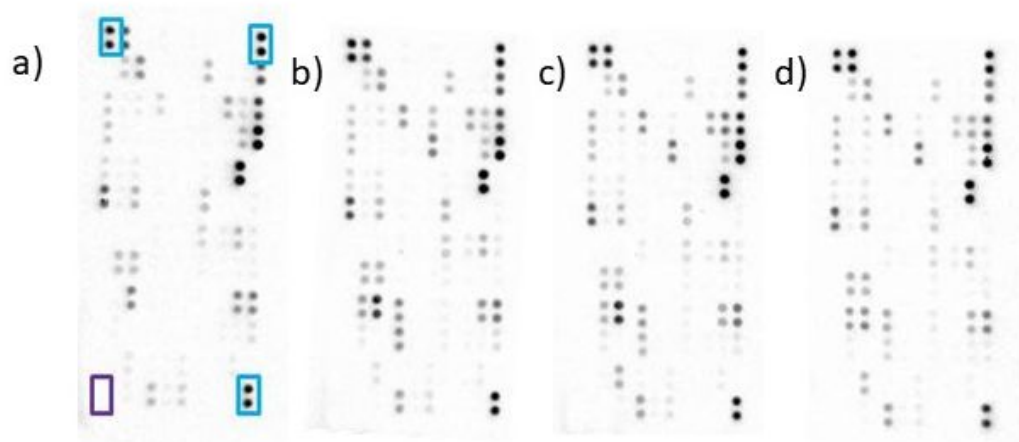


Figure 3.1. Membrane cytokine arrays for 102 soluble mediators. PPP from blood infected for 6 hours (n = 1) was added to cytokine arrays; a) control, b) *E. coli* K12-infected, c) *S. epidermidis* RP62A-infected, and d) *S. aureus* SH1000-infected. The blue boxes indicate the six positive reference spots on a single membrane, and the purple box (bottom left) indicates the position of the two negative reference spots. All plasma used on the above membranes came from the same donor.

For all proteins that showed any exposure change, the mean pixel density was calculated (Table 3.1). In total, 33/102 proteins were detected on the membrane from the 4 samples. Of these 33 proteins, 14 had a high degree of variability between the four samples (Table 3.1, grey and blue). Eight of these had variability in pixel density across treatments that were not significant (Table 3.1, grey), while six of these proteins were identified as having very low or absent pixel density in the control membrane and higher levels in infected samples (Table 3.1, blue). The remaining 19 proteins (Table 3.1, white) had consistent pixel density across all four treatments.

Table 3.1. The 33 soluble mediators identified during screening with membrane cytokine arrays (n = 1 donor). All proteins where two spots were defined on at least one membrane were scanned using ImageJ and values converted to pixels. Values represent the mean pixel density of two protein spots minus the mean of the negative control spots. Grey rows indicate differences in pixel intensity between individual membranes, blue rows substantial differences between the control membrane and at least one infected membrane, white row had consistent pixel density across membranes.

| Cytokine/Chemokine | Control | K12 | RP62A | SH1000 |
|---|---|---|---|---|
| Vitamin D BP | 2591.4 | 2162.8 | 3865 | 2390.4 |
| CD31 | 4061.4 | 2911.8 | 2343.2 | 3505 |
| TIM-3 | 2159.7 | 1947.6 | 1609.2 | 830.6 |
| VCAM-1 | 10542.4 | 10108.2 | 8925.8 | 11297.5 |
| Serpin E1 | 9492.6 | 12203.8 | 8952.4 | 15279.7 |
| SHBG | 3738.8 | 3448.3 | 2801.9 | 2709.5 |
| Thrombospondin-1 | 3798.5 | 3781 | 3171.5 | 4171.2 |
| TNF-α | 538.5 | 5518.4 | 5565.1 | 4556.2 |
| Osteopontin | 6821.7 | 6069.3 | 4286.5 | 5304.3 |
| PF4 | 4200.8 | 3851.7 | 3553.9 | 4983.1 |
| RANTES | 4482.5 | 3714.4 | 3750.8 | 3815.1 |
| RBP-4 | 7358.2 | 16338 | 10638.7 | 6582 |
| Resistin | 1192.4 | 1195.4 | 3868.4 | 3139.8 |
| Lipocalin-2 | 2343.4 | 5846.9 | 5298.5 | 5471.2 |
| MIP-1α | 10.6 | 6433.1 | 4111.4 | 3689.8 |
| MIP-3α | 162 | 8870.6 | 3308.7 | 1899.4 |
| MMP-9 | 4348.7 | 4371.7 | 5330.9 | 5299.6 |
| IL-6 | 83.3 | 2559.3 | -4.5 | 886.1 |
| IL-8 | 201.7 | 8591.9 | 6912.6 | 6982.3 |
| Growth Hormone | 2499.1 | 3165.4 | 2577.9 | 1911.5 |
| IGFBP-2 | 4201.7 | 3569.2 | 3240 | 2969.1 |
| IGFBP-3 | 2304.8 | 1776 | 1768.8 | 1661.3 |
| Endoglin | 5953.3 | 6250.3 | 4506 | 3707.7 |
| Chitinase 3-like 1 | 24036.6 | 4459.2 | 9489.4 | 5380.3 |
| Complement factor D | 5828.8 | 4887.3 | 4549.8 | 3805.3 |
| C-reactive protein | 25379 | 19983.4 | 20952.2 | 9169.7 |
| Cystatin C | 3855 | 2736 | 2384.8 | 2424.7 |
| DPPIV | 7916.3 | 4351.9 | 4202.8 | 2969.5 |
| Adiponectin | 10784.1 | 7104.1 | 10800.9 | 8578.9 |
| Apolipoprotein A-I | 13614.1 | 9024 | 18278.4 | 10572.3 |
| Angiogenin | 22382.1 | 16179.4 | 20794.6 | 18757.9 |
| C5a | 7381.4 | 8614.3 | 8501 | 6704.1 |
| CD14 | 2096.8 | 1562.5 | 1912.4 | 1306.1 |

The six proteins that were absent or very low in the control sample but significantly increased in some infected samples were plotted graphically (Figure 3.2). Tumour necrosis factor-α was increased in all infected PPP, with a 10-fold increase in pixel density in both the *E. coli* K12 and *S. epidermidis* RP62A plasma samples and an 8-fold pixel density increase in the *S. aureus* SH1000 plasma sample. Macrophage inflammatory protein-1α and MIP-1β were increased in all infected plasma samples, with a 606-fold pixel density increase in the K12 plasma sample and a 387-fold pixel density increase in both the RP62A and SH1000 plasma samples. Macrophage inflammatory protein-3α was increased in all infected plasma samples, with a 55-fold pixel density increase in the K12 plasma sample, a 20-fold pixel density increase in the RP62A plasma sample and an 11-fold pixel densityincrease in the SH1000 sample. Interleukin-6 was only increased in the K12 and SH1000 plasma samples, with a 31-fold pixel density increase and an 11-fold pixel density increase, respectively. Interleukin-8 was increased in all infected plasma samples, with a 43-fold pixel density increase in the K12 plasma sample and a 34-fold pixel density increase in both staphylococcal species. Resistin was only increased in the plasma samples infected with *S. aureus* and *S. epidermidis* (3-fold pixel density increase).
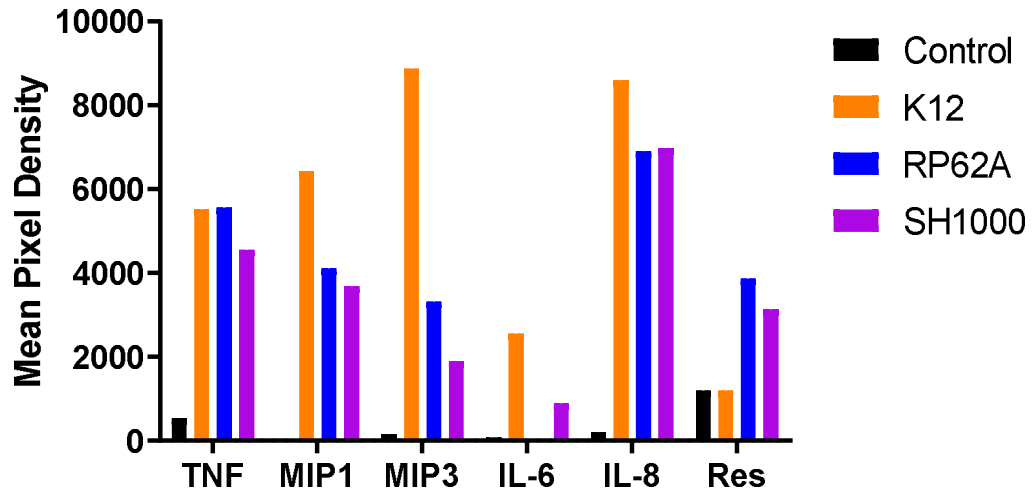
Figure 3.2. Mean pixel density of 6 substantially variable proteins following infection and membrane screening (n = 1 donor). All values represent the mean pixel density of two protein spots minus the mean of the two negative control spots.

The remaining 8 proteins are shown in grey (Table 3.1) had varying degrees of pixel density between the different membranes but was not significant. These were also plotted graphically (Figure 3.3). Of these cytokines, the largest change can be observed in Chitinase 3-like 1 (CHI3L1), CRP and retinol binding protein 4 (RBP-4). The glycoprotein CHI3L1, often associated with inflammation and cancerous processes, was high in the control plasma sample but showed a 5-fold and 3-fold decrease in the mean pixel density of K12/SH1000 plasma samples and RP62A plasma samples, respectively. The APP CRP, was generally decreased in all infected plasma samples, with the greatest reduction being in the SH1000 plasma sample (3-fold pixel density decrease). The retinol transporter protein RBP-4 was only increased up to 2-fold in pixel density in the K12 plasma sample when compared with the control plasma sample. Of the other proteins, TIM-3 was slightly lower in the infected plasma samples, Serpin E1 appeared to be slightly higher in the K12 and SH1000 plasma samples, Lipocalin-2 was slightly higher in the infected plasma samples, and both DPPIV and CD14 were slightly lower in the infected plasma samples (Figure 3.3).
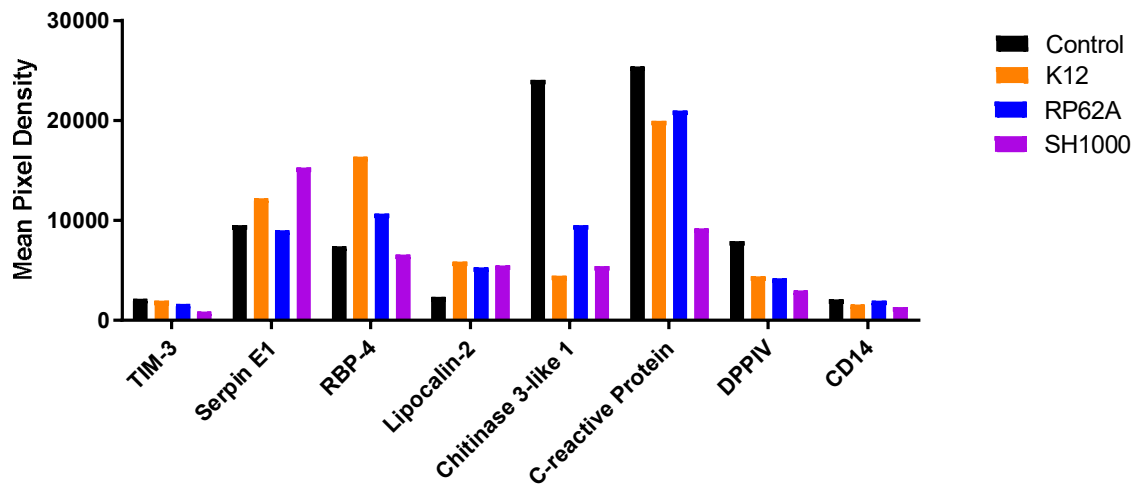
Figure 3.3. Mean pixel density of 8 variable proteins following infection and membrane screening (n = 1 donor). All values represented indicate the mean pixel density of two protein spots minus the mean of the negative control spots.

### 3.3.2. Quantitative Analysis of leading biomarkers during *ex vivo* Whole Blood Infection

Based on the findings from the membrane cytokine array kit (Table 3.1; Figure 3.2) and further reading (Mollnes *et al.,* 2002; Conway Morris *et al.,* 2009; Abe *et al.,* 2010; Alexandraki and Palacio, 2010; Decembrino *et al.,* 2015; Surbatovic *et al.,* 2015; Wang *et al.,* 2018), several cytokines, proteins or chemokines were chosen for quantitative analysis. They were IL-6, MIP-1α, MIP-3α, resistin, calprotectin (S100A8 and S100A8/A9), TF3, C5a and IL-10. Each cytokine was analysed individually and compared at 'Genera' level (*Escherichia* vs *Staphylococcus*), at 'species' level (*E. coli* vs *S. aureus* vs *S.* epidermidis) and finally at 'strain' level (RP62A vs 1457 vs SH1000 vs VAP39 vs ECOR36 vs GMB10 vs K12 vs B) over 6 hours of *ex vivo* infection.

### 3.3.2.1. IL-6

Interleukin-6 (Figure 3.4a) in the plasma of *Escherichia* samples (K12, strain B, GMB10 and ECOR26) was significantly increased compared to *Staphylococcus* infected samples (*S. aureus* SH1000 and VAP39, and *S. epidermidis* 1457 and RP62A), culminating in an extremely elevated concentration of 46593 pg/ml (5000-fold increase vs control) and 10287 pg/ml (1000-fold increase vs control), respectively. Control samples did not change over time ($p = 0.3151$). Significantly more IL-6 was consistently present in the *Escherichia* PPP than both the control and *Staphylococcus* PPP at all time points assessed ($p < 0.0001$ at all-time points).

With respect to species, *E. coli* clearly induced significantly more IL-6 production than both the control or the *S. epidermidis* or *S. aureus* species (Figure 3.4b). Both *Staphylococcus* species induced modest but significant increases in IL-6 expression (compared to the control). At 6 hours, IL-6 concentrations in *E. coli* treated PPP were magnitudes higher than the concentrations of both *Staphylococcus* treated PPP. At all-time points significantly more IL-6 was present in *E. coli* infected blood than with either of the *Staphylococcus* species ($p = 0.0013$ [2 hour], $p = 0.0015$ [4 hour], and $p < 0.00001$ [6 hour]; Figure 3.4b).

Strains of *E. coli* were found to consistently stimulate high levels of IL-6 in PPP at all time points tested (Figure 3.4c). At two hours post-infection, IL-6 induction was highest in ECOR26, with all *E. coli* strains except strain B ($p < 0.0001$) having significantly higher concentrations of IL-6 than the control PPP. Whilst RP62A-induced IL-6, no *Staphylococcus* strains induced significantly greater IL-6 concentration than was found in the healthy control. At 4 hours post-infection, IL-6 concentrations were highest in response to *E. coli* K12, with all *E. coli* strains except GMB10 having significantly higher concentrations of IL-6 than the control. Whilst IL-6 concentrations had increased in response to all *Staphylococcus* strains, no samples induced significantly greater IL-6 concentrations than in the healthy control ($p = 0.0014$). At 6 hours post-infection, all *E. coli* strains induced significantly higher IL-6 concentrations than was seen in the healthy control, with GMB10 inducing the highest concentration ($p < 0.0001$). *Staphylococcus* strains induced a slight increase in IL-6 concentration compared to the uninfected control. This increase however was not significant.

Figure 3.4. Change in IL-6 over time in response to a) Control, *Staphylococcus* and *Escherichia* genera; b) to control, *E. coli*, *S. aureus* and *S. epidermidis* species; c) and each strain plasma samples (n = 5 donors). Error bars represent the mean ± SEM. In (a), * represents significant differences between the infected and control, and * represents significant differences between the *Escherichia* and *Staphylococcus*, in (b) * represents significant differences between *E. coli* and *S. epidermidis* and * between *E. coli* and *S. aureus*, and in (c) significant differences are represented between two strains or control by black lines and asterisks indicating the level of significance between the two PPP. On graphs, asterisks represent the following significant values: * = $p < 0.05$, ** = $p < 0.01$, *** = $p < 0.001$, **** = $p < 0.0001$.

### 3.3.2.2. MIP-1α

*Escherichia* induced a greater MIP-1α response than *Staphylococcus* (Figure 3.5a), with both bacterial Genera showing increasingly higher concentrations over 6 hours. The control sample remained low throughout the experiment ($p = 0.1649$). At the 4-hour time-point, concentrations of MIP-1α decreased in *Escherichia* treated blood but increased again at 6 hours post-infection, although there was no significant differences in these values between the time points. *Escherichia* induced MIP-1α did not significantly increase over time ($p = 0.6979$); in contrast *Staphylococcus* was found to significantly increase over time ($p = 0.0319$). Significantly more MIP-1α was induced in response to *Escherichia* and *Staphylococcus* than in uninfected controls at all time points assessed ($p < 0.0001$ [2 hour], $p = 0.0047$ [4 hour], $p = 0.0008$ [6 hour]; Figure 3.5a).

With respect to species, *E. coli* induced significantly higher MIP-1α concentrations than *S. aureus* at 2 hours post-infection, but not *S. epidermidis* ($p = 0.0083$) (Figure 3.5b). However, at further time points there was no significant difference between species (Figure 3.5b).

With respect to strain induction of MIP-1α (Figure 3.5c), at 2 hours post-infection, only *E. coli* strains ECOR26, GMB10 and B induced significantly higher MIP-1α than the healthy control, whereas *E. coli* K12 induced very low levels in comparison ($p = 0.0068$). No significance was found between *Staphylococcus* strains ($p > 0.05$), which were rather low in comparison. At 4 hours post-infection, no strains induced significant levels of MIP-1α ($p = 0.0543$). At 6 hours post-infection, only strain B induced significantly high concentrations of MIP-1α compared with the healthy control ($p = 0.0312$).

Figure 3.5. Change in MIP-1α over time in response to a) control, *Staphylococcus* and *Escherichia* genera; b) control, *E. coli*, *S. aureus* and *S. epidermidis* species; and c) and each strain plasma samples (n = 5 donors). Error bars represent the mean ± SEM. In (a), * represents significant differences between the infected PPP and control PPP, and * represents significant differences between the *Escherichia* and *Staphylococcus* PPP, in (b), * represents significant differences between *E. coli* PPP and *S. aureus* PPP and in (c) significant differences are represented between two strains or control by black lines and asterisks indicating the level of significance between the two PPP. On graphs, asterisks represent the following significant values: * = $p < 0.05$, ** = $p < 0.01$, *** = $p < 0.001$, **** = $p < 0.0001$.

### 3.3.2.3. MIP-3α

There was significantly more MIP-3α induced by *Escherichia* than by control or *Staphylococcus* genera (Figure 3.6a). Consistent with IL-6 (Figure 3.4) and MIP-1α (Figure 3.5), controls were consistently low in MIP-3α and did not change over the course of the experiment ($p = 0.6430$). Both *Staphylococcus* and *Escherichia* induced significant time dependent increases in MIP-3α ($p < 0.0001$ for both genera) over the 6 hour experiment. Significantly more MIP-3α was induced by *Escherichia* than both uninfected control and *Staphylococcus* at all times tested. *Staphylococcus* significantly induced more MIP-3α than the control at the 4-hour time-point ($p < 0.0001$).

With respect to species, *E. coli* induced significantly more MIP-3α than either *S. aureus* or *S. epidermidis* ($p < 0.0001$ [2hr], $p = 0.0019$ [4hr], $p < 0.0001$ [6hr]; Figure 3.6b). At each time point, *E. coli* induced MIP-3α increased but in contrast remained at similar levels in both *Staphylococcus* species between the 4- and 6-hour time-point (Figure 3.6b).

Macrophage inflammatory protein-3α induction was clearly strain dependent (Figure 3.6c). At 2 hours post-infection, ECOR26 and GMB10 induced significantly more MIP-3α than the uninfected control ($p = 0.0009$). The *Staphylococcus* strains induced lower MIP-3α levels than the *E. coli* strains. At 4 hours post-infection, *E. coli* ECOR26, GMB10 and K12 had significantly greater concentrations of MIP-3α than the uninfected control ($p = 0.0019$, Figure 3.6c). *Staphylococcus* strains induced MIP-3α at 4 hours but were not significantly different to the control ($p > 0.05$). At 6 hours post-infection, all *E. coli* strains induced significantly higher MIP-3α concentrations than uninfected controls, while concentrations of MIP-3α remained consistent with results at 4 hours post-infection following *Staphylococcus* strain stimulation ($p = 0.0003$, Figure 3.6c).
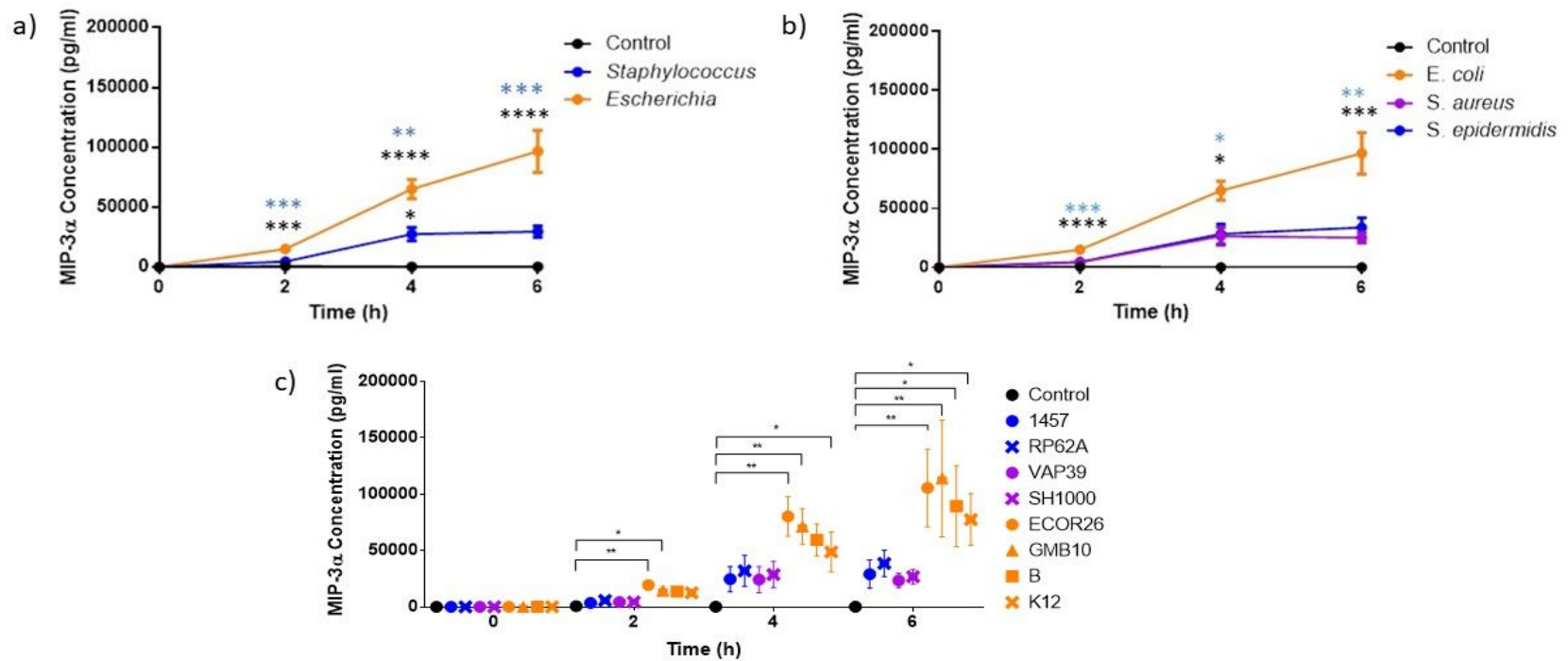
Figure 3.6. Change in MIP-3α concentration over time in response to a) control, *Staphylococcus* and *Escherichia* genera; b) control, *E. coli*, *S. aureus* and *S. epidermidis* species; and c) each strain plasma samples (n = 5 donors). Error bars represent the mean ± SEM. In (a), * represents significant differences between the infected PPP and control PPP, and * represents significant differences between the *Escherichia* and *Staphylococcus* PPP, (b) * represents significant differences between E. coli PPP and *S. aureus* PPP, and * represents significant differences between *E. coli* PPP and *S. epidermidis* PPP, and (c) significant differences are represented between two strains or control by black lines and asterisks indicate the level of significance between the two PPP. On graphs, asterisks represent the following significant values: * = $p < 0.05$, ** = $p < 0.01$, *** = $p < 0.001$, **** = $p < 0.0001$.

### 3.3.2.4. Resistin

Time dependent changes in resistin were observed in response to *Staphylococcus* and *Escherichia* genera and even uninfected control (Figure 3.7a). The control significantly increased between 2 and 4 hours but returned to baseline at 6 hours ($p = 0.0055$). In contrast, both genera induced more resistin than the uninfected control by 4 hours post-infection. However, *Escherichia* treated PPP contained more Resistin at 6 hours than the *Staphylococcus* treated PPP. Both *Staphylococcus* and *Escherichia* induced significant resistin concentrations between 2 and 4 hours compared with the control ($p < 0.0001$ for both). Only at 2 and 6 hours did *Escherichia* induce significantly more resistin than the uninfected control ($p = 0.0287$ and $p = 0.0042$, respectively).

With respect to species, both *E. coli* and *S. aureus* induced slightly more resistin than uninfected control and *S. epidermidis* (but this was not significant; Figure 3.7b). At 4 hours post-infection, all stimuli induced resistin; again, both *E. coli* and *S. aureus* induced higher concentrations than the uninfected control or *S. epidermidis,* but this was not significant. At 6 hours post-infection, this trend continued and demonstrated significant differences between the species ($p = 0.0107$); however, a Dunn's multiple comparison test did not reveal any differences between the treatment groups.

Resistin induction in blood was found to vary between different bacterial strains (Figure 3.7c). At 2 hours post-infection, only GMB10 induced significant increases compared to control ($p = 0.0051$). At 4 hours post-incubation, SH1000, ECOR26 and GMB10 induced significantly higher levels of resistin than the uninfected control ($p = 0.0012$). At 6 hours post-infection, SH1000 and GMB10 induced significant increases in resistin compared to uninfected control. In addition, SH1000 (the highest concentration of resistin detected) induced significantly higher levels of resistin than strain 1457 ($p = 0.0005$).
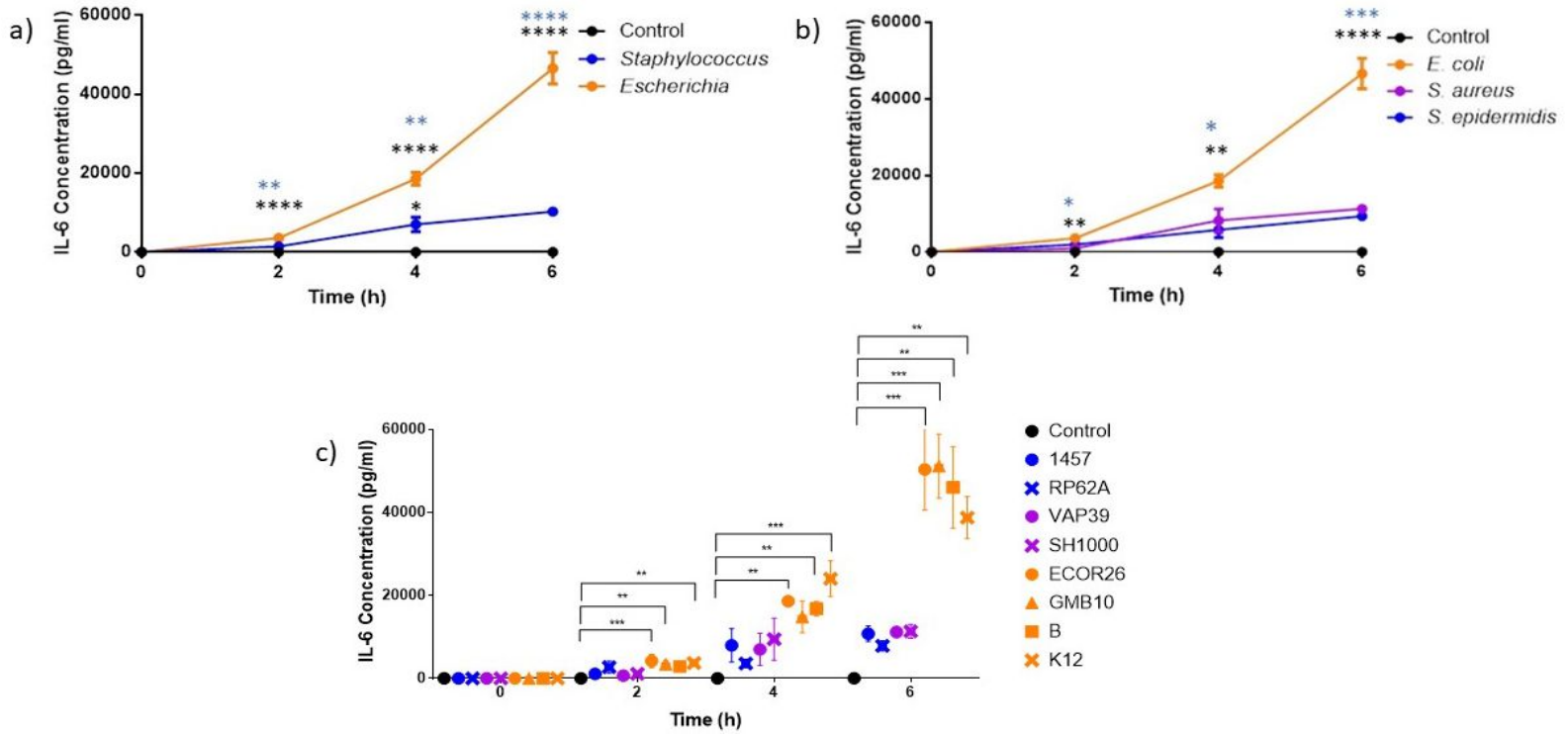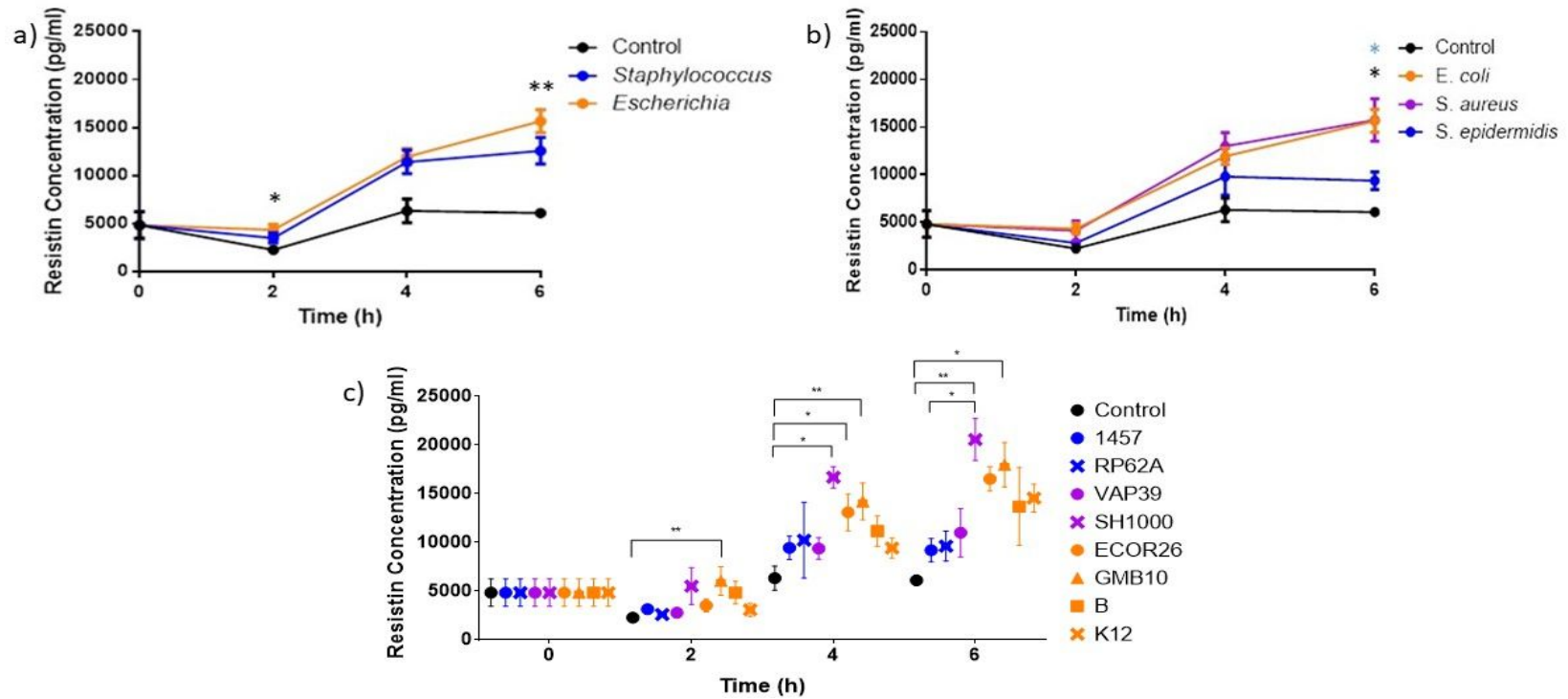
Figure 3.7. Change in resistin concentration over time in response to a) control, *Staphylococcus* and *Escherichia* genera; b) control, *E. coli*, *S. aureus* and *S. epidermidis* plasma species; and c) each strain plasma samples (n = 5 donors). Error bars represent the mean ± SEM. In (a), * represents significant differences between the infected PPP and control PPP, in (b) * represents significant differences between *E. coli* PPP and *S. epidermidis* PPP, and * represents significant differences between *S. aureus* PPP and *S. epidermidis* PPP, and in (c) significant differences are represented between two strains or control by black lines and asterisks indicate the level of significance between two PPP. On graphs, asterisks represent the following significant values: * = $p < 0.05$, ** = $p < 0.01$.

### 3.3.2.5. Calprotectin

Calprotectin in both its active (S100A8/A9) and inactive (S100A8) form was chosen for ELISA analysis to monitor the extent of neutrophil activation in the whole blood model and to analyse its use as a biomarker of antimicrobial activity.

### 3.3.2.5.1. S100A8

The profile of S100A8 production over time was a characteristic 'bell' shape with very little difference between treatments (Figure 3.8a). During the first 2 hours, the concentration of S100A8 rapidly increased in all treatment groups, but after 4 hours and 6 hours all sample groups demonstrated a significant decline in S100A8 concentrations ($p = 0.0478$ [Control], $p = 0.0107$ [*Staphylococcus*] and $p = 0.0007$ [*Escherichia*]). At no time point were any of the treatment groups significantly different in S100A8 concentration ($p = 0.7655$ [2 hour], $p = 0.7650$ [4 hour], $p = 0.1153$ [6 hour]; Figure 3.8a).

A similar trend was seen when bacterial species was assessed (Figure 3.8b). All treatment groups induced a non-significant increase in S100A8 concentration at 2 hours post-infection, with *E. coli* inducing the highest concentration and *S. aureus* the lowest. Then there was a substantial decline in the concentration of S100A8 in all treatment groups up to 6 hours post-infection. At no time-point was there any significant difference between any of the treatment groups ($p = 0.736$ [2 hour], $p = 0.6195$ [4 hour], $p = 0.6552$ [6 hour]; Figure 3.8b).

Induction of S100A8 incubated with different *E. coli, S. aureus* and *S. epidermidis* strains remained consistent to the species and genera grouping (Figure 3.8c) producing a characteristic 'bell' shaped curve. S100A8 was induced by 2 hours post infection in all groups with SH1000 inducing the lowest concentration and RP62A the highest. After the 2-hour time-point, all samples experienced a substantial decline in the concentration of S100A8, with the lowest concentration at the end of the experiment in control PPP and the highest in SH1000 PPP. At no time point was there any significant association between strain and S100A8 concentration ($p = 0.6442$ [2 hour], $p = 0.1537$ [4 hour], $p = 0.0397$ [6 hour]).

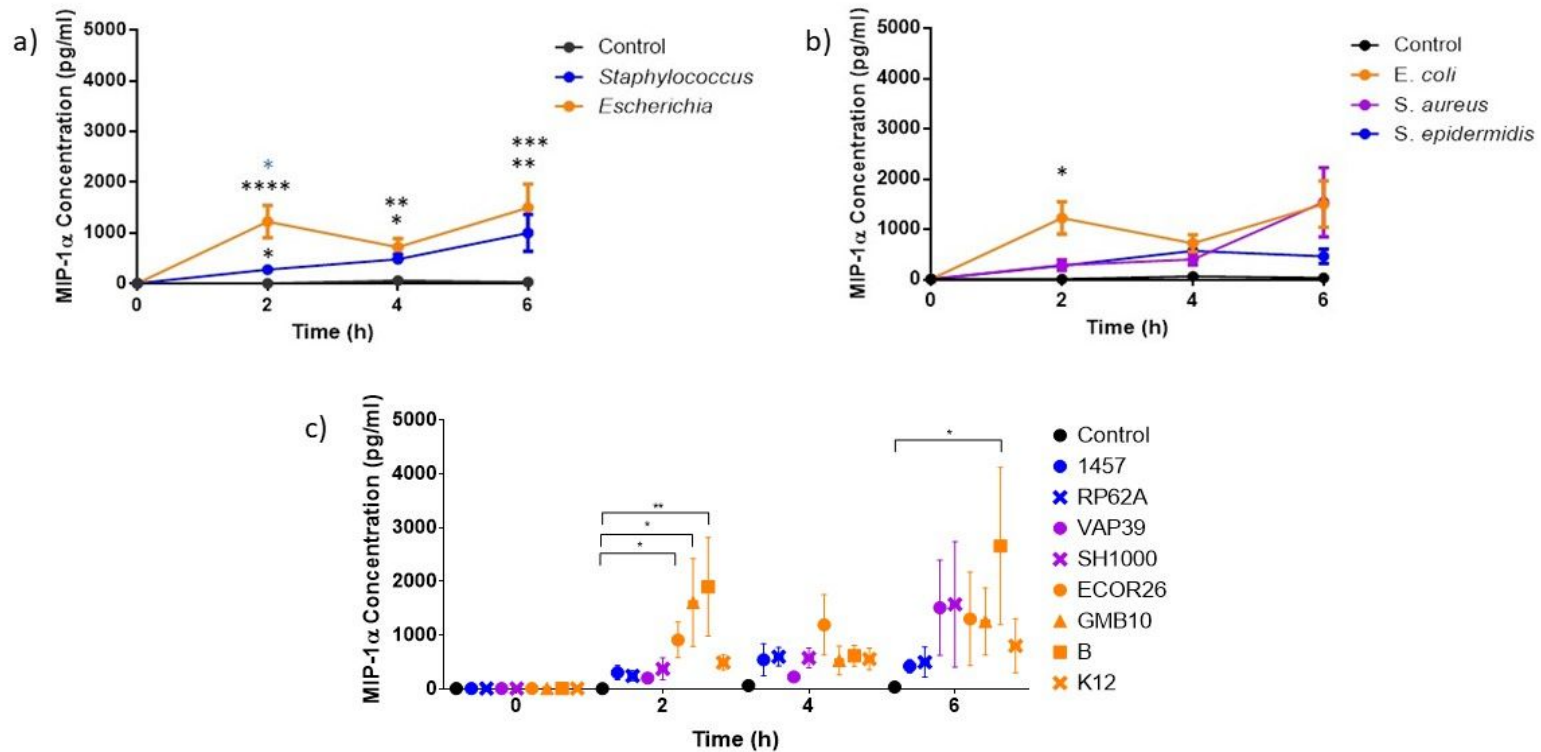Figure 3.8. Change in S100A8 average concentration over time in response to a) control, *Staphylococcus* and *Escherichia* genera; b) control, *E. coli*, *S. aureus* and *S. epidermidis* species; and c) each strain plasma sample (n = 5 donors). Error bars represent the mean ±SEM.

### 3.3.2.5.2. S100A8/A9

The concentration of S100A8/A9 increased in all samples during the infection period (Figure 3.9a). Calprotectin (S100A8/A9) concentration increased, but with no differences between experimental groups at the 2-hour time-point. At no time point was there any significant differences between treatment groups ($p$ = 0.2391 [2 hour], $p$ = 0.2247 [4 hour], $p$ = 0.1455 [6 hour]). There was no significant change in S100A8/A9 concentration over time in control samples ($p$ = 0.1837); however, both *Staphylococcus* ($p$ < 0.0001) and *Escherichia* ($p$ < 0.0001) significantly induced increasing concentrations of S100A8/A9 over the course of the experiment (Figure 3.9a).

A very similar trend in S100A8/A9 was seen with respect to bacterial species (Figure 3.9b). At 2 hours post-infection no significant differences in S100A8/A9 could be detected between control and infected samples. At later time points infected samples induced more S100A8/A9. At 6 hours post-infection, the highest average concentration of S100A8/A9 was induced by *S. aureus* although there were no significant differences. At no time point was there any significant difference between any of the treatment types ($p$ = 0.2306 [2 hour], $p$ = 0.4047 [4 hour], $p$ = 0.0824 [6 hour]; Figure 3.9b).

*Escherichia coli, S. aureus* and *S. epidermidis* strains showed considerable variability in their induction of S100A8/A9 over the time course (Figure 3.9c). While S100A8/A9 increased over the initial 2-hour incubation there were no significant differences between treatments ($p$ = 0.5671). At 4 hours post-infection, considerable variability was observed between individual *Staphylococcus* strains. In particular, SH1000 induced higher S100A8/A9 ($p$ = 0.0868) which reached significance at 6 hours post-infection ($p$ = 0.0136; Figure 3.9c).
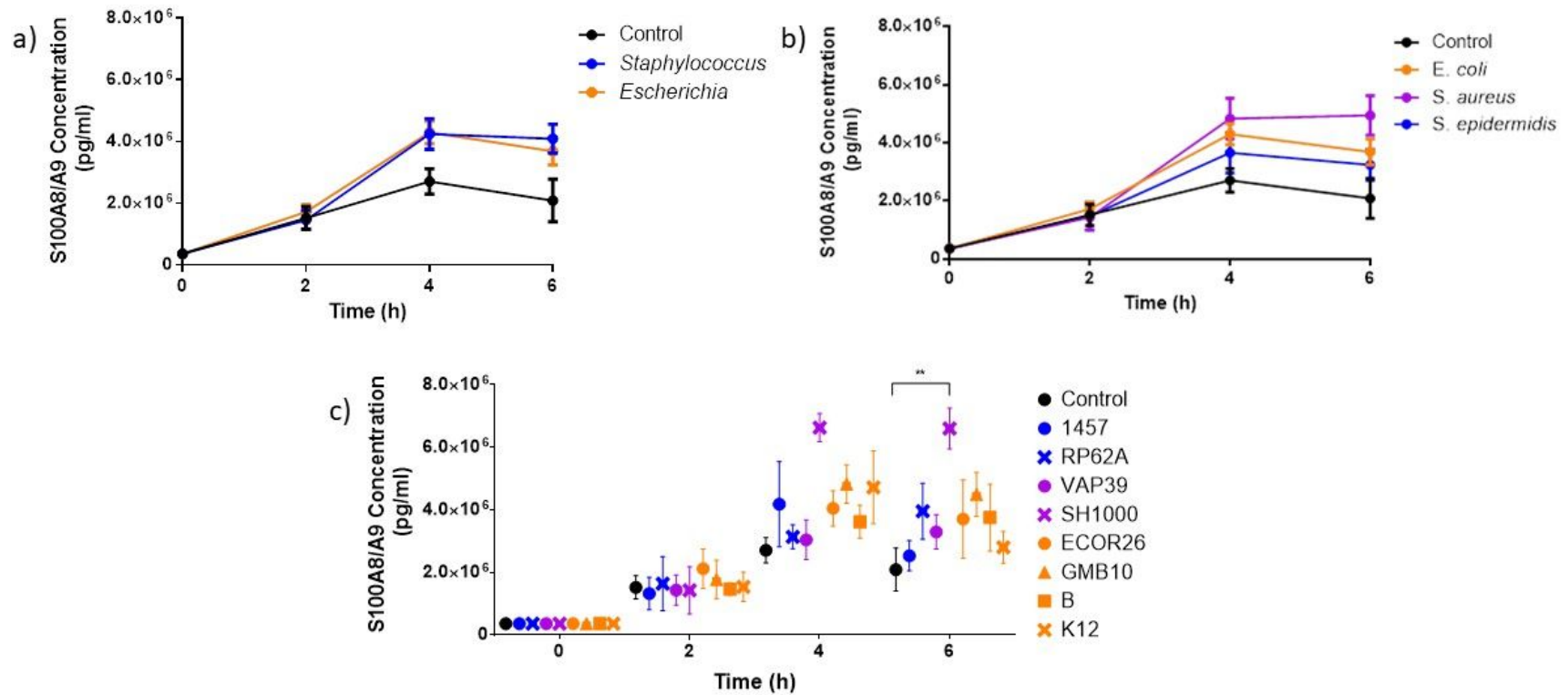
Figure 3.9. Change in S100A8/A9 average concentration over time in response to a) control, *Staphylococcus* and *Escherichia* genera; b) control, *E. coli*, *S. aureus* and *S. epidermidis* species; and c) each strain plasma sample (n = 5 donors). Error bars represented the mean ±SEM. In (c), significant differences are represented between two strains or control by black lines and asterisks indicating the level of significance between the two PPP. On graphs, asterisks represent the following significant values: ** = $p < 0.01$.

### 3.3.2.6. Human Coagulation Factor III/Tissue Factor (TF3)

Tissue factor 3 was not detected in samples taken at 2 and 4 hours post-infection. However, TF3 could be detected at 6 hours post-infection (Figure 3.10a). At genera, species and strain level there was no significant difference between uninfected controls or treatment groups ($p = 1.477$, genera; $p = 0.7839$, species; $p = 0.0683$, strain). Both *S. aureus* and *S. epidermidis* induced very similar concentrations of TF3 at 6 hours post-infection, which were marginally (but not significantly) higher than those induced by *E. coli* or uninfected control (Figure 3.10b). One donor sample induced by *E. coli* K12 was found to contain no TF3.
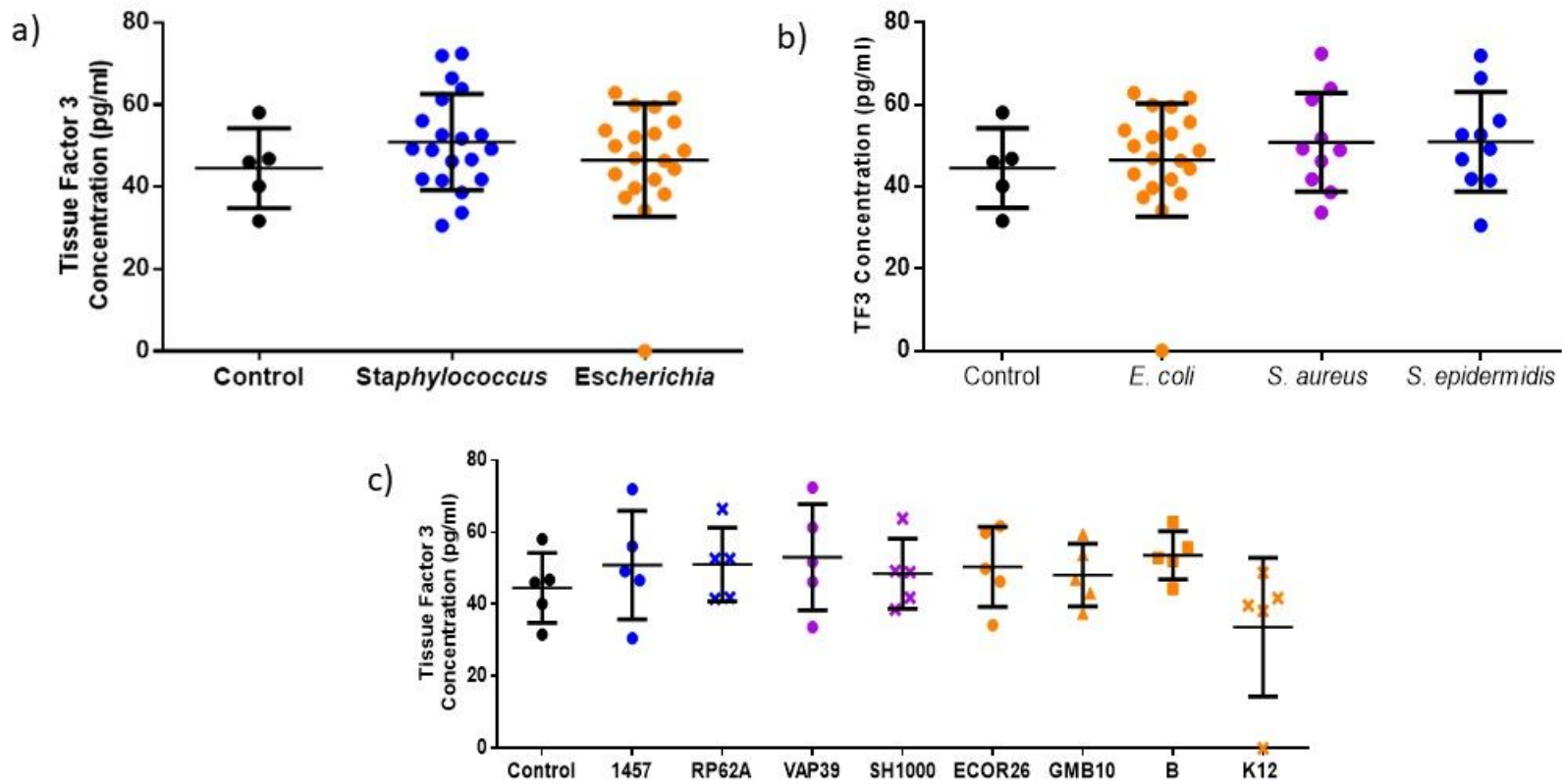
Figure 3.10. Change in TF3 average concentration at 6 hours post-infection in response to a) control, *Staphylococcus* and *Escherichia* genera; b) control, *E. coli*, *S. aureus* and *S. epidermidis* species; and c) each strain plasma sample (n = 5 donors). Error bars represent the mean ±SEM.

### 3.3.2.7. C5a

*Staphylococcus* and *Escherichia* both induced C5a in blood over the 4 hour experiment (Figure 3.11a). No significant differences were identified at 2 hours post-infection ($p = 0.1595$), but at 4 hours *Escherichia* induced significantly more C5a than *Staphylococcus* or control ($p = 0.0044$). The control did not significantly change in C5a concentration with time ($p = 0.0952$) but both *Staphylococcus* and *Escherichia* significantly induced C5a over time ($p < 0.0001$ in both cases).

With respect to bacterial species, the C5a data was consistent with the data on genera (Figure 3.11b). The C5a concentration at 2 hours post-infection was very similar in all treatment groups. *Escherichia coli* induced the highest concentration of C5a at 4 hours post-infection, and both *S. aureus* and *S. epidermidis* induced almost identical average concentrations. However, no differences were found between treatment group and C5a concentration at any time point ($p = 0.4135$ [2 hour], $p = 0.4359$ [4 hour]; Figure 3.11b).

With respect to strain, at 2 hours post-infection, only strain B was found to induce significantly more C5a than the control ($p = 0.0064$). Considerable variation in induction of C5a was seen at 4 hours post-infection (Figure 3.11c). At 4 hours post-infection statistical tests indicated that there was an association between strain and C5a concentration ($p = 0.0424$) but a Dunn's multiple comparison test did not find any associations. The C5a induced at this time point was highly variable in response to most strains, with the highest concentration detected in response to ECOR26 and the lowest in response to K12 (Figure 3.11c).
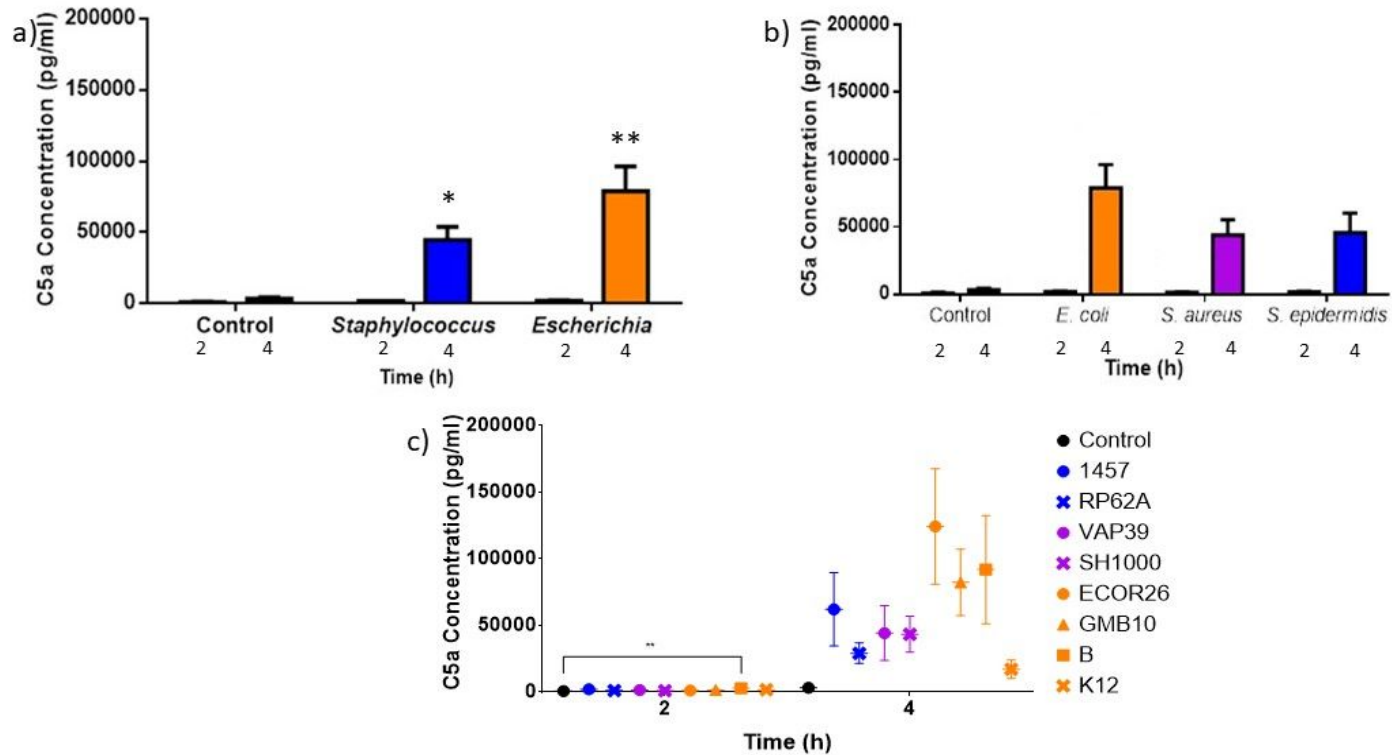
Figure 3.11. Change in C5a average concentration at 2- and 4-hours post-infection in response to a) control, *Staphylococcus* and *Escherichia* plasma samples; b) control, *E. coli*, *S. aureus* and *S. epidermidis* species; and c) each strain plasma sample (n = 5 donors). Error bars represent the mean ±SEM. In (a), * represents significant differences between the infected PPP and control PPP and in (c) significant differences are represented between two strains or control by black lines and asterisks indicating the level of significance between the two PPP. On graphs, asterisks represent the following significant values: * = $p < 0.05$, ** = $p < 0.01$.

### 3.3.2.8. IL-10

No IL-10 was detected at 2- and 4-hours post-infection, therefore only data taken at 6 hours post-infection are shown (Figure 3.12a). In general, relatively low levels of IL-10 were detected in response to all treatments. However, both *Staphylococcus* and *Escherichia* had higher average concentrations of IL-10 than the control, but no significant difference was found between bacterial genera and control induced IL-10 ($p = 0.0823$). With respect to species, results were consistent with that seen for bacterial genera (Figure 3.12b). Again, *E. coli* induced more IL-10 than the staphylococcal species but no significant differences were found between treatment groups ($p = 0.0840$; Figure 3.12b). Considerable variation in IL-10 concentration was evident in blood induced by each strain (Figure 3.12c). The highest average concentration of IL-10 was found in response to GMB10 and the lowest in response to RP62A (Figure 3.12c). No significant differences were found between strains ($p = 0.1322$).
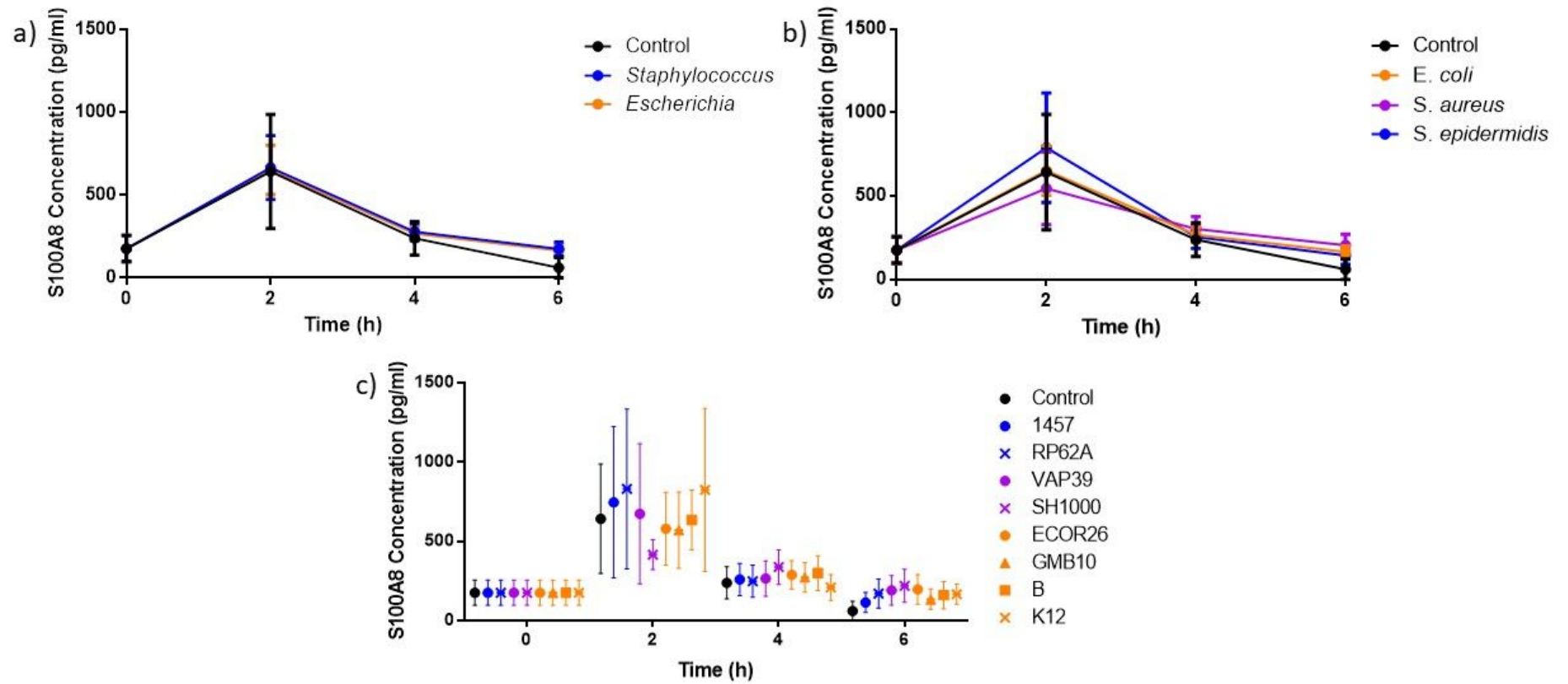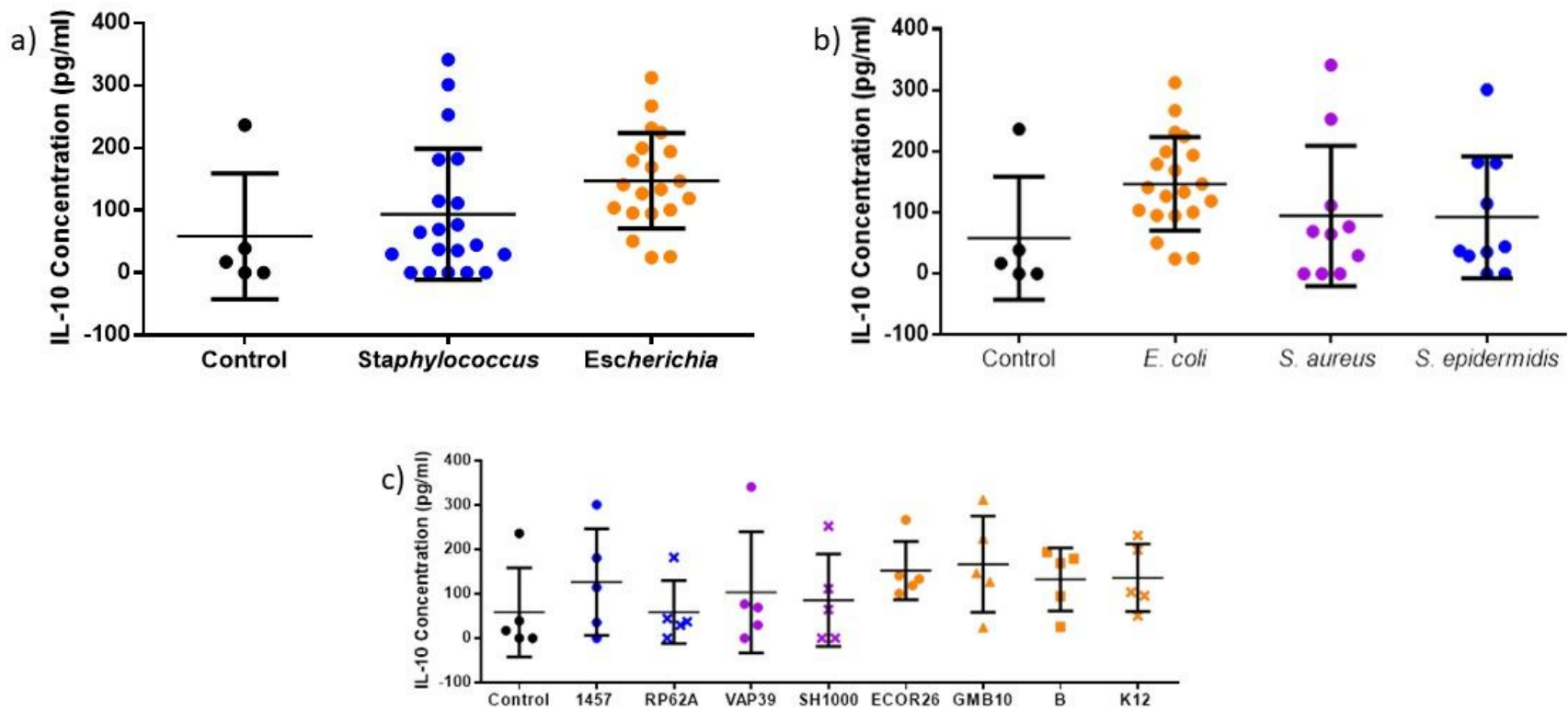
Figure 3.12. Change in IL-10 average concentration at 6 hours post-infection in response to a) control, *Staphylococcus* and *Escherichia* genera; b control, *E. coli*, *S. aureus* and *S. epidermidis* species; and c) each strain plasma sample (n = 5 donors). Error bars represent the mean ±SEM.

## 3.4. Discussion

Sepsis represents one of the most significant challenges in diagnostic medicine due to the complexity and redundancy of the innate immune response. The cytokine storm and subsequent pathologies initiated during the response are multi-factorial, and the causes of both sepsis and SIRS are numerous and difficult to distinguish (Becker *et al.*, 2008). These difficulties are exacerbated further by the requirement of different antibiotics to treat different infections, as choosing the wrong treatment could be detrimental to the patient and would significantly contribute to the current antibiotic resistance crisis (Póvoa, 2002). While bacteria remain the predominant cause of sepsis, diagnosis is further complicated by the influence that different bacterial groups (Gram-positive vs. Gram-negative) have on the immune response. Historically, Gram-negative bacteria were noted as inducing a significantly greater and earlier immune response than seen in Gram-positive infections (Surbatovic *et al.*, 2015). Consistent with this are results in the ICU, where Gram-negative bacteria are the most common cause of septic shock (Fournier and Philpott, 2005; Surbatovic *et al.*, 2015).

In this study, the immune response of 8 proteins were measured using an *ex vivo* whole blood model, in response to 8 bacterial strains (including 2 genera and 3 species) to determine their application as clinical biomarkers of infection and sepsis. The membrane array identified 6 proteins that showed considerable variations between different bacterial strains and uninfected control, four were chosen from this selection, and IL-8 and TNF-α were not chosen to include in further study as they are very early cytokines that are markers of general inflammation and have relatively little discriminatory power (Alexandraki and Palacio, 2010; Ye *et al.*, 2014; Dolin *et al.*, 2018). They have also been the subject of numerous studies in the past (Rigato *et al.*, 1996; Gordon *et al.*, 2004; Hong *et al.*, 2014; Macdonald *et al.*, 2014; Kraft., 2015, Hu *et al.*, 2016; Roderburg *et al.*, 2016), and show relatively poor discriminatory power in distinguishing the cause of sepsis (Biron *et al.*, 2015). Other immune biomarkers, including CRP and PCT, were not included. CRP was not included as it is primarily produced in liver hepatocytes, and therefore change in concentration over time would not be an appropriate measure in the whole blood model alone. The presence of CRP in the cytokine membrane array was surprising, but the finding was more likely due to the donor's inflammatory state prior to bacterial exposure, and similar findings had been noted in a previous study (Pepys and Hirschfield, 2003). We did measure PCT but the ELISAs could not detect any PCT in

either serum or standards, an issue that could not be rectified by using different kits or by using industry grade reagents.

In this study, an *ex vivo* whole blood model was used to investigate potential biomarkers of infection. *Ex vivo* whole blood models have been used previously to investigate bacterial-host cell interactions and human biomarkers of infection and sepsis (Mollnes *et al.*, 2002; Al-Ishaq *et al.*, 2015). They have numerous advantages, as they remove the need to dose healthy volunteers with potentially detrimental LPS and limits the ethical considerations for application (Mollnes *et al.*, 2002). Live bacteria can be applied in laboratory settings to multiple donors that eliminate the risk of exposure. Further, the use of an *ex vivo* model allows for strict control of laboratory and methodological procedures; all samples are treated and dosed the same, and experimental error is minimised by controlling for incubation conditions. Additionally, live bacteria can be applied to the model, which allows for a more accurate representation of clinical sepsis and allows for the testing of multiple strains and species that best reflect the disease. However, limitations also exist with this type of model. There are of course costs to using an *ex vivo* model (£21/donor), and the significant degree of variability observed between donors is still very much evident; this variability is something that can be minimised but cannot be truly eliminated as it reflects the diverse biological variation in humans. Furthermore, this model only allows for acute modelling of early sepsis interactions, as healthy blood cannot be sustained outside the body for longer than 6, perhaps 8 hours. Additionally, collection of healthy blood requires the use of an anti-coagulant that is present throughout the entire experiment. Anti-coagulants interfere with numerous inflammatory processes, particularly the complement and coagulation cascade, and therefore it is difficult to understand interactions in both these pathways, which are heavily involved in the development of severe sepsis. However, the use of anti-coagulants is unavoidable, and other studies (Mollnes *et al.*, 2002; Al-Ishaq *et al.*, 2015), both animal and human models, would have to use anti-coagulants at some point, suggesting that the use of anti-coagulants here are unavoidable. Finally, despite the risk of drop-out being minimised with lower health risks and monetary gain, a good healthy volunteer compliance is needed for scheduled blood draw. This factor is of course beyond the control of the scientist.

Modelling systemic inflammation and sepsis has always been a challenge. Animal models using mice and rats are useful for understanding early immunopathological changes and organ dysfunction. However, such studies are flawed by major inter-species differences in the magnitude of the immune response and the amount of stimuli required to trigger a

response (Andreasen *et al.*, 2008). Mice are most commonly used as sepsis models as they are small, readily available and easily manipulated by laboratory personnel (Fink, 2014). Additionally, numerous strains have been produced genetically and they possess very similar inflammatory mechanisms to humans. However, some strains of mice are hyporesponsive to LPS compared with humans. The $LD_{50}$ is approximately 1-25 mg/kg in mice, a dose 1000-fold higher than is required to induce severe illness in humans, and a dose 1000000-fold higher than the dose used in endotoxaemia human models (Fink, 2014). The human endotoxin model has been used for over 50 years to understand both acute and chronic systemic inflammation in healthy human volunteers (Andreasen *et al.*, 2008). It involves the intravenous application of purified LPS usually from *E. coli*, which induces systemic inflammation similar to that of early sepsis. The highest doses of LPS used range from a bolus injection of 2-4 ng/kg body weight (BW), which simulate acute systemic inflammation, and low doses range from either a bolus injection or continuous infusion of 0.06-0.02 ng/kg body weight, which simulates chronic inflammation. Lipopolysaccharide can be measured in the blood plasma after a few minutes post-injection and is often cleared in the blood after 15 minutes. It is transported to the liver, where it is degraded and excreted in the faeces and urine (Andreasen *et al.*, 2008). This model has been useful for studying the cytokine and chemokine kinetics after endotoxin exposure, and is useful for studying early acute responses during sepsis (Andreasen *et al.*, 2008). However, there are numerous disadvantages to using the human endotoxic model. The highly variable nature of sepsis, both between patients and other aspects of the disease, such as age, gender and comorbidities complicate the majority of clinical studies and experimental models (Kamisoglu *et al.*, 2015). There are considerable ethical considerations, particularly for the patients themselves, as they experience no direct benefits while taking significant risks. Further, the dose of LPS required to mimic severe sepsis is ethically irresponsible and particularly dangerous for the volunteer, and such interactions cannot be investigated (Andreasen *et al.*, 2008). Additionally, using healthy volunteers as opposed to using volunteers with comorbidities such as diabetes and cancer is not representative of the majority that will develop sepsis (Andreasen *et al.*, 2008). Lipopolysaccharide is also an insufficient stimulus for modelling systemic responses, as often live bacteria are the cause of sepsis (Andreasen *et al.*, 2008; Kamisoglu *et al.*, 2015).

A major finding of this chapter was that *E. coli* strains induced an inflammatory response that was magnitudes greater than that induced by either *S. aureus* or *S. epidermidis*. *E. coli* is a Gram-negative bacterium, while *S. aureus* and *S epidermidis* are Gram-positive.

The key distinction between these classes of bacteria are based on cell wall composition; both have cell walls composed of PGN, a macromolecule that is present in a much thicker layer in Gram-positive bacteria. Gram-negative bacteria have a much thinner layer of PGN but are coated with a layer of LPS, also known as endotoxin. Lipopolysaccharide is known to induce an immune response that is magnitudes greater than that of PAMPs from Gram-positive bacteria (Abe et al., 2010). Interleukin-6 and MIP-3α in particular show the greatest promise in distinguishing between these two very different classes of bacteria (Figure 3.13). An association between Gram-negative bacterial sepsis and elevated IL-6 concentrations has been discussed previously, and assertions that IL-6 is not a specific biomarker may be misguided (Abe *et al*., 2010; Alexandraki and Palacio, 2010; Surbatovic *et al*., 2015; Ninkovic *et al*., 2016). Abe *et al* (2010) found that in bacteraemia patients, elevated IL-6 concentration was significantly associated with Gram-negative bacteraemia, and a similar trend was observed by Surbatovic *et al* (2015).  If a bacterial infection is suspected, IL-6 could be used as a biomarker for distinguishing between Gram-positive and Gram-negative infection based on a threshold concentration. Interleukin-6 concentrations slowed across time with *Staphylococcus* samples but continued to substantially increase with *Escherichia* samples. This potentially has applications in monitoring disease severity.
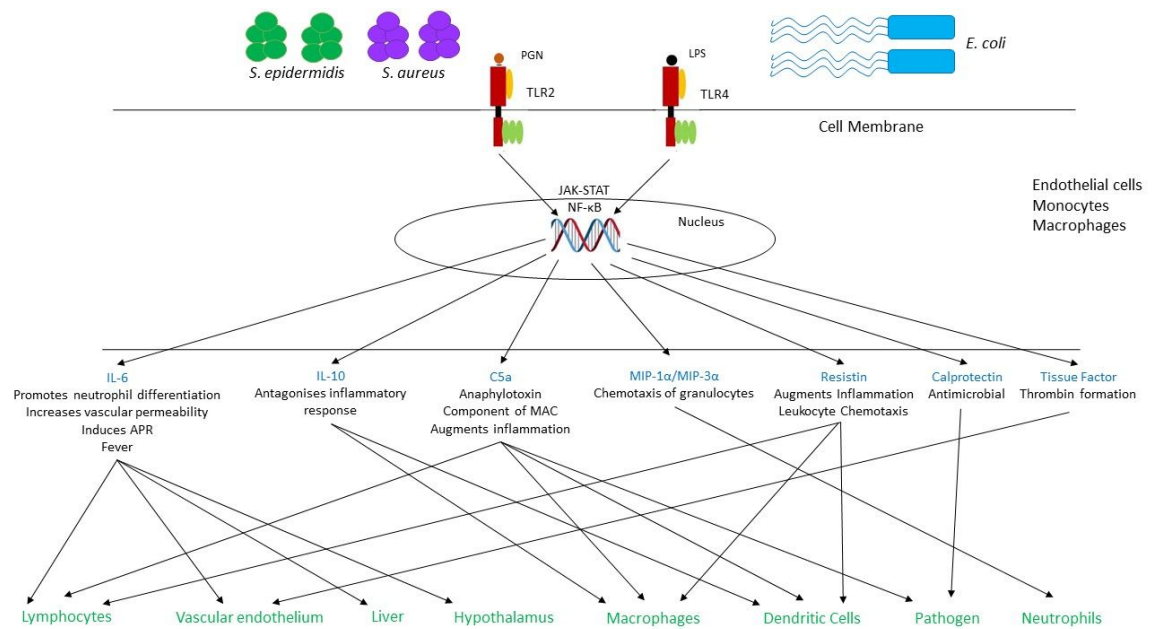
Figure 3.13. Soluble mediators (blue) analysed in this study including their targets (green) and main effect (black).

Macrophage inflammatory protein expression often strongly correlates with IL-6 (Figure 3.13). Most interestingly, the pattern of expression of MIP-3α closely mimicked that of IL-6. Much higher MIP-3α concentrations were detected at the end of the experiment compared with IL-6, which supports the observation that expression of MIP proteins upregulates IL-6 expression during inflammation (O'Grady *et al*., 1999). For both *Staphylococcus* and *Escherichia*, the trend in expression for both proteins is strongly correlated. While there is limited studies on the biomarker potential of MIP-1α and MIP-3α with regards to sepsis, O'Grady *et al* (1999) analysed a limited number of sepsis patients (20 patients, age 2-37) for MIP-1α concentration from admission. They found that MIP-1α concentrations were elevated on admission (24.2 pg/ml) but decreased substantially over the next couple of days (O'Grady *et al.* 1999). This is in contrast with the current findings, as the average concentration of MIP-1α at 4 hours (earliest time of symptom manifestation) was approximately 1000 pg/ml, magnitudes higher than reported here. This could however be an experimental discrepancy, as O'Grady *et al* (1999) used 20 patients of mixed infections whereas in the present study only live bacteria was used in an experimental *ex vivo* model. Confounding factors such as cause of infection and length of time to blood sampling could alter the reported results.

Resistin was surprisingly identified as a potential candidate biomarker by the cytokine array, and at 2- and 6-hours post-infection was found to be significantly ($p < 0.05$) induced by *Escherichia* compared to control. However, it was not found to be significantly greater (p > 0.05) than the resistin induced by *Staphylococcus*. Resistin is a secretory protein that has been linked to obesity and the development of type 2 diabetes, both diseases with significant immunomodulatory dysfunctions (Pang and Le, 2006). Resistin has also been linked to microbial inflammation via the regulation of its expression by IL-6 and TNF-α in human PBMCs (Mazaki-Tovi *et al.,* 2010; Aliefendioglu *et al.*, 2014). Chronic inflammatory conditions such as arthritis and kidney disease are associated with high resistin expression (Mazaki-Tovi *et al.*, 2010). In addition, a role in bacterial inflammation has been proposed due to the upregulation of resistin in PBMCs following challenge with LPS, *E. coli* and streptococcal M1 protein (Johansson *et al.*, 2009; Mazaki-Tovi *et al.*, 2010). During inflammation, resistin may play a role in monocyte-macrophage function, and effects observed in other studies include increasing NFκB and MAPK activity, promoting production of pro-inflammatory cytokines and promoting lipid accumulation in tissue macrophages (Filkova *et al.*, 2009). Several studies have reported that patients with severe inflammation had significantly greater concentrations of resistin in their blood than healthy individuals (Pang and Le, 2006; Mazaki-Tovi *et al.*, 2010; Aliefendioglu *et al.*, 2014). Studies on adult patients with sepsis have found that resistin expression and secretion is elevated in the presence of bacterial infections and has the potential to serve as an indicator of disease severity (Mazaki-Tovi *et al.*, 2010; Aliefendioglu *et al.*, 2014). In the present study, resistin was found at higher concentrations than other inflammatory cytokines in the control sample, supporting the current literature linking resistin to non-infectious chronic inflammation. However, when challenged with both *Escherichia* and *Staphylococcus*, resistin concentrations increased. Whilst there is little evidence that resistin can be used to distinguish between bacterial cause of sepsis, there is more evidence to support using resistin as a biomarker of inflammation in numerous disease processes, and there is evidence to support the use of resistin to monitor disease processes to understand its discriminatory power (Pang and Le, 2006; Johansson *et al.*, 2009, Mazaki-Tovi et al.; 2010).

Calprotectin (S100A8/A9), TF3, C5a and IL-10 were investigated as key mediators of neutrophil degranulation, coagulation, complement and anti-inflammatory processes, all pathways that have been strongly implicated in development of sepsis pathology (Mollnes *et al.,* 2002; Decembrino *al.*, 2015; Wang *et al.*, 2018). Calprotectin is a heterocomplex

granular protein with broad antimicrobial properties (Decembrino *et al.*, 2015; Wang *et al.*, 2018). In healthy patients, it is found in its inactive forms (S100A8 and S100A9) in the cytosol of PBMCs and is rapidly released into the extracellular space after activation of PRRs by PAMPs. Here, it dimerises to form the active protein (S100A8/A9, or calprotectin). Calprotectin has been used as a non-specific marker of the process of degranulation, and recently was noted to increase substantially in the plasma of septic neonates as well as in patients with infections (Decembrino *et al.*, 2015; Jonsson *et al.*, 2017). In this study, inactive (S100A8) and active (S100A8/A9) calprotectin was measured to determine its potential as a biomarker of infection. As expected, S100A8 concentrations increased initially as it was released from PBMCs but then decreased as the infection progressed and the protein dimerised. Active calprotectin was present at substantially high concentrations very early on in the experiment and plateaued between 4- and 6-hours post-infection. Subsequent statistical tests revealed that neither of these proteins were of any benefit in determining inflammation using this experimental procedure, as the control was found to demonstrate similar changes in calprotectin expression. This is potentially a result of neutrophil priming, and thus is not an appropriate biomarker to investigate using this model.

Complement component 5a was found to be substantially variable in different donors and was present at higher than normal levels in the control samples. Due to this, only two time points were recorded (2 and 4 hours). There is some potential that C5a is being induced in control samples by the incubation process. Alternatively, a previous study (Mollnes *et al.*, 2002) found that the use of certain anti-coagulants had an adverse effect on complement activation. In particular, it was found that heparin was found to inhibit complement activation at high concentrations but was also found to promote activation at low concentrations (Mollnes *et al.*, 2002). This is possibly the effect that is being seen in these samples. Complement component 5a does show some promise as a biomarker of inflammation (Conway Morris *et al.,* 2009), if not of bacterial species, and thus it should be investigated again with the use of EDTA or lepirudin as an anti-coagulant to prevent the unnecessary activation of C5a in these samples. Both IL-10 and TF3 were not detected until six hours post-infection, and when they were detected were considerably variable and very similar in average concentration between groups. At such an early time point (six hours) it is difficult to predict how these proteins would behave. Both are produced relatively early on in an infection, within six hours and potentially are appropriate

biomarkers at time points outside the limitations of this study. From these results it is not possible to recommend either proteins as biomarkers for use in sepsis diagnosis.

Collectively, the major results in this chapter identify, IL-6, MIP-1α, MIP-3α and resistin as showing potential as biomarkers of inflammation and perhaps of infection. This study renews interest in IL-6 as a discriminatory cytokine between Gram-positive and Gram-negative sepsis and suggests that clinics should focus more on using this protein in clinical diagnosis. Also provided here is the first evidence that MIP-3α could be a potentially powerful predictor of Gram-negative sepsis in human PPP and supports the use of MIP-1α as a predictor of inflammation. This study also demonstrated resistin as a promising new biomarker candidate of infection, as it has wide-ranging applications. While this chapter investigated soluble biomarkers in the *ex vivo* model the next chapter will investigate changes in leukocytes (chapter 4).

## Chapter 4. Cellular Characterisation of a Whole Blood Model of Sepsis

### 4.1. Introduction

### 4.1.1. Cells of the Immune System

Innate and adaptive immune cells play a pivotal role in the development and pathology of sepsis (Cohen, 2002; Brown *et al.*, 2006; Monneret *et al.*, 2008; Rittirsch et al., 2008; Bosmann and Ward, 2013; Li *et al.*, 2017b; Conway Morris *et al.,* 2018). Innate cells include monocytes, macrophages and neutrophils, and they prevent colonisation and invasion by pathogens through two major mechanisms; phagocytic engulfment of pathogens and production of molecular mediators to stimulate the adaptive immune response (Gasteiger *et al.*, 2017; Li *et al.*, 2017b). Neutrophils make up to 60% of circulating blood leukocytes, and have multiple roles in inflammation, including phagocytosis and killing through ROS and enzyme degradation, together with production of cytokines and chemokines (Lehmann *et al.*, 2000; van Kessel *et al.*, 2014). Of these functions, the key process undertaken by neutrophils is phagocytosis, and adequate phagocytosis is key to resolving infections  (van Kessel *et al.*, 2014). Monocytes and tissue macrophages are pivotal in sensing infections (Arango Duque and Descoteaux, 2014). Macrophages monitor tissues for any sign of damage or pathogen invasion and are often the first cells to sense an infection through PRR on their cell surface (Gasteiger *et al.*, 2017). Once a pathogen has been recognised, macrophages process antigens and present them to other cells of the immune system to promote pathogen clearance and the development and fine tuning of an adaptive immune response (Hoebe *et al.*, 2004). Circulating adaptive immune cells include both B and T lymphocytes, which can be further subdivided into helper CD4+, cytotoxic CD8+ and regulatory T lymphocytes ( Kaiko *et al.*, 2008; Iwasaki and Medzhitov, 2015). Lymphocytes generate specific pathogen immune responses and memory, but the importance of each subset is driven by the type of pathogen causing the infection (Iwasaki and Medzhitov, 2015).

### 4.1.2. Dysregulated Cellular Functions during Sepsis

Sepsis induces a multitude of changes in the behaviour of immune cells that significantly impact on progression into septic shock and multiple organ failure (Cohen, 2002; Bosmann and Ward, 2013; Conway-Morris, 2018). Granulocytes are over-produced to meet the phagocytic demand to eliminate infection (Faix, 2013). As sepsis progresses, these granulocytes become increasingly immature as they are released too early from the bone marrow, an event that significantly impacts on the ability of the body to eliminate

the pathogen (Faix, 2013). These immature neutrophils are further characterised by increasing necrosis and the presence of Dohle bodies in their cytoplasm (Faix, 2013). Increased numbers of immature neutrophils are accompanied by a decrease in apoptotic clearance, which leads to their accumulation in vital organs and subsequent organ damage (Cohen, 2002; Faix, 2013). Macrophages undergo a similar reduction in apoptosis, allowing for the persistence of these cells within infected tissues and subsequent inability to perform their functions, resulting in an immunoparalysis (Umlauf *et al.*, 2013). Both B and T cells undergo an opposite effect; increasing apoptosis results in a diminished capacity to resolve an infection as lymphocyte clones are not generated correctly, and persistent lymphopenia during sepsis is characteristic of immunosuppression in severely ill patients (Cohen, 2002).

### 4.1.3. Cellular Biomarkers of Sepsis

Several cellular biomarkers of infection have previously been explored for diagnosing sepsis. Cell counts are already applied in determining the progression of sepsis (Chalupa *et al.*, 2011). For example, a neutrophil count that is higher, lower or contains 10% immature cells compared to resting counts are all considered markers of severe inflammation and sepsis (Brown *et al.*, 2006). Observational diagnoses from blood smears include the identification of toxic granulations and Dohle bodies within the cytoplasm of neutrophils, both indicators of bacterial infection (Faix, 2013). A depletion in both circulating B and T lymphocytes are also markers of immunoparalysis and severe sepsis (Faix, 2013). Measurable changes in leukocytes during sepsis can also be identified using cell surface markers, such as CD64, CD11b, triggering receptor expressed on myeloid cells 1 (TREM-1) and receptor for advanced glycation products (RAGE; Faix, 2013; Biron *et al.*, 2015). CD64, a high affinity receptor for immunoglobulin is substantially increased in septic patients and has been found to have better specificity than PCT in diagnosing bacterial sepsis, as well as showing considerable promise in diagnosing neonatal sepsis (Faix, 2013; Biron *et al.*, 2015). However, CD64 has been found to be relatively unstable in anti-coagulated blood samples, an issue as all blood samples need to be treated with an anti-coagulant (Faix, 2013). CD11b promotes neutrophil adherence to endothelium lining the vasculature, promoting rolling and migration to inflammatory sites, and has also been associated with an increase during bacterial infections (Faix, 2013). Increase in cell surface expression of TREM-1 has also been associated with sepsis (Faix, 2013; Biron *et al.*, 2015). Similar increases in RAGE have also been shown in sepsis but its efficacy as a sepsis biomarker is complicated by

high resting expression in certain cell types (Faix, 2013). Other cell surface markers that have been associated with sepsis include reduced CD14 and MHC class II expression on NK cells and macrophages (Chalupa *et al*., 2011; Faix, 2013; Conway Morris *et al*., 2018). A reduction in the number of regulatory T cells has also been associated with an increased risk of acquiring a secondary infection in patients with sepsis (Faix, 2013).

Measuring features of apoptosis particularly with regards to B and T cells have shown recent promise in diagnosing severe inflammation (Duplessis *et al.,* 2018). Such features, including expression of apoptotic mediators and the release of cell-free DNA (cfDNA), have been investigated previously (Figure 4.1; Duplessis *et al*., 2018). Both extracellular cfDNA and nucleosome levels reflect the extent of apoptosis within a host. Cell free DNA is derived from necrotic, lytic, apoptotic and secretory processes, and nucleosomes derive from the degradation of chromatin during apoptosis or necrosis (Duplessis *et al.*, 2018). In healthy people, levels of cfDNA and nucleosomes have very short half-lives (approximately 15 minutes) and are cleared by the liver and excreted. However, persistently high levels of these are indicative of excessive tissue damage and liver failure, both hallmarks of sepsis pathology. A recent study has indicated that both cfDNA and nucleosome concentrations correlate strongly with sepsis severity, and both are able to predict the progression into severe septic shock (Duplessis *et al*., 2018).
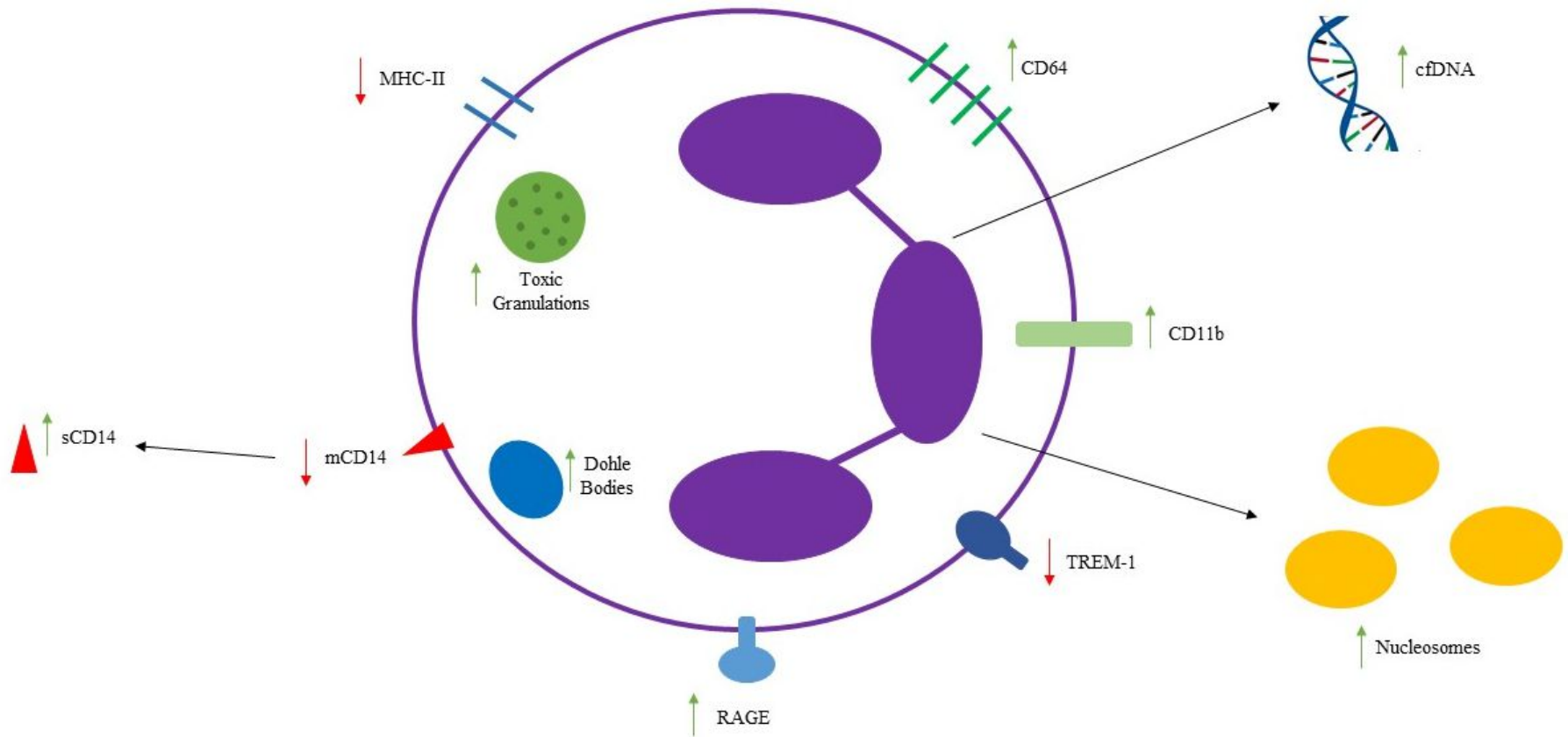
Figure 4.1. Diagram depicting the neutrophil and other leukocyte cellular biomarkers associated with bacterial infection and sepsis (Faix, 2013; Biron, 2015; Duplessis 2018; Conway Morris *et al*., 2018).

### 4.1.4. Aims and Objectives

The aim of the work in this chapter was to measure the effects of sepsis causing organisms on leukocyte cell surface markers and functions in the *ex vivo* blood model. Cell surface markers were determined by flow cytometry and phagocytosis was determined by microscopy. The ability to assay the central cellular changes that immune cells undergo during sepsis in the whole blood model was also important. More specifically the aims were as follows:

- Characterise the phagocytic response of neutrophils to *E. coli, S, aureus* and *S. epidermidis*.
- Identify and characterise leukocyte subsets in whole blood using flow cytometry.
- Characterise *E. coli* K12- and *S. epidermidis* RP62A- induced responses in the whole blood model using flow cytometry;
  - ➤ Changes in leukocyte subset markers.
  - ➤ Changes in cell viability.
  - ➤ Changes in TLR expression.

### 4.2. Methodology

A full description of the methodologies used in this chapter are described in Chapter 2.

### 4.2.1. Microbiology & Whole Blood

Two to three colonies of *E. coli*, *S. aureus* and *S. epidermidis* (8 strains, listed in Table 2.3) were inoculated for up to 24 hours in either 5 ml of TSB or LB at 37°C at 200 r.p.m. Bacterial culture was standardised as described in Section 2.5.4 and added to 1 ml healthy volunteer whole blood described in section 2.5.6.2. The inoculated blood was incubated for 2, 4, 6 or 8 hours at 37°C at 10 r.p.m., and at each interval 100 µl blood was removed and used in either phagocytosis or flow cytometry analysis.

### 4.2.2. Phagocytosis Analysis

After incubation, 100 µl of blood containing the bacteria was processed as described in described in section 2.7.1. Neutrophils were counted and the percentage of phagocytosis calculated as described in section 2.7.1.

### 4.2.3. Flow Cytometry Staining

After incubation, 100 µl of whole blood containing either *E. coli* K12 or *S. epidermidis* RP62A was added to round bottom tubes and processed as described in section 2.7.2.

### 4.2.3.1. Separation of Mononuclear Cells from Whole Blood

Histopaque-1077 was used to isolated mononuclear leukocytes from whole blood and a FITC Annexin V/Dead cell apoptosis kit was used to assess cell viability as described in section 2.7.2.2

### 4.2.3.2. FACS Analysis

Stained samples were analysed using the Novocyte NovoSampler Pro (Acea Biosciences Inc., San Diego, California) as described in section 2.7.2.3. All laser parameters were selected (section 2.7.2.1, table 2.5) and a quality control was run each time.

### 4.2.3.3. Data Analysis

Flow Cytometry data was analysed using FlowJo v10 (BD Biosciences). Compensation was performed using mixed single-stain samples and applied to all experimental samples. A gating strategy was established through which positive populations were isolated based on MFI, histogram distribution and separation of stained populations from unstained populations.

### 4.2.4. Statistical Analysis

Phagocyte and flow cytometry data were analysed using GraphPad Prism version 7. N numbers refer to the number of donors analysed in the test. All data was tested for normality using the Shapiro-Wilks normality test and where this was not possible ( $n < 7$ ) data was assumed to be not normally distributed. For normally distributed data, parametric one-way ANOVAs with Dunn's multiple comparison tests were applied. Non-parametric Kruskal-Wallis tests with Dunn's multiple comparison tests were applied to not normally distributed data. A $p$ value of $<0.05$ was considered significant. On graphs, error is represented by the SEM.

## 4.3. Results

### 4.3.1. Neutrophil Phagocytosis

In order to assess the degree of neutrophil phagocytosis in the whole blood model, the number of neutrophils with and without phagosomes containing either *S. aureus, S. epidermidis* or *E. coli* were counted (Figure 4.2a-f and 4.3a-c) and presented at the level of genera, species and strain (Figure 4.3a-c respectively).
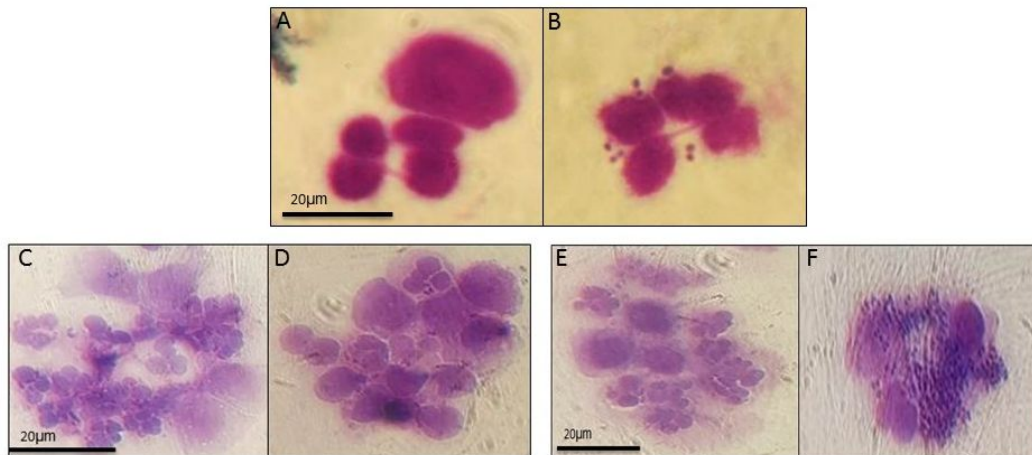


Figure 4.2. Microscopy images of neutrophils in whole blood identified by their multi-lobed nuclei at 2 (images A and B), 4 (images C and D) and 6 hours (images E and F). Image A, C and E were taken from samples incubated with *E. coli*, and image B, D and F are taken from samples incubated with Staphylococci. Scale bar = 20 µm.

Distinct morphological changes occurred throughout the 6-hour infection (Figure 4.2). At 2 hours post-infection, microscopy showed that both *Staphylococcus* and *Escherichia* infected blood had single neutrophils, both with and without bacteria in the cytoplasm, and in some cases, lymphocytes or monocytes were found closely associated with the neutrophils (Figure 4.2a). Neutrophils appeared to be healthy without characteristic signs of apoptosis (condensed nuclei, clumping of cells, loss of membrane integrity etc.). However, at 4- and 6-hours post-infection, all neutrophils were found clustered with other neutrophils and leukocytes in both *Staphylococcus* and *Escherichia* treated samples and lost definition of their multi-lobed nuclei (see Figure 4.2c/d and e/f).

Phagocytosis counts over the same time course were also calculated (Figure 4.3). The uninfected control remained consistently low over the course of the experiment (maximum 5%) and all replicates had very little or no phagocytosis detected. Phagocytosis of *Staphylococcus* was significantly greater ($p < 0.0001$) than that in both the uninfected control and *Escherichia* at all time points studies (Figure 4.3a). Whilst the degree of phagocytosis was elevated in response to *Escherichia* it was not significantly different to the uninfected control ($p > 0.05$).

With respect to species (Figure 4.3b), after 2 hours post-infection, both *S. aureus* and *S. epidermidis* had identical degrees of phagocytosis and were significantly higher than *E. coli* or uninfected control. However, at 4- and 6-hours post-infection, the degree of phagocytosis was higher in the *S. epidermidis* samples than in *S. aureus* samples, but not statistically significant. Phagocytosis of both staphylococcal species remained significantly higher that *E. coli* and uninfected control.

Phagocytosis was strongly strain dependent (Figure 4.3c). At all-time points (2, 4 and 6 hours), *S. epidermidis* strains 1457, RP62A and *S, aureus* SH1000 were phagocytosed significantly more than control. *Staphylococcus aureus* VAP39 was only significantly greater than the control at 2 hours post-infection. At 6 hours, *S. epidermidis* strains 1457 and RP62A  were phagocytosed significantly more than *E. coli* strain B and K12 ($p < 0.0001$). Neutrophil phagocytosis of *E. coli* ECOR26, GMB10, B and K12 all remained consistently low over the 6-hour time course. Phagocytosis of *E. coli* ECOR26 and GMB10 was consistently higher than B and K12, but no significant differences were found.
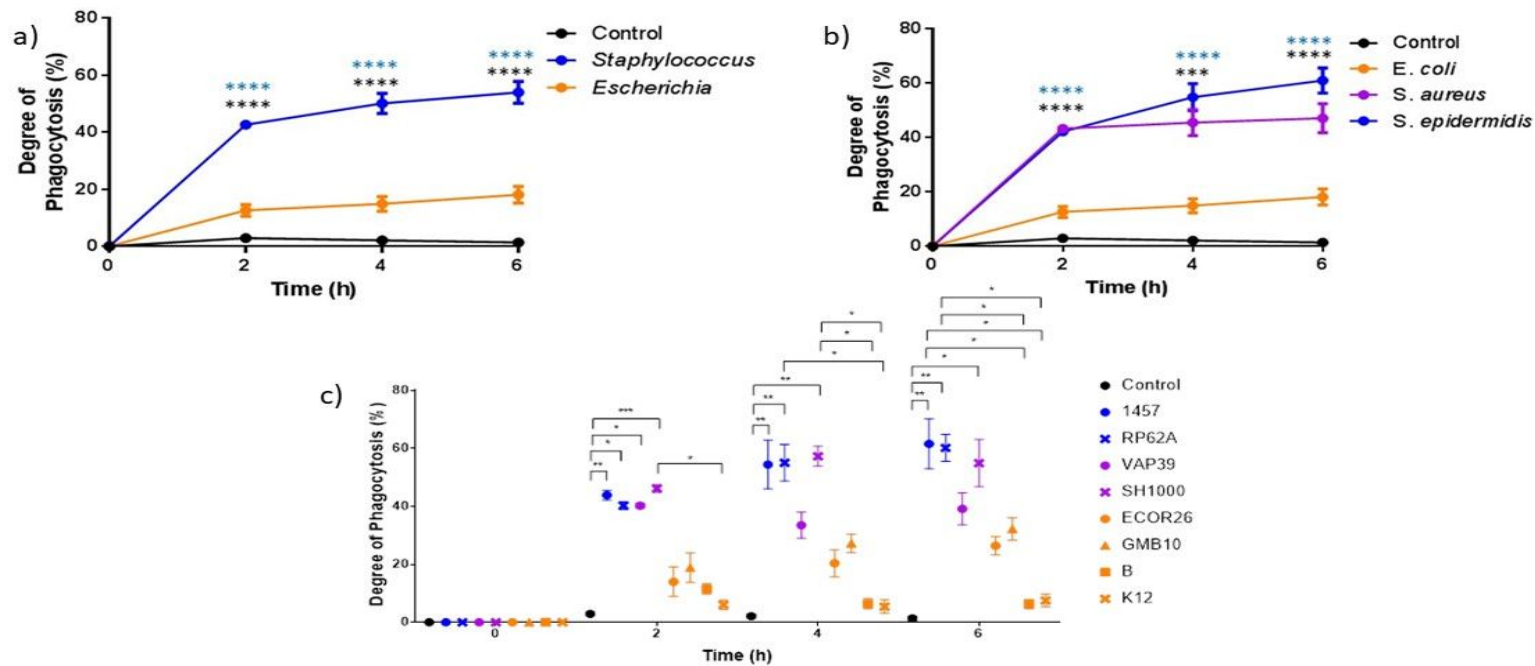
Figure 4.3. Neutrophil phagocytosis (%) over time in blood infected by bacteria; a) changes in the amount of phagocytosis in the control, *Staphylococcus* and *Escherichia* genera (n = 5); b) changes in the amount of phagocytosis in the control, *E. coli*, *S. aureus* and *S. epidermidis* species; c) changes in the amount of phagocytosis in *E. coli*, *S. aureus* and *S. epidermidis* strains (n = 5 donors). Error bars represent the mean ±SEM. In (a), * represents significant difference between the *Staphylococcus*-infected PPP and control PPP, and * represents significant differences between the *Escherichia* and *Staphylococcus* PPP, in (b), * represents significant differences between *E. coli* PPP and *S. aureus* PPP, and * represents significant differences between *E. coli* PPP and *S. epidermidis* PPP, and in (c), significant differences are represented between two strains or control by black lines and asterisks indicating the level of significance between the two PPP. On graphs, asterisks represent the following significant values: * = $p < 0.05$, ** = $p < 0.01$, *** = $p < 0.001$, **** = $p < 0.0001$.

### 4.3.2. Characterisation of Whole Blood Model

The fluorochrome-antibody conjugates outlined in Table 2.1 were used to identify cellular subsets including; Leukocytes (CD45-positive), Monocytes (CD14-positive), T cells (CD3-positive) and B cells (CD19-positive). Granulocytes were identified by their positive staining for CD45 and their high granularity (SSC). A gating strategy (Figure 4.4) was established whereby cells positive for the selected fluorochrome-antibody conjugate (compared with the unstained control) were identified and counted using the 'gating' function on the FlowJo software.
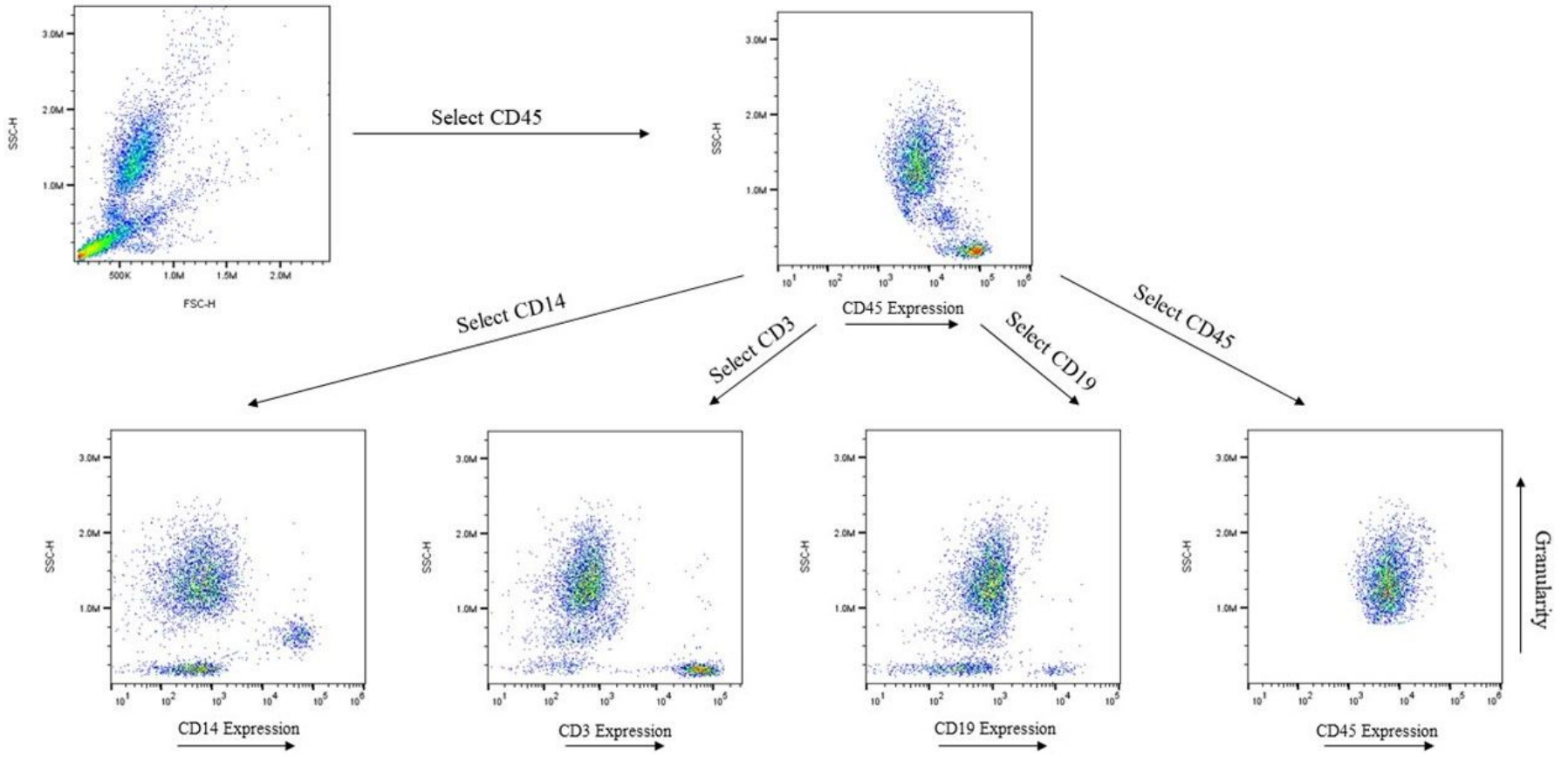
Figure 4.4. Schematic of the gating strategy for characterisation of leukocyte subsets in whole blood using CD marker expression patterns.

This gating strategy was used to investigate changes in leukocyte populations following infection with *E. coli* K12 and *S. epidermidis* RP62A over a 6-hour time course. Prior to infection (~1 hour following phlebotomy), whole blood was stained for leukocyte subsets and a composite dot plot produced to identify leukocyte subsets (Figure 4.5). All leukocytes could be clearly labelled with fluorochrome antibody conjugates and compensation of overlapping fluorescences allowed for complete separation of positive and negative populations.
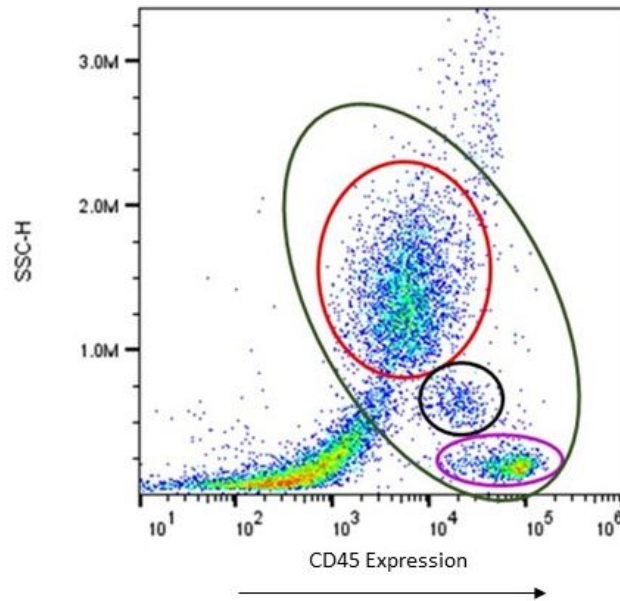


Figure 4.5. Diagram showing the distribution of leukocytes in blood processed within one hour of drawing from the donor. The y axis is side scatter and the x axis is CD45 fluorescence. Green = leukocytes; Red = neutrophils; Black = monocytes; and Purple = lymphocytes.

Composite dot plots (SSC vs CD45) were produced for uninfected control and blood infected with *E. coli* K12 and *S. epidermidis* RP62A for 2, 4 and 6 hours (Figure 4.6). In uninfected control, characteristic populations for neutrophils, monocytes and lymphocytes were identified which did not change with time (Figure 4.6, left column). In blood treated with *E. coli* K12, two global changes were observed. Firstly, the neutrophil population became more uniform in CD45 expression (thinner) in the first 2 hours but with a wider distribution of granularity. Secondly the monocyte population decreased and disappeared by 6 hours post infection. Blood treated with *S. epidermidis* RP62A also had similar global changes but their time course differed. The neutrophil population became more uniform in CD45 expression (thinner) with a wider granularity, but this took the full 6 hours. The monocyte population decreased and disappeared by 6 hours post infection.

Figure 4.6. Scatter plots of the control, *E. coli* K12-treated and *S. epidermidis* RP62A-treated blood selected for CD45 expression at 2-, 4- and 6-hours post-infection.

### 4.3.2.1. Quantification of Leukocyte Cell Counts

Quantification of the changes in cell populations and marker expression observed previously were determined using the techniques described in section 2.7.2.3.

The changes in the populations of monocytes, granulocytes, T cell and B cell populations were determined (Figure 4.7) using the gating strategy outlined previously (Figure 4.4). The monocyte population rapidly decreased 2 hours after the addition of *E. coli* K12 or *S. epidermidis* RP62A and continued to decrease slowly over the 6 hours (Figure 4.7a). *Escherichia coli* K12 induced significant decreases in the monocyte population at 2 hours post-infection ($p = 0.0151$), whilst *S. epidermidis* induced significant decreases in monocytes compared to the control at 4- and 6-hours post-infection ($p < 0.05$). Monocytes were the only leukocyte subset that changed significantly over 6 hours. Granulocytes (Figure 4.7b), T cells (Figure 4.7c) and B cells (Figure 4.7d) remained relatively constant over the course of the experiment. In addition, infection with *E. coli* K12 or *S. epidermidis* RP62A had no effect on their total numbers.
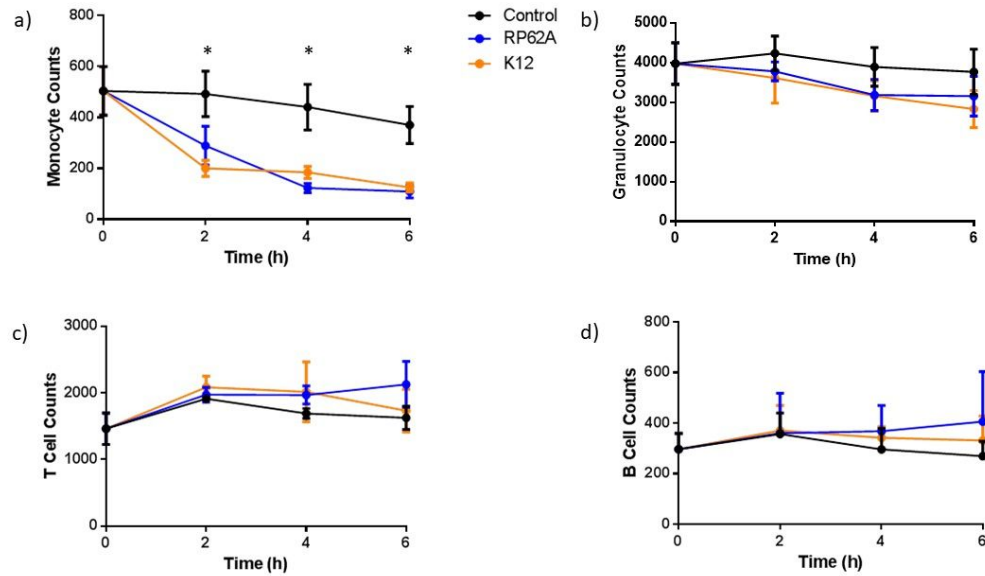
Figure 4.7. Quantification of leukocyte subsets in response to infection; a) monocytes, b) granulocytes, c) T cells, and d) B cells infected with *E. coli* K12 and *S. epidermidis* RP62A over the 6-hour infection period (n = 4 donors). Error bars indicate the mean ±SEM. Asterisks indicate significant differences between the control and at 2 hour K12, and 4 and 6 hour RP62A. On graphs, asterisks represent the following significant values: * = $p < 0.05$.

## 4.3.2.2. Leukocyte Differential Counts

Using counts from the previous gating strategy leukocyte differential counts were calculated (Figure 4.8). Prior to infection (Figure 4.9a) granulocytes represented 59% of the leukocyte population, T cells represented 22%, monocytes represented 7% and B cells represented 4% ,and all fall within ranges expected in healthy whole blood (Huang *et al.,* 2007). Following infection leukocyte differential counts did not change despite the changes in total monocyte counts calculated previously. Thus, differential counts were independent of stimulus (uninfected control, *E. coli* K12 and *S. epidermis* RP62A) and time (Figure 4.8b-d).

135
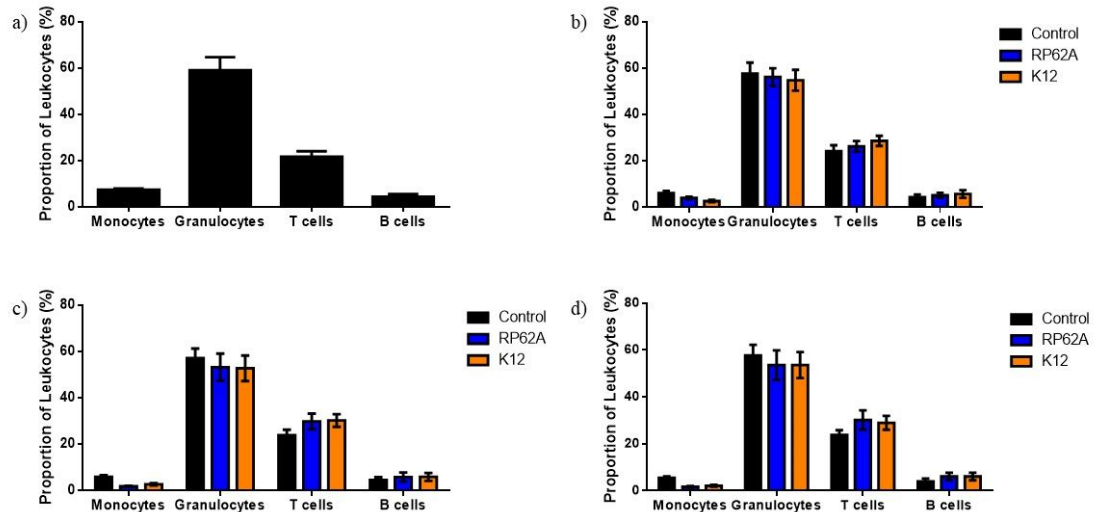
Figure 4.8. Differential counts of whole blood over a 6-hour time course. a) 0 hour, b) 2 hour, c) 4 hour, and d) 6 hour (n = 4 donors).

### 4.3.3. Cell Biomarker Analysis

The expression (MFI) of CD45, CD14, CD3 and CD19 were measured over 6 hours on leukocyte subsets, including monocytes, granulocytes, and lymphocyte populations from whole blood incubated with RPMI (control), *E. coli* K12 and *S. epidermidis* RP62A.

### 4.3.3.1. CD45 Expression

CD45 expression on monocytes was time and stimulus dependent (Figure 4.9a). At 2- and 4-hours post infection, *E. coli* K12 induced significant increases in CD45 expression compared to uninfected control and *S. epidermidis* RP62A ($p = 0.0012$ and $p = 0.0031$ respectively). At 6 hours post-infection only *S. epidermidis* RP62A-treated monocytes had a significantly higher CD45 expression than the control monocytes ($p = 0.0285$). CD45 expression also increased with time on uninfected controls but this was not significant. On granulocytes (Figure 4.9b) both *S. epidermidis* RP62A and *E. coli* K12 induced CD45 expression at 2- and 4-hours post-infection compared to uninfected control. Of the infected groups, only *E. coli* K12 was found to induce significantly more CD45 expression compared to the control ($p = 0.0159$ and $p = 0.0107$ at 2 and 4 hours respectively). At 6 hours post-infection, both *S. epidermidis* RP62A and *E. coli* K12 induced significantly greater expression of CD45 on granulocytes than in the control group ($p = 0.0003$). The highest expression of CD45 was detected on T cells and B cells (Figure 4.10c/d). For both B and T cells (Figure 4.9c and d respectively), CD45

expression remained constant throughout the experiment and was independent of infection.
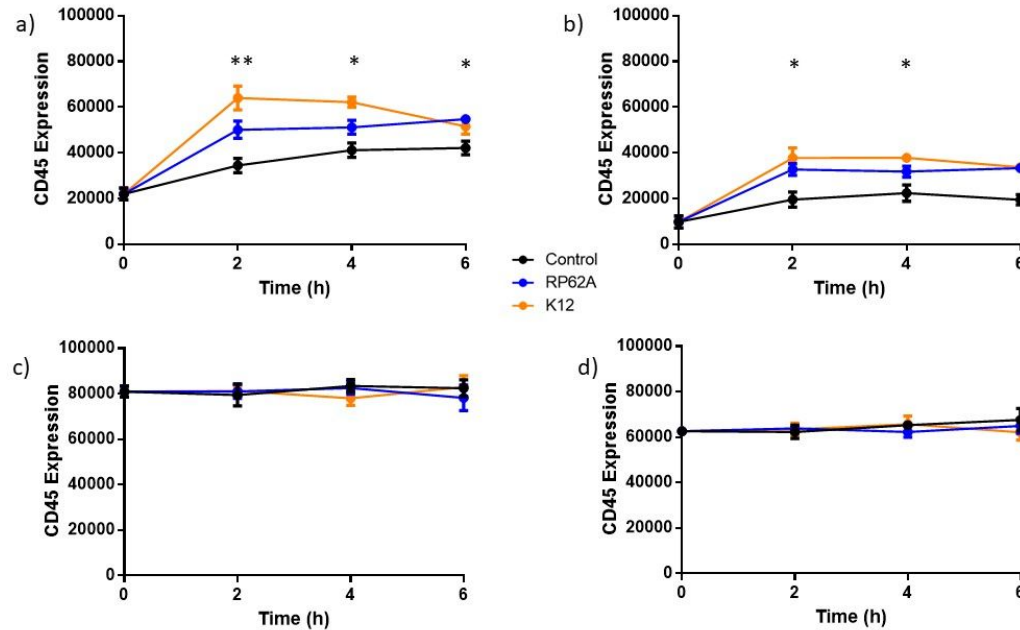


Figure 4.9. Graphs showing CD45 expression over 6-hour infection period in the control, *S. epidermidis* RP62A and *E. coli* K12 samples on, a) monocytes, b) granulocytes, c) B cells and d) T cells (n = 4 donors). Error bars represent the mean ±SEM. In a) asterisks indicate significant differences between the control and *E. coli* K12 at 2- and 4-hour, and the control and *S. epidermidis* RP62A at 6 hour; in b) asterisks indicate significant differences between the control and *E. coli* K12. Asterisks represent the following significant values: $* = p < 0.05$, $** = p < 0.01$.

## 4.3.3.2. CD14 Expression

CD14 could only be detected on monocytes (Figure 4.10a-d). However, there were no significant differences in CD14 expression with time or following induction by *E. coli* K12 or *S. epidermidis* RP62A.
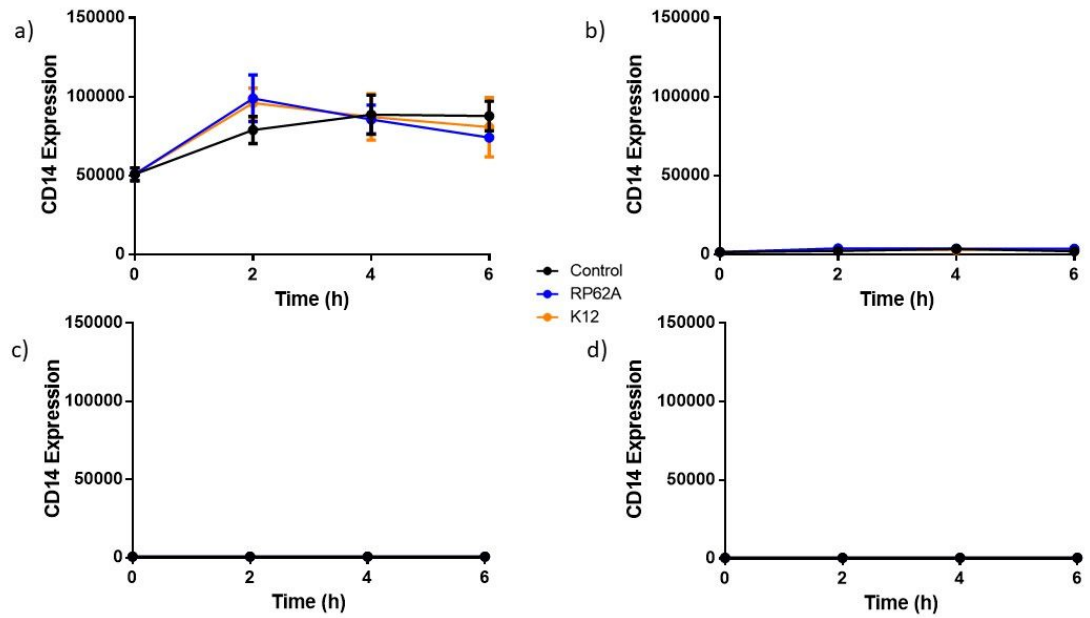
Figure 4.10. Graphs showing CD14 expression over the 6-hour infection period in response to control, *S. epidermidis* RP62A and *E. coli* K12 on, a) monocytes, b) granulocytes, c) T cells and d) B cells (n = 4 donors). Error bars represent the mean ±SEM.

### 4.3.3.3. CD3 Expression

CD3 expression could only be detected on T cells (Figure 4.11a-d). However there were no significant differences in CD3 expression with time or following induction by *E. coli* K12 or *S. epidermidis* RP62A. At 6 hours CD3 expression decreased in response to infection but was not significant.
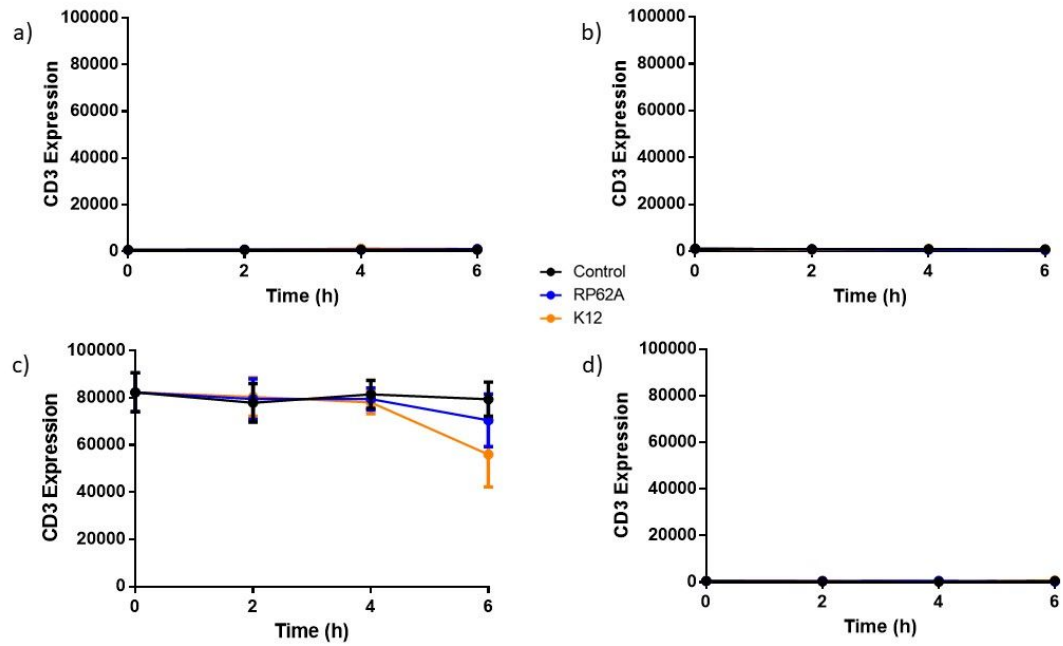
Figure 4.11. Graphs showing CD3 expression over the 6-hour infection period in response to control, *S. epidermidis* RP62A and *E. coli* K12, a) monocytes, b) granulocytes, c) T cells and d) B cells (n = 4 donors). Error bars represent the mean ±SEM.

## 4.3.3.4. CD19 Expression

CD19 expression (Figure 4.13) could be detected at high level on B cells, low levels on monocytes and granulocytes and was undetectable on T cells (Figure 4.12a-d). There were no significant differences in CD19 expression with time or following induction by *E. coli* K12 or *S. epidermidis* RP62A on granulocytes or lymphocytes. *E. coli* K12 induced a significant increase in monocytes CD19 compared to uninfected control at all time points. *S. epidermidis* RP62A also induced a significantly higher expression of CD19 on monocytes than in uninfected control at 6 hours post-infection ($p = 0.0132$).
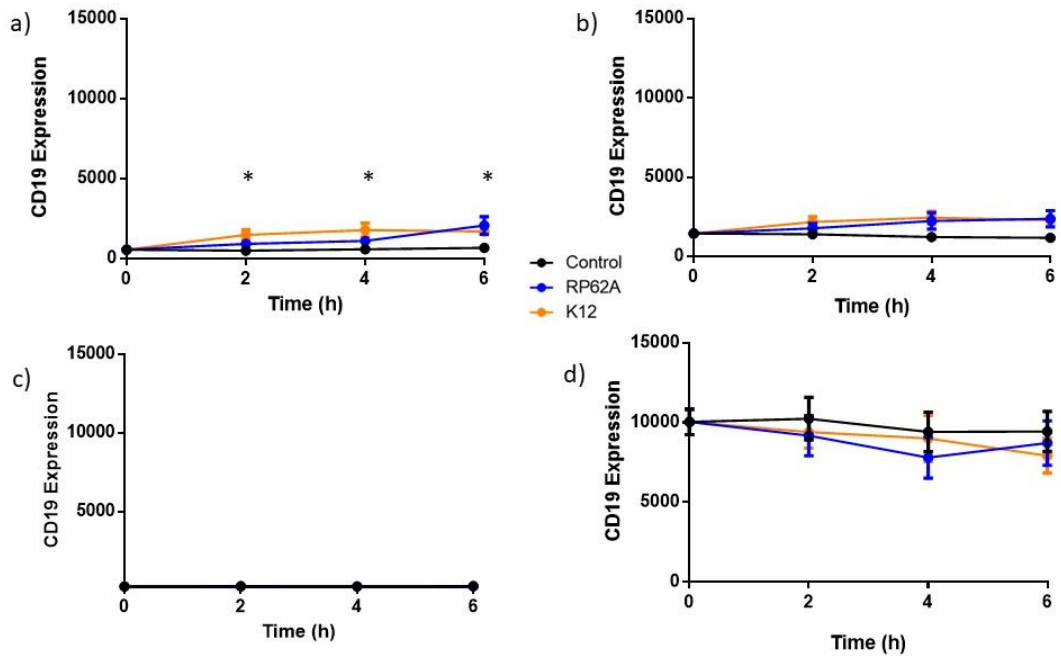
Figure 4.12. CD19 expression over 6-hour infection period in response to control, *S. epidermidis* RP62A and *E. coli* K12 on a) monocytes, b) granulocytes, c) T cells and d) B cells (n = 4 donors). Error bars represent the mean ±SEM. Asterisks indicate significant differences between the control and *E. coli* K12 at 2- and 4 hour, and the control and *S. epidermidis* RP62A at 6 hour. On graphs, asterisks represent the following significant values: $*$ = $p < 0.05$.

### 4.3.4. Live/Dead Cell Assay of Mononuclear Leukocytes

### 4.3.4.1. Staining Profile of Mononuclear Leukocytes

The rapid reduction in CD14-positive monocytes (Figure 4.7) upon addition of bacterial suspension warranted further investigation using a Live/Dead Cell Assay, as the results suggested the cells had undergone cell death. The fluorochromes Annexin-FITC (phosphatidylserine binding) and PI-PE Texas Red (DNA binding) were used to assess for apoptotic and necrotic cells respectively.

Initial experiments used the method described in section 2.7.2.1 however it was clear that BD FACS Lyse Solution used to lyse erythrocytes also permeabilised leukocyte populations resulting in high necrotic staining (results not shown). This effect was confirmed using the U937 monocyte cell line (Figure 4.13). U937 cells treated with BD FACS Lyse showed a large population of PI-positive cells that were not present in the untreated cells. Therefore, BD FACS Lyse was discarded as the lysis procedure interfered with cellular viability and in its place, Histopaque 1077 was used to isolate mononuclear leukocytes from whole blood.
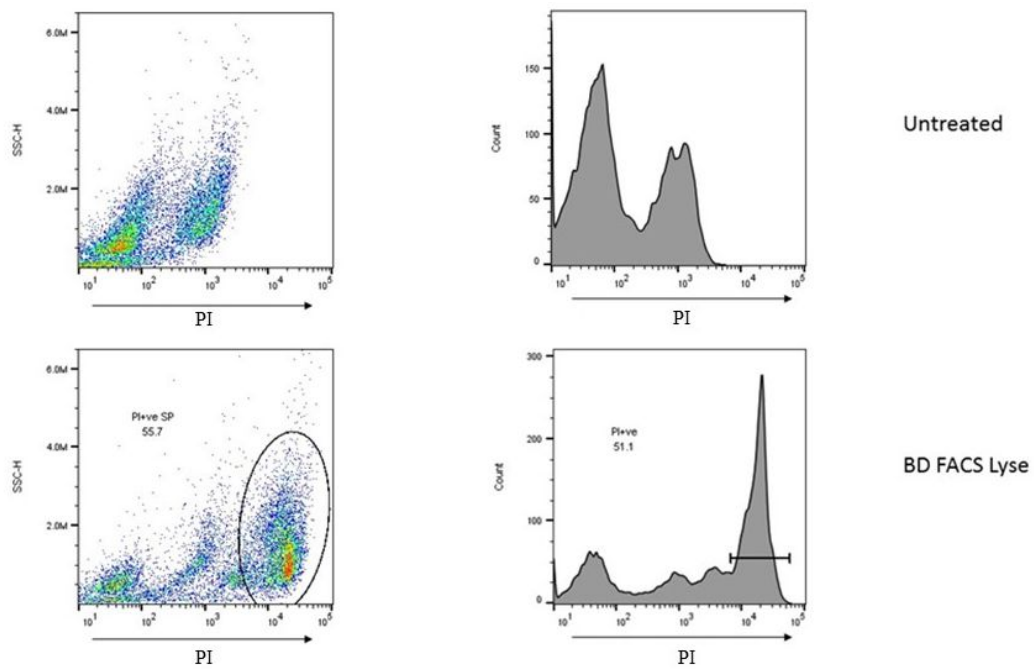
Figure 4.13. Scatter plots and histograms of U937 cells stained with PI. Events outlined in black indicate PI staining in cells treated with BD FACS Lyse.

The SSC vs FSC and staining profile of mononuclear leukocytes (lymphocytes and monocytes; Figure 4.14) isolated from untreated whole blood revealed that cells negative for any Annexin and PI (live cells) were in quadrant 4 (Q4), while cells staining positive for Annexin but negative for PI (apoptotic cells) were in quadrant 3 (Q3), cells staining positive for both Annexin and PI (secondary necrotic cells) were in quadrant 1 (Q1), and cells staining positive for PI only (primary necrotic cells) were in quadrant 2 (Q2). In the untreated control, approximately 1,484 monocytes were isolated using the Histopaque method, and 93.2% were viable (Q4) whilst 6.8% of monocytes were apoptotic (Q3).
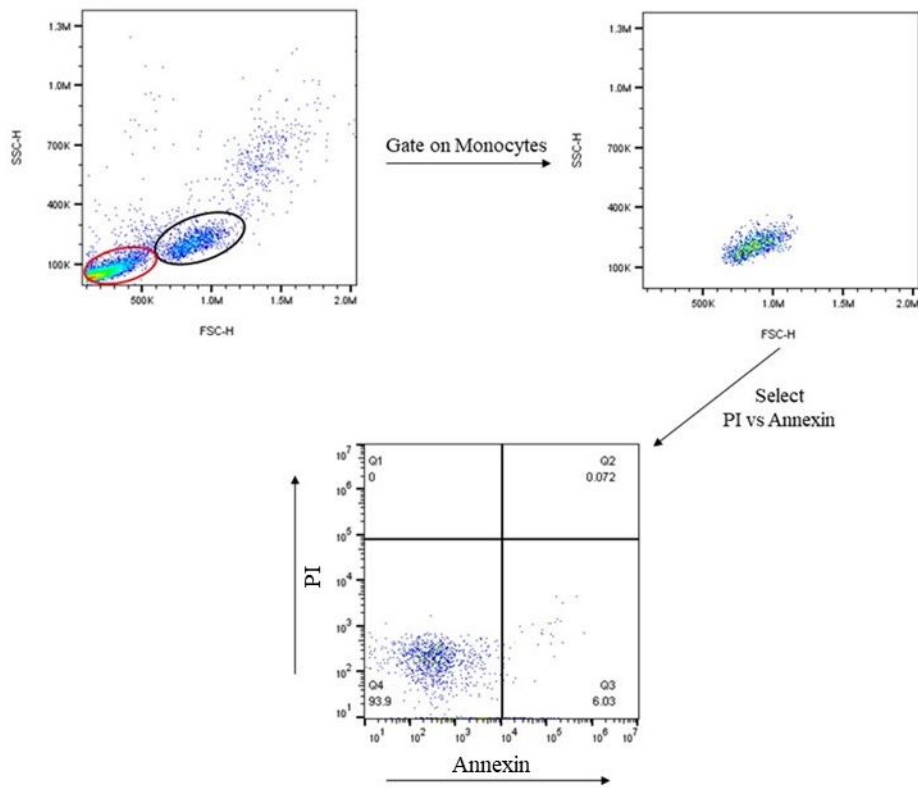
Figure 4.14. Schematic of the gating strategy for monocyte viability. Red circle – lymphocytes, black circle – monocytes.

Composite dot plots (SSC vs FSC) were produced for uninfected control and blood infected with *E. coli* K12 and *S. epidermidis* RP62A after 3 and 6 hours of infection (Figure 4.15). Well-defined populations of lymphocytes and monocytes were recovered in the uninfected control and the treated blood. Two key universal changes were noted in both *E. coli* K12 and *S. epidermidis* treated samples. First, at 3 hours post-infection, the monocyte population became more uniform and less diverse in terms of size (FSC), and secondly a new population of events appeared that were high both in granularity and size. At 6 hours post-infection the second trend decreased, with much less events occurring at high granularity and size in the *E. coli* K12 treated blood. The uninfected control remained relatively unchanged, although the monocyte population did become smaller.
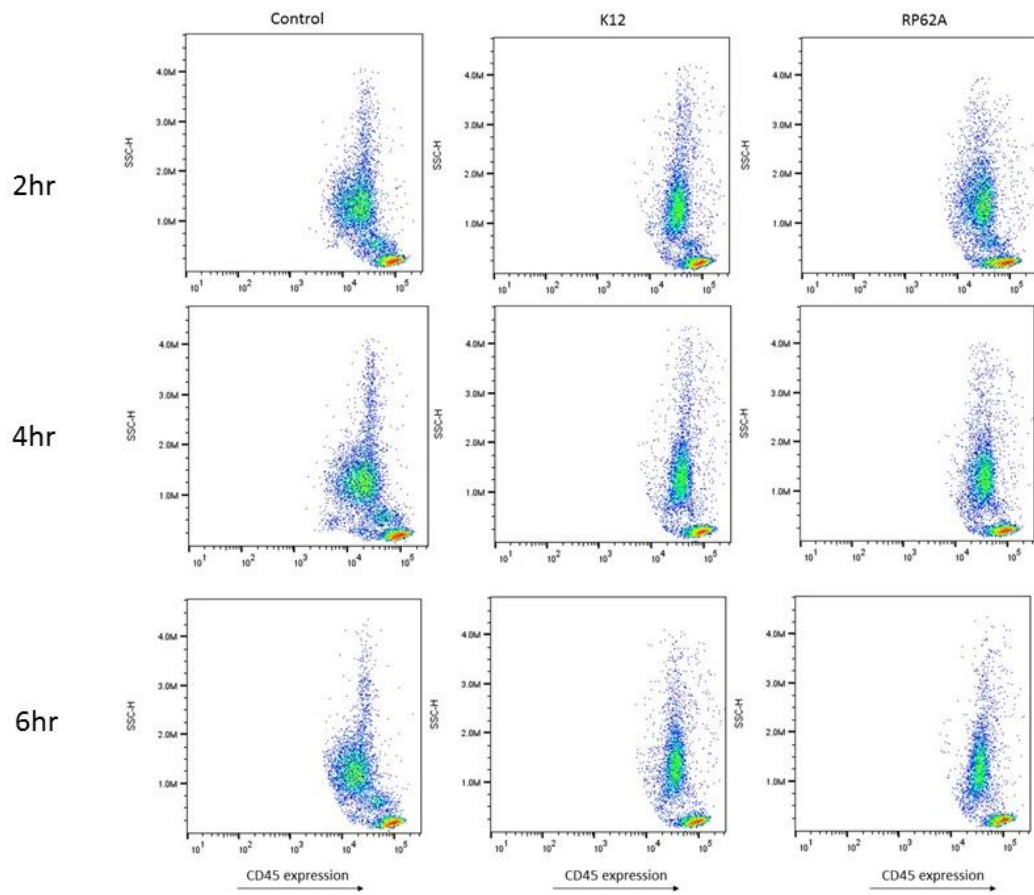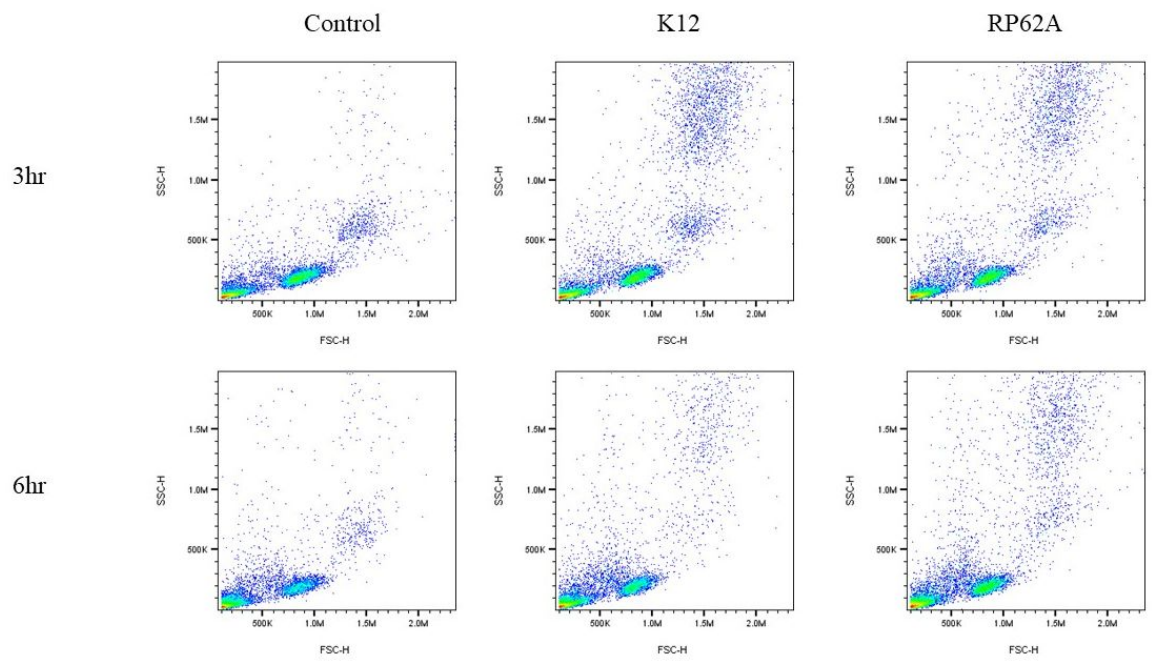
Figure 4.15. Scatter plots of the control, *E. coli* K12-treated and *S. epidermidis* RP62A-treated blood selected for SSC vs FSC at 3- and 6-hours post-infection.

## 4.3.4.2. Monocyte Cell Counts

Monocytes constituted approximately 13.2% of the total mononuclear leukocyte population (Figure 4.16a). Total monocyte counts increased at 3 hours post-infection and then declined at 6 hours post-infection in all groups. Live monocytes followed a similar trend, again in all groups (Figure 4.16b). The number of viable monocytes was almost identical to the number of total monocytes in blood throughout the course of the experiment in all samples (~1900 live, 1700 viable).
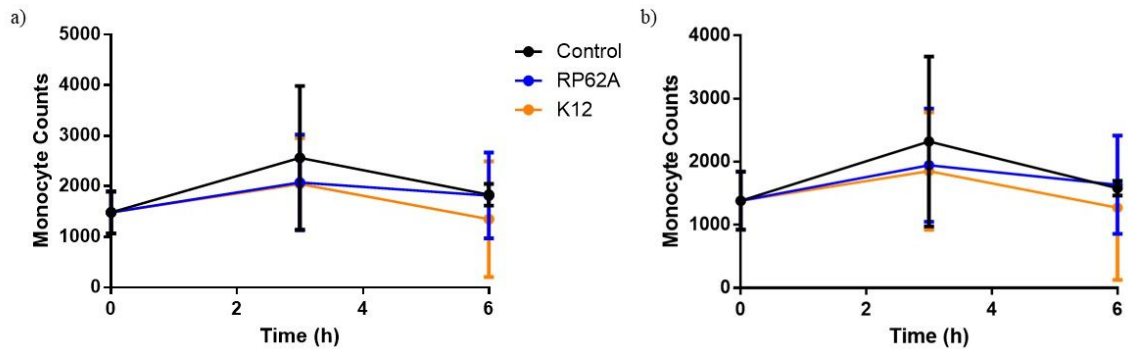


Figure 4.16. Monocyte counts at 0, 3- and 6-hours post-infection with control, *S. epidermidis* RP62A and *E. coli* K12, a) total monocyte counts and b) live monocyte counts (n = 3 donors). Error bars represent the mean ±SEM.

## 4.3.5. TLR Expression on Leukocytes

## 4.3.5.1. Characterisation of TLR Expression

The antibodies TLR2-PE, TLR4-APC and CD45-FITC were used to characterise TLR expression responses to bacteria over an 8-hour infection period. Expression of the TLRs was defined by first gating CD45-positive leukocytes and then selecting for each individual TLR. Expression of both TLRs was determined using histograms and unstained controls (Figure 4.17).
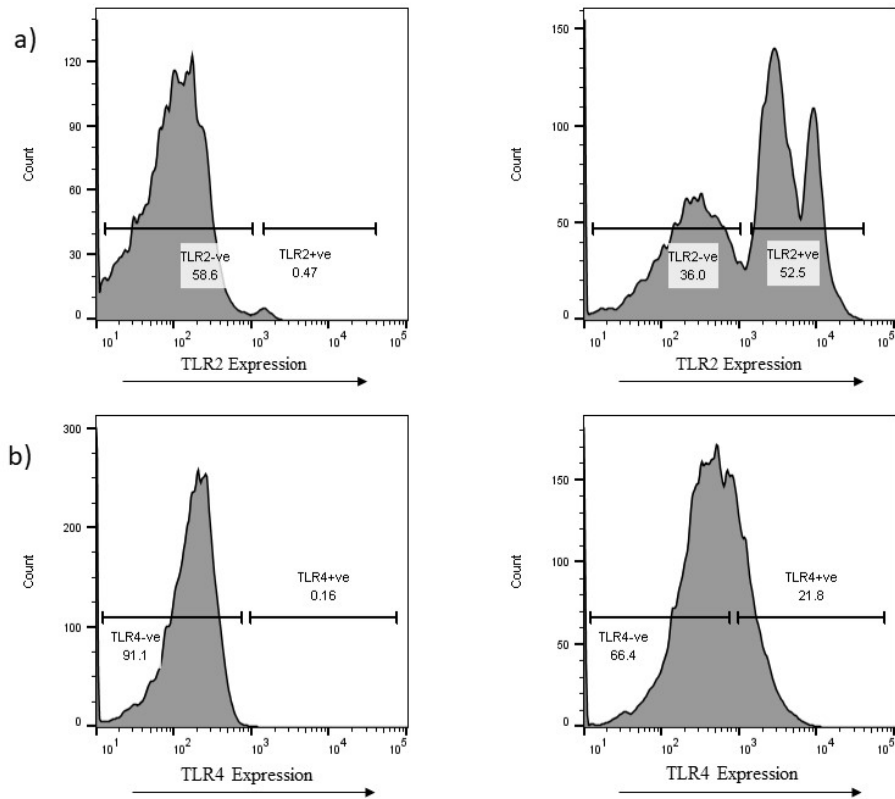
Figure 4.17. Histograms illustrating a) TLR2 and b) TLR4 expression on leukocytes in healthy blood in the unstained (left) and stained (right) control.

Expression profiles of TLR2 and TLR4 for the different experimental samples at each time point are show in Figure 4.19. Toll-like receptor 2 was well defined at each time point (Figure 4.18a) and in all experimental samples had a high expression count. Toll-like receptor 4 was less evident (Figure 4.18b) and was not easily distinguishable from negative populations, but the percentage of positive cells did increase over time as peaks were distinguishable at later time points.
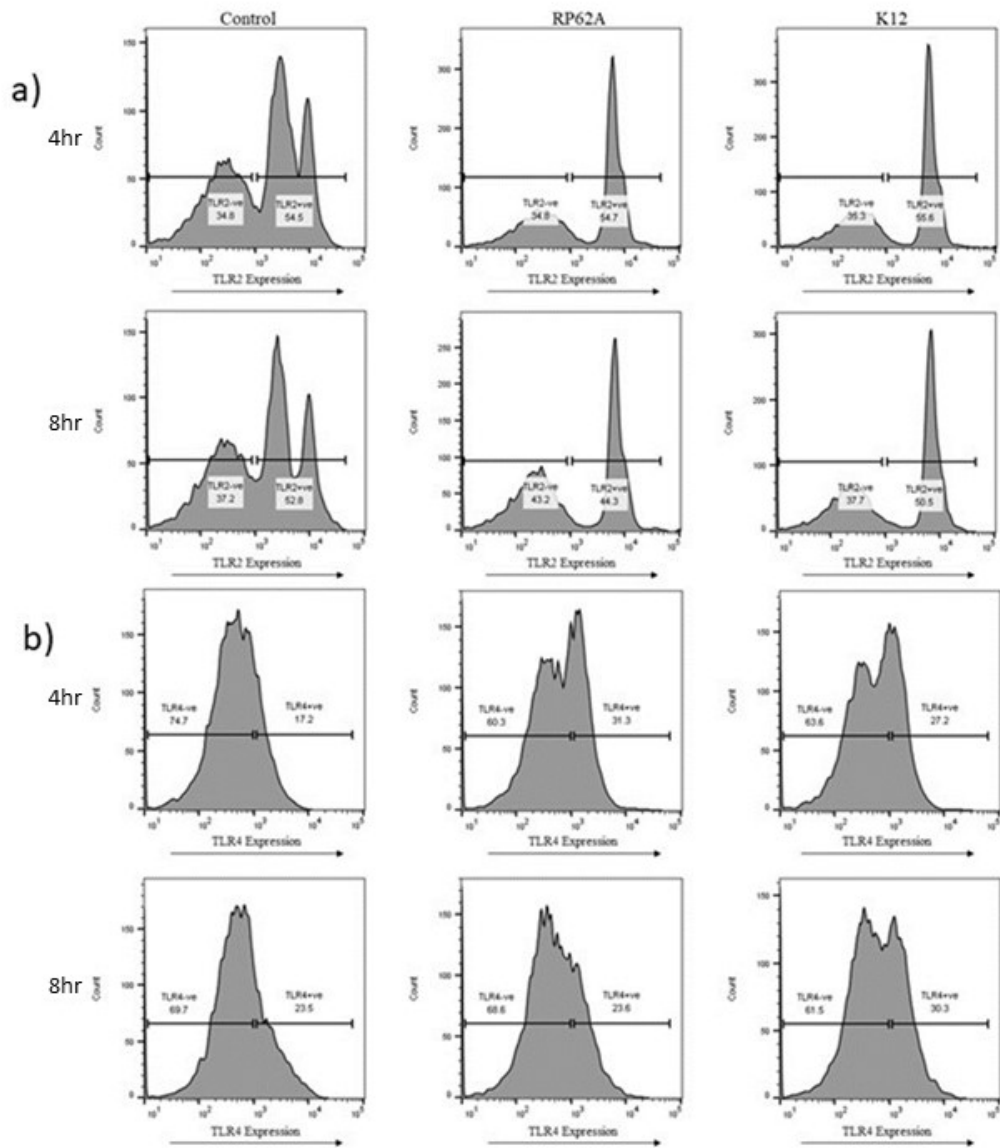
Figure 4.18. Histograms of a) TLR2 and b) TLR4 expression in response to control, *S. epidermidis* RP62A and *E. coli* K12 samples at 4 hour and 8 hour intervals.

#### 4.3.5.2. TLR Expression Profiles

Each cell type was gated appropriately based on CD45 staining patterns and side scatter patterns into leukocytes, monocytes, granulocytes and lymphocytes.

#### 4.3.5.2.1. TLR2

The expression profiles of TLR2 in granulocytes, monocytes and lymphocytes are shown in Figure 4.19. Toll-like receptor 2 expression on granulocytes remained unchanged for the duration of the experiment (Figure 4.19a). Average expression of TLR2 was approximately 2000 (MFI) on granulocytes throughout the time course in all treatments. However, monocytes were found to vary considerably in TLR2 expression over the course of the experiment (Figure 4.19b). Toll-like receptor 2 expression was much higher than what was seen on the granulocytes (MFI of 7466 vs 2000). At 4 hours post-infection, all treatment groups demonstrated a significant increase in TLR2 expression (p = 0.0250), although a Dunn's multiple comparisons test did not identify any sample as being significantly different. The control group increased to 9020 (1.2% increase), the RP62A-treated group increased to 13608 (1.8% increase) and the K12-treated group increased to 11454 (1.5% increase). At 8 hours post-infection, this trend reversed to show a decrease in TLR2 expression on all experimental groups (p = 0.1000). The control group decreased to 8499 (0.9% decrease), the RP62A-treated group decreased to 11796 (0.9% decrease) and the K12-treated group decreased to 8183 (1.4% decrease).

A slight decrease in TLR2 expression was noted on the lymphocytes although most changes were not significant (Figure 4.19c). At 4 hours post-infection, the control group increased in TLR2 expression whereas the infected groups decreased (p = 0.1679). The control group increased to 3331 (0.9% increase), the RP62A-treated group decreased to 2333 (0.8% decrease) and the K12-treated group decreased to 1865 (0.6%). At eight hours post-incubation, all groups except control showed a decrease in TLR2 expression. The control group increased to 3365 (1% increase), the RP62A-treated group decreased to 1765 (0.8% decrease) and the K12-treated group decreased to 1350 (0.7% decrease; p = 0.0036), although a Dunn's multiple comparison test did not identify any sample as being significantly different.
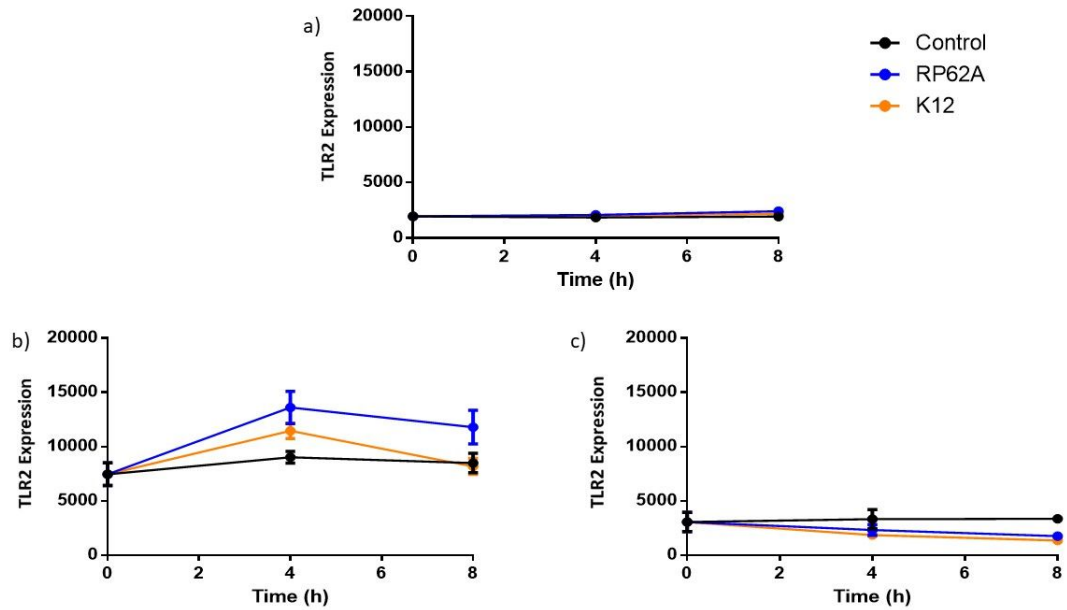
Figure 4.19. Toll-like receptor 2 expression over the 8-hour infection on a) granulocytes, b) monocytes and c) lymphocytes (n = 3 donors). Error bars represent the mean ±SEM.

### 4.3.5.2.2. TLR4

Expression of TLR4 on granulocytes, monocytes and lymphocytes was measured (Figure 4.20). Granulocyte TLR4 expression was found to decrease at 4 hours post-infection but increase again at 8 hours post-infection (Figure 4.20a). Expression at the beginning of the experiment was high (4189) but decreased at 4 hours post-infection to an average expression of 1785 (57% decrease). At 8 hours post-infection, all groups demonstrated an increase in TLR4 expression, which was much greater in the control sample (p = 0.1321). The control increased to 3114 (43% increase), the RP62A-treated group increased to 1954 (9% increase) and the K12-treated group increased to 1865 (4% increase). Toll-like receptor 4 expression was also found to vary on monocytes (Figure 4.20b). Expression was lower at the beginning of the experiment than was seen with the granulocytes (2320), and at 4 hours post-infection increased or remained the same in the infected groups and decreased in the control. The control group decreased to 1781 (23% decrease), the RP62A-treated group remained the same at 2315 and the K12-treated group increased to 3013 (23% increase). At 6 hours post-infection, the control group and the RP62A-treated group showed an increase in TLR4 expression whereas the K12-treated group showed a decrease. The control group increased to 1970 (10% increase), the RP62A-treated group increased to 2596 (11% increase) and the K12-treated group

148

decreased to 2239 (26% decrease). Toll-like receptor 4 expression was not found to vary significantly in the lymphocyte subpopulation of leukocytes (Figure 4.20c).
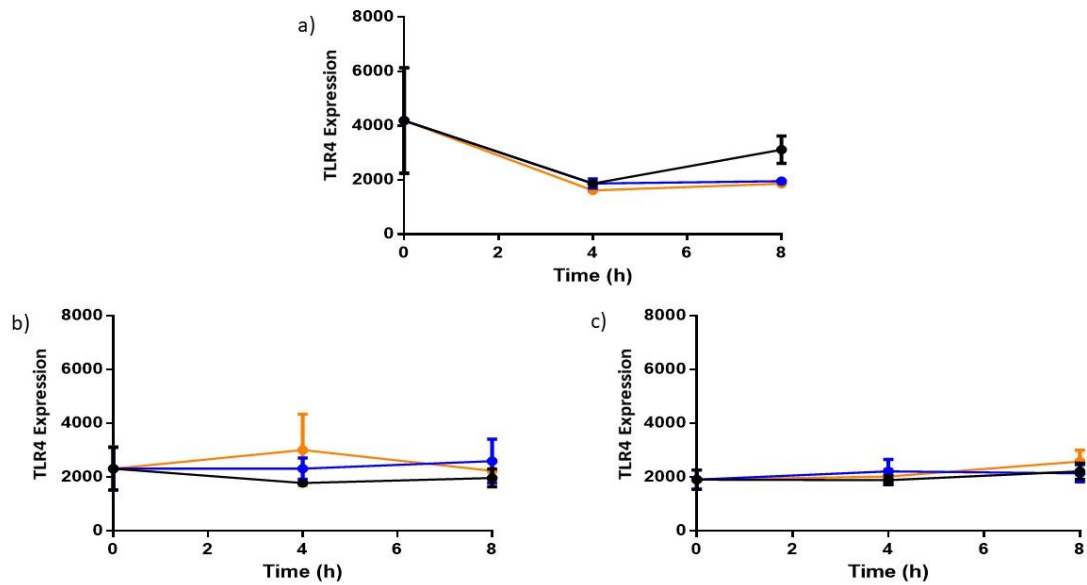


Figure 4.20. Toll-like receptor 4 expression over the 8-hour infection on a) granulocytes, b) monocytes and c) lymphocytes (n = 3 donors). Error bars represent the mean ±SEM.

## 4.4. Discussion

Innate immune cells represent an effective and highly coordinated defence system against infection ( Iwasaki and Medzhitov, 2015; Gasteiger *et al*., 2017; Li and Tablin, 2018). Overstimulation and dysregulation of these cells occurs during severe inflammation and sepsis, representing a key factor in understanding and interpreting its causes (Cohen, 2002). Phagocytosis is an essential process in the removal of pathogens from diseased tissues and preventing excessive inflammation (Li and Tablin, 2018). The professional phagocytic cells (neutrophils) and the antigen-presenting cells (monocytes/macrophages) are key in defending the host from infection and in promoting the development of sepsis and septic shock (Cohen, 2002; Gasteiger *et al*., 2017). However, during sepsis monocytes and neutrophils are unable to participate effectively in the clearance of bacterial invaders ( Rittirsch *et al*., 2008; Umlauf *et al.,* 2013). Thus, measuring phagocytosis of pathogenic bacteria by neutrophils is a useful tool in understanding host-pathogen interactions during the early stages of sepsis.

The light microscopy results found that the neutrophils in all infected samples began to cluster together accompanied by other immune cells, particularly lymphocytes. This clustering reflects a cellular reaction to surround and contain any infected neutrophils and

chemotaxis of lymphocytes towards areas of infection (Sokol and Luster, 2015). This clustering also strongly suggests the formation of NETs, extracellular DNA fibres that serve to eliminate extracellular pathogens while protecting host cells from damage (Li and Tablin, 2018). To confirm this in the future, extracellular staining with a DNA stain (such as Propidium iodide) could highlight these NETs. In addition to this clustering effect, a loss of definition in the multi-lobed nuclei of infected neutrophils was also observed (Figure 4.2). This strongly indicates condensation of the nuclei in such neutrophils, suggesting that these cells are experiencing apoptosis, or infection specific cell death, pyroptosis (Bergsbaken *et al*., 2009).

The most notable outcome of the phagocytosis investigation was that more neutrophils in the *Staphylococci*-treated blood contained intracellular bacteria than was observed in the *E. coli*-treated blood. This trend was evident for all strains tested within each genus and persisted throughout the course of the experiment. One possible explanation for this difference is the different virulence potential of strains used in this experiment. *S .epidermidis* RP62A and 1457, *S. aureus* VAP39 and SH1000 were all isolated from infections, whereas *E. coli* K12, B, ECOR26 and GMB10 were all non-pathogenic strains. However, as was seen in Chapter 3, the *E. coli* strains were responsible for an increased cytokine response compared to the pathogenic *Staphylococcus* strains; thus, the disease potential of the organism is not the reason for the difference in neutrophil uptake.

A possible reason for *E. coli* not being taken up to the same extent as *Staphylococci* is that *E. coli* are capable of persisting within an iron-poor environment, such as human serum, by the production of siderophores to sequester free iron, and is able to avoid complement deposition and phagocyte ingestion via the production of a protective capsule and the synthesis of type 3 secretion systems (TTSSs; Celli and Finlay, 2002; Miajlovic and Smith, 2014; Martin *et al.*, 2017). *Escherichia coli* is capable of synthesising up to four different siderophores: aerobactin, enterobactin, salmochelins and yersiniabactin (Martin *et al*., 2017). *Staphylococcus aureus* is very capable of surviving and replicating with professional phagocytes and are able to resist attempts at killing and limiting the infection ( Malachowa and DeLeo, 2011; Thammavongsa *et al*., 2015). This could perhaps be why there is a greater uptake in this case; the ability to survive within these cells would negate the production of anti-complement and anti-phagocytic mechanisms and therefore these bacteria would not resist uptake. The same is potentially true for *S. epidermidis*, especially as *S. epidermidis* is capable of producing antimicrobial

peptide-neutralising molecules such as sepA (Cheung *et al.*, 2014), which would prevent intracellular killing.

Flow Cytometry analysis of leukocytes from whole blood proved to be a useful and effective tool for monitoring changes in cell density, shape and certain marker expression. Currently, flow cytometric analysis is employed in numerous clinical diagnoses, including diagnosis of leukaemias, lymphomas and identification of infectious diseases such as HIV and sepsis (Umlauf *et al.*, 2013; Mizrahi *et al.*, 2018). In this study, flow cytometry analysis allowed for the monitoring of two specific leukocyte cellular subgroups; the granulocytes and the mononuclear cells. Initially, CD3, CD14, CD19 and CD45 were chosen to identify each subset and monitor progress. Using CD45-FITC, a clear identification of CD45-positive leukocytes was possible and identified approximately 7000 leukocytes per 3-10 μl of lysed and washed cell preparations. This represents approximately 50-60% of the total volume taken up by the cytometer, indicating good recovery of leukocytes and showed the efficacy of using CD45 as a marker for leukocytes. This work correlates well with previous studies (Figure 4.5; Brown and Wittwer, 2000; Cherian *et al.*, 2010; Kahng *et al.,* 2015). Specifically, the high granularity of the neutrophil subgroup and the high staining for CD45 allowed for effective gating of these cells, thus these cells were clearly well-defined from the other cell groups. CD14, the main differentiation marker of monocytes was a very good defining marker of monocytes, and exclusively separated the monocytes from neutrophils and lymphocytes (Zamani *et al.*, 2013). Whilst the fact that both B and T cells have very similar population characteristics (small size and low granularity) it was impossible to separate them using CD45 expression but CD3 (the T cell receptor; Valle *et al.*, 2015), and CD19, a transmembrane glycoprotein present on the cell surface of all B cells (Wang *et al.*, 2012) were able to differentiate B and T cells effectively. Thus, the use of CD3, CD14 and CD19 staining in conjunction with CD45 staining allowed for the accurate separation of both these lymphocyte subtypes, and hence completed the separation of all main leukocytes involved in sepsis development.

Over the course of experimental infection (0-6 hours), there was very little variation in populations in uninfected control blood. This was important as it verified that experimental conditions (such as rotation, temperature, time *etc*.) had little to no effect on the results. Incubation with either *S. epidermidis* RP62A or *E. coli* K12 led to changes in flow plot characteristics over time. An increase in granularity and greater conformity of size in the granulocyte population of *S. epidermidis* RP62A-treated blood could possible reflect the increased uptake of bacteria by neutrophils, and increased clumping of leukocytes and formation of NETs as seen by microscopy. Fuchs *et al*. (2007) demonstrated that within 3 hours of stimulation neutrophils lose their characteristic lobular nucleus (as we observed), degranulating their membranes before dying. DNA fragmentation does not occur in this form of cell death, causing the chromatin to unfold into the extracellular space allowing neutrophils to continue their antimicrobial effects after death via the formation of NETs. This process correlates with increases in granularity at 2 hours (uptake of bacteria) and decrease by 6 hours (degranulation and cell death, NET formation). The use of Histopaque 1077 allowed us to avoid preservation with BD FACS lyse which compromised cell membranes. However, only the mononuclear cells could be recovered via this method. In order to confirm changes in neutrophils, an alternative method of cell isolation could be applied, such as using a Percoll-based density gradient with 33mM NaCl to lyse red blood cells (Kuhns *et al*., 2015) or a Ficoll-Hypaque gradient (Haslett *et al.,* 1985).

Monocytes incubated with *S. epidermidis* RP62A and *E. coli* K12 rapidly lost population definition with subsequent loss of both CD45 and CD14 expression. However, Annexin/PI staining determined that at least 95% were viable. However, it is possible that the isolated monocyte populations do not contain any necrotic cells, as these cells often lose the definition and may sediment differently. Therefore, the entire mononuclear leukocyte cell population was examined to determine any cell death present in the samples. Even in these samples, cell death was very low, and the vast majority of cells were alive, and a very small proportion were apoptotic. This suggests that monocytes are unlikely experiencing cell death via apoptosis or pyroptosis but are more likely differentiating into APCs. In one study, PBMC infection with agonists of viral origin led to a substantial reduction in the number of CD14-positive monocytes within 6 hours of infection, and this trend was consistent with differentiation rather than cell death (Hou *et al.*, 2012). This could have happened in this study, which could be confirmed as

differentiation by using fluorescent antibodies specific for the MHC-II receptors (Reuter and Lang, 2009). MHC-II is only expressed on monocytes and macrophages that have processed pathogenic antigens and presented them on their cell surface, hence becoming an APC (Reuter and Lang, 2009).

Significant increases in CD45 expression were seen on monocytes and granulocytes treated with *S. epidermidis* RP62A and *E. coli* K12. CD45 is a leukocyte specific tyrosine phosphatase that is essential for proper leukocyte antigen receptor signal transduction (Tchilian and Beverley, 2006). All cells of the haemopoietic cell line express certain levels of CD45 on their cell surface (Tchilian and Beverley, 2006). It is particularly important when initiating antigen-specific responses in B and T lymphocytes, particularly cytokine-specific upregulation (Tchilian and Beverley, 2006). Increased expression of CD45 on monocytes and granulocytes could be related to antigen receptor transduction initiation of cytokine regulation, differentiation into APCs, phagocytosis and NETosis (Rosales, 2018). Additionally, increased expression of CD45 may also directly contribute to the prolonged survival of these cells, as CD45 negatively regulates apoptosis, preventing excessive apoptosis in inflammatory periods (Bergsbaken *et al*., 2009).

CD14 expression decreased in monocytes treated with *S. epidermidis* RP62A and *E. coli* K12, resulting in a very low number of positive cells by 6 hours post-infection. CD14 is a co-receptor for TLR4 that detects and binds to LPS in the presence of LPS-binding protein (LBP; Mukherjee *et al*., 2015). It exists in two forms; membrane-bound (mCD14) and a soluble scavenger form (sCD14; Mukherjee *et al*., 2015). Changes in expression of CD14 are likely related to inflammation and infection dynamics – an increase in expression after initial detection of PAMPs would potentially lead to an increase in cell surface expression of mCD14 to promote pro-inflammatory processes such as cytokine secretion and phagocytosis. This gradual increase on neutrophils reflects the important function of this cell type in early host defence. The decrease in mCD14 expression on monocytes at the later experimental time points supports the switch from mCD14 to sCD14, as the monocytes have experienced initial stimulation with PAMPs and scavenge using sCD14 to detect further bacterial cells and to promote neutrophil activity. It is also possible that the decrease in monocytes and the increase in neutrophils reflects the release of mCD14 from monocytes and the binding of these sCD14 forms neutrophils, promoting efficient phagocytosis and cytokine production. Non-survivors of sepsis are noted as having reduced CD14 expression on monocytes harvested during ICU stay, although this association was not significant (Danikas *et al*., 2008).

Both TLR2 and TLR4 expression was evident on a range of leukocytes. Toll-like receptor 2 was found to be more abundantly expressed on a wide range of leukocytes, and TLR4 to a lesser extent. While both were abundant in their expression, there were disparities between the numbers of cells expressing them and the level of expression. Both of these TLRs have a restricted pattern of expression in leukocytes with different levels of regulation, and both are known to be present in monocytes, granulocytes, lymphocytes and dendritic cells (Muzio *et al.*, 2000). Both are expressed maximally on CD14+ cells (monocytes), and a higher level of expression of TLR4 has been noted on granulocytes, which is reflected in the current results (Muzio *et al.*, 2000). A possible explanation is that TLR2 is expressed at a higher level at resting state than TLR4, or less TLR4 molecules were required to initiate a response, hence the lower levels of expression on a subset of leukocytes.

The parameters investigated in the present study (cell count, expression of CD markers, viability and TLR expression) have successfully allowed for the development of whole blood model that can be applied to understand disease processes and infection dynamics. The innate immune system cells offer a rich pool of biomarkers for infection and disease, and the use of an *ex vivo* system allows for these processes to be investigated without the need for animal models. All cells and markers behaved as predicted and were consistent with the literature. The cells also were able to survive outside of the body for up to six hours and showed very little sign of the experimental procedure interfering with their function and health. To conclude, this study has allowed for the development of a model that potentially has very important applications in the future. An example of its application to a potential novel biomarker is presented in chapter 5.

## Chapter 5. Characterisation of Sterol Responses in a Whole Blood Sepsis Model

## 5.1. Introduction

### 5.1.1. Cholesterol

Cholesterol is an abundant molecule found in all animal cells, and is essential for many cellular processes (Cyster *et al.,* 2014). It constitutes approximately 25% of the total lipid content of cell plasma membranes, and is necessary for efficient membrane packing and fluidity. Packing of cholesterol in membranes also serves cell signalling roles by acting to anchor transmembrane receptors and provide membrane integrity (Russell, 2003; Cyster *et al*., 2014). Excess cholesterol is broken down into constituent bile acids in the human liver, converting approximately 500mg of cholesterol per day (Russell, 2003). Bile acids are secreted into the small intestine and act as emulsifiers of dietary lipids and fat-soluble vitamins, participating centrally in digestion (Russell, 2003). Cholesterol biosynthetic pathways are active in all nucleated mammal cells, and involve cholesterol metabolism and utilisation of its downstream products (Cyster *et al*., 2014). These include oxysterols, modified cholesterol that have undergone addition of one or two hydroxyl groups on either the 24th, 25th or 27th carbon (Figure 5.1; Russell, 2003). Previous studies showed that oxysterols, produced during bile acid synthesis, provide a negative feedback mechanism that prevents excessive breakdown of cholesterol (Russell, 2003). However, recent research indicates that oxysterols also play a pivotal role in inflammation and adaptive immunity, as well as critical roles in cholesterol metabolism in the brain (Hughes *et al.*, 2013; Cyster *et al.*, 2014; Tall and Yvan-Charvet, 2015; Ning *et al*., 2017; Testa *et al.*, 2018).
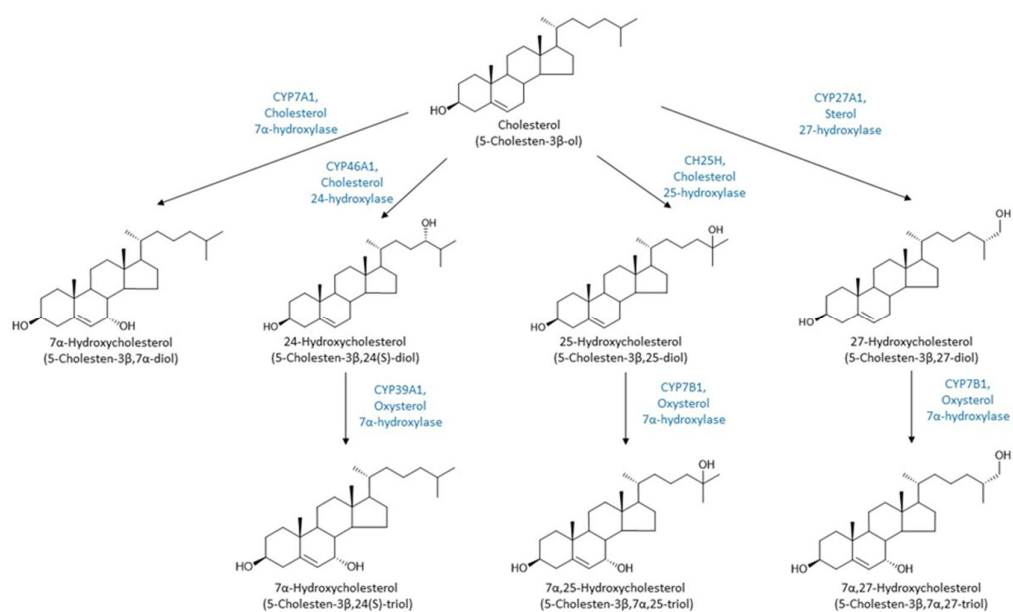
Figure 5.1. Schematic diagram of the sterol biosynthetic pathway. Chemical names are shown below chemical structures and the biosynthetic enzyme is shown adjacent to the arrow indicating the reaction it catalyses (Adapted from Russell, 2003).

### 5.1.2. 25-Hydroxycholesterol

Cholesterol is hydroxylated by the enzyme cholesterol 25-hydroxylase (CH25H), or CYP27A1, which is expressed at relatively low levels in all mammalian tissues (Cyster et al., 2014; Ning et al., 2017). The product of this reaction, 25-hydroxycholesterol (25-HC), is an oxysterol with an additional hydroxyl group (-OH) present on the 25th carbon of the molecule (Cyster et al., 2014). Expression of CH25H is induced in human macrophages upon exposure to Poly I:C, LPS and type I IFN signalling (Russell, 2003; McDonald and Russell, 2010; Cyster et al., 2014; Ning et al., 2017). In vitro, 25-HC has been shown to prevent viral replication and cell membrane fusion, which is linked to its upregulation through IFN signalling (Cyster et al., 2014; Ning et al., 2017). Interferons play a crucial role in dampening the immune response to infections therefore controlling excessive inflammation, particularly through regulating IL-1 expression and inflammasome suppression (Cyster et al., 2014). It follows that 25-HC production via IFN signalling may play a pivotal anti-inflammatory role both in vitro and in vivo (Cyster et al., 2014). Other functions of 25-HC described both in vitro and in vivo include regulation of IgA production and the promotion of macrophage foam cell differentiation and neutrophil chemotaxis (Koarai et al., 2012; Cyster et al., 2014). Pro-inflammatory properties have also been described through the upregulation of pro-inflammatory cytokines (Cyster et al., 2014). Relevant to sepsis, 25-HC has been shown to aid in

recovery of liver function after LPS exposure, and *ch25h*-deficient mice had elevated levels of IL-1β and IL-18 after LPS exposure (Cyster *et al*., 2014; Ning *et al*., 2017).

Research on the role of 25-HC in immunity has been largely investigated using viruses (Amako *et al*., 2009; Anggakusuma *et al*., 2015; Li *et al.,* 2017a; Wang *et al*., 2017; Shawli *et al*., 2019), while in comparison little research has looked at the role of bacteria and bacterial PAMPs on 25-HC induction (Zou *et al*., 2011). One *in vitro* study on 25-HC production noted bacterial infection with *Listeria monocytogenes* promotes upregulation of CH25H in infected macrophages *in vivo*, and is one of the only investigations into the role that 25-HC plays in bacterial infection (Zou *et al*., 2011).

### 5.1.3. Aims and Objectives

The principal aim of this study is to assess the sterol response in whole blood to defined bacterial PAMPs and live bacteria. Following on from soluble mediators in Chapter 3, this chapter also investigates the potential of 25-HC as a host biomarker in bacterial sepsis using the *ex vivo* whole blood model. The chapter has the following objectives:

- Analysis of concentrations of the oxysterols 24-HC, 25-HC, 27-HC, 7α-HC, 7α, 25-diHC and 7α, 27-diHC and cholesterol via LC-MS in platelet poor plasma isolated from whole blood treated with;
  - The PAMPs LPS, PGN and Poly I:C.
  - The whole live bacteria *E. coli* K12 and *S. epidermidis* RP62A.
  - Blocking antibodies for TLR2 and TLR4, to investigate PRR activation by *E. coli*.

## 5.2. Materials and Methods

### 5.2.1. Microbiology and Whole Blood

Up to three colonies of *E. coli* K12 or *S. epidermidis* RP62A were inoculated for up to 24 hours in either 5 ml TSB or LB at 37°C at 200 r.p.m. Bacterial cultures were standardised as described in Section 2.5.4 and were added to 1 ml of healthy volunteer whole blood as outlined in Section 2.5.6.2. Blood was incubated for 2 and 8 hours at 37°C and 10 r.p.m. Blood was removed and centrifuged at 7000 r.p.m for 5 minutes at room temperature before being frozen at -20°C.

### 5.2.2. Solid-phase Extraction of Sterols

To a 1.5 ml microcentrifuge tube, 1.05 ml of prepared standards in ethanol (Appendix A) was added and 100 µl PPP samples or quality control PPP or water was added drop-wise to the corresponding microcentrifuge tube. Samples were sonicated for 5 minutes before adding 350 µl of water and sonicating for a further 5 minutes. Tubes were centrifuged at 17000 g for 30-60 minutes (section 2.9.1.1). During this time, a Vacuum Manifold Processing System was sterilised with 70% ethanol before being fitted with Sep-Pak Vac 3cc (200 mg) tc18 cartridges. The cartridges were pre-conditioned with 100% then 70% ethanol before the PPP or water samples were added and allowed to drip through via gravity. The columns were then washed with 6 ml of 70% ethanol to elute the oxysterols. The sample was split equally between two tubes labelled Fr1A and Fr1B. Columns were washed again with 70% ethanol and cholesterol eluted using 2 ml of 100% ethanol. This sample was split equally between two tubes labelled Fr3A and Fr3B. All samples were dried overnight in a Scanvac scanspeed vacuum concentrator (section 2.9.1.2).

### 5.2.3. Sterol Oxidation and Reverse-phase Extraction

Samples from section 5.2.2 were reconstituted using 100 µl isopropanol and vortexed thoroughly before adding 1 ml $KH_2PO_4$. Samples were vortexed for 1 minute before 3 µl of cholesterol oxidase was added to tubes labelled Fr1A and Fr3A, and incubated at 37°C for 1 hour. After this, the reaction was stopped with 100% methanol and 150 µl of glacial acetic acid. To tubes labelled Fr1A and Fr3A, 190 mg of $D_5$ Girard P was added and to tubes labelled Fr1B and Fr3 150 mg of $D_0$ Girard P was added. All tubes were vortexed until all the Girard reagent had dissolved and then incubated overnight in the dark at room temperature. The next day, a vacuum manifold was sterilised with 70% ethanol and fitted with Oasis HLB 3cc (60 mg) extraction cartridges and preconditioned with 100%, 10%

and 70% methanol, respectively. Each sample was added to its own column and allowed to drip via gravity. Columns were then washed with 35% methanol before the effluent was combined with $H_2O$. The effluent was reapplied to the column, the column washed with 17% methanol and the resulting effluent combined with more $H_2O$, vortexed and reapplied to the column. Th column was washed with 10% methanol and all effluent discarded. The bound sterols were eluted with 3x applications of 1 ml 100% methanol and one application of 1 ml 100% ethanol. Samples were stored at -20$^o$C until analysis.

### 5.2.4. Mass Spectrometry and Chromatogram Analysis

For each sample, the first and second elutions of Fr1A, Fr1B, Fr3A and Fr3B samples were centrifuged at 17000 g for 30-60 minutes. During this, mobile phases A and B for LC-MS were prepared and placed in the LTQ-Orbitrap Velos. HPLC vials were prepared of 19-hydroxycholesterol (19-HC), 50% methanol/50% isopropanol and 95% methanol. Samples were combined using 22.5 µl from each microcentrifuge tube and 60 µl of water. Samples were analysed using the LTQ-Orbitrap Velos.

Chromatogram outputs were processed using Thermo Xcalibur Roadmap. Layouts for each analyte of interest were established using their mass ranges and the scan filter FTMS and TIC/ITMS. Upon identification of each analyte, an area peak was exported from the FTMS chromatogram and the concentration of the internal standard used to calculate the concentration of the unknown analyte.

### 5.2.5. Statistical Analysis

Statistical analysis of sterol data was performed using GraphPad Prism version 7. N numbers refer to the number of donors analysed in the test. Data was assumed to not be normally distributed (n < 7) and Kruskal-Wallis tests with a Dunn's multiple comparison test were applied. Two-way ANOVAs were performed for multivariate data. A p value of < 0.05 was considered significant. On graphs, error is represented by the SEM.

## 5.3. Results

### 5.3.1. Cholesterol & Oxysterol Quantification

Data obtained from LC-MS was analysed using Thermo Xcalibur Roadmap to identify and quantify sterol analytes in plasma samples taken at 2 and 8 hours post-infection. Included with all samples was a control plasma sample from the experimental donor, a QC plasma sample that always originated from the same donor (CRF 131) and a water blank to monitor contamination. The water blank in all extraction batches was found to contain no sterols, indicating no contamination. All QCs from each batch extraction were analysed for their 25-HC concentration (n = 8) and cholesterol concentration (n = 9; Figure 5.2). The CoV for 25-HC and cholesterol were 21.2% and 9.3% respectively, giving good reproducibility.
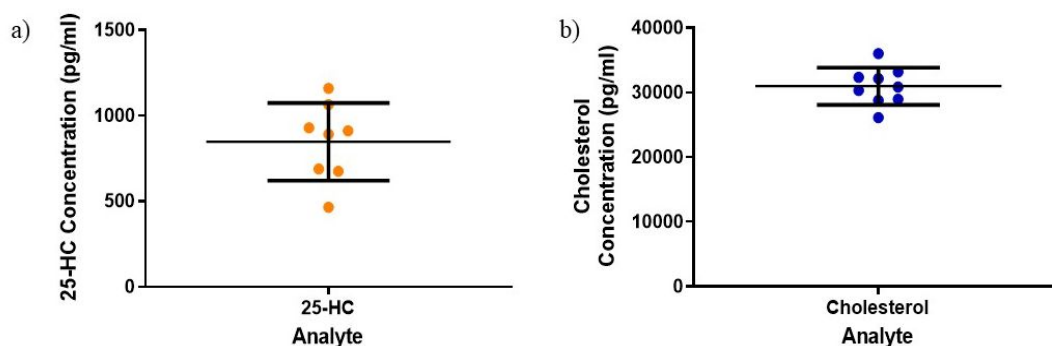


Figure 5.2. 25-hydroxycholesterol (a, n= 8 replicates) and cholesterol (b, n = 9 replicates) concentration in the QC sample replicates. Error bars represent the mean ±SEM.

Chromatograms for all sterols analysed were generated including ion chromatograms for cholesterol (Figure 5.3) and the 6 oxysterols (Figure 5.4) together with FTMS chromatograms (Figure 5.5). All analytes were found to elute from the column at roughly the same retention time, and this retention matched expected times of these analytes (Figure 5.5). The ion fragmentation pattern of cholesterol (Figure 5.4) is characterised by the abundant 411 mass fragment, as well as the 151 and 163 fragment that characterises most cholesterol derivatives. Cholesterol is further characterised by the less abundant peaks 367 and 396. 25-hydroxycholesterol is characterised by the 163 fragment, an abundant 437 peak coupled with a non-existant 394 fragment. Conversely, 24-HC, in both its S and R isomer form, contains this 394 fragment, allowing for resolution of these two analytes (Figure 5.4a and b). 27-hydroxycholesterol is characterised again by the 151 fragment of oxysterols and an abundant 437 peak. In addition to these peaks, the

characteristic 327, 412 and a highly abundant 427 peak characterise this oxysterol (Figure 5.4c). 7α-hydroxycholesterol is characterised by the oxysterol 151 peak and an abundant 437 peak. In addition to these characteristic oxysterol fragmentation peaks, 7α-HC also fragments into the less abundant 394 and 409 peaks (Figure 5.4d). 7α,25-dihydroxycholesterol is characterised by an abundant 453 peak and the less abundant 425 and 435 peaks. 7α,27-dihydroxycholesterol is discriminated from 7α,25-diHC by the presence of low abundance 151 and 410 peaks as well as a highly abundant 443 peak (Figure 5.4e and f). The FTMS chromatograms used to quantify the sterols after they have been identified as described above are shown in Figure 5.5. The peaks highlighted are characteristic of all sterols described.
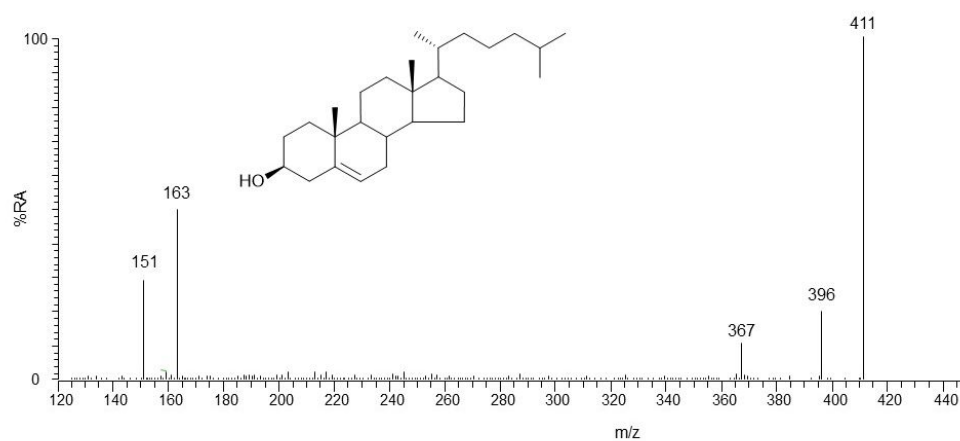


Figure 5.3. Ion fragment chromatogram of cholesterol, highlighting the fragmentation pattern. Chromatogram represents the cholesterol fingerprint in the QC plasma sample.
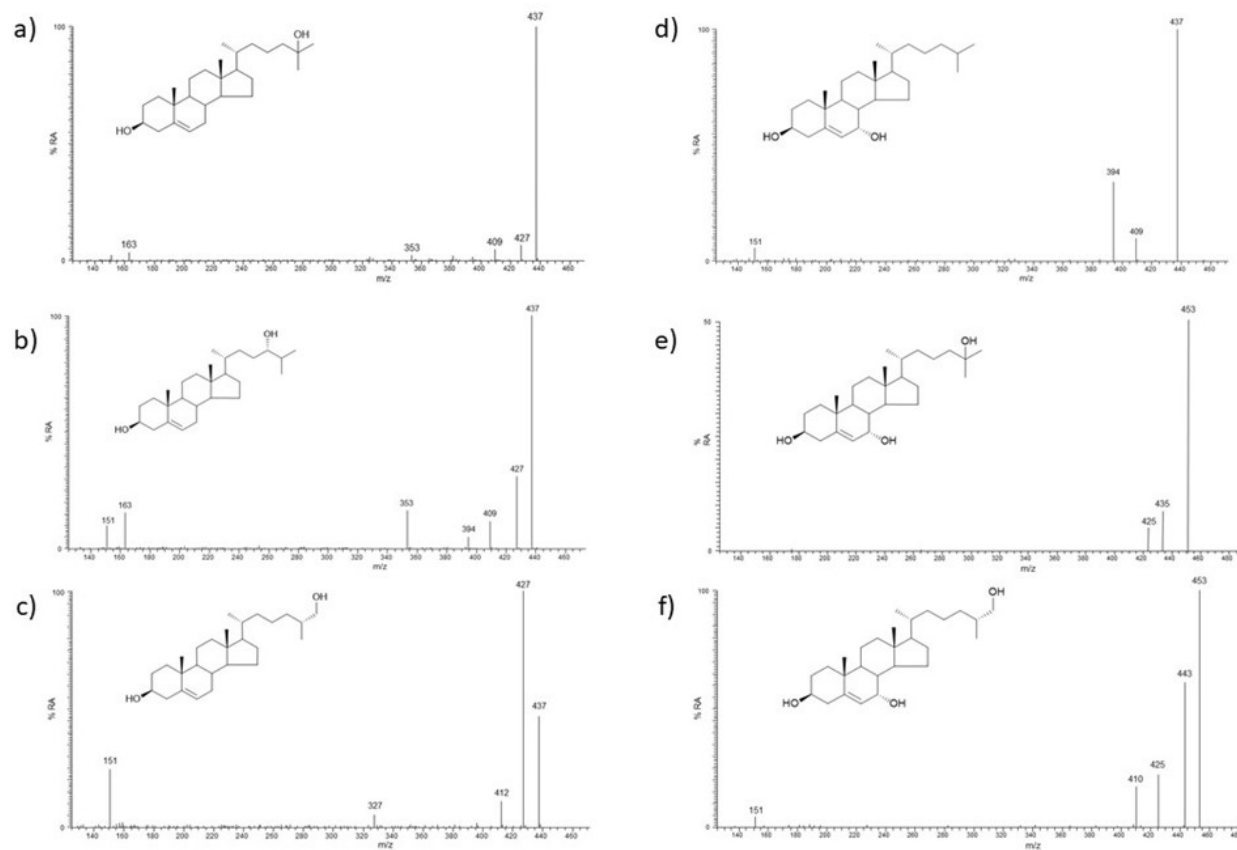
Figure 5.4. Total ion fragment chromatograms (TIC) of the six oxysterols analysed, illustrating their fragmentation pattern; a) 25-hydroxycholesterol; b) 24(S)-hydroxycholesterol; c) 27-hydroxycholesterol; d) 7α-hydroxycholesterol; e) 7α,25-dihydroxycholesterol; f) 7α,27-dihydroxycholesterol. Chromatograms represent the fingerprints in the QC plasma sample.
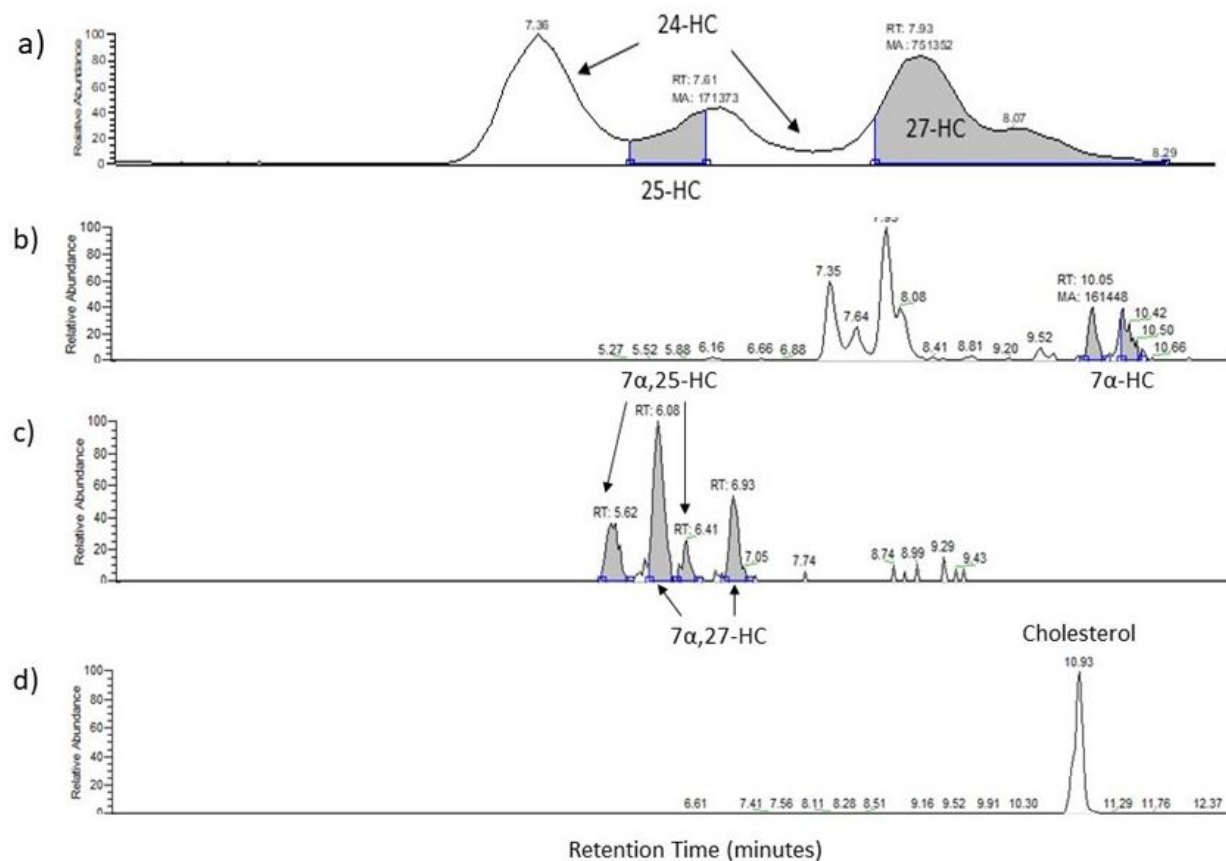
Figure 5.5. Fourier transform mass spectrometry (FTMS) chromatograms used for quantification of the analytes investigated. Retention time in minutes is displayed above each highlighted peak area. Briefly, a) FTMS chromatogram of 24-HC, 25-HC and 27-HC; b) FTMS chromatogram of 7α-HC; c) FTMS chromatogram of 7α,25-diHC and 7α,27-diHC; and d) FTMS chromatogram of cholesterol.

### 5.3.2. Sterol responses to PAMPs and whole live bacteria in *ex vivo* whole blood

#### 5.3.2.1. 25-Hydroxycholesterol

25-hydroxycholesterol was detected in all plasma samples tested, including the control samples (Figure 5.6). The average concentration of 25-HC detected was 1723.744 pg/ml (1.7 ng/ml), which was sufficently low to match expected concentrations of 25-HC in healthy subjects (Crick *et al.*, 2018; Dias *et al.*, 2018) . No significant effect was observed at 2 hours post-infection in any treatment groups ($p = 0.8585$). Similarly, at 8 hours post-infection no significant effects were observed in any treatment groups despite small increases in *E. coli* K12-treated PPP and a significant difference indicated by a Kruskal-Wallis test ($p = 0.0061$). Similarly, a two-way ANOVA determined that that there were no interactions between time and treatment, and that neither factor was significant (Treatment, $p = 0.2976$; Time, $p = 0.2432$; Figure 5.6; Table 5.1**).**

 ($p = 0.0061$);
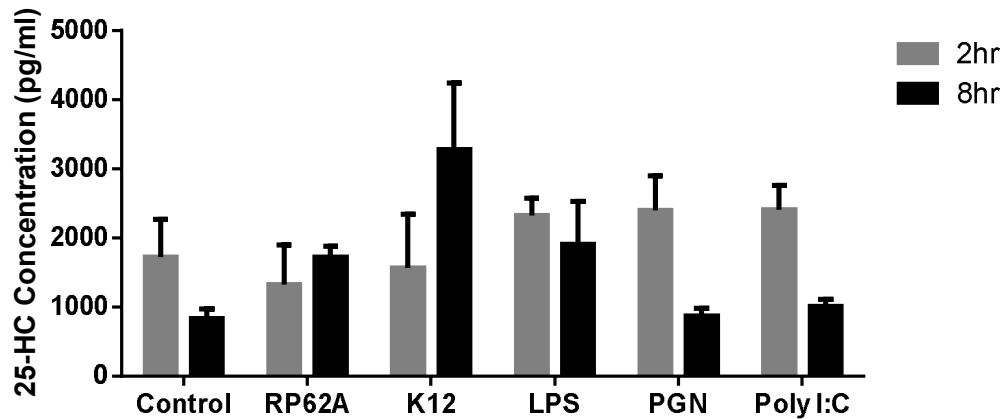


Figure 5.6. The concentration of 25-HC (pg/ml) in response to whole bacteria and PAMPs (n = 3 donors). Grey and black bars represent 2 and 4 hours post-infection respectively. Error bars represent the mean ±SEM.

The relationship between whole live bacteria was analysed further (Figure 5.7). A Kruskal-Wallis test demonstrated that there was signficantly more 25-HC in the blood treated with *E. coli* K12 at this time point than was observed in the control ($p = 0.0036$). Despite 25-HC concentration on *S. epidermidis* RP62A-treated plasma being elevated, no significant association was found at this time point between the bacteria and 25-HC expression.
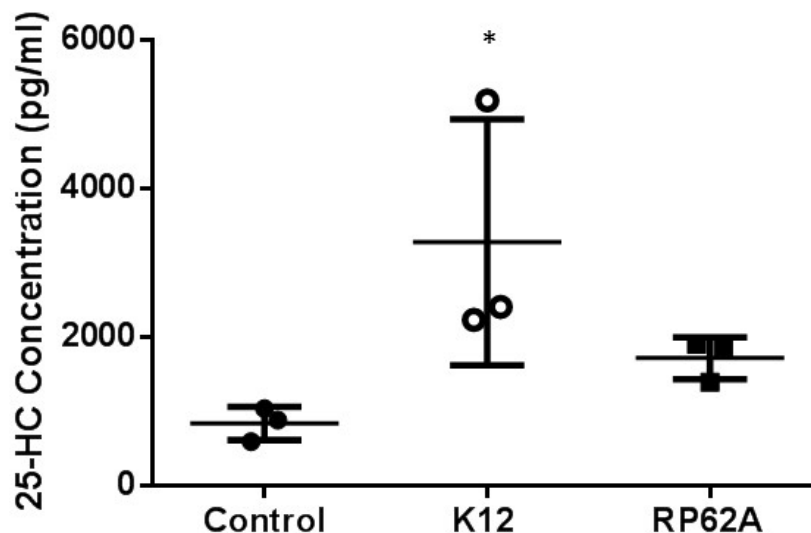
Figure 5.7. The concentration of 25-HC (pg/ml) at 8 hours post-infection in response to control and whole live bacteria-treated samples (n = 3 donors). Error bars represent standard error and the asterisk indicates significant difference between the *E. coli* K12-treated plasma and the control plasma ($p < 0.05$).

### 5.3.2.2. Other Oxysterols

All other oxysterols were investigated (Figure 5.8). The most abundant oxysterol in the uninfected blood was 24-HC (Figure 5.8a), and the least abundant was 7α,25-diHC (Figure 5.8d). Changes were dependent on the oxysterol and time. Specifically 24-HC, 27-HC and 7α-HC demonstrated significant decreases between 2- and 8-hour time points independent of the stimulus ($p = 0.0157$). 27-hydroxycholesterol was the only oxysterol (other than 25-HC) to change significantly following stimulation or infection (Figure 5.8b). Whilst the *S. epidermidis* RP62A- and *E. coli* K12-treated blood remained unchanged at 2 hours post-infection, blood treated with all three PAMPs significantly increased 27-HC concentration ($p = 0.0450$). At 8 hours post-infection this effect was lost and 27-HC was similar to control in all treatments.
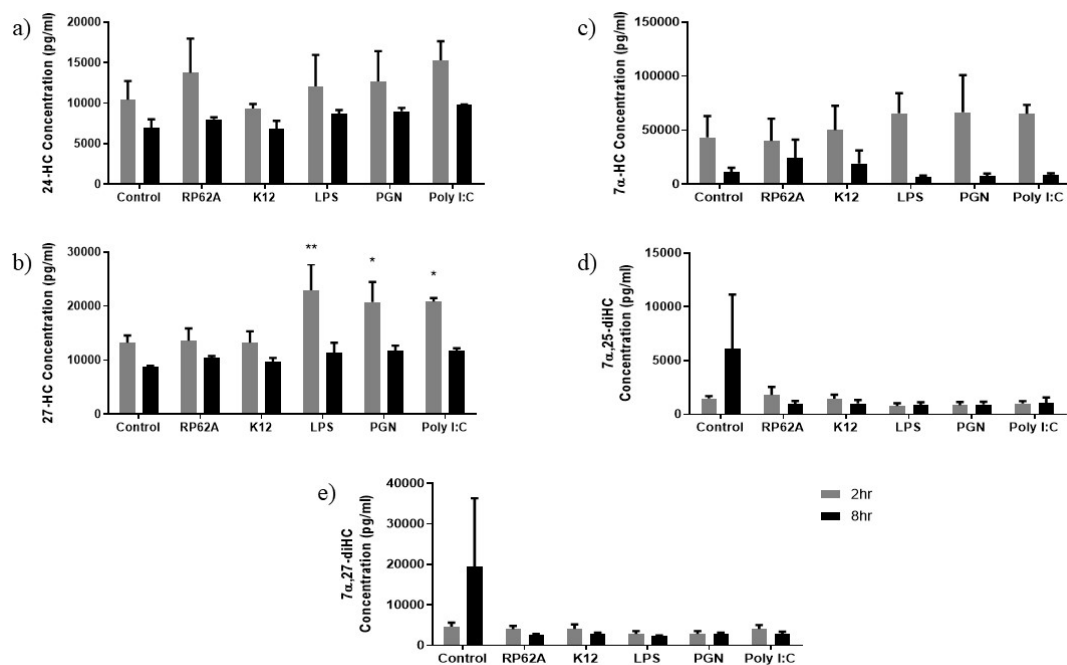
Figure 5.8. Concentration of 24-HC (a), 27-HC (b), 7α-HC (c), 7α,25-diHC (d) and 7α,27-diHC (e) at two- and eight-hours post-incubation (n = 3 donors). Error bars represent the mean ±SEM. On graphs, asterisks represent the following significant values: $* = p < 0.05$, $** = p < 0.01$.

## 5.3.2.3. Cholesterol

Cholesterol was found to be the most abundant sterol in uninfected blood samples investigated (Figure 5.9). Initially, small changes in cholesterol concentrations were noted in all treated samples at the 2-hour time point (not significant). At the 8-hour time-point, there were further changes in cholesterol concentration noted in all treated groups, including the control, whilst the agonist-treated samples remained at the same concentration. No significant changes were found in any of the treatments tested (Table 5.1).
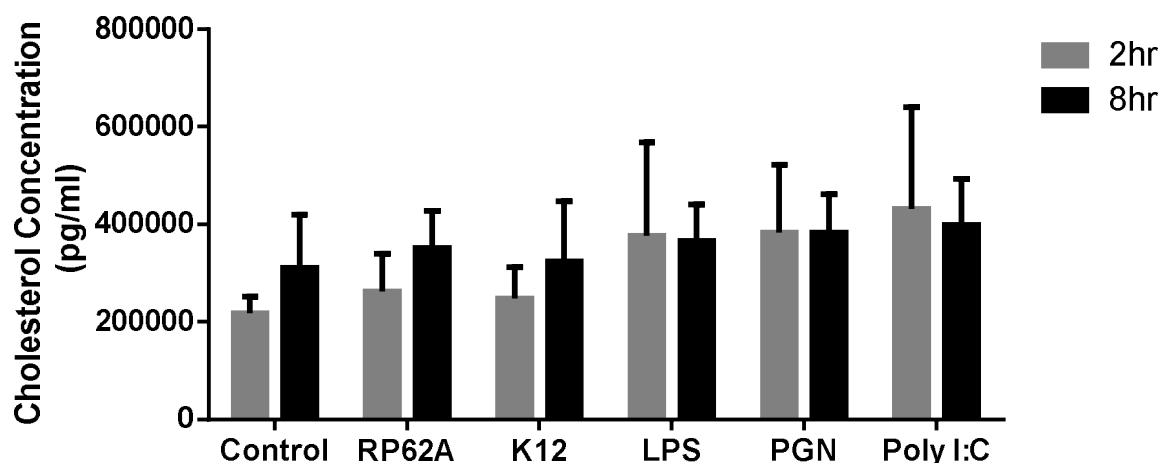
Figure 5.9. The concentration of cholesterol in response to PAMPs and whole live bacteria. Grey and black bars represent 2- and 8-hours post-infection (n = 3 donors). Error bars represent the mean ±SEM.

Table 5.1. Significance values (p < 0.05) of individual 2-way ANOVAs performed on each sterol investigated. Tukey's multiple comparison tests were applied to analyse any significance between treatment groups. Treatment refers to the experimental PPP (Control vs RP62A vs K12 vs LPS vs PGN vs Poly I:C) and Time refers to 2 vs 8 hrs post-infection.

| Sterol | Treatment | Time 2 hours vs. 8 hours |
|---|---|---|
| 25-HC | 0.2976 | 0.2432 |
| 24-HC | 0.3176 | 0.0157 (*) |
| 27-HC | 0.0450 | <0.0001 (****) |
| 7α-HC | 0.9928 | 0.0005 (***) |
| 7α,25-diHC | 0.4478 | 0.4867 |
| 7α,27-diHC | 0.4657 | 0.5304 |
| Cholesterol | 0.4141 | 0.2188 |

### 5.3.3. Influence of TLR2 and TLR4 on PAMP- and bacteria-induced sterols in whole blood

To determine whether TLR pathways were involved in *E. coli* K12-induced sterols, whole blood pre-incubated with blocking antibodies against human TLR2 and TLR4 were added prior to infection with *E. coli* K12 for 8 hours (Figure 5.10). 25-hydroxycholesterol concentration (Figure 5.10a) increased non-significantly in blood treated with *E. coli* K12, an effect that was replicated following preincubation with control PAb or specific TLR2 and TLR4 receptor blocking antibodies. There was no significant decrease in 25-HC between the *E. coli* K12 control and the TLR antibody-treated blood ($p = 0.1140$).

The 24-HC concentrations (Figure 5.10b) remained relatively consistent with or without any treatment with the exception that one donor showed a large non-signficant increase in a sample pre-treated with the TLR2 blocking antibody. This result is considered an anomaly as the other donors did not replicate this response ($p = 0.8771$). Concentrations of 27-HC (Figure 5.10c) were variable across the different treatment groups, with the only change seen in the blood treated with the PAb control, where a decrease was observed, but not a significant one ($p = 0.3056$). 7α-hydroxycholesterol concentrations (Figure 5.10d) were variable in samples taken from the plasma control and *E. coli* K12 control but were less variable when treated with either PAb or the TLR blocking antibodies, where concentrations appeared to be slightly lower, but not statistically significant ($p = 0.5985$). 7α, 25-dihydroxycholesterol (Figure 5.10e) again showed variability in PPP concentration in the blood treated with RPMI control and *E. coli* K12 but seemed to normalise somewhat with preincubation with both PAb and the TLR blocking antibodies. Addition of *E. coli* K12 in all cases appeared to decrease the concentration of 7α, 25-diHC, but this change was not significant ($p = 0.1289$). While overall the 7α, 27-diHC concentration (Figure 5.10f) remained relatively unchanged, and variability was observed between donors for each treatment group ($p = 0.8878$).
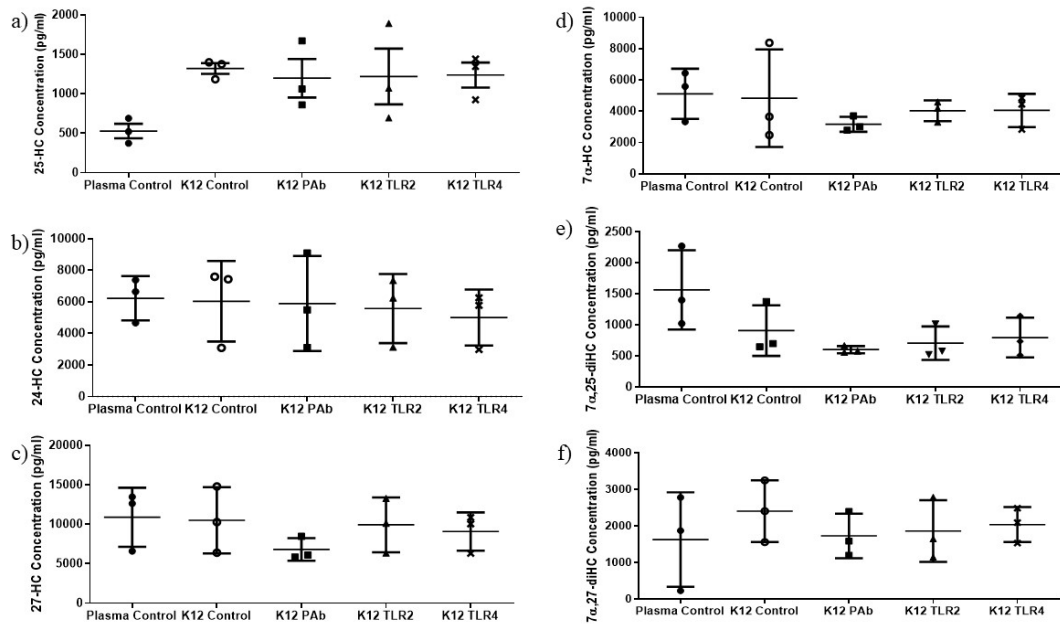
Figure 5.10. Oxysterol concentrations of a) 25-HC; b) 24-HC; c) 27-HC; d) 7α-HC; e) 7α,25-diHC; and f) 7α,27-diHC in the TLR block experiment (n = 3 donors). Error bars represent the mean ±SEM.

A Kruskal-Wallis test performed on the cholesterol concentrations (Figure 5.11) revealed that there were no significant differences between any of the treatment groups ($p = 0.6637$). However, a 2-way ANOVA performed on all the TLR block data revealed that there was a significant trend associated with treatment ($p = 0.0379$) and a significant difference between the concentrations of the sterols ($p < 0.0001$). Evidently, there was substantially more cholesterol present in the PPP samples than any other sterol. As shown in Figure 5.11, addition of *E. coli* K12 to blood regardless of pre-incubation with blocking antibodies led to a reduction in cholesterol concentration, although this was not significant. The addition of control and blocking antibodies seemed to enhance this effect but did not significantly reduce cholesterol concentration (Figure 5.11).
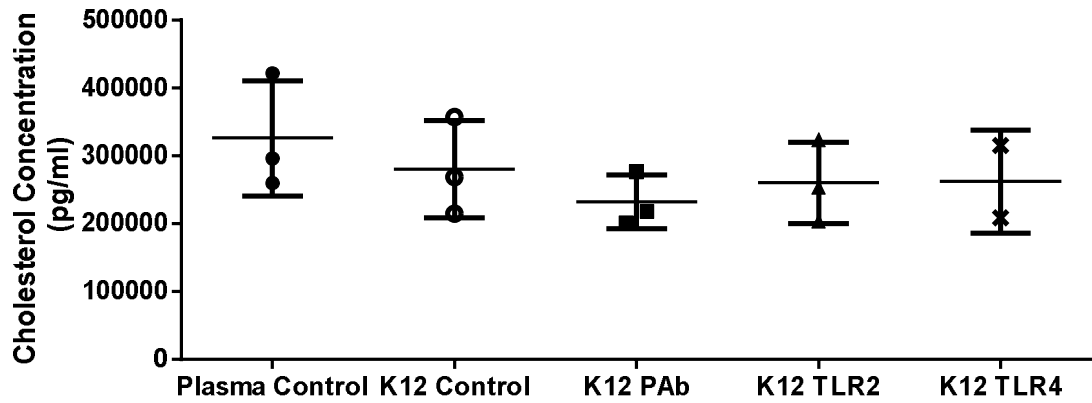
Figure 5.11. Cholesterol concentration in the TLR block experiment (n = 3 donors). Error bars represent the standard error.

As little difference was seen between *E. coli* K12 control and pre-treated TLR2 and TLR4 inhibited blood, the same samples were also analysed by ELISA to determine IL-6 concentration and any changes in response to TLR blocks. As can be seen in Figure 5.12, there was no IL-6 present in control PPP samples, but there was significantly higher concentrations of IL-6 present in blood treated with *E. coli* K12 only ($p = 0.0117$). Antibodies for TLR2 and TLR4 could not inhibit *E. coli* induced IL-6, despite a reduction in the TLR4 treated blood. Interestingly, both TLR2- and TLR4- blocked blood showed marginally decreased levels of IL-6 in PPP, which in the TLR4-blocked blood the average concentration was almost half that of the K12 control. Neither the PAb control, the TLR2-blocked blood nor the TLR4-blocked blood was significantly different to the control.
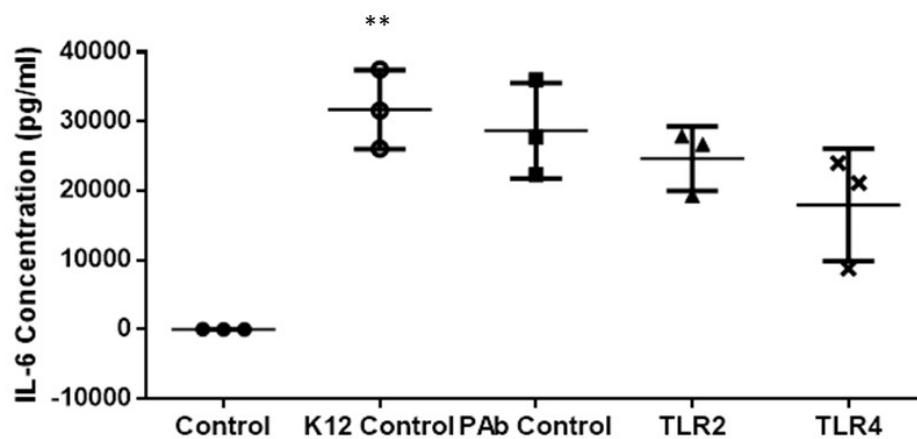
Figure 5.12. Graph showing the concentration of IL-6 in the TLR inhibition experiment (n = 3 donors). Error bars represent the mean ±SEM. Black asterisks indicate where there is significant difference between the control and the *E. coli* K12 control samples ($p < 0.05$).

## 5.4. Discussion

Sterols play a significant role in maintaining lipid homeostasis in mammals (Russell, 2003). Increasingly, the role these molecules play in promoting, mediating and downregulating inflammatory responses is being recognised as key components of inflammatory research (Gold *et al.*, 2014). These molecules may also represent important new biomarkers of inflammatory causes and disease severity (Zmysłowski and Szterk, 2019). A body of research has highlighted several sterols that can be applied in inflammatory diagnostics (Zmysłowski and Szterk, 2019). Mass spectrometry is a widely used clinical technique for identifying and quantifying molecules involved in disease processes and has wide applications in the medical field (Jannetto and Fitzgerald, 2016). In this chapter, LC-MS was used to identify and quantify sterols of the bile acid synthetic pathway in the plasma of experimentally infected healthy blood in order to determine the potential for sterol biomarkers in the diagnosis of sepsis.

25-hydroxycholesterol has received much attention recently over its numerous roles in virus-related inflammation  (Amako *et al.*, 2009; Anggakusuma *et al.*, 2015; Li., 2017a; Wang *et al.*, 2017; Shawli *et al.*, 2019), whilst one study has focused on the role bacteria play in 25-HC activity during an infection (Zou *et al*., 2011). The data in this chapter challenges the body of evidence that supports the idea that 25-HC induction during infection is virus specific by confirming that bacteria are also capable of promoting 25-HC synthesis *ex vivo*. Statistical analysis of 8-hour data demonstrated that *E. coli* K12 significantly upregulated 25-HC production in donor blood, whilst *S. epidermidis* RP62A did not. Whilst there was no significant difference in the 25-HC concentration between

the two different strains, the fact that only K12 induced a significantly higher concentration than the control supports that 25-HC is upregulated more specifically in response to Gram-negative *E. coli* activity. It is also possible that the lower 25-HC concentration induced by *S. epidermidis* RP62A may be due to a delayed or muted response as was seen with the cytokine data in Chapter 3. These results build on the hypothesis that 25-HC does play a role bacterial immunity.

The results clearly indicate that *E. coli* K12 is capable of stimulating a 25-HC response in whole blood samples. *E. coli* K12 is a Gram-negative organism that possesses an abundant pool of LPS on its cell surface (Bachmann, 1972). Previous studies have found that 25-HC production is mediated through TLR4 engagement by LPS *in vivo*, therefore this work is consistent with these previous findings (McDonald and Russell, 2010; Ning *et al.*, 2017). However, when TLR blocking experiments were performed, only a small reduction (non-significant) in 25-HC was observed, thus it is possible that 25-HC production is mediated via a mechanism independent of TLR4. Gram-negative bacteria produce other PAMPs beside LPS such as extracellular DNA, that engage TLRs other than TLR4 (Heumann and Roger, 2002). In addition to this, *E. coli* is responsible for damage to host cells that leads to the generation of DAMPs, stimulating other TLRs and NLRs (Saïd-Sadier and Ojcius, 2012). Any of these PAMPs and DAMPs are capable of stimulating interferon signalling and hence 25-HC production. Therefore, it is likely that 25-HC production is not specific to TLR4 signalling and that its upregulation is a universal feature of the inflammatory response. The increase in 25-HC at the 2-hour time-point in samples treated with purified agonists confirmed to a degree that these PAMPs upregulate 25-HC production. The small volume of agonist used could perhaps explain why little response was seen at eight hours when it would be expected at high levels in normal cell line models of 25-HC production. The 1 µl (of 1 µg/ml) added at the beginning of the experiment was most likely ingested by phagocytes and destroyed very early in the experiment, and a more accurate representation of any interactions could have been achieved by using a higher concentration (Heumann and Roger, 2002).

Surprisingly the experiments also showed the potential importance of 27-HC, as concentrations were found to increase over the first 2 hours in blood treated with PAMP agonists only. 27-hydroxycholesterol is a bile acid that has recently been linked with the development of breast cancer in patients with high dietary cholesterol (Baek *et al.*, 2017), promoting proliferation of cancerous cells in an oestrogen receptor (ER)-dependent manner (Hughes *et al.*, 2013; Baek *et al.*, 2017). In addition to promoting breast tumours,

27-HC has also been linked to the development of Alzheimer's, as high levels of 27-HC have been found in the blood of such patients (Testa *et al*., 2018). 27-hydroxycholesterol has also been associated with viral immunity, in part because the enzyme responsible for its synthesis, CYP27A1, is predominantly expressed in macrophages, much like CH25H (Civra *et al*., 2018). In addition, a recent study found that 27-HC has potent anti-viral activity, and modulation of host oxysterols may be a primary host strategy to combat a broad range of viral infections (Civra *et al*., 2018). Therefore, the upregulation of 27-HC in blood could be related to a broader host strategy of modulating oxysterols during bacterial infections as well as viral infections. However, it is important to note that only the purified agonists elicited such a response and only at the 2-hour time-point; thus, more work is required to further understand this interaction.

The other oxysterols investigated did not show any response to PAMPs, *E. coli* K12 or *S. epidermidis* RP62A. This was not surprising in this model despite functions being reported in other body compartments and diseases ( Amako *et al.*, 2009; Hughes *et al*., 2013; Baek *et al*., 2017; Civra *et al*., 2018; Zmysłowski and Szterk, 2019). For instance, 24-HC is almost exclusively formed in the brain, and circulating levels are low in healthy adults (Testa *et al.,* 2018). The enzyme responsible for its synthesis (CYP46) is mainly located in neurons, and 24-HC readily crosses the blood-brain barrier to modulate cholesterol homeostasis in the brain (Lutjohann and von Bergmann, 2003). Crucially, 24-HC has been linked to the development of Alzheimer's and demyelinating diseases, suggesting that the major role of this oxysterol is in the nervous system (Testa *et al*., 2018). This is perhaps one reason for the low levels in the current model as circulating 24-HC is low to begin with and the enzyme required for its synthesis lies elsewhere in the body. With respect to 7α-HC, it is a product of cholesterol synthesis found to accumulate within atherosclerotic plaques and contribute significantly to inflammatory signalling in the inflamed artery (Cho *et al*., 2017). Indeed, 7α-HC is considered a biomarker for both lipid peroxidation and oxidative stress indicative of impaired glucose tolerance and diabetes (Ferderbar *et al*., 2007). Thus, one reason why levels of this oxysterol are low in our model may be due to its involvement only in localised arterial inflammation during atherosclerosis and not in any pathogenic immune response. While the levels of 7α,25-diHC and 7α,27-diHC were barely detected in PPP, this can be explained by the fact that they have roles in bile acid synthesis, and do not appear to contribute to the inflammatory response (Russell, 2003).

Cholesterol has for a long time been acknowledged for its significant immune functions, both during resting state and during infection (Robertson and Ghazal, 2016). No significant changes in cholesterol were noted in response to stimulus or time. However, during the TLR blocking experiment, decreases were seen in plasma cholesterol concentration in all *E. coli* K12-treated blood (regardless of antibody type), although these changes were not significant. These results are consistent with the fact that during infection, concentrations of plasma cholesterol have been noted to decrease substantially, a reaction that promotes the inflammatory response and prevents excessive inflammation (Tall and Yvan-Charvet, 2015). In fact, sepsis patients have been found to have consistently low plasma cholesterol concentration during the inflammatory event (Feingold and Grunfeld, 2000). These findings are particularly interesting as they support the current literature which reports that cholesterol concentrations significantly decrease in the blood in response to infection ( Feingold and Grunfeld, 2000; Tall and Yvan-Charvet, 2015).

The extraction method used for this analysis was appropriate due to the high sensitivity and specificity of the LC-MS, as confirmed by the QC samples. The results confirmed the accuracy of the method and confirmed that operator error was low, thus variability in the experimental samples was due to donor variations and not to experimental error. Donor samples were found to vary significantly in certain cases, and one or two donors had oxysterol levels that were much higher or lower than in others, signifying that a certain degree of variability in sterol expression exists between different people. In some cases, this variability did not allow for an accurate measure of collective responses to certain stimuli. In future, more donors should be included to narrow this variation and truly represent population responses.

The current method used required the extraction of sterols with different concentrations of ethanol (70-100%) followed by several days of oxidation of target molecules and their reverse-phase extraction with different concentrations of methanol (15-100%), as well as extended time in the LC-MS for analysis. While this method is highly accurate and sensitive, the length of time required to extract and analyse (5-7 days) is not applicable for the diagnosis of severely ill sepsis patients. Sepsis symptoms present within four hours of stimulation of PRRs in the blood, and progression to septic shock can be very rapid in many cases (Cohen, 2002; Bowmann *et al.,* 2013; Conway Morris *et al.,* 2018). Within 24-48 hours, a patient could well be experiencing very severe septic shock. Therefore, the current method is not suitable for clinical diagnosis at this time, but is highly appropriate

for further research into the pathways and mechanisms governing oxysterol interactions during bacterial sepsis and promises for future applications in such research.

To confirm the 25-HC-*E. coli* interactions observed in this study, it is clear that more work needs to be undertaken to elucidate the roles of 25-HC in bacterial immunity. Firstly, more donor samples are required to accurately assess the influence that *E. coli* K12 and perhaps other more pathogenic strains have on 25-HC production *ex vivo*. Secondly, more time-points should be analysed to track concentration changes in these systems. However, donated blood does not last very long outside the body, and after 4-8 hours, blood cells and molecular components begin to degrade and do not represent the healthy, circulating system being investigated (Kuhns *et al.*, 2015). Thirdly, using various mononuclear cell lines would aid in confirming interactions and signalling mechanisms.

The current findings support the growing literature on the concept that certain sterols can act as immune modulators. In particular, a firm groundwork of research is already present to develop a potential new biomarker for discriminating bacterial infections based on genera, species or other phenotype. The findings also challenge the concept that 25-HC upregulation is not a virus-specific defence mechanism; rather, it is a more general response to infection. Further, there is evidence that accumulation of cholesterol intra-cellularly is an infection-specific response to stimulation by pathogens. In conclusion, 25-HC represents a potential novel biomarker of bacterial infection and, together with cholesterol, show promise for the development of new diagnostic techniques for sepsis.

## Chapter 6. Characterisation of a collection of blood culture positive *E. coli* (bacterial sepsis) isolates from South West Wales

### 6.1. Introduction

### 6.1.1. Bacterial Sepsis in Wales

Sepsis represents one of the biggest challenges faced by clinicians due to its multifactorial nature and difficulty in diagnosing the cause (Becker *et al.*, 2009; Monneret and Venet, 2016). In the UK, it is currently the major cause of death among critically ill patients and kills more people than both breast and bowel cancer combined (Charles *et al.*, 2009; Chan and Gu, 2011; McPherson *et al.*, 2013; Monneret and Venet, 2016). In England and Wales, up to 27% of all ICU admissions have been diagnosed with severe sepsis, and almost half of these patients will later die due to sepsis complications (McPherson *et al.*, 2013). Rapid diagnosis is needed but complicated by delayed time to test results and delays in conducting wellness assessments such as SOFA and APACHE, as well as a lack of specific biomarkers (Bouch and Thompson, 2008; Vincent, 2016). In Wales, 1800 deaths occur annually and this equates to approximately £125 million being spent annually on sepsis treatment and care (Szakmany *et al.*, 2016). Treating patients in critical care wards in Wales results in approximately £1932 being spent per intensive care patient per night (NHS Wales, 2016). With over 9,500 patients treated in intensive care in Wales in 2015-2016, treating these patients places a significant financial as well as labour burden on the NHS (NHS Wales, 2016). These figures do not account however for patients who are treated on other wards, as sepsis patients are not restricted to ICU wards and for those with comorbidities recorded as cause of death in lieu of sepsis (Rudd *et al.*, 2020).

Hywel Dda University Health Board (HDUHB) is a large cohort of NHS services providing health care for almost 25% of the land mass of Wales (Figure 6.1). Under its management, over 50 centres of health including major hospitals, community hospitals and general practices provide sufficient health care and monitoring for a population of 384, 000 people. The HDUHB currently has four ICUs stationed at each of the 4 major hospitals. The total number of ICU beds for the whole of West Wales is 29, with the most being located at Glangwili General (Hardisty *et al.*, 2019).

**Hywel Dda Health Board**
384,000 population
11,007 members of staff

Glangwili General
Hospital

Prince Philip
Hospital

Bronglais General
Hospital

Withybush General
Hospital

**Carmarthenshire**
183, 936 population

**Ceredigion**
79, 488 population

**Pembrokeshire**
120, 576 population

**7**
Community hospitals

**48**
General Practices

**42, 060**
Operations Performed

**46, 117**
Emergency Admissions

**27, 760**
Arrivals by
Ambulance

**86.4%**
In-patients receiving Sepsis 6
within 1hr

**91.09**
Rate of *E. coli* cases per
100,000 population

**2%**
Reduction in *E. coli*
sepsis cases

Figure 6.1. Hospital frequency and statistics associated with the Hywel Dda University Health Board (Hardisty *et al.*, 2019). Counties that are part of the HDUHB are circled in green on the map of Wales, which are Carmarthenshire, Powys and Pembrokeshire.

### 6.1.2. *E. coli* Sepsis

An important goal in the Clinical Microbiology of sepsis is the identification of the pathogen responsible for the excessive inflammation (Póvoa, 2002). Bacteria are responsible for most cases of sepsis, depending on geographical location and other determining factors such as age (Feezor *et al.*, 2003; Becker *et al.*, 2009; Abe *et al.*, 2010; Schuetz *et al.*, 2011; Ramachandran, 2014; Singer *et al.*, 2016). In Wales, *E. coli* is the most common Gram-negative bacteria isolated from patients with bacteraemia (Public Health England, 2015). This bacterium asymptomatically colonises the mammalian colon and is present in nearly 100% of the population (Kaper *et al.*, 2004). The bacterium usually benefits the host, contributing to good gut health by metabolising certain nutrients into usable host molecules (particularly molecules involved in glycolysis) and preventing colonisation by pathogenic Enterobacteriaceae (Kaper *et al.*, 2004). Rarely do these strains cause disease outside the gut, and only cause mild to moderate enteritis in immunocompromised patients (Vila *et al.*, 2016).

### 6.1.3. ExPEC Infections

Despite the benefits that colonising *E. coli* confer to the host, a group of *E. coli* exist that are capable of invading and colonising almost any sterile body tissues; these are known as extraintestinal *E. coli* (ExPEC). The most common site of ExPEC infection is the urinary tract, and such *E. coli* are known as uropathogenic *E. coli* (UPEC; Vila *et al.*, 2016). Approximately 150 million people worldwide develop at least one UTI annually, and over 40% of women will experience at least one UTI in their lifetime (Terlizzi *et al.*, 2017), with 80-90% of all sampled UTIs caused by UPEC (Terlizzi *et al.*, 2017). Other sites that can be infected by ExPEC include any organ in the intra-abdominal region (liver, spleen, gallbladder, pancreas and kidneys), the bile ducts, the brain (meningitis) and bone tissue (Vila *et al.,* 2016).

The ability to colonise tissues outside the gut environment is important for ExPEC pathogenesis and arises from the possession of an armoury of VFs that confer considerable genomic plasticity for the pathogen (Emody *et al.*, 2003). ExPEC strains share many characteristics with adherent invasive *E. coli* (AIEC; frequently associated with inflammatory conditions of the gut, including irritable bowel disease), including belonging to the pathogenic phylogenetic groups B2 and D and possessing VFs that enable them to invade and colonise surrounding organ tissues (Martinez-Medina & Garcia-Gil, 2014). Virulence factors are encoded by pathogenicity islands (PAIs) that are

acquired via horizontal gene transfer of plasmids, phages and conjugation. Approximately 50% of the ExPEC genome is composed of PAIs, and unique combinations of these PAIs gives rise to a very genetically diverse strain population that are capable of producing numerous combinations of VFs. Important *E. coli* VFs include adhesins, iron-acquisition systems, invasins, toxins and polysaccharide capsules (Vila *et al*., 2016). Traits that are expressed by production of these VFs include attachment to host tissue, competition against other bacteria, damage to host tissue, acquisition of nutrients and avoiding the host immune system (Vila *et al*., 2016). Common *E. coli* VFs and associated genes and function are well documented and these are outlined in Table 6.1.

Table 6.1. Genes encoding VFs and their function (Emody et al., 2003; Wiles *et al.,* 2008; Kohler and Dobrindt, 2011; Vila *et al*., 2016; Terlizzi *et al*., 2017) .

| Virulence Factor | Gene | Function |
|---|---|---|
| Type 1 fimbriae | *fim, fimH* | Tissue colonisation, biofilm formation |
| Dr fimbriae | *draBC, afa* | Epithelium binding, bacterial internalisation, RBC aggregation |
| Haemagglutinin | *hra, tsh* | RBC aggregation |
| P fimbriae | *papACEFG* | Stimulate cytokine production, colonisation |
| S fimbriae | *sfa, sfaS* | Epithelium adhesion, tissue penetration |
| M fimbriae | *bmaE* | Epithelial invasion |
| *E. coli* common pilus | *ecpA* | Epithelial adhesion |
| F1C fimbriae | *foc* | Epithelial adhesion |
| Adhesion siderophore | *iha* | Adhesion |
| Mat | *mat* | Adhesion, meningitis-related |
| Curli | *crl, csg* | Biofilm formation, pathogenicity |
| Antigen 43 | *agn43, flu* | Adhesion, biofilm formation |
| Invasin | *ibeA,B,C* | Tissue invasion |
| Aerobactin | *iuc, aer, iutA* | Siderophore, iron acquisition |
| Iron repressible protein | *irp* | Synthesis of siderophore yersiniabactin |
| Yersiniabactin receptor | *fyuA* | Siderophore receptor |
| Salmochelin | *iroN* | Siderophore receptor |
| Haemin Receptor | *chu, hma* | Iron acquisition from haemoglobin |
| Iron Transport Protein | *sitA,B,C* | Iron transportation |
| Siderophore Receptor | *ireA* | Iron acquisition |
| Complement Resistance Protein | *traT* | Inhibition of classical complement pathway |
| Capsule | *kpsMI-neuA, kpsMII, K1, K2, K5* | Capsule protection against complement and phagocytosis |
| Outer membrane protein | *omp, ompT* | Intracellular survival, immune evasion |
| Increased serum survival | *iss* | Phagocytosis resistance |
| CoIV Plasmid | *coIV* | Colonisation |
| Colicin | *cvaC* | Promotes colonisation by virulent strains |
| Serine protease autotransporter | *pic* | Mucin degradation, epithelial colonisation, mammalian cell damage |
| Secreted autotransporter toxin | *sat* | Proteolytic activity, mammalian cytotoxicity |
| Vacuolating autotransporter toxin | *vat* | Proteolytic activity |
| Haemolysin A | *hlyA* | Pore formation in host cells, cell lysis |
| α-haemolysin | *hylD* | RBC lysis |
| Cytotoxic necrotising factor | *cnf* | Cell necrosis |
| Cytolethal distending toxin | *cdt* | Mammalian cell apoptosis |
| Invasion of brain endothelium | *ibeA* | Invasion |
| B-glucuronidase | *uidA* | Serum survival |
| Colibactin Synthesis | *clb* | dsDNA breakage |
| Uropathogenic specific protein | *usp* | Genotoxin |

### 6.1.4. Aims and Objectives

The aim of this chapter was to characterise genomically and phenotypically clinical *E. coli* isolates obtained from *E. coli* bacteraemia patients, and to identify traits and VFs associated with origins of infection and bacteraemia. Specific aims were as follows:

- Compare traits of clinical isolates with known traits of UPEC and ExPEC.
- Identify *E. coli* phyla, sequence types and genes associated with origin of infection.
- Identify *E. coli* phyla, sequence type and genes associated with sepsis, commensals or water samples.
- Identify known VFs in clinical *E. coli* isolates.
- Confirm whether a relationship exists between origin of infection and *E. coli* invasion phenotype in human epithelial cell lines.

### 6.2. Methodology

### 6.2.1. Microbiology

Ninety-eight clinically relevant strains of blood culture positive *E. coli* were obtained from Public Health Wales on agar slopes (Appendix B). All isolates originated from the HDUHB (Simmons *et al.*, 2019). Slopes were streaked and bacteria inoculated onto blood agar and incubated at 37°C for up to 24 hours (section 2.5.2.). Of the 98 original isolates, two were non-culturable (Figure 6.2). Glycerol stocks were created of the isolates that grew and were stored at -80°C (section 2.5.2.).

### 6.2.2. DNA Extraction and Sequencing

All DNA extractions were carried out using the QIAamp DNA mini kit according to manufacturer's instructions (section 2.5.5). A single colony from each plate was inoculated in 5 ml of LB media and incubated at 37°C at 200 r.p.m for up to 24 hours. One millilitre of overnight culture was pipetted into a 1.5 ml microcentrifuge tube and centrifuged for 5 minutes before discarding the supernatant and adding a further 1 ml of culture and centrifuged as described above. The DNA (ng/ml) was quantified using the Nanodrop spectrophotometer and frozen at -20°C before being sequenced at the Swansea Genome Centre (Dr Matthew Hitchings).

## 6.2.3. Pan-genome Construction

Of the 96 DNA extractions sent for sequencing, 73 were of sufficient quality and purity to be sequenced (Figure 6.2). Sequences were annotated using Prokka (Seemann, 2014) and the output used to construct the pan-genome using the Roary pan-genome pipeline (Page *et al*., 2015). Included in the pan-genome were the ECOR collection of sequences for reference (Ochman and Selander, 1984). The pan-genome was used to determine the core and accessory genome and to create maximum likelihood trees using iTOL v4 (Letunic and Bork, 2007).

```
                        98 clinical isolates

                          Bacterial Culture

              96 isolates              2 isolates not culturable

                          DNA extraction

   Failed to extract 23 isolates       73 isolates
                                   Illumina Sequencing &
                                        Assembly

   39 Urinary   8 Biliary   10 Intra-abdominal   8 Water   8 Other
```
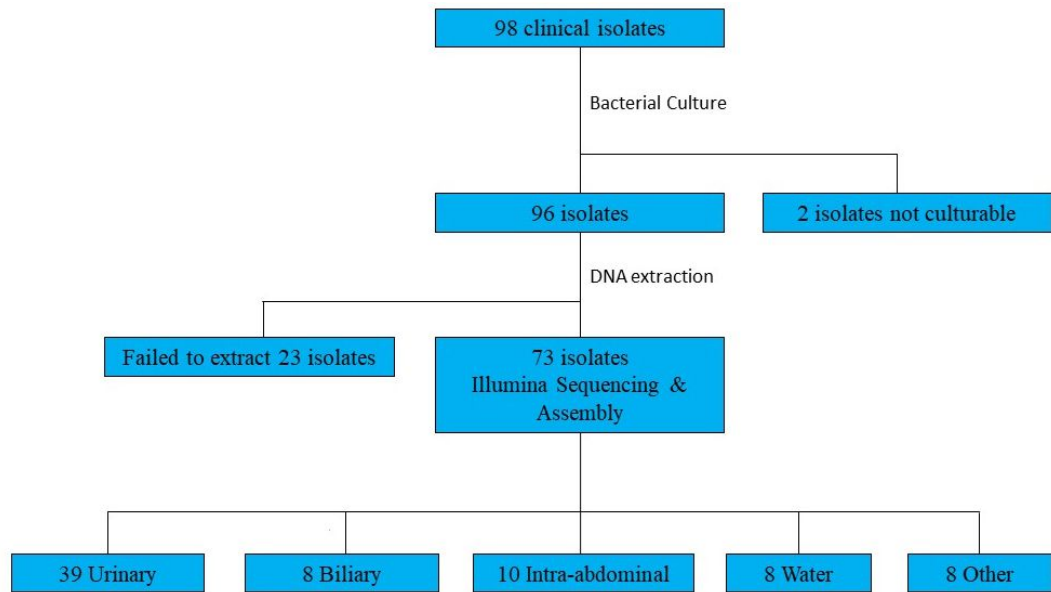
Figure 6.2. Clinical *E. coli* isolates from HDUHB that were cultured, DNA extracted and sequenced from the original collection. Origin of infection is described in the lower tier.

## 6.2.4. Genome-wide Association Study (GWAS)

Scoary microbial pan-GWAS (Brynildsrud *et al*., 2016) was used to assess gene associations within the pan-genome associated with given traits. The traits analysed included "origin of infection" with isolates categorised based on original infection source (clinical decision) from the urinary tract (urinary), bile duct (biliary) intra-abdominal organs (intra-abdominal), undefined or unknown source (other) and environmental sources (water). Other traits analysed included whether isolates were causative of "bacteraemia" or originated elsewhere "non-bacteraemia".

### 6.2.5. Gentamicin Protection Assay

Epithelial cell invasiveness of 4 *E. coli* isolates from each origin of infection (Table 6.2) was assessed using a gentamicin protection assay (sections 2.5.2 and 2.6.5). Confluent UM-UC-3 and CACO-2 cells in 24-well plates were washed and supplemented with antibiotic-free cell culture media. Bacterial cultures were standardised to 0.05 (600 nm) and 100 µl of each suspension added to the cell culture plates and incubated in a 5% $CO_2$ incubator at 37°C for 4 hours. The original bacterial inoculum was serially diluted and the bacterial dose determined. After incubation, cells were washed with PBS and 300 µg/ml gentamicin in PBS added to each well. Plates were incubated for 90 minutes and checked for extracellular bacteria by plating 10 µl from each well. Wells were washed once with PBS and 10 µl plated once again. Plates were washed a further 2x with PBS and 2 ml of 0.1% Triton-100 in PBS added to each well for 10 minutes. Each well was serially diluted and plated onto blood agar and incubated for up to 24 hours. Counts were determined and used to calculate the percentage of the original inoculum invaded. The invasion index was then calculated using this value divided by the multiplicity of infection (MOI; number of bacteria added divided by the number of cells seeded). This experiment was repeated three times for each bacteria tested.

Table 6.2. Isolates used in the gentamicin protection assay.

| Isolate | Origin of Infection |
|---|---|
| K12 | Reference |
| 17/122 | Urinary |
| B17E00 4409 | Urinary |
| 17/106 | Intra-abdominal |
| 3757 | Intra-abdominal |
| B17E00 4376 | Biliary |
| BHE00 4183 | Biliary |
| E18E500522 | Water |
| E18E500166 | Water |
| 17/107 | Urinary |
| 17/104 | Urinary |
| B4053 | Biliary |
| B4019 | Biliary |
| 1124046916 | Intra-abdominal |
| 1124046973 | Intra-abdominal |
| E17E505761 | Water |
| E17E505979 | Water |

## 6.2.6. Statistical Analysis

Statistical analysis of gene and invasion data was performed using GraphPad Prism version 7. Chi squared tests were performed on each gene in Table 6.9. Data was assumed to not be normally distributed (n < 7) and two-way ANOVAs were applied. A p value of < 0.05 was considered significant.

## 6.3. Results

### 6.3.1. The *E. coli* Pangenome

The pan-genome constructed by Roary contained a total of 29763 genes from 136 *E. coli* genomes (73 clinical isolates, 63 ECOR collection). The core genome (genes shared by all or most strains) was composed of 2184 genes and the accessory genome (genes not present in all strains) was composed of 27579 genes. The combined core and accessory genome represents the pangenome (Table 6.3).

Table 6.3. Number of genes recovered by the pangenome in 136 clinical and ECOR isolates. Core and soft-core genes are shared by nearly all isolates, whilst shell and cloud genes are classed under the accessory genome. % represents the percentage of isolates that these genes are present in.

| Pangenome | Genes | Number |
|---|---|---|
| Core | Core Genes (99-100%) | 32 |
|  | Soft-core Genes (95-99%) | 2152 |
| Accessory | Shell Genes (15-95%) | 3816 |
|  | Cloud Genes (0-15%) | 23763 |
|  | Total Genes (0-100%) | 29763 |

Of these genes, 18862 were hypothetical proteins and 10901 were previously identified proteins. As expected, pangenome analysis confirmed that as the number of genomes increased, the number of conserved genes decreased and the number of total genes increased (Figure 6.3a). In addition, as the number of genomes increased the number of new genes decreased, and the number of unique genes increased (Figure 6.3b); this indicates that the pangenome was created successfully.
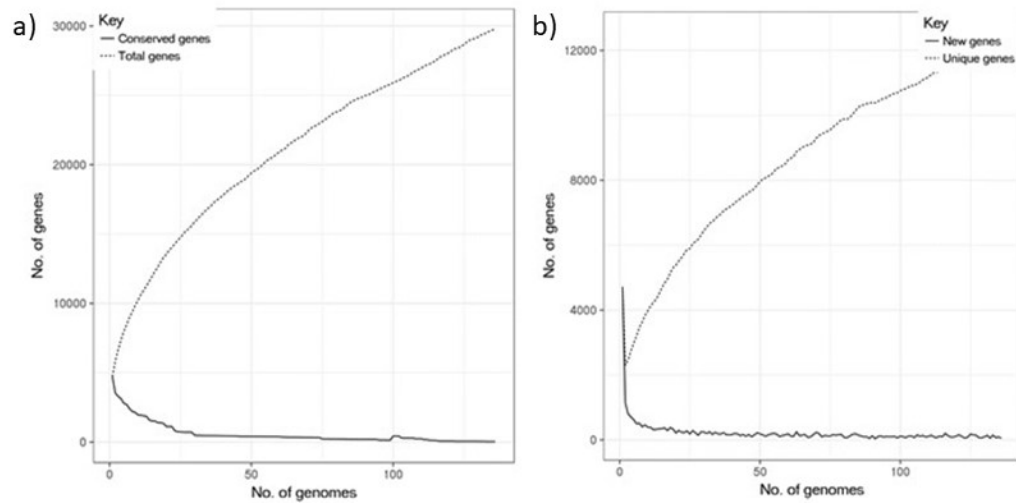
Figure 6.3. *Escherichia coli* pangenome analysis. The total number of genes and the number of conserved genes against; a) the number of genomes included in the study; and b) the total number of new and unique genes against the number of genomes.

As expected, pangenome analysis confirmed that as the number of genomes increased, the number of both new and conserved genes decreased (Figure 6.4a and b) while the number of genes in the pangenome increased (Figure 6.4c). The number of unique genes also increased as the number of genomes increased (Figure 6.4d). Genes with 97% blast identity were found to have the greatest number of blast results (Figure 6.4e). This indicates that the pangenome was created successfully.
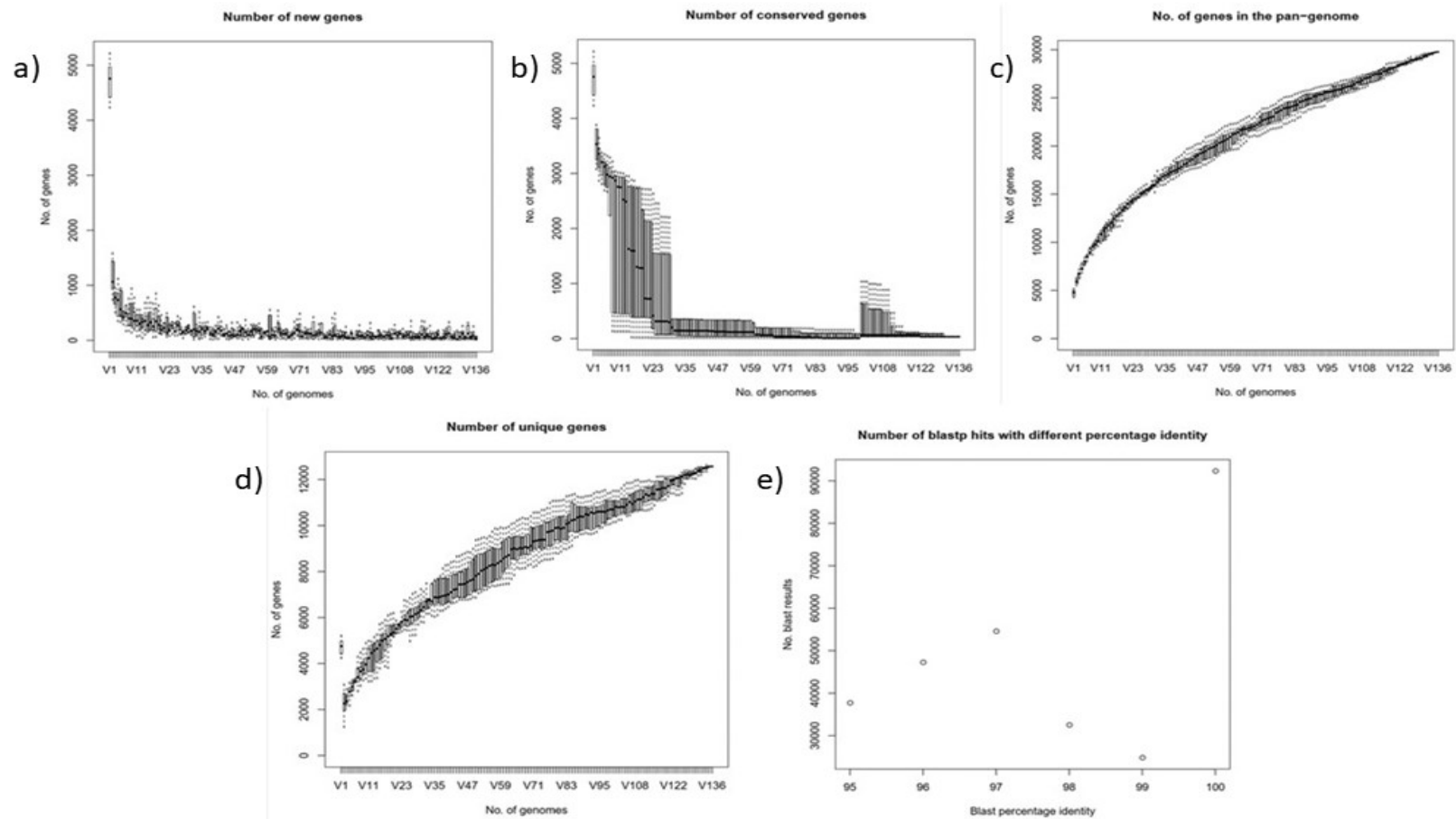
Figure 6.4. *Escherichia coli* pangenome analysis. Numbers of a) new, b) conserved and d) unique genes as well as c) the number of genes in the pan-genome against the number of genomes. Also showing e) the number of blastp hits with different percentage identity.

Roary analysis showed the presence and absence of genes in all isolates studied (Figure 6.5). The Roary matrix confirmed the presence of genes (dark blue) is stronger in the core genome, which begins to the left of the matrix (Figure 6.5). As the core genome is shared by all or the majority of isolates, more dark blue was observed. As genes become less common, less presence was seen and more absence was noticed, as indicated by the increasing light blue colour as the matrix is read left to right.  Several isolates were found to contain a high proportion of absent genes (red dots in Figure 6.5) and were found to contain few annotated genes, indicating poor sequence quality (Table 6.4).
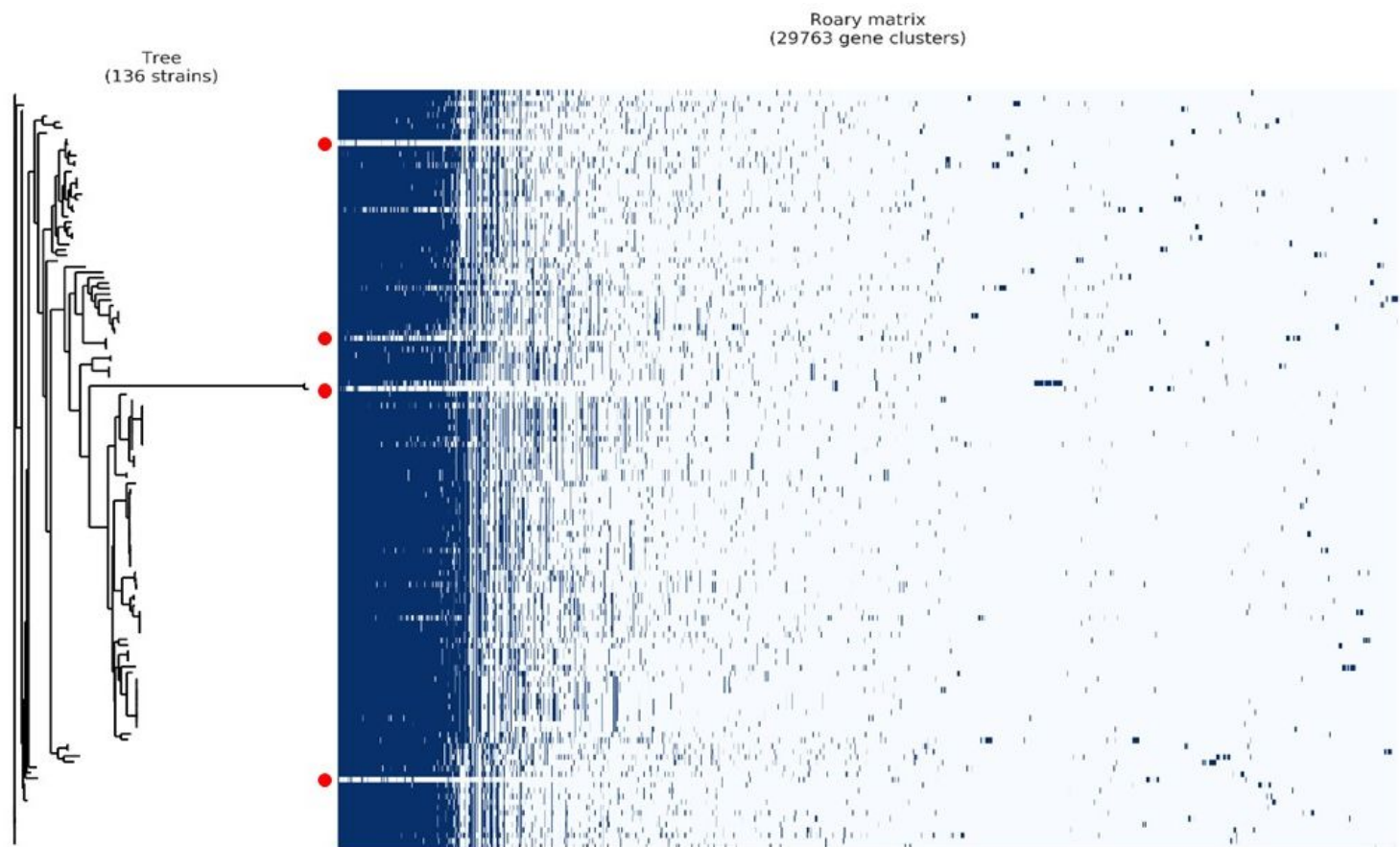
Figure 6.5. Presence (dark blue) and absence (light blue) of genes in both the core genome (left) and accessory genome (right). As genes become less common, light blue colouring becomes more frequent. Red dots indicate isolates with poor sequencing.

Table 6.4. Clinical isolates sequenced with low gene number.

| Isolate | Number of Genes |
|---------|-----------------|
| E18E500522 | 477 |
| E17E505024 | 726 |
| B17E008958 | 2336 |
| E17E50558 | 3349 |

### 6.3.1.1. Phylogenetic Neighbour Joining Trees

Phylogenetic analysis of the *E. coli* collection confirmed the diverse nature of the isolates (Figure 6.6). *Escherichia coli* with different origins of infection were found scattered throughout the tree, and no clustering was observed based on origin of infection in urinary tract, biliary tract or intra-abdominal region. Eight phylogroups were assigned to the clinical and ECOR isolates according to the Clermont method (Clermont *et al*., 2000; Clermont *et al*., 2015). Sixty four out of the 168 isolates belonged to phylogroup B2 where the majority of pathogenic isolates belong (Clermont *et al.,* 2000; Clermont *et al.,* 2015). The other pathogenic phylogroup identified was group D, which had 10 isolates. Of these, four were ECOR, three were urinary, two were intra-abdominal and one was a water isolate. The typically commensal group A was assigned to 23 isolates, and all but two belonged to the ECOR collection, and of the clinical isolates one was a water strain and the other a urinary isolate present in a patient with clinical pneumonia (other). Other phylogroups identified were F (7 isolates), B1 (16), C (5), E (5) and cryptic (6; Figure 6.6).
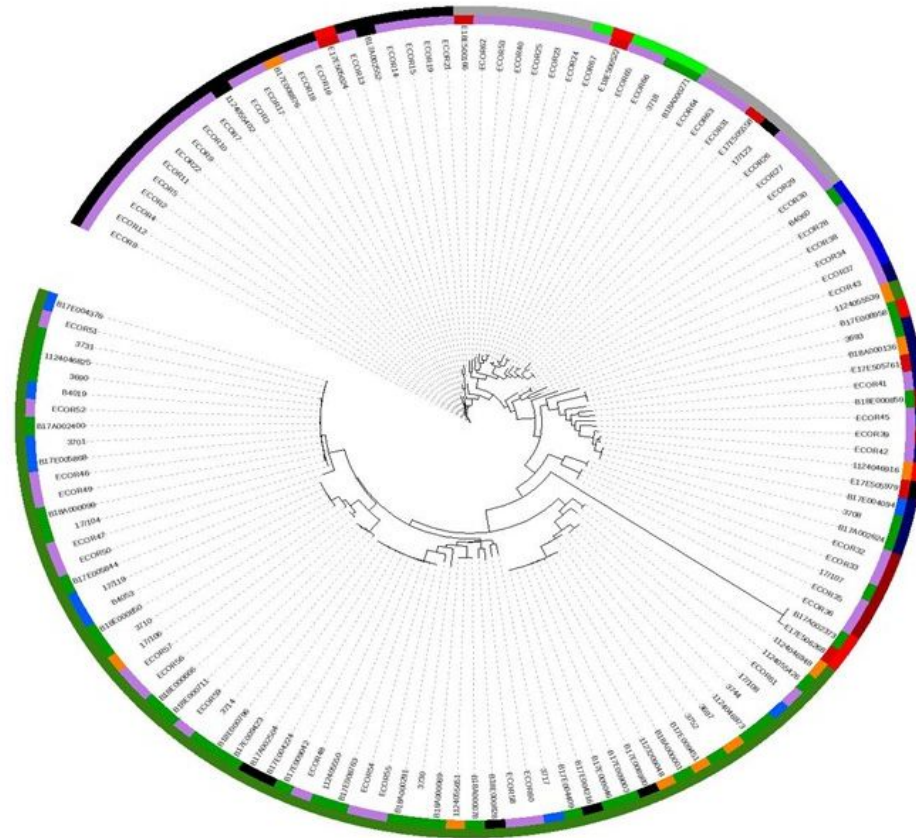
Figure 6.6. Circular phylogenetic tree of the pan-genome constructed with 168 *E. coli* strains. Key refers to the origin of infection (inner circle) and the phylogroup (outer circle).

Warwick MLST analysis based on six virulence genes identified sequence types (STs) for each isolate. Two clinical isolates were found to belong to ST10, a clonal complex that does not possess any virulence-associated genes but is associated with extended spectrum β-lactamase (ESBL) carriage in the gut of a diverse range of mammalian and avian hosts. These strains were isolated from the urine and the intra-abdominal region (Table 6.5). Four STs found to be strongly associated with ExPEC infections (ST69, ST73, ST95 and ST131) were identified in the clinical collection. Of these, two belonged to ST69, nine belonged to ST73, three belonged to ST95 and six belonged to ST131. Of ST69, one isolate was isolated from the urine and the other from a water source, ST73 isolates originated from the urine (four isolates), the intra-abdominal region (two isolates), and the biliary tract (three isolates); ST95 isolates originated from the biliary tract (two isolates) and the intra-abdominal region (one isolate) and ST131 isolates originated from the urine (four isolates), the biliary tract (one isolate) and from an unidentified source (one isolate; Table 6.5). The majority of isolates did not belong to STs associated with ExPEC infections, and 14 isolates could not be assigned a known ST.

Table 6.5. Sequence types identified using the Warwick MLST scheme based on six virulence genes.

| Isolate | Phylogroup | Sequence Type |
|---|---|---|
| 17/104 | B2 | 73 |
| 17/106 | B2 | 95 |
| 17/107 | F | 62 |
| 17/108 | B2 | 131 |
| 17/119 | B2 | 95 |
| 17/123 | B1 | 2628 |
| 3690 | B2 | 131 |
| 3693 | D | 62 |
| 3697 | B2 | 73 |
| 3701 | B2 | None Assigned |
| 3708 | D | 550 |
| 3710 | B2 | 978 |
| 3714 | B2 | 88 |
| 3717 | B2 | 144 |
| 3718 | C | 73 |
| 3730 | B2 | 131 |
| 3731 | B2 | 64 |
| 3744 | B2 | 350 |
| 3752 | B2 | 73 |
| B17E008763 | B2 | 75 |
| B17E008876 | A | 12 |
| B17E008958 | U/Cryptic | 12 |
| B17E009042 | B2 | 79 |
| B17E009451 | B2 | 79 |
| B17E008980 | B2 | 80 |
| B17E009003 | B2 | 14 |
| B17E009046 | B2 | 10 |
| 1124046916 | No match | None Assigned |
| 1124046948 | B2 | 429 |
| 1124046825 | B2 | 73 |
| 1124046973 | B2 | 131 |
| 1124055539 | B2 | None Assigned |
| 112405550 | B2 | 12 |
| 1124055651 | B2 | 127 |
| 1124055426 | B2 | 429 |
| 1124055402 | A | 6318 |
| B17A002373 | U/Cryptic | None Assigned |
| 1123209048 | B2 | 73 |
| B17A002400 | B2 | 12 |
| B17A002504 | B2 | 1838 |
| B17A002552 | A | 69 |
| B17A002624 | D | 127 |
| B18A000069 | B2 | 38 |
| B18A000136 | D | 73 |
| B18A000099 | B2 | None Assigned |

| | | |
|---|---|---|
| B18A000001 | B2 | 127 |
| B18A000078 | B2 | 10 |
| B18A000291 | B2 | 88 |
| B18A000271 | C | 12 |
| B17E009423 | B2 | None Assigned |
| B18E000859 | F | None Assigned |
| B18E000850 | B2 | 1064 |
| B18E000828 | B2 | 12 |
| B18E000796 | B2 | 404 |
| B18E000711 | B2 | 404 |
| B18E000666 | B2 | 10 |
| E17E505558 | B1 | 4118 |
| E17E505761 | D | None Assigned |
| E17E505979 | A | 1205 |
| E18E500166 | B1 | None Assigned |
| E18E500522 | Cryptic | None Assigned |
| E17E506268 | U/Cryptic | None Assigned |
| E17E505024 | U/Cryptic | 43 |
| B17E004094 | D | 69 |
| B17E004216 | B2 | 131 |
| B17E004224 | B2 | 12 |
| B17E004376 | B2 | 73 |
| B17E004409 | B2 | 131 |
| B17E005844 | B2 | 140 |
| B17E005868 | B2 | 73 |
| B4019 | B2 | 73 |
| B4053 | B2 | 95 |
| B4060 | E | 118 |

## 6.3.1.2. Core Genome Analysis

Core genes were present in 135/136 isolates, with four genes (*rplP, rpmC, yigL, bioD1_2*) shared by all isolates. All genes were involved in essential cellular processes, including:

- Metabolism & Biosynthesis (*yigL, bioD1_2, limB, argD, glpX, sfsA, dapF, yjfC*).
- Respiration (*nadD, atpA, ypjD*).
- rRNA synthesis and mRNA translation (*rplP, rpmC, rpmF, rpsQ, fis, rlmD, rhlB, yceD*).
- Antibiotic biosynthesis (*cetB*).
- Biofilm persistence (*bsmA*).
- tRNA function (*dus*).
- DNA and protein repair (*hupB, uvrA, degP*).
- DNA replication (*udp, holA*).
- Membrane transport (*metQ, tamB*).
- Cell signalling (*dgkA, cpdA*).

Eight genes were found to be involved in rRNA synthesis and mRNA translation, and functions included coding for the 50S and 30S ribosomal subunits and for the translation of mRNA. Eight genes also coded for proteins involved in diverse metabolic and biosynthetic processes, such as cofactor biosynthesis, limonene metabolism, amino acid metabolism, carbohydrate metabolism and sugar metabolism. Fewer genes were found to code for proteins involved with damage and repair, as well as persistence and antibiotic production.

### 6.3.2. Antimicrobial Resistance (AMR) Genes

Antimicrobial resistance genes were found in all but one clinical *E. coli* isolates, and the vast majority of isolates including water-sourced isolates were found to have resistance genes for at least one antibiotic (Table 6.6). There was only 1 isolate that was found to have no antibiotic resistance genes which was the urinary isolate B4060. Genes conferring resistance to β-lactams, polymyxin, bicyclomycin, macrolides, tetracyclines, aminoglycosides, fosfomycin and penicillin were identified in the majority of isolates (Table 6.6). The AMR genes found in abundance were those conferring resistance to various antimicrobials (49 total genes/alleles) and the least abundant were genes conferring resistance against fosfomycin (Table 6.6).

Table 6.6.Antimicrobial resistance genes present in clinically relevant *E. coli* isolates.

| Antimicrobial | Genes | Present In (%) |
|---|---|---|
| Various | *acrA, acrB, emrD, mdfA mdtE, mdtF, mdtG, mdtH, mdtK, mdtL, mdtM, mdtN, mdtO, emrE, acrZ, acrR, acrF, acrE, mexA* 50 total genes/alleles | Urinary (97.44%) Biliary (100%) Intra-abdominal (100%) Other (100%) Water (100%) |
| Cephalosporins Ampicillin | *ampC, bla* 11 total genes/alleles | Urinary (94.87%) Biliary (100%) Intra-abdominal (90%) Other (100%) Water (62.5%) |
| Polymyxin | *arnA* 1 gene/allele | Urinary (94.87%) Biliary (100%) Intra-abdominal (100%) Other (100%) Water (62.5%) |
| Bicyclomycin | *bcr* 4 total genes/alleles | Urinary (97.44%) Biliary (100%) Intra-abdominal (100%) Other (100%) Water (75%) |
| Aminoglycosides | *aacA, neo, yokD, aadB* 6 total genes/alleles | Urinary (12.82%) Biliary (37.5%) Intra-abdominal (10%) Other (12.5%) Water (12.5%) |
| Fosfomycin | *fosA* 1 gene/allele | Urinary (2.56%) Biliary, Intra-abdominal, Other, Water (0%) |

## 6.3.3. Genome-Wide Association Studies (GWAS)

## 6.3.3.1. Origin of Infection

Genes significantly associated with origin of infection of the clinical *E. coli* were identified using Scoary analysis (Brynildsrud *et al.,* 2016). The analysis revealed that 1084 genes were associated with an isolation source, with 531 of these genes identified as hypothetical proteins. Genes associated with sensitivity and specificity lower than 75% were removed from the analysis and genes that met the criteria can be seen in Table 6.7. No genes could be identified in the intra-abdominal and water groups that met this criteria.

Table 6.7. Genes identified by Scoary analysis as being associated with origin of infection of the bacteria. Hypothetical proteins were filtered out and genes were chosen based on sensitivity and specificity >75%.

| Gene | Annotation | Origin of Infection | Sensitivity | Specificity | Naïve P value | Bonferonni P value |
|---|---|---|---|---|---|---|
| *tufA* | Elongation factor Tu 1 | Biliary | 100 | 79.6875 | 7.72E-06 | 0.229592 |
| *tufB* | Elongation factor Tu 2 | Urinary | 82.05 | 79.38 | <0.00001 | <0.00001 |
| *folP_2* | Dihydropteroate synthase | Other | 75 | 85.94 | 0.0004 | 1 |
| *pemK* | Endoribonuclease PemK | Other | 75 | 82.03 | 0.0012 | 1 |
| *pemI* | Antitoxin PemI | Other | 75 | 82.03 | 0.0012 | 1 |
| *rusA_3* | Crossover junction endodeoxyribonuclease RusA | Other | 75 | 75.78 | 0.0052 | 1 |
| *alIS* | HTH-type transcriptional activator AlIS | Other | 75 | 75.78 | 0.0052 | 1 |

### 6.3.3.1. Bacteraemia/Non-bacteraemia

Genes significantly associated with *E. coli* from patients with bacteraemia or from non-bacteraemia sources (water and ECOR) were identified using Scoary analysis. The analysis revealed that 2965 genes were associated with either bacteraemia or non-bacteraemia, and 1140 genes were identified as hypothetical proteins. Genes associated with sensitivity and specificity lower than 75% were removed from the analysis and up to 10 genes that met the criteria can be seen in Table 6.8.

One gene was found to have high sensitivity and specificity in both groups (*oppA*), suggesting that a large percentage of the *E. coli* isolates have this gene (Table 6.8).

Table 6.8. Genes associated with bacteraemia or non-bacteraemia. Hypothetical proteins were filtered out and genes were chosen based on sensitivity and specificity >75%.

| Gene | Annotation | Bacteraemia vs Non-bacteraemia | Sensitivity | Specificity | Naïve P Value | Bonferroni P value |
|---|---|---|---|---|---|---|
| *group_15737* | tRNA-Ala(tgc) | Bacteraemia | 98.48 | 95.71 | <0.00001 | <0.00001 |
| *tufB* | Elongation factor Tu 2 | Bacteraemia | 77.27 | 98.57 | <0.00001 | <0.00001 |
| *dsbL* | Thiol:disulphide interchange protein DsbL | Bacteraemia | 86.36 | 70 | <0.00001 | <0.00001 |
| *oppA* | Periplasmic oligopeptide-binding protein | Bacteraemia | 77.27 | 78.57 | <0.00001 | <0.00001 |
| *oppA* | Periplasmic oligopeptide-binding protein | Non-bacteraemia | 75.71 | 78.79 | <0.00001 | <0.00001 |
| *hyfA_1* | Hydrogenase-4 component A | Non-bacteraemia | 75.71 | 77.27 | <0.00001 | 0.00002 |

### 6.3.4. Genes associated with Virulence

The complete gene presence/absence file was searched for any genes identified as known VFs (Table 6.1; Emody *et al.,* 2003; Dale & Woodford, 2015; Vila *et al.,* 2016; Sarowska *et al.,* 2019). A total of 63 VF genes were found that had previously been described as important VFs in ExPEC and UPEC strains. These genes were further subdivided; 26 genes related to mammalian cell adhesion, 21 genes related to both invasion of host cells and bacterial cell protection, 5 genes related to iron acquisition, 10 genes related to toxin production and 1 gene related to other pathogenic processes (Table 6.9). Forty-one genes were found to present in >50% of isolates, with the most abundant genes shared between isolates (>95% presence) all related to curli formation (*csgC, csgE, csgG*) and the least abundant gene (<5% presence) was associated with production of α-haemolysin (*hlyB*; Table 6.9).

Chi squared tests were applied to each gene to determine whether any origins of infection had significantly less or more strains positive for that gene. Five genes in total (*ecpA* [p = 0.0012], *flu* [p = 0.0028], *papA* [p = 0.0496], *ompC* [p < 0.0001], *ompG* [p = 0.0008], *fyuA* [p = 0.0012]) were determined to be significantly less present in the water group than the other pathogenic groups. These genes are related to pilus formation (*ecpA, papA*), host cell adhesion and invasion (*flu, ompC, ompG*) and iron acquisition (*fyuA*).

Table 6.9. Genes associated with the production of VFs identified in the pan-genome. The percentage presence within each origin of infection is described. Fields denoted with asterisks indicate where the percentage presence for that origin of infection is significantly different from other origins of infection for that particular gene as determined by individual chi squared tests. Asterisks represent the following significant values: * = $p < 0.05$, ** = $p < 0.01$, *** = $p < 0.001$, **** = $p < 0.0001$.

| Gene | Annotation | Virulence Group | No. of Alleles | % of Total Clinical Isolates | % of Urinary | % of Biliary | % of IA | % of Water | % of Other |
|---|---|---|---|---|---|---|---|---|---|
| afaE3 | Afimbrial adhesin AFA-III | Adhesins | 3 | 5.8 | 7.7 | 0 | 10 | 0 | 0 |
| cdtB | Cytolethal distending toxin subunit B | Toxins | 1 | 6.8 | 10.3 | 0 | 0 | 0 | 12.5 |
| crl | Sigma factor-binding protein Crl | Adhesins | 2 | 91.8 | 92.3 | 100 | 100 | 62.5 | 100 |
| csgA | Major curlin subunit | Adhesins | 1 | 93.6 | 92.3 | 100 | 100 | 62.5 | 100 |
| csgB | Minor curlin subunit | Adhesins | 2 | 94.5 | 97.4 | 100 | 100 | 62.5 | 100 |
| csgC | Curli assembly protein CsgC | Adhesins | 1 | 95.9 | 97.4 | 100 | 100 | 62.5 | 100 |
| csgD | CsgBAC operon transcriptional regulatory protein | Adhesins | 3 | 93.2 | 94.9 | 100 | 100 | 62.5 | 100 |
| csgE | Curli production assembly/transport component CsgE | Adhesins | 1 | 95.9 | 97.4 | 100 | 100 | 62.5 | 100 |
| csgG | Curli production assembly/transport component CsgG | Adhesins | 1 | 95.9 | 97.4 | 100 | 100 | 62.5 | 100 |
| cvaA | Colicin V secretion protein CvaA | Protectins & Invasins | 3 | 31.5 | 33.3 | 50 | 20 | 12.5 | 37.5 |

200

| | | | | | | | | | |
|---|---|---|---|---|---|---|---|---|---|
| *cvaC* | Colicin-V | Protectins & Invasins | 1 | 13.7 | 12.8 | 12.5 | 10 | 25 | 12.5 |
| *cvpA* | Colicin V production protein | Protectins & Invasins | 1 | 91.8 | 94.9 | 100 | 90 | 62.5 | 100 |
| *ecpA* | Common pilus major fimbrillin subunit EcpA | Adhesins | 3 | 90.4 | 92.3 | 100 | 100 | 50 ** | 100 |
| *ecpB* | putative fimbrial chaperone EcpB | Adhesins | 1 | 93.2 | 94.9 | 100 | 100 | 62.5 | 100 |
| *ecpD* | Fimbria adhesin EcpD | Adhesins | 4 | 93.2 | 94.9 | 100 | 100 | 62.5 | 100 |
| *ecpE* | putative fimbrial chaperone EcpE | Adhesins | 4 | 93.2 | 94.9 | 100 | 100 | 62.5 | 100 |
| *fimA* | Type-1 fimbrial protein, A chain | Adhesins | 14 | 93.2 | 97.4 | 100 | 100 | 62.5 | 87.5 |
| *flu* | Antigen 43 | Adhesins | 22 | 75.3 | 84.6 | 100 | 70 | 25 ** | 62.5 |
| *focC* | Chaperone protein FocC | Adhesins | 6 | 82.2 | 84.6 | 100 | 90 | 62.5 | 62.5 |
| *fyuA* | Pesticin receptor | Toxins | 2 | 79.4 | 87.2 | 100 | 80 | 25 ** | 75 |

| | | | | | | | | | |
|---|---|---|---|---|---|---|---|---|---|
| *hemR* | Hemin receptor | Iron Acquisition | 7 | 75.3 | 74.4 | 87.5 | 80 | 50 | 87.5 |
| *hlyA* | Hemolysin, chromosomal | Toxins | 6 | 35.6 | 41 | 37.5 | 20 | 12.5 | 50 |
| *hlyB* | Alpha-hemolysin translocation ATP-binding protein HlyB | Toxins | 2 | 2.7 | 0 | 0 | 0 | 25 | 0 |
| *hlyC* | Hemolysin-activating lysine-acyltransferase HlyC | Toxins | 2 | 30.1 | 33.3 | 37.5 | 10 | 12.5 | 50 |
| *hlyD* | Hemolysin secretion protein D, chromosomal | Toxins | 2 | 31.5 | 38.5 | 37.5 | 10 | 0 | 50 |
| *hlyE* | Hemolysin E, chromosomal | Toxins | 4 | 52.1 | 46.2 | 12.5 | 90 | 50 | 75 |
| *iucA* | N(2)-citryl-N(6)-acetyl-N(6)-hydroxylysine synthase | Iron Acquisition | 5 | 46.6 | 51.3 | 62.5 | 40 | 37.5 | 25 |
| *iucC* | Aerobactin synthase | Iron Acquisition | 1 | 53.4 | 56.4 | 75 | 50 | 25 | 50 |
| *iucD* | L-lysine N6-monooxygenase | Iron Acquisition | 4 | 71.2 | 51.3 | 62.5 | 40 | 37.5 | 25 |
| *iutA* | Ferric aerobactin receptor | Iron Acquisition | 2 | 53.4 | 59 | 75 | 50 | 25 | 37.5 |
| *kpsD* | Polysialic acid transport protein KpsD | Protectins & Invasins | 4 | 93.1 | 94.9 | 100 | 100 | 62.5 | 100 |
| *kpsF* | Arabinose 5-phosphate isomerase KpsF | Protectins & Invasins | 1 | 63 | 28.2 | 37.5 | 50 | 62.5 | 37.5 |

| | | | | | | | | | |
|---|---|---|---|---|---|---|---|---|---|
| *kpsM* | Polysialic acid transport protein KpsM | Protectins & Invasins | 5 | 68.5 | 74.4 | 62.5 | 60 | 50 | 75 |
| *kpsT* | Polysialic acid transport ATP-binding protein KpsT | Protectins & Invasins | 9 | 64.4 | 66.7 | 62.5 | 50 | 25 | 75 |
| *kpsU* | 3-deoxy-manno-octulosonate cytidylyltransferase | Protectins & Invasins | 1 | 63 | 71.8 | 62.5 | 50 | 37.5 | 62.5 |
| *omp38* | Outer membrane protein Omp38 | Protectins & Invasins | 1 | 94.5 | 97.4 | 100 | 100 | 62.5 | 100 |
| *ompA* | Outer membrane protein A | Protectins & Invasins | 3 | 93.2 | 100 | 100 | 90 | 50 | 100 |
| *ompC* | Outer membrane protein C | Protectins & Invasins | 8 | 91.8 | 97.4 | 100 | 100 | 37.5 **** | 100 |
| *ompD* | Outer membrane porin protein OmpD | Protectins & Invasins | 12 | 82.2 | 87.2 | 100 | 70 | 62.5 | 75 |
| *ompF* | Outer membrane protein F | Protectins & Invasins | 4 | 93.2 | 94.9 | 100 | 100 | 62.5 | 100 |
| *ompG* | Outer membrane protein G | Protectins & Invasins | 1 | 79.5 | 82.1 | 100 | 80 | 25 *** | 100 |

| | | | | | | | | | |
|---|---|---|---|---|---|---|---|---|---|
| *ompL* | Porin OmpL | Protectins & Invasins | 1 | 6.8 | 7.7 | 0 | 10 | 12.5 | 0 |
| *papA* | Pap fimbrial major pilin protein | Adhesins | 24 | 63 | 76.9 | 62.5 | 50 | 25 * | 50 |
| *papE* | Fimbrial protein PapE | Adhesins | 10 | 53.4 | 64.1 | 50 | 30 | 25 | 62.5 |
| *papG* | Fimbrial adhesin PapG | Adhesins | 6 | 52.1 | 64.1 | 37.5 | 30 | 25 | 62.5 |
| *papG* | Fimbrial adhesin PapG | Adhesins | 6 | 2.7 | 2.6 | 0 | 10 | 0 | 0 |
| *papH* | PAP fimbrial minor pilin protein | Adhesins | 4 | 63 | 69.2 | 50 | 40 | 25 | 75 |
| *papK* | Fimbrial adapter PapK | Adhesins | 4 | 50.7 | 61.5 | 50 | 20 | 25 | 62.5 |
| *pic* | Serine protease pic autotransporter | Adhesins Protectins & Invasins | 4 | 27.4 | 30.8 | 25 | 30 | 12.5 | 25 |
| *sat* | Serine protease sat autotransporter | Toxins | 2 | 32.9 | 28.2 | 37.5 | 20 | 25 | 12.5 |
| *sfaA* | S-fimbrial protein subunit SfaA | Adhesins | 7 | 21.9 | 30.8 | 37.5 | 0 | 0 | 12.5 |
| *sfaG* | S-fimbrial protein subunit SfaG | Adhesins | 5 | 94.5 | 97.4 | 100 | 100 | 62.5 | 100 |
| *sfaH* | S-fimbrial protein subunit SfaH | Adhesins | 5 | 95.9 | 100 | 100 | 100 | 62.5 | 100 |

| sfaS | S-fimbrial adhesin protein SfaS | Adhesins | 9 | 94.5 | 97.4 | 100 | 100 | 62.5 | 100 |
|------|--------------------------------|----------|---|------|------|-----|-----|------|-----|
| tsh | Temperature-sensitive hemagglutinin tsh autotransporter | Toxins | 9 | 19.2 | 17.9 | 25 | 30 | 25 | 0 |
| uidA | Beta-glucuronidase | Other | 4 | 93.2 | 97.4 | 100 | 100 | 50 | 100 |

## 6.3.5. Invasion of Gut and Urinary Epithelial Cells

The invasion index of four *E. coli* strains from each origin of infection (16 isolates) was investigated using the gentamicin protection assay on CACO-2 (gut) and UM-UC-3 (bladder) human epithelial cells (Figure 6.7). There was a trend towards higher invasion for all bacteria (including the *E. coli* K12 control) with bladder UM-UC-3 cells compared with gut CACO-2 cells ($p < 0.0001$). No significant difference ($p > 0.05$) was found between the invasion of isolates within each origin of between bladder and gut epithelial cells (Figure 6.7).

*Escherichia coli* isolates from water sources were found to be most invasive in CACO-2 cells and intra-abdominal isolates were found to be most invasive in UM-UC-3 cells (did not reach significance). Least invasive of the clinical isolates were intra-abdominal *E. coli* in CACO-2 cells and urinary *E. coli* in UM-UC-3 cells (Figure 6.7).

*Escherichia coli* K12 invasion into CACO-2 was found to be significantly lower than intra-abdominal, biliary and water *E. coli* into UM-UC-3. In addition, invasion of *E. coli* urinary isolates into CACO-2 cells were found to be significantly less than invasion of intra-abdominal isolates into UM-UC-3 cells.
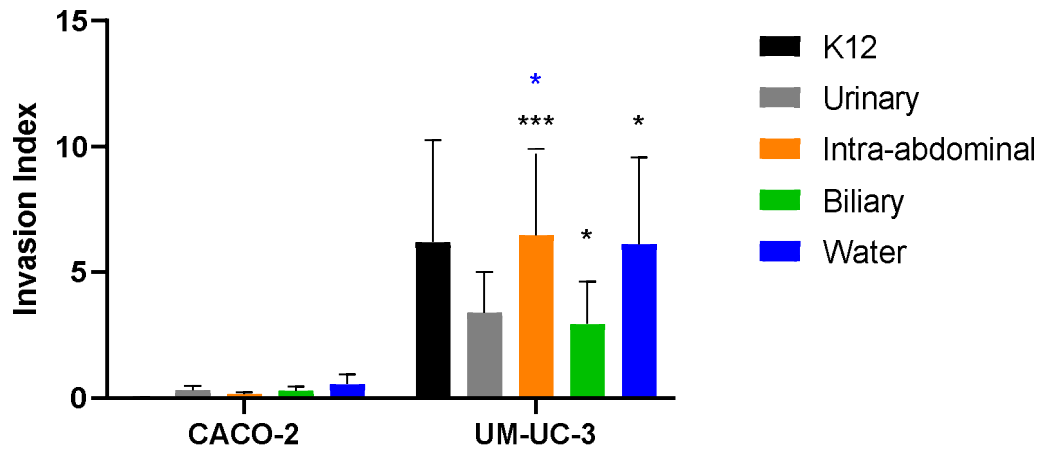


Figure 6.7. Invasion Index of ExPEC in gut (CACO-2) and bladder (UM-UC-3) epithelial cells. Error bars represent the SEM. Black asterisks indicate where the data is significantly different to the CACO-2 *E. coli* K12 control and the blue asterisk indicates where the data is significantly different to the CACO-2 *E. coli* urinary data. Asterisks represent the following significant values: * = $p < 0.05$, *** = $p < 0.001$.

## 6.4. Discussion

The emergence of next generation sequencing (NGS) technologies and software analysis pipelines has allowed for the genomic composition of pathogenic bacteria to be more fully characterised. The microbial pangenome describes the full complement of genes that are shared within a bacterial species (Page *et al.*, 2015). In this chapter, the *E. coli* pangenome constructed using the pan-genome pipeline Roary (Page *et al.,* 2015) describes the full complement of genes shared by 136 different *E. coli* genomes, 71 of which were new blood culture positive *E. coli* from the HDUHB. Roary is capable of generating a pangenome in a reasonable amount of time (overnight in this case) while reducing the RAM usage, allowing for large datasets to be analysed on a desktop PC in a relatively short amount of time (Page *et al*., 2015). Genes are annotated using Prokka (Seemann, 2014), which is extremely fast and is fully compatible with Roary. Outputs from Roary include summary statistics of the coding sequences as well as a gene presence/absence file with information on genes and their presence within any isolate of interest. Further analysis can be done to determine any genes that are significantly associated with a given "trait", such as origin of infection or high/low invasiveness, by employing a GWAS using Scoary (Brynildsrud *et al.*, 2016).

The clinical isolates used in this chapter came from three major origins of infection; the urinary tract, the biliary duct and the abdomen, as well as others that were unspecified. What was immediately evident was that more urinary *E. coli* were isolated compared to the other groups. This was not surprising as urosepsis is one of the most common presentations of *E. coli* sepsis in hospitals, and this is the case for HDUHB, especially where ExPEC are concerned (Kaper *et al.*, 2004; Hardisty *et al.*, 2019). Approximately 80-90% of all UTIs are caused by UPEC strains, and 150 million people annually develop a UTI (Terlizzi *et al*., 2017). These factors coupled together would help explain why the urinary tract was the most common origin of infection of ExPEC in this collection.

As demonstrated in Figures 6.5 and 6.6, the isolates were phylogenetically diverse, and origin of infection was not associated with a defined ST. The clinical isolates were found to be principally separate from the ECOR collection, which perhaps reflects the pathogenicity of the HDUHB isolates and the lack of pathogenicity in the ECOR collection. Sequence types that have been strongly associated with ExPEC infection (ST69, 73, 95 and 131; Doumith *et al*., 2015) were all found in the present study. However, only ~30% (20 of 73) of the isolates were found to belong to these STs, and these were not closely associated, suggesting that the isolates are not closely related.

Further, the genetic diversity of these isolates suggests that the origin of the infections was likely from the community as opposed to the hospitals, as hospital outbreaks tend to be due to one or two defined clones (Hacek *et al*., 2004; Domenech de Cellès *et al*., 2012; Ruppe *et al.*, 2017). One water isolate was found to belong to ST69, which is worrying as this environmental isolate can possible cause serious infection if it is able to invade sterile body tissues. Of the remaining 51 isolates, 15 were unable to be assigned a ST, suggesting that perhaps further STs exist that are associated with sepsis. It is also possible that the Warwick MLST scheme used to determine the STs in this study was unable to assign a ST that it did not recognise (Clermont *et al*., 2000; Clermont *et al*., 2015).

All but one of the isolates were found to contain at least one antibiotic resistance gene, and the majority were found to contain genes conferring multi-drug resistance. This result is troubling. To have all ExPEC and even some isolates from a water source possessing at least one or more genes conferring resistance to more than one antibiotic poses a significant public health risk. First-line antibiotics such as cephalosporins, fluoroquinolones and trimethoprim-sulfamethoxazole are commonly used to treat both community- and hospital-acquired ExPEC infections (Pitout, 2012). Several studies across Europe and the American continent observed that between 20-45% of ExPEC were resistant to these first line antibiotics (Foxman, 2010). The fact that, in all of the isolates (except one), there were genes conferring resistance to cephalosporins, which are so widely used, is very troubling. Susceptibility testing will be performed in the future to confirm if the strains are resistant to any of the antibiotics discussed. Further, the presence of *arnA,* a gene conferring resistance to polymyxin, in the vast majority of the isolates is of particular concern. Polymyxin is a last resort antibiotic treatment for multi-drug resistant Gram-negative infections, particularly by *K. pneumoniae* and *E. coli* (Velkov *et al*., 2013). The isolates in the present study, while being genetically resistant to common first-line antibiotics, also carry genes that potentially confer resistance to last-resort antibiotics; this poses a significant problem for treating multi-drug resistant ExPEC not only in the HDUHB hospitals but in the rest of Wales and beyond.

Two genes that were found to be strongly associated with UPEC, biliary infections and sepsis in this study were *tufA* and *tufB*. These genes encode for the bacterial elongation factors thermo-unstable 1 and 2 (EF-tu 1 and 2), which are important components of the ribosomal decoding pathway that ensures rapid and accurate translation (Yikilmaz *et al*., 2014). Whilst this process is central to translation, these genes were not present in the core genome and have not previously been described as VFs in ExPEC. However, a recent

study by Widjaja *et al.* (2017) found that pathogenic strains of *S. aureus, Mycoplasma pneumoniae* and *M. hyopneumoniae* produced EF-tu that bound to plasminogen. This binding promoted the conversion of plasminogen to plasmin in the presence of plasminogen activators (Widjaja *et al.*, 2017), a key step in fibrinolysis, the process that prevents the formation of excessive blood clots (Chapin and Hajjar, 2015). The ability of EF-tu to promote this conversion suggests that it may have serine protease activity (Chapin and Hajjar, 2015). In addition, work on *S. pneumoniae* has associated EF-tu production with binding to complement factors, which facilitates immune evasion and invasion of host tissue (Sarkar *et al.*, 2013). Thus, EF-tu is a potential VF that has been previously unexplored and may confer an advantage on ExPEC in supporting survival in the blood stream and prevent their subsequent elimination by leukocytes. This may also confer upon ExPEC further ability to disseminate within the host and invade tissue. That *tufA* and *tufB* were both found to be strongly associated not only with biliary and urinary isolates but also with sepsis suggests that these two genes could potentially be excellent biomarkers of ExPEC in the future.

VFs could be identified in most isolates, which is to be expected within the ExPEC pathotype. The extent of their presence in water isolates is a cause for concern. Hospital environments are ideal for the persistence of pathogenic water-borne pathogens, such as *Legionella* and *Pseudomonas*, capable of survival in large, complex systems that are vulnerable to areas of stagnation and biofilm growth. This, coupled with the elevated presence of vulnerable individuals, puts many patients at risk of developing severe water-borne infections (Decker and Palmore, 2013). Further checks on the origin of these isolates are required to determine if this is a potential public health risk and a possible vehicle for ExPEC infection.

Bacterial invasion into human epithelial cells has been explored previously using the gentamicin protection assay (Hamrick *et al.*, 2003; John *et al.*, 2017; VanCleave *et al.*, 2017). Here, a subset of the *E. coli* strains were tested for their ability to invade urinary (UM-UC-3) and colon (CACO-2) epithelial cells to determine whether there were differences in the invasiveness of *E. coli* from each origin of infection (urinary, intra-abdominal, biliary, water) in relevant tissues. While the findings of this study are preliminary, it is evident that the invasiveness of each group of isolates in each cell line is different (Figure 6.7). First, *E. coli* invaded more readily into urinary epithelial cells than colon epithelial cells, and the most invasive group of isolates were the water isolates. While it is not unusual that isolates would readily invade urinary epithelial cells (ExPEC

possess invasins and adhesins that facilitate invasion of mammalian cells), it is unusual that of all the isolates the ones sampled from water were the most invasive (similar to intra-abdominal isolates). Again, the fact that the water isolates were highly invasive is of great concern for the acquisition of ExPEC via drinking sources. Other infective *E. coli,* such as enterotoxigenic *E. coli,* are both highly invasive and are acquired via the ingestion of contaminated food or water (Nataro and Kaper, 1998), which would perhaps explain the highly invasive nature of our isolates. Compared to the urinary epithelial cells, the most invasive in this group were the intra-abdominal isolates, which did possess in abundance genes associated with invasion.

Whilst the preliminary results of the gentamicin protection assay are interesting, the assay itself had some limitation (Friis *et al.,* 2005). The epithelial cells while confluent at the beginning of the experiment, were easily lifted from the base of the wells when gently washed, suggesting poor adhesion or *E. coli* induced toxicity. Cell detachment was only noted after 4-hour incubation with *E. coli*, and it is possible that the activity of these ExPEC were responsible for the loss in adherence and viability of these cells. Twelve of the isolates tested contained at least one toxin that is toxic to mammalian cells, making it possible for epithelial cell killing to occur. Furthermore, the high concentration of gentamicin used (300 µg/ml), whilst well above the MIC for *E. coli* (2 µg/ml, determined by EUCAST, 2019), did not always kill all strains in the collection when plating the clinical strain at wash stage. This was not noted in control and *E. coli* K12 wells. Therefore, perhaps gentamicin is not an appropriate antibiotic to use with these isolates. Gentamicin is typically used for antibiotic protection assays due to its broad-spectrum activity and its high molecular weight preventing it from crossing mammalian cell membranes (Kaneko *et al*., 2016). Alternatively, kanamycin could be used, which also has high molecular weight and broad-spectrum activity, although susceptibility profiles would need to be determined. Whilst no gentamicin resistance was found in the genome of the isolates, it is still possible that a novel gene is present that confers resistance to this antibiotic, although this is very unlikely.

In conclusion, *E. coli* blood culture positive isolates from patients with sepsis in west Wales hospitals present on a diverse phylogenetic background with a variety of STs and possess an armoury of virulence genes that confer upon them the ability to establish ExPEC infections derived from diverse body tissues. Widespread multi-drug resistance and the presence of VFs in water isolates may represent a significant future risk for the treatment and the acquisition of the most common bacteria causing sepsis in Wales.

## Chapter 7. Final Discussion

### 7.1. Sepsis

Sepsis is one of the largest challenges facing healthcare professionals today (Monneret and Venet, 2016). Symptoms are often non-specific and are present in a wide range of inflammatory diseases, and include fever, confusion, extreme shivering, muscle pain and severe breathlessness (Cohen, 2002; UK Sepsis Trust, 2019). The high number of cases and deaths is also heavily influenced by complications associated with diagnosis and treatment, as well as the increase in antibiotic resistance (Charles *et al.*, 2009; Singer *et al.*, 2016). The most commonly isolated bacteria associated with sepsis in England and Wales is *E. coli* (Public Health England, 2015)*,* which can originate from infections of the lung, intra-abdominal region, urinary tract, skin and soft tissue as well as from indwelling medical devices (Calandra and Cohen, 2005). Defining the cause of sepsis is critical to diagnosis and treatment and identifying the organism responsible for the septic episode is critical to guiding empirical antibiotic therapy (Vincent, 2016), but this can take up to 48 hours (Jin and Khan, 2010). The ideal molecular biomarker of sepsis would not only be rapid but would also discriminate between bacterial, viral or fungal infections, as well as informing on correct treatment (Vincent, 2016). The discovery of potential biomarkers of sepsis is constantly evolving, and blood samples from patients with different stages of sepsis have informed on both new and old molecular markers that could be applied in the clinic (Di Gaudio *et al.,* 2018; Mangioni *et al.,* 2019).

### 7.2. Thesis Aims

The major aim of this thesis was to investigate host molecular and cellular biomarkers of sepsis and determine bacterial genomic biomarkers of septic *E. coli*, with the following objectives:

- Characterisation of the host innate immune response towards model and pathogenic strains of *Staphylococcus* and *E. coli* in healthy whole blood in order to identify novel biomarkers of bacterial infection. These biomarkers were characterised using ELISAs.
- Characterisation of the host cellular response towards *S. epidermidis* RP62A and *E. coli* K12 in healthy whole blood in order to determine the efficacy of the whole blood model for understanding bacteria – host cell interactions. This was characterised using microscopy and flow cytometry.

- Characterisation of the sterol response towards *S. epidermidis* RP62A and *E. coli* K12 in healthy whole blood in order to determine any associations between bacterial infection and sterol regulation. This was characterised using LC-MS.

- Genomic analysis of sepsis-causing *E. coli* strains from Welsh hospitals in order to understand the occurrence and virulence of certain strains. A GWAS was used to determine genes associated with origins of infection and sepsis.

- Characterisation of the invasiveness of certain sepsis-causing *E. coli* using the gentamicin protection assay in bladder UM-UC-3 and colon CACO-2 epithelial cells.

## 7.3. The Whole Blood Sepsis Model: A Promising Alternative?

Part of the work in this thesis further developed an *ex vivo* whole blood model previously used within the Microbiology and Infectious Disease group (Al-Ishaq *et al.*, 2015). The *ex vivo* whole blood sepsis model allows for analysis of systemic inflammation using a diverse range of stimuli (such as PAMPs) and whole bacterial species whilst minimising risk to donors. Further advantages allow for the manipulation of different sepsis environments, such as promoting senescence of immune cells to mimic conditions in older or immunocompromised patients. In Chapter 3, the model was used in conjunction with bacterial strains relevant to sepsis, namely *E. coli, S. epidermidis* and *S. aureus* to measure early biomarker responses. Interleukin-6, MIP-1α, MIP-3α and resistin were shown to be reproducible between tests and absent in the control. Furthermore in Chapter 4, flow cytometry confirmed that control cells that undergo the same experimental conditions to the infected groups remain unchanged throughout the course of the experiments. Overall, this model represents a robust and ethical means of measuring early sepsis interactions and determining potential future biomarkers of infection prior to clinical validation. Similar models have been used to study systemic infection (Nolte *et al.*, 2002; Hunniger *et al*., 2014; Vivas-Alegre *et al*., 2015; do Nascimento *et al*., 2018; Prausse *et al.*, 2018; Strobel and Johswich, 2018) in response to numerous pathogens. The application of whole blood modelling to sepsis diagnosis by measuring *E. coli* and *Staphylococcus* responses represents a novel application for this model.

### 7.4. Molecular Biomarkers of Sepsis

A biomarker is a medical characteristic that can be measured and interpreted to identify a normal or pathogenic process. The test for this biomarker should also be accurate and reproducible, allowing a clinician to accurately identify the pathological process taking place (Strimbu and Tavel, 2010). The molecular biomarkers investigated in Chapter 3 demonstrated a clear distinction in cytokine profiling between whole blood infected with *E. coli* and *Staphylococcus,* thus agreeing with previous findings (Abe et al., 2010), and revealed the potential of several new biomarkers of *E. coli* and *Staphylococcus* sepsis (Figure 7.1). In *E. coli* infected blood, high expression of IL-6, MIP-1α, MIP-3α and C5a directly contrasted with significantly lower expression in whole blood infected with *Staphylococcus*.

Results in this thesis support the importance of *E. coli*-induced IL-6 as a biomarker for sepsis. This correlates with Celik *et al.* (2015), who found that blood samples from neonatal sepsis patients contained significantly higher concentrations of IL-6 if the patient was infected with Gram-negative bacteria, compared to Gram-positive and fungal infections. A study by Skovbjerg *et al.* (2010) found that whilst Gram-positive bacteria induced greater expression of IL-12, IFN-γ and TNF, Gram-negative bacteria induced substantially more IL-6, IL-8 and IL-10. Several other studies have also found IL-6 preferentially highly expressed in patients with Gram-negative infections than with Gram-positive infections (Kragsbjerg *et al*., 1998; Abe *et al*., 2010; Ye *et al*., 2014; Surbatovic *et al.,* 2015; Shao *et al.*, 2018).

This thesis found that high levels of MIP-1α are preferentially expressed in whole blood in response to *E. coli* and represents a potential biomarker of *E. coli* sepsis. Macrophage inflammatory proteins have previously been investigated as biomarkers in sepsis diagnosis (Fujishima *et al*., 1996; O'Grady *et al*., 1999). These studies found that MIP-1α was elevated in patients within 24 hours of sepsis and correlated with levels of TNF-α and IL-6 (O'Grady *et al.,* 1999), and that in the blood of 38 septic patients the levels of MIP-1α strongly correlated with those of CRP, IL-6 and TNF-α, all of which are substantially elevated during sepsis, and was also found to be a predictor of high mortality (Fujiishima *et al.,* 1996). In the current study, MIP-1α could also be correlated with IL-6 levels. Vermont *et al.* (2006) found that high levels of MIP-1α correlated with juvenile nonsurvivors of meningococcal sepsis and was a better predictor of mortality than early alarm cytokines like TNF-α and IL-6. Despite these findings, to our knowledge no studies have investigated the discriminatory power of MIP-1α as a biomarker of bacterial sepsis.

With regard to MIP-3α, there is a paucity of data investigating its role in sepsis. Tsai *et al.* (2013) found that MIP-3α was elevated in patients with sepsis and was significantly higher in nonsurvivors. Other studies have also had similar findings (Akahoshi *et al.,* 2003; Kitagawa *et al.,* 2013; Klaus *et al.,* 2016; Warford *et al.,* 2017). To the best of our knowledge, this thesis presents the first evidence that MIP-3α is preferentially overexpressed in blood treated with *E. coli* compared with blood treated with *Staphylococcus*.

The measurement of MIP proteins and IL-6 in healthcare settings would be relatively easy and rapid to perform. They are easy to detect using blood tests, and here we found that they were easily tested by a specific sandwich ELISA. However, ELISAs can take up to 7 hours to perform, and plates must be pre-coated the night before. In the clinic, a robust and rapid method of determining concentration of analyte in a blood sample is to perform a Luminex assay (R & D Systems, 2019). A Luminex assay consists of mixing the analyte source (blood, urine, *etc.*) with a solution of coloured beads that have been pre-coated with capture antibodies specific to the analyte of interest. This is a rapid (12,800 tests/hour) and cost-effective assay as it can be performed in a multi-well plate, allowing for multiple samples to be tested at once, and as multiplexing is possible with the assay, up to 100 analytes can be tested using a very small sample, minimising the amount of blood drawn required from severely ill people. Thus Luminex could offer a rapid cost-effective means of measuring IL-6, MIP-1α, MIP-3α and perhaps resistin in a healthcare setting.
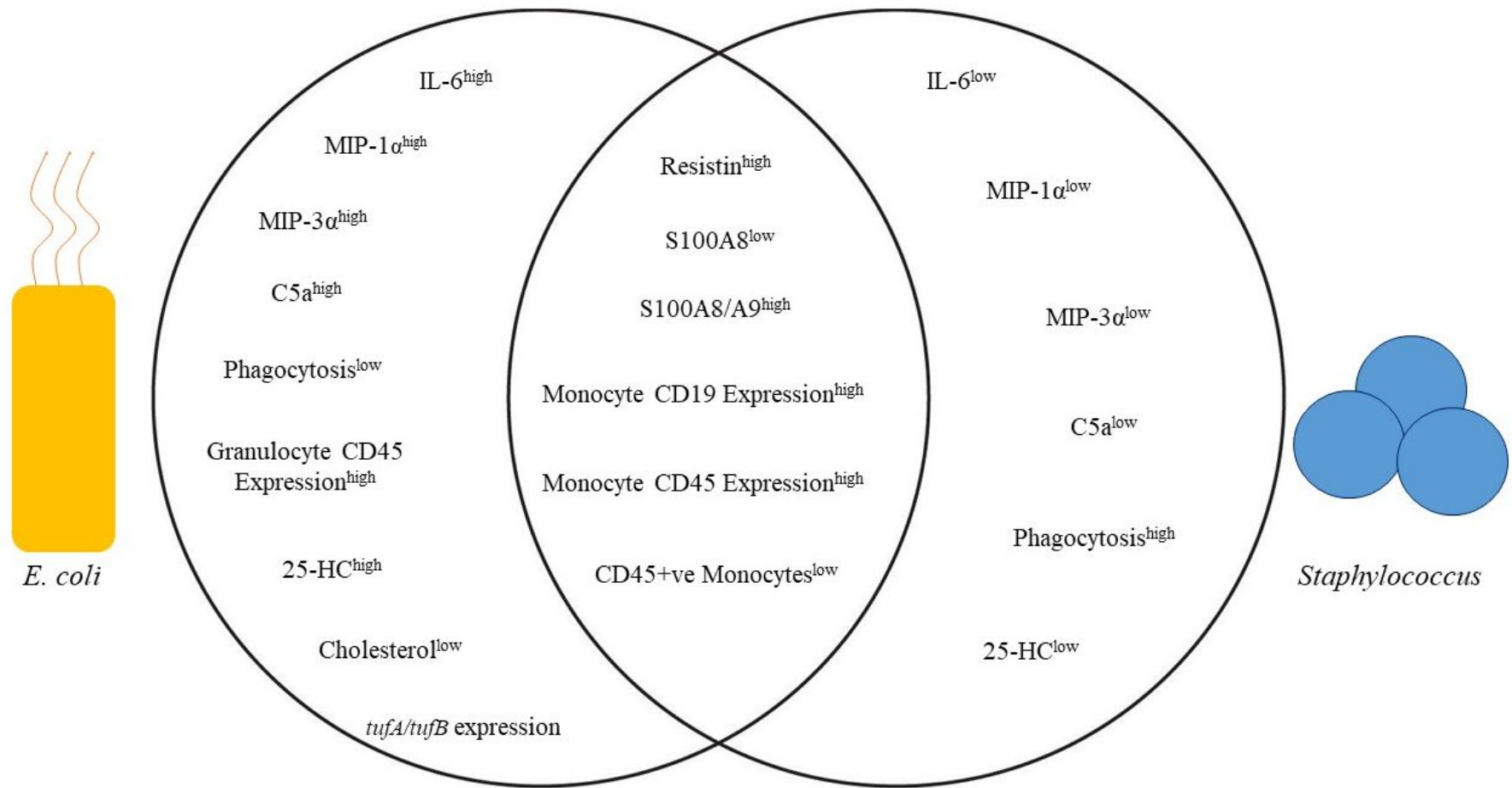
Figure 7.1. Biomarkers of *E. coli* and *Staphylococcus* infection.

## 7.5. Cellular Biomarkers of Sepsis

In addition to identifying molecular biomarkers of infection, Chapter 4 investigated and identified cellular biomarkers (Figure 7.1). Elevated CD45 expression on granulocytes and monocytes and low phagocytosis were found to all be markers of *E. coli* K12 infection. In contrast, high phagocytosis was found to be markers of *S. epidermidis* RP62A infection.

Changes in CD45 expression has been poorly investigated in bacterial sepsis but is nevertheless used as a means to identify leukocytes in blood and other fluids. However, one study has identified significant increases in CD45 mRNA expression in the brains of endotoxaemic mice (Jacob *et al.*, 2007). CD45 has also been found to be critical to the *S. aureus* infection response by playing essential roles in neutrophil and B cell chemotaxis and differentiation of T cells (Zhu *et al.*, 2011). Despite few advances in using CD45 as a biomarker, this thesis found good evidence of increased CD45 expression in response to infection, and temporal changes in CD45 expression on leukocyte subsets allowed for *E. coli* and *S. epidermidis* infection to be distinguished. *E. coli* infections lead to an increase in CD45 expression on both monocytes and granulocytes (specifically neutrophils), whilst *S. epidermidis* infections lead to an increase on monocytes. Dual monitoring of CD45 expression patterns on both these cell types by flow cytometry may allow for discrimination between these two infections.

In a healthcare setting CD45 expression could be measured relatively easily using flow cytometry as it has long been used clinically to diagnose infections such as HIV (CD4$^+$ T cell counts Brown and Wittwer, 2000; Clift, 2015) and a variety of blood cancers (SSC/CD45; Orfao *et al.*, 1999). Assessing cell surface CD45 could be processed and analysed within 2 hours of blood being drawn, allowing for rapid disease diagnosis. Antibodies for these markers are relatively inexpensive, and inclusion in routine flow cytometry blood testing would not negatively impact routine testing in clinics. Further to this, relatively little blood (100 µl) is required for testing, minimising impact on the patient. Phagocytosis, despite being measured using microscopy here, can also be determined using flow cytometry (Lehmann *et al.*, 2000), where the ability to tag and monitor internalisation of bacteria by neutrophils was investigated (Lehmann *et al.,* 2000), and this can be achieved with live bacteria. It is possible to maintain a library of fluorochrome-bound antibodies that can be easily applied to a blood sample, processed and measured in less than 2 hours. Different bacterial species can be targeted using species-specific antigens, such as the O antigen of pathogenic *E. coli* (Stenutz *et al.*, 2006)

or the immunodominant surface antigen B of *S. aureus* (Mackey-Lawrence *et al.*, 2009). Once internalised, fluorescently-tagged bacteria can be tracked using flow cytometry or visualised using ImageStream technology, which allow users to visualise individual cells. Thus, high throughput monitoring of phagocytosis could easily be performed in the clinic.

It was suggested by Linder *et al.* (2019) that it was the individual microorganism that determined the extent of the immune response rather than the Gram type. They found that the blood of patients with septic shock had the highest levels of cytokines when infected with *Neisseria meningitidis* (Gram-negative) or *S. pneumoniae* (Gram-positive) and the lowest when infected with *Enterococcus faecalis* (Gram-positive). Hence, it is possible that the same effect was seen in this current study; despite using only one species of Gram-negative (*E. coli*) and two of Gram-positive bacteria from the same genus (*S. aureus* and *S. epidermidis*). Thus, more species and bacteria genera need to be tested to confirm if the responses are truly due to Gram type or to individual microorganisms.

## 7.6. Oxysterols and their role in diagnosis

There is limited research into the role that 25-HC plays in bacterial infection, but there is an abundance of research into the role that it plays in viral infections (Bauman *et al.,* 2009; Blanc *et al.,* 2013; Li *et al.,* 2013; Anggakasuma *et al.,* 2015; Shawli *et al.,* 2019). This thesis extended the whole blood model to provide the first evidence that 25-HC is preferentially synthesised in response to *E. coli* K12 infection. The work also potentially provides the first evidence that 25-HC can be produced in immune cells other than tissue macrophages, but the mechanism underlying this induction was only partly investigated. Roles during infection that have been identified to date include regulating IgA production (immune function of mucous membranes), promote formation of macrophage foam cells (important in atherosclerosis), amplify inflammatory cytokines, promote neutrophil chemotaxis and suppress the activity of the inflammasome. These roles are clearly established in bacterial infections, and in this model it is likely that similar roles are being carried out.

Whilst the original hypothesis suggested that 25-HC may be a good biomarker to predict sepsis, its application in a healthcare setting may be more difficult. Despite being a potential new biomarker for *E. coli* infection, there are numerous issues that suggest proceeding with caution. The mass spectrometry method used in this study was extremely sensitive and allowed for an accurate means of identifying and quantifying oxysterols present in samples (Crick *et al.,* 2015). However, one major drawback with the method

was the extended period of time required to extract and analyse the molecules. Progression to severe sepsis and septic shock can take place in as little as 48 hours after sepsis symptoms first present, and the total extraction and analysis time for this current method was up to 7 days. Currently one dedicated technician would be needed to complete this technique, and this does not make financial sense. However, testing blood lipid levels with a simple blood test is routine in general practice, and the rapid testing of total cholesterol can be achieved using the Hitachi 704 analyser spectrophotometer (Lentjes *et al.*, 1987). This machine is also used for routine testing of triglycerides and other lipid measurements, as well as numerous other biological parameters. Hence, if these can be tested routinely in a diagnostic laboratory, it stands to reason that 25-HC and other oxysterols could also be incorporated into routine lipid testing in the future.

## 7.7. Genomic Biomarkers: The future of Identifying Sepsis Pathogens

Genome-wide expression studies have been previously used to investigate bacterial factors that predict and lead to infection (Tettelin *et al.*, 2005; Nourdin-Galindo *et al.*, 2017; Griesenauer *et al.*, 2019). One particular study by Dix *et al.* (2015) investigated the transcriptional profile of *E. coli, S. aureus, C. albicans* and *A. fumigatis* when inoculated in a whole blood model. Using this method, they identified 38 biomarker genes that had previously been associated with sepsis and showed potential applications in the future in anti-pathogen strategies. Studies such as this are essential for identifying novel means of diagnosing sepsis, and the central theme in these studies is the genome or expression profile of the pathogen of interest.

Advances in sequencing technology and statistical analysis of whole genomes have allowed for investigations into collections of pathogens to determine genes that are associated with certain traits. Hence, this study is not the first to investigate genetic links between sepsis and *E. coli*, and several studies have analysed genomic factors such as phylogenetic group and antibiotic resistance profiles (Moradigavarand *et al.*, 2018; Paniagua-Contreras *et al.*, 2019; Salinas *et al.*, 2019; Zhang *et al.*, 2019). Daga *et al.* (2019) found that the gene *afa* was associated with sepsis mortality during *E. coli* infections, and that the VFs found in abundance among sepsis isolates included *traT, kpsMT* II, the $K_5$ capsule and the yersiniabactin *fyuA*. In the current work, the majority (42.5%) of the sepsis isolates belonged to phylogenetic group B2, which was also the group that the majority of VFs and PIs were found. Out of the isolates, 16.7% were found to be genetically resistant to 3rd generation cephalosporins. These results reveal key

molecular and epidemiological characteristics of *E. coli* bacteraemias that can aid in recognising and treating difficult infections.

This study used *E. coli* blood culture positive isolates from South-West Wales and the HDUHB, and analysis revealed two novel genes that could be applied to identify sepsis pathogens; *tufA* and *tufB*. As discussed in Chapter 6, *tufA* and *tufB* are elongation factors that have been previously associated with *Mycoplasma* virulence by functioning as adhesins (Balasubramanian *et al.*, 2008). No such association with *E. coli* has been found to the best of our knowledge. The implications here suggest a pathway of adhesion in *E. coli* which potentially represents a novel method of identifying ExPEC in blood cultures. Both presence of *tufA* and *tufB* in *E. coli* can be easily analysed in the clinic using a PCR method, particularly aimed at the genomic level rather than the expression level. This would confirm the presence of these genes quickly (less than 2 hours) and allow a diagnostic technician to identify ExPEC strains in the clinic. These two genes as well as the others identified could be applied to rapid PCR detection methods and would aid greatly in identifying ExPEC in vulnerable patients.

To conclude, this study has identified several molecular and cellular biomarkers of bacterial sepsis that have wide-ranging applications in healthcare settings. Genomic analysis revealed two key genes (*tufA* and *tufB*) that can accurately distinguish between ExPEC and non-ExPEC strains of *E. coli*. New and easily detectable markers of bacterial sepsis (IL-6, MIP-1α, MIP-3α) that have been discovered show great promise for the future of sepsis diagnosis and improvements in patient care.

## Future Perspectives

This study has revealed may lines of enquiry for future work and expansion into other research areas. The whole blood model has multiple applications, and in the future there is the potential to analyse interactions with multiple species of bacteria, not just *E. coli* and *Staphylococcus*. There are other pathogens that are also associated with sepsis in the ICU, including *P. aeruginosa, Klebsiella* spp. and *S. pneumoniae,* to name but a few (Opota *et al.,* 2015). It is very likely that our findings are bacterial species dependent, and there is untapped potential for discovering other markers for different pathogens.

Other future work would include investigating interactions at longer time intervals, going beyond 6 hours post-infection and aiming towards monitoring interactions at 24 hours and further. Although whole blood often begins to lyse beyond 6 hours *ex vivo,* it is worth gradually extending the incubation time, especially as 8 hours post-infection flow cytometry results suggest that the uninfected control blood remains unchanged throughout the incubation period. As severe sepsis and septic shock can take up to 24 hours to develop, extending this model to include this time point would be beneficial. Further, performing immunosuppressed modelling using dexamethasone in whole blood would mimic more accurately the condition of patients that typically develop sepsis clinically (Al-Ishaq *et al.,* 2015).

The current collection of *E. coli* obtained from the Hywel Dda University Health Board represents a significant collection to be explored further. Expanding the current collection would be of great benefit, as it would allow for more isolates from each isolation source to be collected, particularly isolates that are not UPEC (intra-abdominal, biliary etc.). This would significantly increase the power of the data set and would allow for more robust testing. Obtaining specific patient information would also be beneficial, as traits such as age, gender and comorbidities could be assessed with the genomic data to determine if any *E. coli* genes are associated with these traits. Ethical approval for this is currently under application (IRAS 262334). None of the isolates were applied to the whole blood model in the current study, this would also be important to complete in the future, as would completing further GWAS based on, for example, high/low expression of IL-6, MIP proteins and Resistin, as well as other factors such as invasion, phagocytosis and mammalian cell killing. Such work would allow for further genes to be discovered that confer these traits on ExPEC. Refining the invasion model as well as building a more robust one would be advantageous in the future. Currently, we hope to build a 3D model of infection based on the UM-UC-3 cells, which would involve layers of a collagen matrix

as well as dosing adherent cells with differentiated macrophages. 3D models are currently being used in clinical research to understand pathological interactions, although few focus on bacterial invasion (Ferraretto *et al*., 2018, Horsley *et al*., 2018). This would allow us to mimic conditions during UPEC infections and improve our understanding of the interactions and genetic factors that influence invasion and proliferation in these tissues. Multiple parameters could be tested, which include expression of cytokines, rate of invasion into UM-UC-3 and migration across collagen matrices, and expression of genes associated with ExPEC infections assessed using PCR-based methods. Further testing of ExPEC-related pathogenicity should also be performed, including assessing motility of isolates, measuring transcription of *tuf* genes in ExPEC grown in serum and using knockout *E. coli* K12 mutants of target genes (the Keio knockout collection; Baba *et al*., 2006) to determine role in ExPEC virulence.

**Limitations**

Whilst the current study has identified numerous candidates for clinical validation in sepsis diagnosis and understanding genetic influence on ExPEC infections, there are limitations that need to be addressed in future studies. The whole blood model is an efficient and ethical way of measuring systemic responses to infection and has numerous advantages over animal models and human endotoxaemia models. However, there are several drawbacks to working with the whole blood model. The largest limitation was finding suitable donors, as many donors did not turn up despite being compensated for their time, and those that did give had to wait three months between donations. This is a limitation that cannot be overcome in future studies but should be considered. Despite this, we were able to obtain a sufficient number of donors for our study and therefore a suitable sample amount, which provided interesting results.

Another limitation was the realistic time frame needed for blood to be incubated and sampled. Blood is not viable outside the body for extended periods of time, and with constant agitation from the rotator and repeated centrifugations of the plasma, this can limit time course experiments. Attempts were made to incubate blood with bacteria for up to 24 hours. This was not ideal as certain strains (specifically *S. aureus* SH1000) induced erythrocyte lysis, making separation of plasma from erythrocytes impossible, thus such strains could not be included in prolonged incubation experiments. However, in the future it would be beneficial to test such samples in order to determine the extent of cytokine production via ELISA and any damage to the cells via flow cytometry. We found that no damage was evident in control samples taken at 6 hours, therefore it is likely that we may see no damage at 8 and 10 hours, respectively.

Another important limitation experienced during the course of this study was the length of time required to extract, process and analyse oxysterols in experimentally infected blood. As mentioned, 7 days to completely process and analyse the samples is unacceptable for the diagnosis of critically ill patients. This major drawback meant that only 10 samples could be processed at a time. The length of time to analysis and the limited space on the vacuum manifold meant that only two bacteria, *E. coli* K12 and *S. epidermidis* RP62A could be assessed. This scenario was similar for the flow cytometry work, as expanding the number of samples resulted in poor staining and inappropriate cell lysis, ultimately resulting in poor scatter plots. However, the results obtained using only these two bacteria were still very interesting and invaluable in determining changes in response to infection.

One major flaw with the apoptosis assay in Chapter 4 was the inability to include polymorphonuclear immune cells in the test. This was due to leukocyte permeabilisation by the use of BD FACS lyse as a means of removing erythrocytes from the samples but resulted in overstaining with PI. The alternative used was to remove the erythrocytes using Histopaque 1077 which did not allow for granulocyte isolation. This method also took an additional hour and a half to completely isolate mononuclear cells, and then the assay was incomplete without the granulocytes. This can be investigated using a phosphatidylserine specific antibody, such as the Annexin we used and with BD FACS lyse.

Finally, an important limitation in Chapter 6 was the cell culture work. Whilst the cells used were relatively easy to culture, when incubated with bacteria the cells were found to slough away easily when washed with warm PBS. This was concerning as any bacteria that had invaded these cells were also potentially washed away. Possible reasons for the detachment of the cells include cell senescence or the direct effect of the pathogenic *E. coli* i.e. toxicity. An alternative that could be applied here would be to centrifuge and isolate the infected cells before washing to prevent their removal. Lysis could then be performed on the remaining cells to give an accurate representation of the final colony counts. Despite the washing away of a significant amount of the cells, high colony counts were determined at the end of the experiment. This was also problematic, as it could not be determined if this was directly from the lysed cells (and hence invaded bacteria) or if the cells were derived from those that had adhered to the base of the plates after cells had been washed away. Both UPEC and ExPEC are known for their possession of adhesion VFs that enable them to adhere to multiple surfaces (Emody *et al.,* 2003; Vila *et al.,* 2016). Further to this, after incubation with 300 µg/ml gentamicin colonies were noted in plates derived from both the sterile control gentamicin solution and the wash solution. This is either means that the gentamicin concentration used was too low (MIC for gentamicin is 2 µg/ml) or that there was gentamicin resistance in certain strains. It should be noted that *E. coli* K12 was the only strain that was killed by gentamicin incubation. A further limitation here concerns the FBS used in the cell culture work. The batch number of FBS used in this study was not noted before 5 ml aliquots were made and frozen; subsequently, no batch testing was performed on the FBS to ensure that there was little impact on cellular growth. As molecular composition and quality can vary between FBS batches this could have had an impact on the growth of the CACO-2 and UM-UC-3 cell lines. To test and prevent this in the future, testing the new batch against the old by testing cellular

viability with a tetrazolium reduction assay would confirm any impact on growth and viability. Further, these cells grown in a new batch of FBS should be allowed to grow for a further length of time than usual (up to two weeks) to allow the cells to adapt to the change.

**Bibliography**

ABE, R., ODA, S., SADAHIRO, T., NAKAMURA, M., HIRAYAMA, Y., TATEISHI, Y., SHINOZAKI, K. & HIRASAWA, H. 2010. Gram-negative bacteremia induces greater magnitude of inflammatory response than Gram-positive bacteremia. *Crit Care,* 14**,** R27-R27.

ADHIKARI, R. P., AJAO, A. O., AMAN, M. J., KARAUZUM, H., SARWAR, J., LYDECKER, A. D., JOHNSON, J. K., NGUYEN, C., CHEN, W. H. & ROGHMANN, M. C. 2012. Lower antibody levels to Staphylococcus aureus exotoxins are associated with sepsis in hospitalized adults with invasive S. aureus infections. *J Infect Dis,* 206**,** 915-23.

AKAHOSHI, T., SASAHARA, T., NAMAI, R., MATSUI, T., WATABE, H., KITASATO, H., INOUE, M. & KONDO, H. 2003. Production of macrophage inflammatory protein 3alpha (MIP-3alpha)(CCL20) and MIP-3beta (CCL19) by human peripheral blood neutrophils in response to microbial pathogens. *Infect Immun,* 71, 524-526.

AL-ISHAQ, R., ARMSTRONG, J., GREGORY, M., O'HARA, M., PHIRI, K., HARRIS, L. G., ROHDE, H., SIEMSSEN, N., FROMMELT, L., MACK, D. & WILKINSON, T. S. 2015. Effects of polysaccharide intercellular adhesin (PIA) in an ex vivo model of whole blood killing and in prosthetic joint infection (PJI): A role for C5a. *Int J Med Microbiol,* 305**,** 948-956.

ALEXANDER, C. & RIETSCHEL, E. T. 2001. Bacterial lipopolysaccharides and innate immunity. *J Endotoxin Res,* 7**,** 167-202.

ALEXANDRAKI, I. & PALACIO, C. 2010. Gram-negative versus Gram-positive bacteremia: what is more alarmin(g)? *Crit Care,* 14**,** 161-161.

ALIEFENDIOGLU, D., GURSOY, T., CAGLAYAN, O., AKTAS, A. & OVALI, F. 2014. Can resistin be a new indicator of neonatal sepsis? *Pediatr Neonatol,* 55**,** 53-7.

AMAKO, Y., SARKESHIK, A., HOTTA, H., YATES, J., 3RD & SIDDIQUI, A. 2009. Role of oxysterol binding protein in hepatitis C virus infection. *J Virol,* 83**,** 9237-46.

AMMORI, B. J., BECKER, K. L., KITE, P., SNIDER, R. H., NYLEN, E. S., WHITE, J. C., LARVIN, M. & MCMAHON, M. J. 2003. Calcitonin precursors in the prediction of severity of acute pancreatitis on the day of admission. *Br J Surg,* 90**,** 197-204.

ANDREASEN, A. S., KRABBE, K. S., KROGH-MADSEN, R., TAUDORF, S., PEDERSEN, B. K. & MOLLER, K. 2008. Human endotoxemia as a model of systemic inflammation. *Curr Med Chem,* 15**,** 1697-705.

ANGGAKUSUMA, ROMERO-BREY, I., BERGER, C., COLPITTS, C. C., BOLDANOVA, T., ENGELMANN, M., TODT, D., PERIN, P. M., BEHRENDT, P., VONDRAN, F. W., XU, S., GOFFINET, C., SCHANG, L. M., HEIM, M. H., BARTENSCHLAGER, R., PIETSCHMANN, T. & STEINMANN, E. 2015. Interferon-inducible cholesterol-25-hydroxylase restricts hepatitis C virus replication through blockage of membranous web formation. *Hepatology,* 62**,** 702-14.

ARANGO DUQUE, G. & DESCOTEAUX, A. 2014. Macrophage cytokines: involvement in immunity and infectious diseases. *Front Immunol,* 5**,** 491.

ASSINGER, A., SCHROTTMAIER, W. C., SALZMANN, M. & RAYES, J. 2019. Platelets in Sepsis: An Update on Experimental Models and Clinical Data. *Front Immunol,* 10.

BABA, T., ARA, T., HASEGAWA, M., TAKAI, Y., OKUMURA, Y., BABA, M., DATSENKO, K. A., TOMITA, M., WANNER, B. L. & MORI, H. 2006. Construction of *Escherichia coli* K-12 in-frame, single-gene knockout mutants: the Keio collection. *Mol Syst Biol,* 2**,** 2006.0008.

BACHMANN, B. J. 1972. Pedigrees of some mutant strains of *Escherichia coli* K-12. *Bacteriol Rev,* 36**,** 525-557.

BAEK, A. E., YU, Y.-R. A., HE, S., WARDELL, S. E., CHANG, C.-Y., KWON, S., PILLAI, R. V., MCDOWELL, H. B., THOMPSON, J. W., DUBOIS, L. G., SULLIVAN, P. M., KEMPER, J. K., GUNN, M. D., MCDONNELL, D. P. & NELSON, E. R. 2017. The cholesterol metabolite 27 hydroxycholesterol facilitates breast cancer metastasis through its actions on immune cells. *Nat Commun,* 8**,** 864.

BALASUBRAMANIAN, S., KANNAN, T. R. & BASEMAN, J. B. 2008. The Surface-Exposed Carboxyl Region of *Mycoplasma pneumoniae* Elongation Factor Tu Interacts with Fibronectin. *Infect Immun,* 76**,** 3116-3123.

BAUMAN, D. R., BITMANSOUR, A. D., MCDONALD, J. G., THOMPSON, B. M., LIANG, G. & RUSSELL, D. W. 2009. 25-Hydroxycholesterol secreted by macrophages in response to Toll-like receptor activation suppresses immunoglobulin A production. *PNAS,* 106**,** 16764–16769.

BECKER, K. L., SNIDER, R. & NYLEN, E. S. 2008. Procalcitonin assay in systemic inflammation, infection, and sepsis: clinical utility and limitations. *Crit Care Med,* 36.

BECKER, K. L., SNIDER, R. & NYLEN, E. S. 2009. Procalcitonin in sepsis and systemic inflammation: a harmful biomarker and a therapeutic target. *Br J Pharmacol,* 159.

BEENKEN, K. E., DUNMAN, P. M., MCALEESE, F., MACAPAGAL, D., MURPHY, E., PROJAN, S. J., BLEVINS, J. S. & SMELTZER, M. S. 2004. Global gene expression in *Staphylococcus aureus* biofilms. *J Bacteriol,* 186**,** 4665-84.

BERGSBAKEN, T., FINK, S. L. & COOKSON, B. T. 2009. Pyroptosis: host cell death and inflammation. *Nat Rev Microbiol,* 7**,** 99-109.

BERUBE, B. J. & WARDENBURG, J. B. 2013. *Staphylococcus aureus* α-Toxin: Nearly a Century of Intrigue. *Toxins,* 5**,** 1140-1166.

BIRON, B. M., AYALA, A. & LOMAS-NEIRA, J. L. 2015. Biomarkers for Sepsis: What Is and What Might Be? *Biomark Insights,* 10**,** 7-17.

BLACK, S., KUSHNER, I. & SAMOLS, D. 2004. C-reactive Protein. *J Biol Chem,* 279**,** 48487–48490.

BLANC, M., HSIEH, WEI Y., ROBERTSON, KEVIN A., KROPP, KAI A., FORSTER, T., SHUI, G., LACAZE, P., WATTERSON, S., GRIFFITHS, SAMANTHA J., SPANN, NATHANAEL J., MELJON, A., TALBOT, S., KRISHNAN, K., COVEY, DOUGLAS F., WENK, MARKUS R., CRAIGON, M., RUZSICS, Z., HAAS, J., ANGULO, A., GRIFFITHS, WILLIAM J., GLASS, CHRISTOPHER K., WANG, Y. & GHAZAL, P. 2013. The Transcription Factor STAT-1 Couples Macrophage Synthesis of 25-Hydroxycholesterol to the Interferon Antiviral Response. *Immunity,* 38**,** 106-118.

BOSMANN, M. & WARD, P. A. 2013. The inflammatory response in sepsis. *Trends Immunol,* 34**,** 129-36.

BOUCH, D. C. & THOMPSON, J. P. 2008. Severity scoring systems in the critically ill. *BJA Education,* 8**,** 181-185.

BOURNAZOS, S., WANG, T. T., DAHAN, R., MAAMARY, J. & RAVETCH, J. V. 2017. Signaling by Antibodies: Recent Progress. *Annu Rev Immunol,* 35**,** 285-311.

BROWN, A. J. & SHARPE, L. J. 2016. Cholesterol Synthesis. *Biochemistry of Lipids, Lipoproteins and Membranes: Sixth Edition,* 327-358.

BROWN, K. A., BRAIN, S. D., PEARSON, J. D., EDGEWORTH, J. D., LEWIS, S. M. & TREACHER, D. F. 2006. Neutrophils in development of multiple organ failure in sepsis. *Lancet,* 368**,** 157-69.

BROWN, M. & WITTWER, C. 2000. Flow Cytometry: Principles and Clinical Applications in Hematology. *Clin Chem,* 46**,** 1221-1229.

BRYNILDSRUD, O., BOHLIN, J., SCHEFFER, L. & ELDHOLM, V. 2016. Rapid scoring of genes in microbial pan-genome-wide association studies with Scoary. *Genome Biol,* 17**,** 238.

BURDETTE, S. D., PARILO, M. A., KAPLAN, L. J. & BAILEY, H. 2010. *Systemic Inflammatory Response Syndrome* [Online]. WebMD. Available: http://intranet.santa.lt/thesaurus/no_crawl/inf%20endo/Systemic%20Inflammatory%20Response%20Syndrome.htm [Accessed 2016].

CALANDRA, T. & COHEN, J. 2005. The international sepsis forum consensus conference on definitions of infection in the intensive care unit. *Crit Care Med,* 33**,** 1538-48.

CAO, C., YU, M. & CHAI, Y. 2019. Pathological alternation and therapeutic implications of sepsis-induced immune cell apoptosis. *Cell Death Dis,* 10, 782.

CAPUZZO, M., VOLTA, C. A., TASSINATI, T., MORENO, R. P., VALENTIN, A., GUIDET, B.IAPICHINO, G., MARTIN, C. *et al.* 2014. Hospital mortality of adults admitted to

Intensive Care Units in hospitals with and without Intermediate Care Units: a multicentre European cohort study. *Crit. Care,* 18:551.

CARTWRIGHT, M., ROTTMAN, M., SHAPIRO, N. I., SEILER, B., LOMBARDO, P., GAMINI, N., TOMOLINOS, J. *et al.* 2016. A broad-spectrum infection diagnostic that detects pathogen-associated molecular patterns (PAMPs) in whole blood. *EBioMedicine,* 9, 217-227.

CELIK, I. H., DEMIREL, G., URAS, N., OGUZ, E. S., ERDEVE, O. & DILMEN, U. 2015. The role of serum interleukin-6 and C-reactive protein levels for differentiating aetiology of neonatal sepsis. *Arch Argent Pediatr,* 113**,** 534-7.

CELLI, J. & FINLAY, B. B. 2002. Bacterial avoidance of phagocytosis. *Trends Microbiol,* 10**,** 232-7.

CHALUPA, P., BERAN, O., HERWALD, H., KASPRIKOVA, N. & HOLUB, M. 2011. Evaluation of potential biomarkers for the discrimination of bacterial and viral infections. *Infection,* 39**,** 411-7.

CHAN, T. & GU, F. 2011. Early diagnosis of sepsis using serum biomarkers. *Expert Rev Mol Diagn,* 11**,** 487-96.

CHAPIN, J. C. & HAJJAR, K. A. 2015. Fibrinolysis and the control of blood coagulation. *Blood Rev,* 29**,** 17-24.

CHARLES, P. E., TINEL, C., BARBAR, S., AHO, S., PRIN, S., DOISE, J. M., OLSSON, N. O., BLETTERY, B. & QUENOT, J. P. 2009. Procalcitonin kinetics within the first days of sepsis: relationship with the appropriateness of antibiotic therapy and the outcome. *Crit Care,* 13**,** 1-11.

CHERIAN, S., LEVIN, G., LO, W. Y., MAUCK, M., KUHN, D., LEE, C. & WOOD, B. L. 2010. Evaluation of an 8-color flow cytometric reference method for white blood cell differential enumeration. *Cytometry B Clin Cytom,* 78B**,** 319-328.

CHEUNG, G. Y., JOO, H. S., CHATTERJEE, S. S. & OTTO, M. 2014. Phenol-soluble modulins-critical determinants of staphylococcal virulence. *FEMS Microbiol Rev,* 38**,** 698-719.

CHILLER, K., SELKIN, B. A. & MURAKAWA, G. J. 2001. Skin microflora and bacterial infections of the skin. *J Investig Dermatol Symp Proc,* 6, 170-4.

CHO, H.-R., SON, Y., KIM, S.-M., KIM, B.-Y., EO, S.-K., PARK, Y. C. & KIM, K. 2017. 7α-Hydroxycholesterol induces monocyte/macrophage cell expression of interleukin-8 via C5a receptor. *PLOS ONE,* 12**,** e0173749.

CHRISTENSEN, G. D., BISNO, A. L., PARISI, J. T., MCLAUGHLIN, B., HESTER, M. G. & LUTHER, R. W. 1982. Nosocomial septicemia due to multiply antibiotic-resistant *Staphylococcus epidermidis*. *Ann Intern Med,* 96 (1), 1-10.

CIVRA, A., FRANCESE, R., GAMBA, P., TESTA, G., CAGNO, V., POLI, G. & LEMBO, D. 2018. 25-Hydroxycholesterol and 27-hydroxycholesterol inhibit human rotavirus infection by sequestering viral particles into late endosomes. *Redox Biol,* 19**,** 318-330.

CLAEYS, R., VINKEN, S., SPAPEN, H., VER ELST, K., DECOCHEZ, K., HUYGHENS, L. & GORUS, F. K. 2002. Plasma procalcitonin and C-reactive protein in acute septic shock: clinical and biological correlates. *Crit Care Med,* 30.

CLERMONT, O., BONACORSI, S. & BINGEN, E. 2000. Rapid and Simple Determination of the *Escherichia coli* Phylogenetic Group. *Appl Environ Microbiol,* 66**,** 4555-4558.

CLERMONT, O., GORDON, D. & DENAMUR, E. 2015. Guide to the various phylogenetic classification schemes for *Escherichia coli* and the correspondence among schemes. *Microbiology,* 161**,** 980-8.

CLIFT, I. C. 2015. Diagnostic Flow Cytometry and the AIDS Pandemic. *Lab Med,* 46**,** e59-64.

COATES, M., BLANCHARD, S. & MACLEOD, A. S. 2018. Innate antimicrobial immunity in the skin: a protective barrier against bacteria, viruses, and fungi. *PLOS Pathogens,* 14(12).

COHEN, J. 2002. The immunopathogenesis of sepsis. *Nature,* 420**,** 885-91.

CONWAY MORRIS, A., DATTA, D., SHANKAR-HARI, M., STEPHEN, J., WEIR, C. J., RENNIE, J., ANTONELLI, J., BATEMAN, A., WARNER, N., JUDGE, K., KEENAN, J., WANG, A., BURPEE, T., BROWN, K. A., LEWIS, S. M., MARE, T., ROY, A. I., HULME, G., DIMMICK, I., ROSSI, A. G., SIMPSON, A. J. & WALSH, T. S. 2018.

Cell-surface signatures of immune dysfunction risk-stratify critically ill patients: INFECT study. *Intensive Care Med,* 44**,** 627-635.

CONWAY MORRIS, A., KEFALA, K., WILKINSON, T. S., DHALIWAL, K., FARRELL, L., WALSH, T., MACKENZIE, S. J., REID, H., DAVIDSON, D. J., HASLETT, C., ROSSI, A. G., SALLENAVE, J. M. & SIMPSON, A. J. 2009. C5a mediates peripheral blood neutrophil dysfunction in critically ill patients. *Am J Respir Crit Care Med,* 180**,** 19-28.

CRICK, P. J., BENTLEY, T. W., WANG, Y. & GRIFFITHS, W. J. 2015. Revised sample preparation for the analysis of oxysterols by enzyme-assisted derivatisation for sterol analysis (EADSA). *Anal Bioanal Chem,* 407**,** 5235-9.

CYSTER, J. G., DANG, E. V., REBOLDI, A. & YI, T. 2014. 25-Hydroxycholesterols in innate and adaptive immunity. *Nat Rev Immunol,* 14**,** 731-743.

D'HERELLE, F. 1918. Sur le role du microbe filtrant bacteriophage dans la dysenterie bacillaire. *C R Seances Acad Sci III,* 167**,** 970-972.

DAGA, A. P., KOGA, V. L., SONCINI, J. G. M., DE MATOS, C. M., PERUGINI, M. R. E., PELISSON, M., KOBAYASHI, R. K. T. & VESPERO, E. C. 2019. *Escherichia coli* Bloodstream Infections in Patients at a University Hospital: Virulence Factors and Clinical Characteristics. *Front Cell Infect Microbiol,* 9**,** 191.

DANIELS, R. 2011. Surviving the first hours in sepsis: getting the basics right (an intensivist's perspective). *J Antimicrob Chemother,* 66 Suppl 2**,** ii11-23.

DANIKAS, D. D., KARAKANTZA, M., THEODOROU, G. L., SAKELLAROPOULOS, G. C. & GOGOS, C. A. 2008. Prognostic value of phagocytic activity of neutrophils and monocytes in sepsis. Correlation to CD64 and CD14 antigen expression. *Clin Exp Immunol,* 154**,** 87-97.

DECEMBRINO, L., DE AMICI, M., POZZI, M., DE SILVESTRI, A. & STRONATI, M. 2015. Serum Calprotectin: A Potential Biomarker for Neonatal Sepsis. *J ImmunolRes,* 2015**,** 147973-147973.

DECKER, B. K. & PALMORE, T. N. 2013. The role of water in healthcare-associated infections. *Curr Opin Infect Dis,* 26**,** 345-51.

DEGN, S. E. & THIEL, S. 2013. Humoral pattern recognition and the complement system. *Scand J Immunol,* 78**,** 181-93.

DEITCH, E. A. 2012. Gut-origin sepsis: Evolution of a concept. *The Surgeon,* 10, 350-356.

DELBRÜCK, M. 1945. Interference Between Bacterial Viruses: III. The Mutual Exclusion Effect and the Depressor Effect. *J Bacteriol,* 50**,** 151-170.

DEUTSCHMAN, C. S., TRACEY, K. J. 2014. Sepsis: current dogma and new perspectives. *Immunity,* 40, 463-75.

DIAS, I. K., MILIC, I., LIP, G. Y. H., DEVITT, A., POLIDORI, M. C. & GRIFFITHS, H. R. 2018. Simvastatin reduces circulating oxysterol levels in men with hypercholesterolaemia. *Redox Biol,* 16, 139-145.

DI GAUDIO, F., INDELICATO, S., INDELICATO, S., TRICOLI, M. R., STAMPONE, G. & BONGIORNO, D. 2018. Improvement of a rapid direct blood culture microbial identification protocol using MALDI-TOF MS and performance comparison with SepsiTyper kit. *J Microbiol Methods,* 155, 1-7.

DIX, A., HÜNNIGER, K., WEBER, M., GUTHKE, R., KURZAI, O. & LINDE, J. 2015. Biomarker-based classification of bacterial and fungal whole-blood infections in a genome-wide expression study. *Front Microbiol,* 6.

DIX, A., FJELL, C. D., INGHAMMAR, M., HSU, J., WALLEY, K. R., BOYD, J. H. & RUSSELL, J. A. 2019. The Specific Organism: Not Bacterial Gram Type: Drives the Inflammatory Response in Septic Shock. *J Innate Immun***,** 1-9.

DO NASCIMENTO, N. C., GUIMARAES, A. M. S., DOS SANTOS, A. P., CHU, Y., MARQUES, L. M. & MESSICK, J. B. 2018. RNA-Seq based transcriptome of whole blood from immunocompetent pigs (*Sus scrofa*) experimentally infected with Mycoplasma suis strain Illinois. *Vet Res,* 49**,** 49.

DOLIN, H. H., PAPADIMOS, T. J., STEPKOWSKI, S., CHEN, X. & PAN, Z. K. 2018. A Novel Combination of Biomarkers to Herald the Onset of Sepsis Prior to the Manifestation of Symptoms. *Shock (Augusta, Ga.),* 49**,** 364-370.

DOMENECH DE CELLÈS, M., SALOMON, J., MARINIER, A., LAWRENCE, C., GAILLARD, J.-L., HERRMANN, J.-L. & GUILLEMOT, D. 2012. Identifying More Epidemic Clones during a Hospital Outbreak of Multidrug-Resistant *Acinetobacter baumannii*. *PLOS ONE,* 7**,** e45758.

DONG, Y. & SPEER, C. P. 2014. The role of *Staphylococcus epidermidis* in neonatal sepsis: guardian angel or pathogenic devil? *Int J MedMicrobiol,* 304**,** 513-520.

DONLAN, R. M. 2002. Biofilms: microbial life on surfaces. *Emerg Infect Dis,* 8**,** 881-90.

DOUMITH, M., DAY, M., CIESIELCZUK, H., HOPE, R., UNDERWOOD, A., REYNOLDS, R., WAIN, J., LIVERMORE, D. M. & WOODFORD, N. 2015. Rapid identification of major *Escherichia coli* sequence types causing urinary tract and bloodstream infections. *J Clin Microbiol,* 53**,** 160-6.

DUPLESSIS, C., GREGORY, M., FREY, K., BELL, M., TRUONG, L., SCHULLY, K., LAWLER, J., LANGLEY, R. J., KINGSMORE, S. F., WOODS, C. W., RIVERS, E. P., JAEHNE, A. K., QUACKENBUSH, E. B., FOWLER, V. G., TSALIK, E. L. & CLARK, D. 2018. Evaluating the discriminating capacity of cell death (apoptotic) biomarkers in sepsis. *J Intensive Care,* 6**,** 72.

DZIARSKI, R. & GUPTA, D. 2005. Peptidoglycan recognition in innate immunity. *J Endotoxin Res,* 11**,** 304-10.

EMODY, L., KERENYI, M. & NAGY, G. 2003. Virulence factors of uropathogenic *Escherichia coli*. *Int J Antimicrob Agents,* 22 Suppl 2**,** 29-33.

EVAVOLD, C. L., KAGAN, J. C. 2019. Inflammasomes: Threat-Assessment Organlles of the Innate Immune System. *Immunity,* 51, 609-624.

FAIX, J. D. 2013. Biomarkers of sepsis. *Crit Rev Clin Lab Sci,* 50**,** 23-36.

FAKANYA, W. & TOTHILL, I. 2014. Detection of the Inflammation Biomarker C-Reactive Protein in Serum Samples: Towards an Optimal Biosensor Formula. *Biosensors,* 4**,** 340.

FEEZOR, R. J., OBERHOLZER, C., BAKER, H. V., NOVICK, D., RUBINSTEIN, M., MOLDAWER, L. L., PRIBBLE, J., SOUZA, S., DINARELLO, C. A., ERTEL, W. & OBERHOLZER, A. 2003. Molecular characterization of the acute inflammatory response to infections with Gram-negative versus Gram-positive bacteria. *Infect Immun,* 71**,** 5803-13.

FEINGOLD, K. R. & GRUNFELD, C. 2000. The Effect of Inflammation and Infection on Lipids and Lipoproteins. *Endotext.* South Dartmouth (MA): MDText.com, Inc.

FERDERBAR, S., PEREIRA, E. C., APOLINARIO, E., BERTOLAMI, M. C., FALUDI, A., MONTE, O., CALLIARI, L. E., SALES, J. E., GAGLIARDI, A. R., XAVIER, H. T. & ABDALLA, D. S. 2007. Cholesterol oxides as biomarkers of oxidative stress in type 1 and type 2 diabetes mellitus. *Diabetes Metab Res Rev,* 23**,** 35-42.

FERRARETTO, A., BOTTANI, M., DE LUCA, P., CORNAGHI, L., ARNABOLDI, F., MAGGIONI, M., FIORILLI, A. & DONETTI, E. 2018. Morphofunctional properties of a differentiated Caco2/HT-29 co-culture as an in vitro model of human intestinal epithelium. *Bioscience reports,* 38**,** BSR20171497.

FILKOVA, M., HALUZIK, M., GAY, S. & SENOLT, L. 2009. The role of resistin as a regulator of inflammation: Implications for various human pathologies. *Clin Immunol,* 133**,** 157-70.

FINK, M. P. 2014. Animal models of sepsis. *Virulence,* 5**,** 143-153.

FOSTER, T. J., GEOGHEGAN, J. A., GANESH, V. K. & HOOK, M. 2014. Adhesion, invasion and evasion: the many functions of the surface proteins of *Staphylococcus aureus. Nat Rev Microbiol,* 12 (1), 49-62.

FOURNIER, B. & PHILPOTT, D. J. 2005. Recognition of *Staphylococcus aureus* by the Innate Immune System. *ClinMicrobiol Rev,* 18**,** 521-540.

FOXMAN, B. 2010. The epidemiology of urinary tract infection. *Nat Rev Urol,* 7**,** 653-60.

FRIIS, L.M., PIN, C., PEARSON, B. M. & WELLS, J. M. 2005. *In vitro* cell culture methods for investigating *Campylobacter* invasion mechanisms. *J Microbiol Methods,* 61, 145-160.

FUCHS, T. A., ABED, U., GOOSMANN, C., HURWITZ, R., SCHULZE, I., WAHN, V., WEINRAUCH, Y., BRINKMANN, V. & ZYCHLINSKY, A. 2007. Novel cell death program leads to neutrophil extracellular traps. *J Cell Biol,* 176**,** 231-41.

FUJISHIMA, S., SASAKI, J., SHINOZAWA, Y., TAKUMA, K., KIMURA, H., SUZUKI, M., KANAZAWA, M., HORI, S. & AIKAWA, N. 1996. Serum MIP-1 alpha and IL-8 in septic patients. *Intensive Care Med,* 22**,** 1169-75.

GABAY, C. & KUSHNER, I. 1999. Acute-phase proteins and other systemic responses to inflammation. *N Engl J Med,* 340**,** 448-54.

GALLO, R. L. & NIZET, V. 2008. Innate barriers against infection and associated disorders. *Drug Discov Today Dis Mech,* 5**,** 145-152.

GASTEIGER, G., D'OSUALDO, A., SCHUBERT, D. A., WEBER, A., BRUSCIA, E. M. & HARTL, D. 2017. Cellular Innate Immunity: An Old Game with New Players. *J Innate Immun,* 9**,** 111-125.

GENDREL, D. & BOHUON, C. 2000. Procalcitonin as a marker of bacterial infection. *Pediatr Infect Dis J,* 19**,** 679-87; quiz 688.

GIANNAKOPOULOS, K., HOFFMANN, U., ANSARI, U., BERTSCH, T., BORGGREFE, M., AKIN, I. & BEHNES, M. 2017. The Use of Biomarkers in Sepsis: A Systematic Review. *Curr Pharm Biotechnol,* 18**,** 499-507.

GILBERT, P., EVANS, D. J. & BROWN, M. R. W. 1993. Formation and dispersal of bacterial biofilms in vivo and in situ. *J Appl Bacteriol,* 74**,** 67S-78S.

GOLD, E. S., DIERCKS, A. H., PODOLSKY, I., PODYMINOGIN, R. L., ASKOVICH, P. S., TREUTING, P. M. & ADEREM, A. 2014. 25-Hydroxycholesterol acts as an amplifier of inflammatory signaling. *PNAS,* 111**,** 10666-10671.

GORDON, A. C., LAGAN, A. L., AGANNA, E., CHEUNG, L., PETERS, C. J., MCDERMOTT, M. F., MILLO, J. L., WELSH, K. I., HOLLOWAY, P., HITMAN, G. A., PIPER, R. D., GARRARD, C. S. & HINDS, C. J. 2004. TNF and TNFR polymorphisms in severe sepsis and septic shock: a prospective multicentre study. *Genes Immun,* 5**,** 631-40.

GORDON, R. J. & LOWY, F. D. 2008. Pathogenesis of Methicillin-Resistant *Staphylococcus aureus* Infection. *Clin Infect Dis,* 46**,** S350-S359.

GOTO, Y. & KIYONO, H. 2012. Epithelial barrier: an interface for the cross-communication between gut flora and immune system. *Immunol Rev,* 245**,** 147-63.

GRIFFITHS, W. J., CRICK, P. J., WANG, Y., OGUNDARE, M., TUSCHL, K., MORRIS, A. A., BIGGER, B. W., CLAYTON, P. T. & WANG, Y. 2013. Analytical strategies for characterization of oxysterol lipidomes: liver X receptor ligands in plasma. *Free Radic Biol Med,* 59**,** 69-84.

GRIESENAUER, B., TRAN, T. M., FORTNEY, K. R., JANOWICZ, D. M., JOHNSON, P., GAO, H., BARNES, S. *et al.* 2019. Determination of an Interaction Network between an Extracellular Bacterial Pathogen and the Human Host. *mBio,* 10.

GRUYS, E., TOUSSAINT, M. J. M., NIEWOLD, T. A. & KOOPMANS, S. J. 2005. Acute phase reaction and acute phase proteins. *J Zhejiang Univ Sci B,* 6**,** 1045-1056.

HACEK, D. M., CORDELL, R. L., NOSKIN, G. A. & PETERSON, L. R. 2004. Computer-assisted surveillance for detecting clonal outbreaks of nosocomial infection. *J Clin Microbiol,* 42**,** 1170-5.

HALLE, S., HALLE, O. & FORSTER, R. 2017. Mechanisms and Dynamics of T Cell-Mediated Cytotoxicity In Vivo. *Trends Immunol,* 38**,** 432-443.

HAMERS, L., KOX, M. & PICKKERS, P. 2015. Sepsis-induced immunoparalysis: mechanisms, markers, and treatment options. *Minerva Anestesiol,* 81**,** 426-39.

HAMPSON, P., DINSDALE, R. J., WEARN, C. M., BAMFORD, A. L., BISHOP, J. R. B., HAZELDINE, J., MOIEMEN, N. S., HARRISON, P. & LORD, J. M. 2017. Neutrophil Dysfunction, Immature Granulocytes, and Cell-free DNA are Early Biomarkers of Sepsis in Burn-injured Patients: A Prospective Observational Cohort Study. *Ann Surg,* 265**,** 1241-1249.

HAMRICK, T. S., DIAZ, A. H., HAVELL, E. A., HORTON, J. R. & ORNDORFF, P. E. 2003. Influence of Extracellular Bactericidal Agents on Bacteria within Macrophages. *InfectImmun,* 71**,** 1016-1019.

HARBARTH, S., HOLECKOVA, K., FROIDEVAUX, C., PITTET, D., RICOU, B., GRAU, G. E., VADAS, L. & PUGIN, J. 2001. Diagnostic value of procalcitonin, interleukin-6, and interleukin-8 in critically ill patients admitted with suspected sepsis. *Am J Respir Crit Care Med,* 164.

HARDISTY, J., MOORE, S. & REES, B. 2019. Hywel Dda University Health Board Annual Reports and Accounts 2018/2019. *In:* WALES, N. (ed.).

HASLETT, C., GUTHRIE, L. A., KOPANIAK, M. M., JOHNSTON, JR, R . B. & HENSON, P. M. 1985. Modulation of multiple neutrophil functions by preparative methods or trace concentrations of bacterial lipopolysaccharide. *Am J Pathol,* 119, 101-110.

HAUSNER, M. & WUERTZ, S. 1999. High rates of conjugation in bacterial biofilms as determined by quantitative in situ analysis. *Appl Environ Microbiol,* 65**,** 3710-3.

HENTSCHEL, D., OLIVIER, C. B., BODE, C. & DIEHL, P. 2014. The Role of Procalcitonin in Septic Patients – A Brief Overview. *TranslMed,* 4.

HEUMANN, D. & ROGER, T. 2002. Initial responses to endotoxins and Gram-negative bacteria. *Clin Chim Acta,* 323**,** 59-72.

HOEBE, K., JANSSEN, E. & BEUTLER, B. 2004. The interface between innate and adaptive immunity. *Nat Immunol,* 5**,** 971-4.

HONG, T. H., CHANG, C. H., KO, W. J., LIN, C. F., LIU, H. H., CHOW, L. P., HUANG, C. T., YU, S. L. & CHEN, Y. S. 2014. Biomarkers of early sepsis may be correlated with outcome. *J Transl Med,* 12**,** 146.

HORSBURGH, M. J., AISHA, J. L., WHITE, I. J., SHAW, L., LITHGOW, J. K. & FOSTER, S. J. 2002. SigmaB modulates virulence determinant expression and stress resistance: characterisation of a functional rsbU strain derived from *Staphylococcus aureus* 8325-4. *J Bacteriol,* 184 (19), 5457-67.

HORSLEY, H., DHARMASENA, D., MALONE-LEE, J. & ROHN, J. L. 2018. A urine-dependent human urothelial organoid offers a potential alternative to rodent models of infection. *Sci Rep,* 8**,** 1238.

HOU, T., HUANG, D., ZENG, R., YE, Z. & ZHANG, Y. 2015. Accuracy of serum interleukin (IL)-6 in sepsis diagnosis: a systematic review and meta-analysis. *Int J Clin Exp Med,* 8**,** 15238-15245.

HOU, W., GIBBS, J. S., LU, X., BROOKE, C. B., ROY, D., MODLIN, R. L., BENNINK, J. R. & YEWDELL, J. W. 2012. Viral infection triggers rapid differentiation of human blood monocytes into dendritic cells. *Blood,* 119**,** 3128-31.

HU, D., WANG, H., HUANG, X., JIANG, Y., QIN, Y., XIONG, B., QIN, G., SOORANNA, S. R. & PINHU, L. 2016. Investigation of association between IL-8 serum levels and IL8 polymorphisms in Chinese patients with sepsis. *Gene,* 594**,** 165-170.

HUGHES, T. M., ROSANO, C., EVANS, R. W. & KULLER, L. H. 2013. Brain cholesterol metabolism, oxysterols, and dementia. *J Alzheimers Dis,* 33**,** 891-911.

HUNNIGER, K., LEHNERT, T., BIEBER, K., MARTIN, R., FIGGE, M. T. & KURZAI, O. 2014. A virtual infection model quantifies innate effector mechanisms and *Candida albicans* immune escape in human blood. *PLoS Comput Biol,* 10**,** e1003479.

IWASAKI, A. & MEDZHITOV, R. 2015. Control of adaptive immunity by the innate immune system. *Nat Immunol,* 16**,** 343-53.

JACOB, A., HENSLEY, L. K., SAFRATOWICH, B. D., QUIGG, R. J. & ALEXANDER, J. J. 2007. The role of the complement cascade in endotoxin-induced septic encephalopathy. *Lab Invest,* 87**,** 1186-94.

JANNETTO, P. J. & FITZGERALD, R. L. 2016. Effective Use of Mass Spectrometry in the Clinical Laboratory. *Clin Chem,* 62**,** 92-8.

JIN, M. & KHAN, A. I. 2010. Procalcitonin: Uses in the Clinical Laboratory for the Diagnosis of Sepsis. *Lab Med,* 41**,** 173-177.

JIN, T., XU, X. & HERELD, D. 2008. Chemotaxis, chemokine receptors and human disease. *Cytokine,* 44**,** 1-8.

JOHANSSON, L., LINNÉR, A., SUNDÉN-CULLBERG, J., HAGGAR, A., HERWALD, H., LORÉ, K., TREUTIGER, C.-J. & NORRBY-TEGLUND, A. 2009. Neutrophil-Derived Hyperresistinemia in Severe Acute Streptococcal Infections. *J Immunol,* 183**,** 4047-4054.

JOHN, D. A., WILLIAMS, L. K., KANAMARLAPUDI, V., HUMPHREY, T. J. & WILKINSON, T. S. 2017. The Bacterial Species *Campylobacter jejuni* Induce Diverse Innate Immune Responses in Human and Avian Intestinal Epithelial Cells. *Front Microbiol,* 8**,** 1840.

JONES, S. A. 2005. Directing transition from innate to acquired immunity: defining a role for IL-6. *J Immunol,* 175**,** 3463-8.

JONSSON, N., NILSEN, T., GILLE-JOHNSON, P., BELL, M., MARTLING, C. R., LARSSON, A. & MÅRTENSSON, J. 2017. Calprotectin as an early biomarker of bacterial infections in critically ill patients: an exploratory cohort assessment. *Crit Care Resusc,* 19 (3), 205-213.

KACZMAREK, A., VANDENABEELE, P. & KRYSKO, D. V. 2013. Necroptosis; the release of damage-associated molecular patterns and its physiological relevance. *Immunity,* 38, 209-23.

KAHL, B., HERRMANN, M., EVERDING, A. S., KOCH, H. G., BECKER, K., HARMS, E., PROCTOR, R. A. & PETERS, G. 1998. Persistent infection with small colony variant strains of *Staphylococcus aureus* in patients with cystic fibrosis. *J Infect Dis,* 177**,** 1023-9.

KAHNG, J., KIM, Y., KIM, M., OH, E.-J., PARK, Y.-J. & HAN, K. 2015. Flow cytometric white blood cell differential using CytoDiff is excellent for counting blasts. *Ann LabMed,* 35**,** 28-34.

KAIKO, G. E., HORVAT, J. C., BEAGLEY, K. W. & HANSBRO, P. M. 2008. Immunological decision-making: how does the immune system decide to mount a helper T-cell response? *Immunology,* 123**,** 326-38.

KAMISOGLU, K., HAIMOVICH, B., CALVANO, S. E., COYLE, S. M., CORBETT, S. A., LANGLEY, R. J., KINGSMORE, S. F. & ANDROULAKIS, I. P. 2015. Human metabolic response to systemic inflammation: assessment of the concordance between experimental endotoxemia and clinical cases of sepsis/SIRS. *Crit Care,* 19**,** 71.

KANEKO, M., EMOTO, Y. & EMOTO, M. 2016. A Simple, Reproducible, Inexpensive, Yet Old-Fashioned Method for Determining Phagocytic and Bactericidal Activities of Macrophages. *Yonsei MedJ,* 57**,** 283-290.

KAPER, J. B., NATARO, J. P. & MOBLEY, H. L. T. 2004. Pathogenic *Escherichia coli*. *Nat Rev Micro,* 2**,** 123-140.

KIBE, S., ADAMS, K. & BARLOW, G. 2011. Diagnostic and prognostic biomarkers of sepsis in critical care. *J Antimicrob Chemother,* 66 Suppl 2**,** ii33-40.

KITAGAWA, Y., KIKUCHI, S., ARITA, Y., NISHIMURA, M., MIZUNO, K., OGASAWARA, H., KAWANO, T., OCHIAI, T., OTSUJI, E. & IMAI, T. 2013. Inhibition of CCL20 increases mortality in models of mouse sepsis with intestinal apoptosis. *Surgery,* 154, 78-88.

KLAUS, D. A., SEEMANN, R., ROTH-WALTER, F., EINWALLNER, E., MOTAL, M. C., TUDOR, B., LEBHERZ-EICHINGER, D., WIEGELE, M., KRENN, C. G. & ROTH, G. A. 2016. Plasma levels of chemokine ligand 20 and chemokine receptor 6 in patients with sepsis: A case control study. *Eur J Anaesthesiol,* 33, 348-355.

KLOOS, W. E. & MUSSELWHITE, M. S. 1975. Distribution and persistence of *Staphylococcus* and *Micrococcus* species and other aerobic bacteria on human skin. *Appl Microbiol,* 30, 381-385.

KLOS, A., TENNER, A. J., JOHSWICH, K. O., AGER, R. R., REIS, E. S. & KOHL, J. 2009. The role of the anaphylatoxins in health and disease. *Mol Immunol,* 46**,** 2753-66.

KOARAI, A., YANAGISAWA, S., SUGIURA, H., ICHIKAWA, T., KIKUCHI, T., FURUKAWA, K., AKAMATSU, K., HIRANO, T., NAKANISHI, M., MATSUNAGA, K., MINAKATA, Y. & ICHINOSE, M. 2012. 25-hydroxycholesterol enhances cytokine release and toll-like receptor 3 response in airway epithelial cells. *RespirRes,* 13**,** 63-63.

KOHLER, C. D. & DOBRINDT, U. 2011. What defines extraintestinal pathogenic *Escherichia coli*? *Int J Med Microbiol,* 301**,** 642-7.

KRAFT, R., HERNDON, D. N., FINNERTY, C. C., COX, R. A., SONG, J. & JESCHKE, M. G. 2015. Predictive Value of IL-8 for Sepsis and Severe Infections After Burn Injury: A Clinical Study. *Shock,* 43**,** 222-7.

KRAGSBJERG, P., SODERQUIST, B., HOLMBERG, H., VIKERFORS, T. & DANIELSSON, D. 1998. Production of tumor necrosis factor-alpha and interleukin-6 in whole blood

stimulated by live Gram-negative and Gram-positive bacteria. *Clin Microbiol Infect,* 4**,** 129-134.

KRATOFIL, R. M., KUBES, P. & DENISET, J. F. 2017. Monocyte Conversion During Inflammation and Injury. *Arterioscler Thromb Vasc Biol,* 37**,** 35-42.

KUBICEK-SUTHERLAND, J. Z., VU, D. M., NOORMOHAMED, A., MENDEZ, H. M., STROMBERG, L. R., PEDERSEN, C. A., HENGARTNER, A. *et al.* 2019. Direct detection of bacteraemia by exploiting host-pathogen interactions of lipoteichoic acid and lipopolysaccharide. *Sci Rep,* 9 (1), 6203.

KUHNS, D. B., LONG PRIEL, D. A., CHU, J. & ZAREMBER, K. A. 2015. Isolation and Functional Analysis of Human Neutrophils. *Curr Protoc Immunol,* 111**,** 7.23.1-16.

LANDSEM, A., FURE, H., CHRISTIANSEN, D., NIELSEN, E. W., OSTERUD, B., MOLLNES, T. E. & BREKKE, O. L. 2015. The key roles of complement and tissue factor in *Escherichia coli*-induced coagulation in human whole blood. *Clin Exp Immunol,* 182**,** 81-9.

LANG, Y., JIANG, Y., GAO, M., WANG, W., WANG, N., WANG, K., ZHANG, H., CHEN, G., LIU, K., LIU, M., YANG, M. & XIAO, X. 2017. Interleukin-1 Receptor 2: A New Biomarker for Sepsis Diagnosis and Gram-Negative/Gram-Positive Bacterial Differentiation. *Shock,* 47**,** 119-124.

LEHMANN, A. K., SORNES, S. & HALSTENSEN, A. 2000. Phagocytosis: measurement by flow cytometry. *J Immunol Methods,* 243**,** 229-42.

LENTJES, E. G. W. M., HARFF, G. A. & BACKER, E. T. 1987. Evaluation of the Hitachi 704 automatic analyser. *Clin Chem,* 33**,** 2089-92.

LETUNIC, I. & BORK, P. 2007. Interactive Tree Of Life (iTOL): an online tool for phylogenetic tree display and annotation. *Bioinformatics,* 23**,** 127-8.

LEVER, A. & MACKENZIE, I. 2007. Sepsis: definition, epidemiology, and diagnosis. *BMJ,* 335**,** 879-883.

LI, C., DENG, Y. Q., WANG, S., MA, F., ALIYARI, R., HUANG, X. Y., ZHANG, N. N., WATANABE, M., DONG, H. L., LIU, P., LI, X. F., YE, Q., TIAN, M., HONG, S., FAN, J., ZHAO, H., LI, L., VISHLAGHI, N., BUTH, J. E., AU, C., LIU, Y., LU, N., DU, P., QIN, F. X., ZHANG, B., GONG, D., DAI, X., SUN, R., NOVITCH, B. G., XU, Z., QIN, C. F. & CHENG, G. 2017a. 25-Hydroxycholesterol Protects Host against Zika Virus Infection and Its Associated Microcephaly in a Mouse Model. *Immunity,* 46**,** 446-456.

LI, R. H. L. & TABLIN, F. 2018. A Comparative Review of Neutrophil Extracellular Traps in Sepsis. *Front Vet Sci,* 5.

LI, X., XU, Z., PANG, X., HUANG, Y., YANG, B., YANG, Y., CHEN, K., LIU, X., MAO, P. & LI, Y. 2017b. Interleukin-10/lymphocyte ratio predicts mortality in severe septic patients. *PloS one,* 12**,** e0179050-e0179050.

LIESENFELD, O., LEHMAN, L., HUNFELD, K. P. & KOST, G. 2014. Molecular diagnosis of sepsis: New aspects and recent developments. *Eur J Microbiol  Immunol,* 4**,** 1-25.

LINDER, A., FJELL, C. D., INGHAMMER, M., HSU, J., WALLEY, K. R., BOYD, J. H. & RUSSELL, J. A. 2019. The Specific Organism: Not Bacterial Gram Type: Drives the Inflammatory Response in Septic Shock. *J Innate Immun,* 26, 1-9.

LIPSCOMB, M. F. & MASTEN, B. J. 2002. Dendritic cells: immune regulators in health and disease. *Physiol Rev,* 82**,** 97-130.

LIU, H. H., ZHANG, M. W., GUO, J. B., LI, J. & SU, L. 2016. Procalcitonin and C-reactive protein in early diagnosis of sepsis caused by either Gram-negative or Gram-positive bacteria. *Ir J Med Sci*, 186 (1), 207-212.

LIU, S. Y., ALIYARI, R., CHIKERE, K., LI, G., MARSDEN, M. D., SMITH, J. K., PERNET, O., GUO, H., NUSBAUM, R., ZACK, J. A., FREIBERG, A. N., SU, L., LEE, B. & CHENG, G. 2013. Interferon-inducible cholesterol-25-hydroxylase broadly inhibits viral entry by production of 25-hydroxycholesterol. *Immunity,* 38**,** 92-105.

LOTZE, M. T., ZEH, H. J., RUBARTELLI, A., SPARVERO, L. J., AMOSCATO, A. A., WASHBURN, N. R., DEVERA, M. E., LIANG, X., TOR, M. & BILLIAR, T. 2007. The grateful dead: damage-associated molecular pattern molecules and reduction/oxidation regulate immunity. *Immunol Rev,* 220.

LUTJOHANN, D. & VON BERGMANN, K. 2003. 24S-hydroxycholesterol: a marker of brain cholesterol metabolism. *Pharmacopsychiatry,* 36 Suppl 2, S102-6.

MACDONALD, S. P., STONE, S. F., NEIL, C. L., VAN EEDEN, P. E., FATOVICH, D. M., ARENDTS, G. & BROWN, S. G. 2014. Sustained elevation of resistin, NGAL and IL-8 are associated with severe sepsis/septic shock in the emergency department. *PLoS One,* 9, e110678.

MACK, D., SIEMSSEN, N. & LAUFS, R. 1992. Parallel induction by glucose of adherence and a polysaccharide antigen specific for plastic-adherent *Staphylococcus epidermidis*: evidence for functional relation to intercellular adhesion. *Infect Immun,* 60, 2048-57.

MACKEY-LAWRENCE, N. M., POTTER, D. E., CERCA, N. & JEFFERSON, K. K. 2009. *Staphylococcus aureus* immunodominant surface antigen B is a cell-surface associated nucleic acid binding protein. *BMC Microbiol,* 9, 61.

MAIER, M., WUTZLER, S., LEHNERT, M., SZERMUTZKY, M., WYEN, H., BINGOLD, T., HENRICH, D., WALCHER, F. & MARZI, I. 2009. Serum procalcitonin levels in patients with multiple injuries including visceral trauma. *J Trauma,* 66, 243-9.

MALACHOWA, N. & DELEO, F. R. 2011. *Staphylococcus aureus* survival in human blood. *Virulence,* 2, 567-569.

MANGIONI, D., PERI, A. M., ROSSOLINI, G. M., VIAGGI, B., PERNO, C. F., GORI, A. & BANDERA, A. 2019. Towards Rapid Sepsis Diagnosis and Patients Stratification: What's New From Microbiology and Omics Science. *J Infect Dis,* 221 (7), 1039-1047.

MARTIN, P., TRONNET, S., GARCIE, C. & OSWALD, E. 2017. Interplay between siderophores and colibactin genotoxin in *Escherichia coli*. *IUBMB Life,* 69, 435-441.

MARTINEZ-MEDINA, M. & GARCIA-GIL, L. J. 2014. *Escherichia coli* in chronic inflammatory bowel diseases: an update on adherent invasive *Escherichia coli* pathogenicity. *World J Gastrointest Pathophysiol,* 5 (3), 213-227.

MARUNA, P., NEDĚLNÍKOVĂ, K. & GŰRLICH, R. 2000. Physiology and Genetics of procalcitonin. *Physiol Res,* 49.

MATERA, G., QUIRINO, A., GIANCOTTI, A., PULICARI, M. C., RAMETTI, L., RODRÍGUEZ, M. L., LIBERTO, M. C. & FOCÀ, A. 2012. Procalcitonin neutralizes bacterial LPS and reduces LPS-induced cytokine release in human peripheral blood mononuclear cells. *BMC Microbiology,* 12, 1-9.

MATWIYOFF, G. N., PRAHL, J. D., MILLER, R. J., CARMICHAEL, J. J., AMUNDSON, D. E., SEDA, G. & DAHESHIA, M. 2012. Immune regulation of procalcitonin: a biomarker and mediator of infection. *Inflamm Res,* 61, 401-9.

MAZAKI-TOVI, S., VAISBUCH, E., ROMERO, R., KUSANOVIC, J. P., CHAIWORAPONGSA, T., KIM, S. K., OGGE, G., YOON, B. H., DONG, Z., GONZALEZ, J. M., GERVASI, M. T. & HASSAN, S. S. 2010. Hyperresistinemia – a Novel Feature in Systemic Infection During Human Pregnancy. *Am J ReprodImmunol,* 63, 358-369.

MCDONALD, J. G. & RUSSELL, D. W. 2010. Editorial: 25-Hydroxycholesterol: a new life in immunology. *J Leukoc Biol,* 88, 1071-1072.

MCGREGOR, C. 2014. Improving time to antibiotics and implementing the Sepsis 6. *BMJ Qual ImprovRep,* 2 (2).

MCPHERSON, D., GRIFFITHS, C., WILLIAMS, M., BAKER, A., KLODAWSKI, E., JACOBSON, B. & DONALDSON, L. 2013. Sepsis-associated mortality in England: an analysis of multiple cause of death data from 2001 to 2010. *BMJ Open,* 3.

MEISNER, M., TSCHAIKOWSKY, K., HUTZLER, A., SCHICK, C. & SCHUTTLER, J. 1998. Postoperative plasma concentrations of procalcitonin after different types of surgery. *Intensive Care Med,* 24, 680-4.

MENENDEZ, R., TORRES, A., REYES, S., ZALACAIN, A., CAPELASTEGUI, A., ASPA, J., BORDERIAS, L. *et al.* 2012. Initial management of pneumonia and sepsis: factors associated with improved outcome. *Eur Respir J,* 39, 156-162.

MENTEN, P., WUYTS, A. & VAN DAMME, J. 2002. Macrophage inflammatory protein-1. *Cytokine Growth Factor Rev,* 13, 455-81.

MERIC, G., MIRAGAIA, M., DE BEEN, M., YAHARA, K., PASCOE, B., MAGEIROS, L., MIKHAIL, J., HARRIS, L. G., WILKINSON, T. S., ROLO, J., LAMBLE, S., BRAY, J.

E., JOLLEY, K. A., HANAGE, W. P., BOWDEN, R., MAIDEN, M. C., MACK, D., DE LENCASTRE, H., FEIL, E. J., CORANDER, J. & SHEPPARD, S. K. 2015. Ecological Overlap and Horizontal Gene Transfer in *Staphylococcus aureus* and *Staphylococcus epidermidis*. *Genome Biol Evol,* 7**,** 1313-28.

MIAJLOVIC, H., AOGAIN, M. M., COLLINS, C. J., ROGERS, T. R. & SMITH, S. G. 2016. Characterization of *Escherichia coli* bloodstream isolates associated with mortality. *J Med Microbiol,* 65**,** 71-9.

MIAJLOVIC, H. & SMITH, S. G. 2014. Bacterial self-defence: how Escherichia coli evades serum killing. *FEMS Microbiol Lett,* 354**,** 1-9.

MILES, A. A., MISRA, S. S. & IRWIN, J. O. 1938. The estimation of the bactericidal power of the blood. *J Hyg (Lond),* 38**,** 732-749.

MIZRAHI, O., ISH SHALOM, E., BANIYASH, M. & KLIEGER, Y. 2018. Quantitative Flow Cytometry: Concerns and Recommendations in Clinic and Research. *Cytometry B Clin Cytom,* 94**,** 211-218.

MOLLNES, T. E., BREKKE, O. L., FUNG, M., FURE, H., CHRISTIANSEN, D., BERGSETH, G., VIDEM, V., LAPPEGARD, K. T., KOHL, J. & LAMBRIS, J. D. 2002. Essential role of the C5a receptor in E coli-induced oxidative burst and phagocytosis revealed by a novel lepirudin-based human whole blood model of inflammation. *Blood,* 100**,** 1869-77.

MONNERET, G. & VENET, F. 2016. Sepsis-induced immune alterations monitoring by flow cytometry as a promising tool for individualized therapy. *Cytometry B Clin Cytom,* 90**,** 376-86.

MONNERET, G., VENET, F. & PACHOT, A. 2008. Monitoring dysfunctions in the septic patient. A new skin for the old ceremony. *Mol Med,* 14.

MORADIGARAVAND, D., PALM, M., FAREWELL, A., MUSTONEN, V., WARRINGER, J. & PARTS, L. 2018. Prediction of antibiotic resistance in *Escherichia coli* from large-scale pan-genome data. *PLOS Comput Biol,* 14 (12).

MORGAN, S. A. 2019. The infusion nurse's role in antibiotic stewardship. *J Infus Nurs,* 42, 75-80.

MORRIS, A. C., BRITTAN, M., WILKINSON, T. S., MCAULEY, D. F., ANTONELLI, J., MCCULLOCH, C., BARR, L. C., MCDONALD, N. A., DHALIWAL, K., JONES, R. O., MACKELLAR, A., HASLETT, C., HAY, A. W., SWANN, D. G., ANDERSON, N., LAURENSON, I. F., DAVIDSON, D. J., ROSSI, A. G., WALSH, T. S. & SIMPSON, A. J. 2011. C5a-mediated neutrophil dysfunction is RhoA-dependent and predicts infection in critically ill patients. *Blood,* 117**,** 5178-88.

MUKHERJEE, R., KANTI BARMAN, P., KUMAR THATOI, P., TRIPATHY, R., KUMAR DAS, B. & RAVINDRAN, B. 2015. Non-Classical monocytes display inflammatory features: Validation in Sepsis and Systemic Lupus Erythematous. *Sci Rep,* 5**,** 13886.

MUZIO, M., BOSISIO, D., POLENTARUTTI, N., D'AMICO, G., STOPPACCIARO, A., MANCINELLI, R., VAN'T VEER, C., PENTON-ROL, G., RUCO, L. P., ALLAVENA, P. & MANTOVANI, A. 2000. Differential expression and regulation of toll-like receptors (TLR) in human leukocytes: selective expression of TLR3 in dendritic cells. *J Immunol,* 164**,** 5998-6004.

NATARO, J. P. & KAPER, J. B. 1998. Diarrheagenic *Escherichia coli. Clin Microbiol Rev,* 11**,** 142-201.

NGUYEN, H. B., RIVERS, E. P., ABRAHAMIAN, F. M., MORAN, G. J., ABRAHAM, E., TRZECIAK, S., HUANG, D. T., OSBORN, T., STEVENS, D. & TALAN, D. A. 2006. Severe Sepsis and Septic Shock: Review of the Literature and Emergency Department Management Guidelines. *Ann Emerg Med,* 48**,** 54.e1.

NHS WALES 2016. The Annual Quality Statement for NHS Wales 2016. *In:* GOVERNMENT, W. (ed.).

NING, Y., KIM, J. K., MIN, H. K. & REN, S. 2017. Cholesterol metabolites alleviate injured liver function and decrease mortality in an LPS-induced mouse model. *Metabolism,* 71**,** 83-93.

NINKOVIC, J., ANAND, V., DUTTA, R., ZHANG, L., SALUJA, A., MENG, J., KOODIE, L., BANERJEE, S. & ROY, S. 2016. Differential effects of Gram-positive and Gram-

negative bacterial products on morphine induced inhibition of phagocytosis. *Sci Rep,* 6**,** 21094.

NOLT, B., TU, F., WANG, X., HA, T., WINTER, R., WILLIAMS, D. L. & LI, C. 2018. Lactate and Immunosuppression in Sepsis. *Shock,* 49, 120-125.

NOLTE, O., RICKERT, A., EHRHARD, I., LEDIG, S. & SONNTAG, H. G. 2002. A modified ex vivo human whole blood model of infection for studying the pathogenesis of *Neisseria meningitidis* during septicemia. *FEMS Immunol Med Microbiol,* 32**,** 91-5.

NOURDIN-GALINDO, G., SANCHEZ, P., MOLINA, C. F., ESPINOZA-ROJAS, D. A., OLIVER, C., RUIZ, P., VARGAS-CHACOFF, L. *et al.* 2017. Comparative Pan-Genome Analysis of *Piscirickettsia salmonis* Reveales Genomic Divergences within Genogroups. *Cell Infect Microbiol,* 7.

NYLEN, E. S., AL ARIFI, A., BECKER, K. L., SNIDER, R. H., JR. & ALZEER, A. 1997. Effect of classic heatstroke on serum procalcitonin. *Crit Care Med,* 25**,** 1362-5.

NYLÉN, E. S., ROHATGI, P., BECKER, K. L., SNIDER, R. H., JR. & THOMPSON, K. A. 1996. Pneumonitis-Associated Hyperprocalcitoninemia. *Am J Med Sci,* 312**,** 12-18.

O'GRADY, N. P., TROPEA, M., PREAS, I. I. H. L., REDA, D., VANDIVIER, R. W., BANKS, S. M. & SUFFREDINI, A. F. 1999. Detection of Macrophage Inflammatory Protein (MIP)-1α and MIP-β during Experimental Endotoxemia and Human Sepsis. *J Infect Dis,* 179**,** 136-141.

O'NEILL, J. 2016. Tackling Drug-Resistant Infections Globally: Final Report and Recommendations. *The Review on Antimicrobial Resistance.*

OBERHOLZEN, A., OBERHOLZEN, C. & MOLDAWER, L. L. 2002. Interleukin 10 a complex role in the pathogenesis of sepsis syndrome and its potential as an anti-inflammatory drug. *Crit Care Med,* 30.

OCHMAN, H. & SELANDER, R. K. 1984. Standard reference strains of *Escherichia coli* from natural populations. *J Bacteriol,* 157**,** 690-3.

OPAL, S. M. & COHEN, J. 1999. Clinical gram-positive sepsis: does it fundamentally differ from gram-negative bacterial sepsis? *Crit Care Med,* 27**,** 1608-16.

OPOTA, O., JATON, K. & GREUB, G. 2015. Microbial diagnosis of bloodstream infection: towards molecular diagnosis directly from blood. *Clin Microbiol Infect*, 21, 323-331.

ORFAO, A., SCHMITZ, G., BRANDO, B., RUIZ-ARGUELLES, A., BASSO, G., BRAYLAN, R., ROTHE, G., LACOMBE, F., LANZA, F., PAPA, S., LUCIO, P. & SAN MIGUEL, J. F. 1999. Clinically useful information provided by the flow cytometric immunophenotyping of hematological malignancies: current status and future directions. *Clin Chem,* 45**,** 1708-17.

OTTO, M. 2009. *Staphylococcus epidermidis* – the "accidental" pathogen. *Nat Rev Microbiol,* 7**,** 555-567.

OTTO, M. 2014. *Staphylococcus aureus* toxins. *CurrOpin Microbiol,* 17**,** 32-37.

PAGE, A. J., CUMMINS, C. A., HUNT, M., WONG, V. K., REUTER, S., HOLDEN, M. T., FOOKES, M., FALUSH, D., KEANE, J. A. & PARKHILL, J. 2015. Roary: rapid large-scale prokaryote pan genome analysis. *Bioinformatics,* 31**,** 3691-3.

PANG, S. S. & LE, Y. Y. 2006. Role of resistin in inflammation and inflammation-related diseases. *Cell Mol Immunol,* 3**,** 29-34.

PANIAGUA-CONTRERAS, G. L., MONROY-PEREZ, E., DIAZ-VALASQUEZ, C. E., URIBE-GARCIA, A., LABASTIDA, A., PENALOZA-FIGUEROA, F. DOMINGUEZ-TREJO, P. *et al.* 2019. Whole-genome sequence analysis of multidrug-resistant uropathogenic strains of *Escherichia coli* from Mexico. *Infect Drug Resist,* 12, 2363-2377.

PARSEK, M. R. & SINGH, P. K. 2003. Bacterial biofilms: an emerging link to disease pathogenesis. *Annu Rev Microbiol,* 57**,** 677-701.

PEPYS, M. B. & HIRSCHFIELD, G. M. 2003. C-reactive protein: a critical update. *J Clin Invest,* 111**,** 1805-12.

PESTKA, S. 2007. The interferons: 50 years after their discovery, there is much more to learn. *J Biol Chem,* 282**,** 20047-51.

PITOUT, J. D. 2012. Extraintestinal pathogenic *Escherichia coli*: an update on antimicrobial resistance, laboratory diagnosis and treatment. *Expert Rev Anti Infect Ther,* 10**,** 1165-76.

POKHAREL, S. M., SHIL, N. K., JEEVAN, B. G. C., COLBURN, S. T., SEGOVIA, J. A., CHANG, T. *et al.* 2019. Integrin activation by the lipid molecule 25-hydroxycholesterol induces a proinflammatory response. *Nat Comm,* 10 (1482).

PÓVOA, P. 2002. C-reactive protein: a valuable marker of sepsis. *Intensive Care Med,* 28**,** 235-243.

PRAUSSE, M. T. E., LEHNERT, T., TIMME, S., HUNNIGER, K., LEONHARDT, I., KURZAI, O. & FIGGE, M. T. 2018. Predictive Virtual Infection Modeling of Fungal Immune Evasion in Human Whole Blood. *Front Immunol,* 9**,** 560.

PUBLIC HEALTH ENGLAND 2015. Health matters: antimicrobial resistance [Online]. Available: https://www.gov.uk/government/publications/health-matters-antimicrobial-resistance/health-matters-antimicrobial-resistance [Accessed 5/3/2019].

QURESHI, K. & RAJAH, A. 2008. Septic Shock: A Review Article. *Br J Medical Pract,* 2**,** 7-12.

R & D Systems 2019. Luminex Assay Principle [Online]. Available: https://www.rndsystems.com/resources/technical/luminex-assay-principle [Accessed].

RAMACHANDRAN, G. 2014. Gram-positive and Gram-negative bacterial toxins in sepsis: a brief review. *Virulence,* 5**,** 213-8.

RASBAND, W. S. 2018. *ImageJ* [Online]. Available: https://imagej.nih.gov/ij/ [Accessed].

RAWAT, D. & NAIR, D. 2010. Extended-spectrum beta-lactamases in Gram negative Bacteria. *J Glob Infect Dis,* 2**,** 263-74.

REBOLDI, A., DANG, E. V., MCDONALD, J. G., LIANG, G., RUSSELL, D. W. & CYSTER, J. G. 2014. 25-hydroxycholesterol suppresses interleukin-1-driven inflammation downstream of type I interferon. *Science,* 345**,** 679-684.

REINHART, K., BAUER, M., RIEDEMANN, N. C. & HARTOG, C. S. 2012. New approaches to sepsis: molecular diagnostics and biomarkers. *Clin Microbiol Rev,* 25**,** 609-34.

REUTER, S. & LANG, D. 2009. Life span of monocytes and platelets: importance of interactions. *Front Biosci (Landmark Ed),* 14**,** 2432-47.

RIGATO, O., UJVARI, S., CASTELO, A. & SALOMAO, R. 1996. Tumor necrosis factor alpha (TNF-alpha) and sepsis: evidence for a role in host defense. *Infection,* 24**,** 314-8.

RITTIRSCH, D., FLIERI, M. A. & WARD, P. A. 2008. Harmful molecular mechanisms in sepsis. *Nat Rev Immunol,* 8.

ROBERTSON, K. A. & GHAZAL, P. 2016. Interferon Control of the Sterol Metabolic Network: Bidirectional Molecular Circuitry-Mediating Host Protection. *Front Immunol,* 7**,** 634.

RODERBURG, C., BENZ, F., SCHÜLLER, F., POMBEIRO, I., HIPPE, H.-J., FREY, N., TRAUTWEIN, C., LUEDDE, T., KOCH, A., TACKE, F. & LUEDDE, M. 2016. Serum Levels of TNF Receptor Ligands Are Dysregulated in Sepsis and Predict Mortality in Critically Ill Patients. *PLOS ONE,* 11**,** e0153765.

ROGER, T., FROIDEVAUX, C., LE ROY, D., REYMOND, M. K., CHANSON, A.-L., MAURI, D., BURNS, K., RIEDERER, B. M., AKIRA, S. & CALANDRA, T. 2009. Protection from lethal Gram-negative bacterial sepsis by targeting Toll-like receptor 4. *PNAS USA,* 106**,** 2348-2352.

ROSALES, C. 2018. Neutrophil: A Cell with Many Roles in Inflammation or Several Cell Types? *Front Physiol,* 9**,** 113.

ROWTHER, F. B., RODRIGUES, C. S., DESHMUKH, M. S., KAPADIA, F. N., HEGDE, A., MEHTA, A. P. & JOSHI, V. R. 2009. Prospective comparison of eubacterial PCR and measurement of procalcitonin levels with blood culture for diagnosing septicemia in intensive care unit patients. *J Clin Microbiol,* 47**,** 2964-9.

RUDD, K. E., JOHNSON, S. C., AGESA, K. M., SHACKELFORD, K. A., KIEVLAM, D. R., COLOMBARA, D. V., IKUTA, K. S., KISSOON, N *et al.* 2020. Global, regional, and national sepsis incidence and mortality, 1990-2017: analysis for the Global Burden of Disease Study. *Lancet,* 395 (10219), 200-211.

RUPPE, E., OLEARO, F., PIRES, D., BAUD, D., RENZI, G., CHERKAOUI, A., GOLDENBERGER, D., HUTTNER, A., FRANCOIS, P., HARBARTH, S. & SCHRENZEL, J. 2017. Clonal or not clonal? Investigating hospital outbreaks of KPC-

producing Klebsiella pneumoniae with whole-genome sequencing. *Clin Microbiol Infect,* 23**,** 470-475.

RUSSELL, D. W. 2003. The enzymes, regulation, and genetics of bile acid synthesis. *Annu Rev Biochem,* 72**,** 137-74.

SAÏD-SADIER, N. & OJCIUS, D. M. 2012. Alarmins, Inflammasomes and Immunity. *Biomed J,* 35**,** 437-449.

SAKR, Y., JASCHINSKI, U., WITTEBOLE, X., SZAKMANY, T., LIPMAN, J., NAMENDYS-SILVA, S. A., MARTIN-LOECHES, I. *et al.* 2018. Sepsis in Intensive Care Unit Patients: worldwide data from the intensive care over nations audit. *Open Forum Infect Dis*, 5(12).

SARKAR, S., HALLSTRÖM, T., HAMMERSCHMIDT, S., SKERKA, C. & ZIPFEL, P. 2013. Elongation Factor Tu (Tuf) is a new virulence factor of *Streptococcus pneumoniae* that binds human complement factors, aids in immune evasion and host tissue invasion. *Mol Immunol,* 56**,** 312.

SARMA, J. V. & WARD, P. A. 2011. The complement system. *Cell Tissue Res,* 343**,** 227-35.

SCHAAF, B., LUITJENS, K., GOLDMANN, T., VAN BREMEN, T., SAYK, F., DODT, C., DALHOFF, K. & DROEMANN, D. 2009. Mortality in human sepsis is associated with downregulation of Toll-like receptor 2 and CD14 expression on blood monocytes. *Diagn Pathol,* 4**,** 12.

SCHRODER, K., HERTZOG, P. J., RAVASI, T. & HUME, D. A. 2004. Interferon-gamma: an overview of signals, mechanisms and functions. *J Leukoc Biol,* 75**,** 163-89.

SCHUETZ, P., ALBRICH, W. & MUELLER, B. 2011. Procalcitonin for diagnosis of infection and guide to antibiotic decisions: past, present and future. *BMC Medicine,* 9**,** 107-107.

SCHUETZ, P., MUELLER, B. & TRAMPUZ, A. 2007. Serum procalcitonin for discrimination of blood contamination from bloodstream infection due to coagulase-negative staphylococci. *Infection,* 35**,** 352-5.

SEEMANN, T. 2014. Prokka: rapid prokaryotic genome annotation. *Bioinformatics,* 30**,** 2068-9.

SEILER, B. T., CARTWRIGHT, M., DINIS, A. L. M., DUFFY, S., LOMBARDO, P., CARTWRIGHT, D., SUPER, E. H. *et al.* 2019. Broad-spectrum capture of clinical pathogens using engineered Fc-mannose-binding lectin enhanced by antibiotic treatment. *F1000Res,* 8, 108.

SELIGMAN, R., MEISNER, M., LISBOA, T. C., HERTZ, F. T., FILIPPIN, T. B., FACHEL, J. M. & TEIXEIRA, P. J. 2006. Decreases in procalcitonin and C-reactive protein are strong predictors of survival in ventilator-associated pneumonia. *Crit Care,* 10.

SEYMOUR, C. W., GESTEN, F., PRESCOTT, H. C., FRIEDRICH, M. E., IWASHYNA, T. J., PHILLIPS, G. S. STANLEY, M. A. S. *et al.* 2017. Time to Treatment and Mortality during Mandated Emergency Care for Sepsis. *N Engl J Med,* 376, 2235-2244.

SHAH, C., HARI-DASS, R. & RAYNES, J. G. 2006. Serum amyloid A is an innate immune opsonin for Gram-negative bacteria. *Blood,* 108 (5), 1751-1757.

SHANKARI-HARI, M., PHILLIPS, G. S., LEVY, M. L., SEYMOUR, C. W., LIU, V. X., DEUTSCHMAN, C. S., ANGUS, D. C., RUBENFELD, G. D., SINGER, M. 2016. Developing a new definition and assessing new clinical criteria for septic shock: for the third international consensus definitions for sepsis and septic shock (sepsis -3). *JAMA,* 315, 775-87.

SHAO, W. X., YU, D. J., ZHANG, W. Y. & WANG, X. J. 2018. Clinical Significance of Interleukin-6 in the Diagnosis of Sepsis and Discriminating Sepsis Induced by Gram-negative Bacteria. *Pediatr Infect Dis J,* 37**,** 801-805.

SHAWLI, G. T., ADEYEMI, O. O., STONEHOUSE, N. J. & HEROD, M. R. 2019. The Oxysterol 25-Hydroxycholesterol Inhibits Replication of Murine Norovirus. *Viruses,* 11.

SHEN, L. 2012. Tight junctions on the move: molecular mechanisms for epithelial barrier regulation. *Ann N Y Acad Sciences,* 1258, 9-18.

SIMMONS, M. D., DANIELS, S. & TEMPLE, M. 2019. Sepsis programme successes are responsible for the increased detection of bacteraemia. *J Hosp Infect,* 101, 93-99.

SINGER, M., DEUTSCHMAN, C. S., SEYMOUR, C. & ET AL. 2016. The third international consensus definitions for sepsis and septic shock (sepsis-3). *JAMA,* 315**,** 801-810.

SKOVBJERG, S., MARTNER, A., HYNSJO, L., HESSLE, C., OLSEN, I, DEWHIRST, F. E., THAM, W. & WOLD, A. E. 2010. Gram-positive and gram-negative bacteria induce

different patterns of cytokine production in human mononuclear cells irrespective of taxonomic relatedness. *J Interferon Cytokine Res,* 30**,** 23-32.

SOKOL, C. L. & LUSTER, A. D. 2015. The chemokine system in innate immunity. *Cold Spring Harb Perspect Biol,* 7.

STENUTZ, R., WEINTRAUB, A. & WIDMALM, G. 2006. The structures of *Escherichia coli* O-polysaccharide antigens. *FEMS Microbiol Rev,* 30**,** 382-403.

STEPPAN, C. M. & LAZAR, M. A. 2002. Resistin and obesity-associated insulin resistance. *Trends Endocrinol Metab,* 13**,** 18-23.

STRIMBU, K. & TAVEL, J. A. 2010. What are Biomarkers? *Curr Opin HIV AIDS,* 5 (6), 463-466.

STRNAD, P., TACKE, F., KOCH, A., TRAUTWEIN, C. 2017. Liver - guardian, modifier and target of sepsis. *Nat Rev Gastroenterol Hepatol,* 14, 55-66.

STROBEL, L. & JOHSWICH, K. O. 2018. Anticoagulants impact on innate immune responses and bacterial survival in whole blood models of *Neisseria meningitidis* infection. *Sci Rep,* 8**,** 10225.

SURBATOVIC, M., POPOVIC, N., VOJVODIC, D., MILOSEVIC, I., ACIMOVIC, G., STOJICIC, M., VELJOVIC, M. & *AL., E.* 2015. Cytokine profile in severe gram-positive and gram-negative abdominal sepsis. *Sci Rep* 5 (11355).

SZAKMANY, T., LUNDIN, R. M., SHARIF, B., ELLIS, G., MORGAN, P., KOPCZYNSKA, M., DHADDA, A., MANN, C., DONOGHUE, D., ROLLASON, S., BROWNLOW, E., HILL, F., CARR, G., TURLEY, H., HASSALL, J., LLOYD, J., DAVIES, L., ATKINSON, M., JONES, M., JONES, N., MARTIN, R., IBRAHIM, Y. & HALL, J. E. 2016. Sepsis Prevalence and Outcome on the General Wards and Emergency Departments in Wales: Results of a Multi-Centre, Observational, Point Prevalence Study. *PLoS One,* 11**,** e0167230.

TALL, A. R. & YVAN-CHARVET, L. 2015. Cholesterol, inflammation and innate immunity. *Nat Rev Immunol,* 15**,** 104-16.

TANAKA, T., NARAZAKI, M. & KISHIMOTO, T. 2014. IL-6 in Inflammation, Immunity, and Disease. *Cold Spring Harb Perspect Biol*, 6 (10).

TCHILIAN, E. Z. & BEVERLEY, P. C. 2006. Altered CD45 expression and disease. *Trends Immunol,* 27**,** 146-53.

TECCHIO, C., MICHELETTI, A. & CASSATELLA, M. A. 2014. Neutrophil-Derived Cytokines: Facts Beyond Expression. *Front Immunol,* 5.

TERLIZZI, M. E., GRIBAUDO, G. & MAFFEI, M. E. 2017. Uropathogenic *Escherichia coli* (UPEC) Infections: Virulence Factors, Bladder Responses, Antibiotic, and Non-antibiotic Antimicrobial Strategies. *Front Microbiol,* 8**,** 1566.

TETTELIN, H., MASIGNANI, V., CIESLEWICZ, M. J., DONATI, C., MEDINI, D., WARD, N. L., ANGIUOLI, S. V., CRABTREE, J. *et al.* 2005. Genome analysis of multiple pathogenic isolates of *Streptococcus agalactiae:* Implications for the microbial "pan-genome". *PNAS,* 102, 13950-13955.

TESTA, G., STAURENGHI, E., GIANNELLI, S., GARGIULO, S., GUGLIELMOTTO, M., TABATON, M., TAMAGNO, E., GAMBA, P. & LEONARDUZZI, G. 2018. A silver lining for 24-hydroxycholesterol in Alzheimer's disease: The involvement of the neuroprotective enzyme sirtuin 1. *Redox Biol,* 17**,** 423-431.

THAMMAVONGSA, V., KIM, H. K., MISSIAKAS, D. & SCHNEEWIND, O. 2015. Staphylococcal manipulation of host immune responses. *Nat Rev Microbiol,* 13**,** 529-43.

THE EUROPEAN COMMITTEE ON ANTIMICROBIAL SUSCEPTIBILITY TESTING 2019. Breakpoint table for interpretation of MICs and zone diameters, version 9.0. http://eucast.org/clinical_breakpoints/

THE UK SEPSIS TRUST 2019. About Sepsis [Online]. Available: https://sepsistrust.org/about/about-sepsis/ [Accessed 5/3/2019].

TSAI, W. H., SHIH, C. H., YU, Y. B. & HSU, H. C. 2013. Plasma levels in sepsis patients of annexin A1, lipoxin A4, macrophage inflammatory protein-3a, and neutrophil gelatinase-associated lipocalin. *J Chin Med Assoc,* 76**,** 486-90.

TURVEY, S. E. & BROIDE, D. H. 2010. Innate immunity. *J Allergy Clin Immunol,* 125**,** S24-32.

UMLAUF, V. N., DRESCHERS, S. & ORLIKOWSKY, T. W. 2013. Flow Cytometry in the Detection of Neonatal Sepsis. *IntJ Pediatr* 2013.

VALLE, A., BARBAGIOVANNI, G., JOFRA, T., STABILINI, A., PEROL, L., BAEYENS, A., ANAND, S., CAGNARD, N., GAGLIANI, N., PIAGGIO, E. & BATTAGLIA, M. 2015. Heterogeneous CD3 Expression Levels in Differing T Cell Subsets Correlate with the In Vivo Anti-CD3–Mediated T Cell Modulation. *J Immunol,* 194**,** 2117-2127.

VAN KESSEL, K. P. M., BESTEBROER, J. & VAN STRIJP, J. A. G. 2014. Neutrophil-Mediated Phagocytosis of *Staphylococcus aureus*. *Front Immunol,* 5**,** 467.

VANCLEAVE, T. T., PULSIFER, A. R., CONNOR, M. G., WARAWA, J. M. & LAWRENZ, M. B. 2017. Impact of Gentamicin Concentration and Exposure Time on Intracellular *Yersinia pestis*. *Front Cell Infect Microbiol,* 7**,** 505.

VELKOV, T., ROBERTS, K. D., NATION, R. L., THOMPSON, P. E. & LI, J. 2013. Pharmacology of polymyxins: new insights into an 'old' class of antibiotics. *Future Microbiol,* 8**,** 711-24.

VERMONT, C. L., HAZELZET, J. A., DE KLEIJN, E. D., VAN DEN DOBBELSTEEN, G. P. & DE GROOT, R. 2006. CC and CXC chemokine levels in children with meningococcal sepsis accurately predict mortality and disease severity. *Crit Care,* 10**,** R33.

VILA, J., SAEZ-LOPEZ, E., JOHNSON, J. R., ROMLING, U., DOBRINDT, U., CANTON, R., GISKE, C. G., NAAS, T., CARATTOLI, A., MARTINEZ-MEDINA, M., BOSCH, J., RETAMAR, P., RODRIGUEZ-BANO, J., BAQUERO, F. & SOTO, S. M. 2016. *Escherichia coli*: an old friend with new tidings. *FEMS Microbiol Rev,* 40**,** 437-463.

VINCENT, J. L., SAKR, Y., SPRUNG, C. L., RANIERI, V. M., REINHART, K., GERLACH, H., MORENO, R., CARLET, J., LE GALL, J. R. *et al.* 2006. Sepsis in European intensive care units: results of the SOAP study. *Crit Care Med,* 34, 344-53.

VINCENT, J. L., RELLO, J., MARSHALL, J., SILVA, E., ANZUETO, A., MARTIN, C. D., MORENO, R., LIPMAN, J., GOMERSALL, C. *et al.* 2009. International study of the prevalence and outcomes of infection in intensive care units. *JAMA,* 302, 2323-9.

VINCENT, J. L. 2016. The Clinical Challenge of Sepsis Identification and Monitoring. *PLoS Med,* 13**,** e1002022.

VIVAS-ALEGRE, S., FERNANDEZ-NATAL, I., LOPEZ-FIDALGO, E. & RIVERO-LEZCANO, O. M. 2015. Preparation of inocula for experimental infection of blood with *Streptococcus pneumoniae*. *Methods,* 2**,** 463-8.

VON HEIMBURG, D., STIEGHORST, W., KHORRAM-SEFAT, R. & PALLUA, N. 1998. Procalcitonin--a sepsis parameter in severe burn injuries. *Burns,* 24**,** 745-50.

WARD, P. A. 2010. The Harmful Role of C5a on Innate Immunity in Sepsis. *J Innate Immun,* 2**,** 439-445.

WANG, J., ZENG, L., ZHANG, L., GUO, Z. Z., LU, S. F., MING, S. L., LI, G. L., WAN, B., TIAN, K. G., YANG, G. Y. & CHU, B. B. 2017. Cholesterol 25-hydroxylase acts as a host restriction factor on pseudorabies virus replication. *J Gen Virol,* 98**,** 1467-1476.

WANG, K., WEI, G. & LIU, D. 2012. CD19: a biomarker for B cell development, lymphoma diagnosis and therapy. *Exp Hematol Oncol,* 1**,** 36-36.

WANG, G. 2014. Human antimicrobial peptides and proteins. *Pharmaceuticals (Basel),* 13, 545-594

WANG, S., SONG, R., WANG, Z., JING, Z., WANG, S. & MA, J. 2018. S100A8/A9 in Inflammation. *Front Immunol,* 9**,** 1298-1298.

WARFORD, J., LAMPORT, A. C., KENNEDY, B. & EASTON, A. S. 2017. Human Brain Chemokine and Cytokine Expression in Sepsis: A Report of Three Cases. *Can J Neurol Sci,* 44, 96-104.

WEBSTER, S. J., DAIGNEAULT, M., BEWLEY, M. A., PRESTON, J. A., MARRIOTT, H. M., WALMSLEY, S. R., READ, R. C., WHYTE, M. K. & DOCKRELL, D. H. 2010. Distinct cell death programs in monocytes regulate innate responses following challenge with common causes of invasive bacterial disease. *J Immunol,* 185**,** 2968-79.

WIDJAJA, M., HARVEY, K. L., HAGEMANN, L., BERRY, I. J., JAROCKI, V. M., RAYMOND, B. B. A., TACCHI, J. L., GRÜNDEL, A., STEELE, J. R., PADULA, M. P., CHARLES, I. G., DUMKE, R. & DJORDJEVIC, S. P. 2017. Elongation factor Tu is a multifunctional and processed moonlighting protein. *Sci Rep,* 7**,** 11227.

WIERSINGA, W. J., DE VOS, A. F., WIELAND, C. W., LEENDERTSE, M., ROELOFS, J. J. & VAN DER POLL, T. 2008. CD14 impairs host defense against gram-negative sepsis caused by *Burkholderia pseudomallei* in mice. *J Infect Dis,* 198.

WILES, T. J., KULESUS, R. R. & MULVEY, M. A. 2008. Origins and Virulence Mechanisms of Uropathogenic *Escherichia coli*. *Exp Mol Pathol,* 85**,** 11-19.

WILKINS, C. & GALE, M. 2013. Sterol-izing Innate Immunity. *Immunity,* 38**,** 3-5.

WILKINSON, T. S., CONWAY MORRIS, A., KEFALA, K., O'KANE, C. M., MOORE, N. R., BOOTH, N. A., MCAULEY, D. F., DHALIWAL, K., WALSH, T. S., HASLETT, C., SALLENAVE, J. M. & SIMPSON, A. J. 2012. Ventilator-associated pneumonia is characterized by excessive release of neutrophil proteases in the lung. *Chest,* 142**,** 1425-1432.

WILLIAMS, T. A., HO, K. M., DOBB, G. J., KNUIMAN, M. & WEBB, S. A. 2010. Effect of length of stay in intensive care unit on hospital and long-term mortality of critically ill adult patients. *Br J Anaesth*, 104, 459-64.

WOBETO, V. P. A., ZACCARIOTTO, T. R. & SONATI, M. F. 2008. Polymorphism of human haptoglobin and its clinical importance. *Genet Mol Biol,* 31 (3), 602-620.

YE, H., ZHANG, X. W., MU, R., FANG, L. K., GU, J. R., LIN, J., DU, J. F., CHEN, J. W., CHEN, Y. J., WU, L. J., PANG, X. F. & LI, Z. G. 2014. Anti-TNF therapy in patients with HBV infection--analysis of 87 patients with inflammatory arthritis. *Clin Rheumatol,* 33**,** 119-23.

YIKILMAZ, E., CHAPMAN, S. J., SCHRADER, J. M. & UHLENBECK, O. C. 2014. The interface between *Escherichia coli* elongation factor Tu and aminoacyl-tRNA. *Biochemistry,* 53**,** 5710-20.

YU, S. L., CHEN, H. W., YANG, P. C., PECK, K., TSAI, M. H., CHEN, J. J. & LIN, F. Y. 2004. Differential gene expression in Gram-negative and Gram-positive sepsis. *Am J Respir Crit Care Med,* 169**,** 1135-43.

ZAMANI, F., ZARE SHAHNEH, F., AGHEBATI-MALEKI, L. & BARADARAN, B. 2013. Induction of CD14 Expression and Differentiation to Monocytes or Mature Macrophages in Promyelocytic Cell Lines: New Approach. *Adv Pharm Bull,* 3**,** 329-332.

ZHANG, N. & BEVAN, M. J. 2011. CD8(+) T cells: foot soldiers of the immune system. *Immunity,* 35**,** 161-8.

ZHANG, X., XIAO, S., JIANG, X., LI, Y., FAN, Z., YU, Y., WANG, P., LI, D., ZHAO, X. & LIU, C. 2019. Genomic characterisation of *Escherichia coli* LCT-EC001, an extremely multidrug-resistant strain with an amazing number of resistance genes. *Gut Pathog,* 11.

ZHU, J. W., DOAN, K., PARK, J., CHAU, A. H., ZHANG, H., LOWELL, C. A. & WEISS, A. 2011. Receptor-like tyrosine phosphatases CD45 and CD148 have distinct functions in chemoattractant-mediated neutrophil migration and response to *S. aureus*. *Immunity,* 35**,** 757-69.

ZMYSŁOWSKI, A. & SZTERK, A. 2019. Oxysterols as a biomarker in diseases. *Clinica Chimica Acta,* 491**,** 103-113.

ZOU, G., HE, J., REN, B., XU, F., XU, G. & ZHANG, W. 2016. The delta high-density lipoprotein cholesterol ratio: a novel parameter for Gram-negative sepsis. *Springerplus,* 5**,** 1044.

ZOU, T., GARIFULIN, O., BERLAND, R. & BOYARTCHUK, V. L. 2011. *Listeria monocytogenes* Infection Induces Prosurvival Metabolic Signaling in Macrophages. *Infect Immun,* 79**,** 1526-1535.

## Appendices

## Appendix A

Specifications of the standards used in the extraction of oxysterols from plasma samples.

| Sterol Name | Stock Solution Concentration | Stock Date | Working Solution Concentration | Working Solution Date | ng of ISTD required per sample | Volume taken for HMC per sample (µl) | x80 (µl) |
|---|---|---|---|---|---|---|---|
| 24R/S-OHC-D7 | 100 ng/µl | 16/09-2013-JA | 4 ng/µl | 04/12/2017-EY | 20 | 5 | 400 |
| 7α-OHC-D7 | 48.74 ng/µl | 31/08/2017-EY | 4 ng/µl | 31/08/2017-EY | 20 | 5 | 400 |
| 22R-3-oxo-OHC-D7 | 5 ng/µl | 20/01/2017-JA | 5 ng/µl | 22/05/2017-AD | 20 | 4 | 320 |
| 7α,25-DiHC-D6 | 100 ng/µl | 16/09/2013-JA | 4 ng/µl | 31/08/2017-EY | 2 | 0.5 | 40 |
| 25OH-VitD3-D6 | 100 ng/µl | 20/08/2013-JA | 4 ng/µl | 31/08/2017-EY | 2 | 0.5 | 40 |
| Cholesterol-D7 | 1 µg/µl | 22/05/2017-EY | 1 µg/µl | 22/05/2017-EY | 20000 | 20 | 1600 |
| EtOH | | | | | | 15 | 1200 |
| | | | | | Total | 50 | 4000 |
| | | | | | On day of use, add EtOH | 1000 | |
| | | | | | Total Volume (µl) | 1050 | |

## Appendix B

*E. coli* clinical isolates used in phenotypic studies.

| Strain | Clinical Identified Source |
|---|---|
| ATCC 35218 | Canine Reference Strain |
| ATCC 25922 | FDA Clinical Isolate Reference Strain |
| B5934 | Urine |
| B5946 | Intra-abdominal |
| B4076 | Other Hepatorenal failure |
| B4019 | Biliary |
| B4060 | Urine |
| B4053 | Biliary |
| B/7E00 4082 | Other Recent Chemotherapy |
| B/7500 4141 | Biliary |
| BHE00 4183 | Biliary |
| B.17E00 9094 | Intra-abdominal |
| B.4297 | Urine |
| B.4298 | Intra-abdominal |
| B17E00 4376 | Biliary |
| B17E00 5844 | Urine |
| B17E00 5868 | Biliary |
| B17E00 4216 | Other |

| | |
|---|---|
| | Unknown |
| B17E00 4224 | Other |
| | Unknown |
| B17E00 4409 | Urine |
| 17/119 | Biliary |
| 17/123 | Other |
| | Clinical Pneumonia |
| | *E. coli* in urine |
| 17/122 | Urine |
| 17/124 | Urine |
| 17/127 | Urine |
| 17/128 | Unknown |
| 17/129 | Urine |
| 17/131 | Urine |
| 3729 | Urine |
| 3736 | Urine |
| 3737 | Urine |
| 3743 | Urine |
| 3747 | Biliary |
| 3757 | Intra-abdominal |
| 17/104 | Urine |
| 17/106 | Intra-abdominal |
| 17/107 | Urine |
| 17/108 | Biliary |

| | |
|---|---|
| 3710 | Urine |
| 3697 | Intra-abdominal |
| 3701 | Biliary |
| 3693 | Urine |
| 3714 | Urine |
| 3718 | Urine |
| 3717 | Biliary |
| 3708 | Urine |
| 3690 | Urine |
| 3730 | Urine |
| 3731 | Urine |
| 3744 | Urine |
| 3745 | Biliary |
| 3756 | Unknown Other |
| 3752 | Urine |
| B17E00 8857 | Urine |
| B17E00 8763 | Urine |
| B17E00 8876 | Intra-abdominal |
| B17E00 8958 | Urine |
| B17E00 9042 | Urine |
| B17E00 9451 | Intra-abdominal |
| B17E00 8980 | Other Unknown |

| | |
|---|---|
| B17E00 9003 | Urine |
| B17E00 9046 | Urine |
| 1124046916 | Intra-abdominal |
| 1124046948 | Intra-abdominal |
| 1124046825 | Urine |
| 1124046973 | Urine |
| 1124055539 | Intra-abdominal |
| 112405550 | Urine |
| 1124055651 | Intra-abdominal |
| 1124055426 | Urine |
| 1124055402 | Other<br><br>Unknown |
| B17A002373 | Urine |
| 1123209048 | Intra-abdominal |
| B17A002400 | Urine |
| B17A002624 | Urine |
| B18A000069 | Urine |
| B18A000136 | Abdominal |
| B18A000099 | Urine |
| B18A000001 | Urine |
| B18A000078 | Urine |
| B18A000291 | Urine |
| B18A000271 | Urine |
| B18A000271 | Other |

| | |
|---|---|
| B17E009423 | Urine |
| B18E000859 | Urine |
| B18E000850 | Urine |
| B18E000828 | Other |
| B18E000796 | Urine |
| B18E000711 | Urine |
| B18E000666 | Urine |
| B18E000643 | Respiratory |
| E17E505558 | Water |
| E17E505761 | Water |
| E17E505979 | Water |
| E18E500166 | Water |
| E18E500522 | Water |
| E17E506268 | Water |
| E17E505024 | Water |

## Appendix C

ECOR isolates used as reference genomes in Chapter 6.

| Isolate | Host | Country of Isolation | Pathogenesis |
|---|---|---|---|
| ECOR10 | Human | Sweden | Coloniser |
| ECOR11 | Human | Sweden | UTI and Acute Cystitis |
| ECOR12 | Human | Sweden | Coloniser |
| ECOR13 | Human | Sweden | Coloniser |
| ECOR14 | Human | Sweden | UTI and Acute Pyelonephritis |
| ECOR15 | Human | Sweden | Coloniser |
| ECOR16 | Leopard | U.S.A. | Coloniser |
| ECOR17 | Pig | Indonesia | Coloniser |
| ECOR18 | Celebese Ape | U.S.A. | Coloniser |
| ECOR19 | Celebese Ape | U.S.A. | Coloniser |
| ECOR2 | Human | U.S.A. | Coloniser |
| ECOR21 | Steer | Bali | Coloniser |
| ECOR22 | Steer | Bali | Coloniser |
| ECOR23 | Elephant | U.S.A. | Coloniser |
| ECOR24 | Human | Sweden | Coloniser |
| ECOR25 | Dog | U.S.A. | Coloniser |
| ECOR26 | Human Infant | U.S.A. | Coloniser |
| ECOR27 | Giraffe | U.S.A. | Coloniser |
| ECOR28 | Human Child | U.S.A. | Coloniser |
| ECOR29 | Kangaroo Rat | U.S.A. | Coloniser |
| ECOR3 | Dog | U.S.A. | Coloniser |
| ECOR30 | Bison | Canada | Coloniser |
| ECOR31 | Leopard | U.S.A. | Coloniser |
| ECOR32 | Giraffe | U.S.A. | Coloniser |
| ECOR33 | Sheep | U.S.A. | Coloniser |
| ECOR34 | Dog | U.S.A. | Coloniser |
| ECOR35 | Human | U.S.A. | Coloniser |
| ECOR36 | Human | U.S.A. | Coloniser |
| ECOR37 | Marmoset | U.S.A. | Coloniser |
| ECOR38 | Human | U.S.A. | Coloniser |
| ECOR39 | Human | Sweden | Coloniser |
| ECOR4 | Human Child | U.S.A. | Coloniser |
| ECOR40 | Human | Sweden | UTI and Acute Pyelonephritis |
| ECOR41 | Human | Tonga | Coloniser |
| ECOR42 | Human | U.S.A. | Coloniser |
| ECOR43 | Human | Sweden | Coloniser |
| ECOR45 | Pig | Indonesia | Coloniser |
| ECOR46 | Ape | U.S.A. | Coloniser |
| ECOR47 | Sheep | New Guinea | Coloniser |
| ECOR48 | Human | Sweden | UTI and Acute Cystitis |
| ECOR49 | Human | Sweden | Coloniser |
| ECOR5 | Human | U.S.A. | Coloniser |
| ECOR50 | Human | Sweden | UTI and Acute Pyelonephritis |

| | | | |
|---|---|---|---|
| ECOR51 | Human Infant | U.S.A. | Coloniser |
| ECOR52 | Orangutan | U.S.A. | Coloniser |
| ECOR53 | Human Child | U.S.A. | Coloniser |
| ECOR54 | Human | U.S.A. | Coloniser |
| ECOR55 | Human | Sweden | Coloniser |
| ECOR56 | Human | Sweden | Coloniser |
| ECOR57 | Gorilla | U.S.A. | Coloniser |
| ECOR58 | Lion | U.S.A. | Coloniser |
| ECOR59 | Human | U.S.A. | Coloniser |
| ECOR60 | Human | Sweden | UTI and Acute Cystitis |
| ECOR61 | Human | Sweden | Coloniser |
| ECOR62 | Human | Sweden | UTI and Acute Pyelonephritis |
| ECOR63 | Human | Sweden | Coloniser |
| ECOR64 | Human | Sweden | UTI and Acute Cystitis |
| ECOR65 | Celebese Ape | U.S.A. | Coloniser |
| ECOR66 | Celebese Ape | U.S.A. | Coloniser |
| ECOR67 | Goat | Indonesia | Coloniser |
| ECOR7 | Orangutan | U.S.A. | Coloniser |
| ECOR8 | Human | U.S.A. | Coloniser |
| ECOR9 | Human | Sweden | Coloniser |